**SANDIA REPORT**
SAND2006-7511
Unlimited Release
Printed December 2006

# Two Dimensional Unstable Scar Statistics

Larry K. Warne, Roy E. Jorgenson, Joseph D. Kotulski, Sandia National Laboratories
Kelvin S. H. Lee, ITT Industries/AES

Prepared by
Sandia National Laboratories
Albuquerque, New Mexico 87185 and Livermore, California 94550

Sandia is a multiprogram laboratory operated by Sandia Corporation,
a Lockheed Martin Company, for the United States Department of Energy's
National Nuclear Security Administration under Contract DE-AC04-94AL85000.



Issued by Sandia National Laboratories, operated for the United States Department of Energy by Sandia Corporation.



Available to DOE and DOE contractors from
U.S. Department of Energy
Office of Scientific and Technical Information
P.O. Box 62
Oak Ridge, TN 37831

Telephone: (865) 576-8401
Facsimile: (865) 576-5728
E-Mail: reports@adonis.osti.gov
Online ordering: http://www.osti.gov/bridge

Available to the public from
U.S. Department of Commerce
National Technical Information Service
5285 Port Royal Rd.
Springfield, VA 22161

Telephone: (800) 553-6847
Facsimile: (703) 605-6900
E-Mail: orders@ntis.fedworld.gov
Online order: http://www.ntis.gov/help/ordermethods.asp?loc=7-4-0#online

SAND2006-7511
Unlimited Release
Printed December 2006

# Two Dimensional Unstable Scar Statistics

Larry K. Warne, Roy E. Jorgenson, Joseph D. Kotulski
Electromagnetics and Plasma Physics Analysis Dept.
Sandia National Laboratories
P. O. Box 5800
Albuquerque, NM 87185-1152

Kelvin S. H. Lee
ITT Industries/AES
1033 Gayley Avenue
Suite 215
Los Angeles, CA 90024

**Abstract**

This report examines the localization of time harmonic high frequency modal fields in two dimensional cavities along periodic paths between opposing sides of the cavity. The cases where these orbits lead to unstable localized modes are known as scars. This paper examines the enhancements for these unstable orbits when the opposing mirrors are both convex and concave. In the latter case the construction includes the treatment of interior foci.

# Contents

**1 INTRODUCTION** ..... **19**

**2 CONVEX MIRRORS AND BOW TIE CAVITY** ..... **20**

2.1 Geometry ..... 20

2.2 Previous Bow Tie Scar Model ..... 21

2.3 Elliptical High Frequency Analysis ..... 24

2.3.1 high frequency approximation ..... 25

2.4 Spatial Variations of Eigenfunctions ..... 28

2.5 Normalization of Eigenfunctions ..... 29

2.6 Projections Along Orbit ..... 38

2.6.1 fourier projection ..... 38

2.6.2 scar projection ..... 39

2.6.3 elliptic system projection ..... 40

2.6.4 random plane wave projection ..... 41

2.6.5 random plane wave projection with elliptical projection operator ..... 43

2.6.6 projection comparisons ..... 45

2.7 Integral Of Square Along Scar ..... 45

2.7.1 average of random plane wave over interval ..... 48

2.7.2 comparison of integral of square ..... 50

2.8 Alternative Eigenfunction Representation and Integral Along Scar ..... 50

2.9 Point Value Statistics ..... 58

2.9.1 point statistics from simulations . . . 61

2.10 Odd Symmetry Along Orbit . . . 62

2.10.1 high frequency elliptical solution . . . 62

2.10.2 energy theorem normalization . . . 65

2.10.3 projection operation . . . 68

2.10.4 random plane wave projection . . . 69

2.11 Odd Symmetry Perpendicular To Orbit . . . 72

2.11.1 second normalization condition . . . 73

2.11.2 odd normal scar problem . . . 75

2.11.3 random plane wave odd projection . . . 79

2.12 Asymmetric Bow Tie Cavity . . . 81

2.12.1 first normalization condition . . . 81

2.12.2 even and odd decomposition . . . 84

2.12.3 comparisons of even-odd theory with asymmetric simulations . . . 86

**3 CONCAVE MIRRORS AND STADIUM CAVITY . . . 89**

3.1 Geometry . . . 89

3.2 Elliptical High Frequency Analysis In Outer Two Regions . . . 93

3.2.1 modal description in region one: between foci . . . 95

3.2.2 modal description in region two: outside foci . . . 98

3.2.3 more symmetrical version of region two solution . . . 100

3.2.4 more general version of region two solution . . . 100

3.2.5 modified region one solution . . . 101

3.3 Behavior Near Focal Region And Matching . . . 102

3.3.1 approach of focal point . . . 102

3.3.2 small shift in focal position . . . 103
3.3.3 focal region three . . . 103
3.3.4 evenness conditions on scar . . . 105
3.3.5 summary of conditions . . . 106
3.3.6 final set of conditions . . . 107
3.3.7 focal shift in simulations . . . 108
3.3.8 focal shift examples . . . 109
3.4 Field Comparisons On Axis . . . 116
3.4.1 distribution of shifts . . . 139
3.4.2 focal continuity condition when s is zero . . . 141
3.5 Normalization of Eigenfunctions . . . 142
3.5.1 carrying out the integration . . . 144
3.6 Trigonometric Projection Operator . . . 148
3.6.1 no amplitude factors . . . 148
3.6.2 no amplitude factors and elimination of phase shifts . . . 150
3.6.3 amplitude factors present with no phase shifts . . . 150
3.6.4 no amplitude factors and focal point shift . . . 152
3.6.5 projection without amplitude factors but with phase factors and focal point shift . . . 153
3.6.6 projection of next scar component . . . 154
3.6.7 random plane wave projection . . . 155
3.7 Elliptical Projection Operator . . . 158
3.7.1 next components and orthogonality . . . 164
3.7.2 random plane wave projection . . . 165
3.8 Integral Of Square Along Scar . . . 168
3.8.1 addition of random plane wave . . . 170

3.8.2 comparison of histograms ... 177

3.9 Point Value Statistics ... 180

3.9.1 value at focus ... 181

3.9.2 value for eigenvalue equal to scar frequency ... 182

3.9.3 value at fixed point ... 183

3.9.4 histograms in stadium from numerical simulations ... 186

**4 CONCLUSIONS ... 205**

**5 REFERENCES ... 205**

**A APPENDICES FOR BOW TIE CAVITY ... 208**

A.1 Bow Tie Cavity Area ... 208

A.2 Peak Of Scar Curve ... 210

A.3 Calculation of Random Plane Wave Projection ... 211

A.3.1 contributions to summation of p components ... 214

A.4 Ray Reflection and Stability ... 216

A.5 Higher Order Bow Tie Cavity ... 220

A.5.1 boundary conditions ... 225

A.6 Asymptotic Orthogonality In The Bow Tie ... 226

A.7 Comparison of Source and Boundary Forms Of Energy Theorem And Normalization ... 230

A.7.1 source free form of energy theorem ... 230

A.7.2 source free symmetric bow tie trigonometric series ... 231

A.7.3 source form with entire eigenfunction current ... 231

A.7.4 source form with single component ... 231

A.7.5 comments on source current strength ... 232

**B APPENDICES FOR STADIUM CAVITY . . . . . 233**

B.1 Higher Order Stadium . . . . . 233

B.1.1 region one . . . . . 233

B.1.2 region two . . . . . 234

B.1.3 region three . . . . . 238

B.1.4 matching . . . . . 242

B.2 Asymptotic Orthogonality In The Stadium . . . . . 244

B.2.1 trigonometric approximation . . . . . 244

B.2.2 scar functions from elliptical analysis . . . . . 247

B.2.3 orthogonality with normal derivative . . . . . 251

B.3 Normalization in Stadium Cavity And Focal Point Contribution . . . . . 253

B.3.1 transition to region three . . . . . 254

B.3.2 Cartesian justification of principal value . . . . . 256

B.3.3 region three correction for s equal to zero . . . . . 258

B.4 Focal Point Correction To Projection Operator . . . . . 262

B.4.1 correction for s equal to zero . . . . . 267

B.4.2 subtraction of averaged values . . . . . 270

B.4.3 shifted projection operator . . . . . 272

B.4.4 subtraction of averaged values from shifted projection . . . . . 274

B.4.5 including higher order terms in the oscillatory functions of the projection operator . . . 276

B.5 Random Plane Wave Representations And Treatment Of Integral Near Focal Point . . . . . 278

B.5.1 random plane wave projection . . . . . 278

B.5.2 another approach to stadium integral of the square . . . . . 280

# Figures


**1. Quarter bowtie cavity geometry.** . . . . . **21**

**2. Comparison of bow tie scar projection, random plane wave projection, and numerical histogram from a boundary element moment method solution.** . . . . . **24**

**3. Ellitical geometry applied to bow tie cavity along horizontal bouncing ball orbit.** . . . . . **25**

**4. Electric field intensity plot for quarter bow tie cavity at a frequency of 3.2266 GHz, which is near a vertical scar frequency.** . . . . . **29**

**5. Spatial distribution of electric field along vertical scarred orbit compared to the simple sinusoid and scar construction.** . . . . . **30**

**6. Electric field intensity plot for quarter bow tie cavity at a frequency of 2.9171 GHz, which is near a horizontal scar frequency.** . . . . . **31**

**7. Spatial distribution of electric field along horizontal scarred orbit compared to the simple sinusoid and scar construction.** . . . . . **32**

**8. Comparison of scar projections and previous Fourier projections (using Fourier series solution) for both scar theory and random plane wave field for $L = 2$ m and $R = 10$ m.** . . . . . **46**

**9. Comparison of scar projections and previous Fourier projections (using Fourier series solution) for both scar theory and random plane wave field for $L = 2$ m and $R = 2$ m.** . . . . . **47**

**10. Comparison of the mean of the integral of square of eigenfunction minus the square of the random plane wave for various numbers of terms included in the summation. The Fourier expansion is used here.** . . . . . **51**

**11. Comparison of trigonometric functions versus elliptical functions.** . . . . . **51**

**12. Histogram for the mean integral of the square of the eigenfunction minus the random plane wave from numerical simulation of quarter bow tie cavity with $L = 2$ m and $R = 10$ m as a function of $\mu = (k - k_p)\,\ell/\pi$.** . . . . . **52**

**13. Histogram for the mean integral of the square of the eigenfunction over the scarred orbit from the numerical simulation of the quarter bow tie cavity with $L = 2$ m and $R = 10$ m as a function of $\mu = (k - k_p)\,\ell/\pi$.** . . . . . **53**

**14. Point histogram of the electric field at the center of the bow tie cavity (on both $x$ and $y$ symmetry planes).** . . . . . **62**

**15. Point histogram of the electric field along $y$ axis at $y = 0.2$ m where $L = 2$ m and $R = 10$ m.** . . . . . **63**

**16. Point histogram of electric field along $y$ axis at $y = 0.6$ m, with $L = 2$ m and $R = 10$ m.** . . . . . **63**

**17. Point histogram of electric field out in the volume with $x = y = 0.5$ m.** . . . . . **64**

**18. Comparison of scar projection and random plane wave projection for electric field which is odd with respect to the normal of the orbit. Geometry is $L = 2$ m and $R = 10$ m. The dotted curve is the asymptotic scar projection for large $s_p$.** . . . . . **82**

**19. Odd problem in symmetric bow tie cavity. Histogram is for the projection of the normal derivative of the field on orbit (magnetic field). Theory is odd scar mode projection and odd random plane wave projection.** . . . . . **83**

**20. Comparison of histogram for the projection of the electric field along the orbit in the asymmetrical bow tie cavity with the even theory and random plane wave projection.** . . . . . **87**

**21. Histogram is for the projection of the normal derivative of the field on the orbit (magnetic field) in the asymmetric bow tie cavity. Theory is odd scar mode projection and odd random plane wave projection.** . . . . . **88**

**22. The electric field intensity of a typical eigenfunction in the asymmetric bow tie cavity showing random behavior.** . . . . . **89**

**23. Vertical scar electric field intensity in asymmetric bow tie cavity $k\ell \approx 45.654$ and with $p = 15$, $k_p\ell \approx 45.5531$.** . . . . . **90**

**24. Another vertical scar electric field intensity plot with $k\ell \approx 58.065$ and with $p = 19$, $k_p\ell \approx 58.12$.** . . . . . **90**

**25. Horizontal scar electric field intensity in asymmetric bow tie cavity.** . . . . . **91**

**26. Bouncing ball mode along horizontal axis in stadium cavity at 4.205 GHz. The geometry has $L = 0.55$ m and $R = 0.25$ m. . . . . 93**

**27. Elliptic cylinder geometry for modeling stadium horizontal scar. . . . . 94**

**28. Elliptical cylinder geometry showing the three regions about the focal point used in modeling the horizontal scar. . . . . 96**

**29. Comparison between simulation of eigenfunction (red curve) and $p = 8$ scar. The black curves are Region 1 and Region 2 formulas (the green curves are the same with $k = k_p$ in the cosine distributions). The tan curve is the Region 3 focal point region, shifted by the theoretical focal point shift. . . . . 119**

**30. Comparison between simulation of eigenfunction (red curve) and $p = 9$ scar. The black curves are Region 1 and Region 2 formulas (the green curves are the same with $k = k_p$ in the cosine distributions). The tan curve is the Region 3 focal point region, shifted by the theoretical focal point shift. . . . . 120**

**31. Bouncing ball mode along horizontal axis in stadium cavity at 4.768 GHz. The geometry has $L = 0.55$ m and $R = 0.25$ m. . . . . 121**

**32. Black and white simplified comparison between simulation of eigenfunction (diamonds) and $p = 9$ scar. The solid dot curves are Region 1 and Region 2 formulas. The open dot curve is the Region 3 focal point region, shifted by the theoretical focal point shift. . . . . 122**

**33. Comparison between simulation of eigenfunction (red curve) and $p = 10$ scar. The black curves are Region 1 and Region 2 formulas (the green curves are the same with $k = k_p$ in the cosine distributions). The tan curve is the Region 3 focal point region, shifted by the theoretical focal point shift. . . . . 123**

**34. Comparison between simulation of another eigenfunction (red curve) and $p = 10$ scar. The black curves are Region 1 and Region 2 formulas (the green curves are the same with $k = k_p$ in the cosine distributions). The tan curve is the Region 3 focal point region, shifted by the theoretical focal point shift. . . . . 124**

**35. Bouncing ball mode along horizontal axis in stadium cavity at 5.3307 GHz. The geometry has $L = 0.55$ m and $R = 0.25$ m. . . . . 125**

**36. Comparison between simulation of eigenfunction (red curve) and $p = 11$ scar. The black curves are Region 1 and Region 2 formulas (the green curves are the same with $k = k_p$ in the cosine distributions). The tan curve is the Region 3 focal point region, shifted by the theoretical focal point shift. . . . . 126**

**37. Comparison between simulation of eigenfunction (red curve) and $p = 12$ scar. The black curves are Region 1 and Region 2 formulas (the green curves are the same with $k = k_p$ in the cosine distributions). The tan curve is the Region 3 focal point region, shifted by the theoretical focal point shift.** . . . . . **127**

**38. Comparison between simulation of eigenfunction (red curve) and $p = 13$ scar. The black curves are Region 1 and Region 2 formulas (the green curves are the same with $k = k_p$ in the cosine distributions). The tan curve is the Region 3 focal point region, shifted by the theoretical focal point shift.** . . . . . **128**

**39. Bouncing ball mode along horizontal axis in stadium cavity at $6.9674$ GHz. The geometry has $L = 0.55$ m and $R = 0.25$ m.** . . . . . **129**

**40. Comparison between simulation of eigenfunction (red curve) and $p = 14$ scar. The black curves are Region 1 and Region 2 formulas (the green curves are the same with $k = k_p$ in the cosine distributions). The tan curve is the Region 3 focal point region, shifted by the theoretical focal point shift.** . . . . . **130**

**41. Comparison between simulation of eigenfunction (red curve) and $p = 15$ scar. The black curves are Region 1 and Region 2 formulas (the green curves are the same with $k = k_p$ in the cosine distributions). The tan curve is the Region 3 focal point region, shifted by the theoretical focal point shift.** . . . . . **131**

**42. Comparison between simulation of eigenfunction (red curve) and $p = 16$ scar. The black curves are Region 1 and Region 2 formulas (the green curves are the same with $k = k_p$ in the cosine distributions). The tan curve is the Region 3 focal point region, shifted by the theoretical focal point shift.** . . . . . **132**

**43. Comparison between simulation of eigenfunction (red curve) and $p = 17$ scar. The black curves are Region 1 and Region 2 formulas (the green curves are the same with $k = k_p$ in the cosine distributions). The tan curve is the Region 3 focal point region, shifted by the theoretical focal point shift.** . . . . . **133**

**44. Bouncing ball mode along horizontal axis in stadium cavity at $9.0707$ GHz. The geometry has $L = 0.55$ m and $R = 0.25$ m.** . . . . . **134**

**45. Black and white simplified comparison between simulation of eigenfunction (diamonds) and $p = 17$ scar. The solid dot curves are Region 1 and Region 2 formulas. The open dot curve is the Region 3 focal point region, shifted by the theoretical focal point shift.** . . . . . **135**

**46. Comparison between simulation of another eigenfunction (red curve) and $p = 17$ scar. The black curves are Region 1 and Region 2 formulas (the green curves are the same with $k = k_p$ in the cosine distributions). The tan curve is the Region 3 focal**

**point region, shifted by the theoretical focal point shift.** . . . . . **136**

**47. Bouncing ball mode along horizontal axis in stadium cavity at $9.1735$ GHz. The geometry has $L = 0.55$ m and $R = 0.25$ m.** . . . . . **137**

**48. Comparison between simulation of eigenfunction (red curve) and $p = 18$ scar. The black curves are Region 1 and Region 2 formulas (the green curves are the same with $k = k_p$ in the cosine distributions). The tan curve is the Region 3 focal point region, shifted by the theoretical focal point shift.** . . . . . **138**

**49. Cumulative distribution of focal point shifts for $8 \leq p \leq 36$ (and $-5 \leq s \leq 5$ for blue curve which includes correction).** . . . . . **140**

**50. An attempt at locating the shifted focal point locations by maximizing the elliptic projection operator as a function of $d_e$.** . . . . . **141**

**51. Comparison of projections with and without amplitude factors. The phase shifts are neglected in both regions.** . . . . . **152**

**52. Effect of applying average focal point shift without phase factors or amplitude divergence factors.** . . . . . **153**

**53. Comparison of trigonometric projection and numerical histogram for short stadium cavity along horizontal bouncing ball scar. The scar theory used an average shifted focal point $d_e \approx 0.094$ m.** . . . . . **154**

**54. Comparison of various trigonometric projections without amplitude divergence factors. The effect of phase factors reducing the tails of the peak, the reduction of the peak due to the average focal shift, and the lack of othogonality of the trigonometric operator with respect to the scar components are the effects illustrated.** . . . . . **156**

**55. Comparison of scar projection and numerical histogram using geometrical focal location. Also shown for reference is the bow tie scar theory. Finally the random plane wave projection is plotted.** . . . . . **161**

**56. Comparison of scar projection and numerical histogram using average shift focal location of $0.092$ m. The projection of the random plane wave is plotted. Also shown for reference is the bow tie scar theory.** . . . . . **162**

**57. Comparison of scar projection and numerical histogram using average shift focal location of $0.092$ m in the theory but the functional shift from the theory to define the projection operator in the numerical histogram. The projection of the random plane wave is plotted. Also shown for reference is the bow tie scar theory.** . . . . . **163**

**58. The black curve shows the scar projection using the geometrical focal point. The solid blue curve (which is almost zero) shows the projection for the $m = 1$ next component. The solid purple curve (again nearly zero) shows the projection for the $m = 2$ next component. The solid green curve is the random plane wave projection. The dotted blue and purple curves show the trigonometric projections of the $m = 1$ and $m = 2$ components.** . . . . . **165**

**59. The phase and exponential factors have been dropped in the projection resulting in the red curve, which approaches the scar function. Note that the abscissa has the same values as $s$.** . . . . . **169**

**60. Integral of the square of the $p$th scar component along the horizontal orbit of the stadium cavity.** . . . . . **171**

**61. Comparison of random plane wave projections from original approach and from correlation function approach.** . . . . . **176**

**62. Integral of the square of the eigenfunction $p$th component minus the random plane wave projection for the stadium cavity. Also shown are the bow tie cavtiy results discussed previously scaled by the ratio of bow tie to stadium cavity areas (to put it on the same scale as the stadium results).** . . . . . **178**

**63. Numerical histogram results for the integral of the square of the field along the horizontal orbit minus the random plane wave integral in the stadium cavity.** . . . . . **178**

**64. Numerical histogram results for the integral of the square of the field along the horizontal orbit in the stadium cavity.** . . . . . **179**

**65. Plot of the scaled amplitude near the focal point for $k = k_p$.** . . . . . **184**

**66. Scar component $p$ statistics as a function of $s$ at fixed location $x_0 = 0.103$ m along the horizontal orbit of the stadium. The focal point shifts according to the phase matching formulas, taking the first solution greater than or equal to $d$.** . . . . . **185**

**67. Numerical histogram of point value statistics along the horizontal orbit in the stadium cavity at location $x_0 = 0.103$ m.** . . . . . **186**

**68. Histogram for point value of field for $x = y = 0.05$ m.** . . . . . **187**

**69. Histogram for point value of field for $x = y = 0.10$ m.** . . . . . **187**

**70. Histogram for point value of field for $x = y = 0.15$ m.** . . . . . **188**

**71. Histogram for point value at $x = 0$ and $y = 0.245$ m.** . . . . . **188**

**72. Histogram for point value at $x = 0$ and $y = 0.20$ m.** . . . . . **189**

**73. Histogram for point value at $x = 0$ and $y = 0.15$ m.** . . . . . **189**

**74. Histogram for point value at $x = 0$ and $y = 0.10$ m.** . . . . . **190**

**75. Histogram for point value at $x = 0$ and $y = 0.05$ m.** . . . . . **191**

**76. Histogram for point value at the center $x = y = 0$.** . . . . . **192**

**77. Histogram for point value on scar orbit at $x = 0.05$ m and $y = 0$.** . . . . . **193**

**78. Histogram for point value on scar orbit at $x = 0.08$ m and $y = 0$.** . . . . . **193**

**79. Histogram for point value on scar orbit at $x = 0.0833$ m (just to the right of the geometrical focal point) and $y = 0$.** . . . . . **194**

**80. Histogram for point value on scar orbit at $x = 0.085$ m and $y = 0$.** . . . . . **194**

**81. Histogram for point value on scar orbit at $x = 0.090$ m and $y = 0$.** . . . . . **195**

**82. Histogram for point value on scar orbit at $x = 0.095$ m and $y = 0$.** . . . . . **195**

**83. Histogram for point value on scar orbit at $x = 0.096$ m and $y = 0$.** . . . . . **196**

**84. Histogram for point value on scar orbit at $x = 0.097$ m and $y = 0$.** . . . . . **196**

**85. Histogram for point value on scar orbit at $x = 0.098$ m and $y = 0$.** . . . . . **197**

**86. Histogram for point value on scar orbit at $x = 0.099$ m and $y = 0$.** . . . . . **197**

**87. Histogram for point value on scar orbit at $x = 0.100$ m and $y = 0$.** . . . . . **198**

**88. Histogram for point value on scar orbit at $x = 0.101$ m and $y = 0$.** . . . . . **198**

**89. Histogram for point value on scar orbit at $x = 0.102$ m and $y = 0$.** . . . . . **199**

**90. Histogram for point value on scar orbit at $x = 0.103$ m and $y = 0$.** . . . . . **199**

**91. Histogram for point value on scar orbit at $x = 0.104$ m and $y = 0$.** . . . . . **200**

**92. Histogram for point value on scar orbit at $x = 0.105$ m and $y = 0$.** . . . . . **200**

**93. Histogram for point value on scar orbit at $x = 0.106$ m and $y = 0$.** . . . . . **201**

**94. Histogram for point value on scar orbit at $x = 0.107$ m and $y = 0$.** . . . . . **201**

**95. Histogram for point value on scar orbit at $x = 0.108$ m and $y = 0$.** . . . . . **202**

**96. Histogram for point value on scar orbit at $x = 0.110$ m and $y = 0$.** . . . . . **202**

**97. Histogram for point value on scar orbit at $x = 0.15$ m and $y = 0$.** . . . . . **203**

**98. Histogram for point value on scar orbit at $x = 0.20$ m and $y = 0$.** . . . . . **203**

**99. Histogram for point value on scar orbit at $x = 0.25$ m and $y = 0$.** . . . . . **204**

**100.Histogram for point value on scar orbit at $x = 0.27$ m and $y = 0$.** . . . . . **204**

**1. Geometry of bow tie cavity and circular walls used in the calculation of the interior area.** . . . . . **209**

**1. Integral values of correction from Region 3. The solid curve has the trigonometric functions subtracted and the dashed curve has the averaged values subtracted.** . . . . . **271**

# Two Dimensional Unstable Scar Statistics

Larry K. Warne, Roy E. Jorgenson, Joseph D. Kotulski
Electromagnetics and Plasma Physics Analysis Dept.
Sandia National Laboratories
P. O. Box 5800
Albuquerque, NM 87185-1152

Kelvin S. H. Lee
ITT Industries/AES
1033 Gayley Avenue
Suite 215
Los Angeles, CA 90024

## 1 INTRODUCTION

Calculations of steady state electromagnetic shielding in a linear system make use of conservation of power [1]. At high frequencies such calculations frequently make assumptions about the homogeneity of the fields inside the shielded volume or cavity, and make use of free space or unloaded transmission and receiving properties of apertures and antennas [1]. When losses are sufficient to result in a high degree of modal overlap, statistical homogeneity of the fields are often assumed. This approach is used in mode stirred chambers (with mechanical or other modal stirring) and in other calculations [2]. Transmission and receiving properties of apertures and antennas in this limit also approach free space unloaded levels [3], [4].

Interest in high frequency (or high energy) behavior of modal fields has been of considerable interest in recent years [5]. The idea of high frequency modal fields being composed of a random distribution of plane waves [6], leading to normal distributions of the field amplitude [7], [5] has been used in various areas, including problems in electromagetics [8]. Recently antenna radiation and coupling problems have been investigated using these chaotic field assumptions [9], [10], [11], [12], [13]. Many experimental verifications of predictions have also been carried out [14], [15], [16], [17].

Cavities which have boundary shapes supporting interior regions of stability can exhibit various types of confined modes. These include whispering gallery and bouncing ball modes [18], [19], as well as modes along closed geodesic curves [20]. These modes may be identified by means of ray tracing and examination of stability exponents for the closed orbits. High frequency asymptotic methods have been developed to examine these types of modes [18], [19], [20]. Such localized modes exhibit nonhomogeneous field behavior and may have higher or lower quality factors than the homogeneous field distributions (depending on the type of mode). Antennas and apertures in these regions will couple into these localized modes.

Enhancements along unstable periodic orbits also exist and have been called scars [21], [22], [23]. These have been investigated extensively for the Schroedinger equation and use has been made of high frequency (energy) semiclassical techniques [24], [25], [26], [27], [28]. Recently there has appeared discussions of bounding levels at interior foci [29]. A method was also introduced to treat constant energy scarring for convex wall geometries (without foci) [30], which is convenient for treatment of the time harmonic electromagnetic problems that are the focus of this report.

This report is directed at understanding the high frequency behavior of modal fields in two dimensional

cavities. In particular, the localization of the eigenfunctions about unstable periodic orbits, is investigated. The approach used by Antonsen [30], on convex mirror geometries in two dimensions, is generalized by introducing the elliptical high frequency formalism, used previously by Vaynshteyn [18] on stable orbits. This combined approach not only gives a feel for the accuracy in the convex mirror case but also enables us to treat unstable orbits with concave mirrors. The method is illustrated by investigating the horizontal bouncing ball scars in the stadium cavity.

The first half of the report combines the elliptic geometry approach with the random phase reflection coefficient in the convex boundary example of the bow tie cavity. A slightly different description of the eigenfunctions is adopted here than in previous work, regarding the eigenfunction as asymptotically made up of scarred projections and a random plane wave component. This view is useful in the second half of the report on the stadium cavity. Projections of the eigenfunction and integrals of the square are calculated and compared to previous results and to statistics assembled by numerical simulations of the eigenfunctions. The main reason for this first half on the convex walls is to illustrate the method in a simpler geometry than that encountered in the concave case. We also briefly consider the asymptotic nature of the construction and how higher order approximations can be found. The asymmetrical bow tie geometry is also briefly discussed and the odd problem statistics are constructed.

The second half of the report generalizes the method to the concave boundary example of the stadium cavity. The complicating feature here is the presence of interior foci along the scarred orbit that must be treated. Separate regions at the focus and on either side of it are used to construct the eigenfunction along the orbit. The random phase reflection coefficient in this case needed to be modified to have conjugate forms on either side of the focus. Matching of the solutions in the various regions could only be accomplished by allowing a subwavelength shift of the focal region. The normalization using the electromagnetic energy theorem results in a principal value evaluation at the focus. Projections of the eigenfunctions and integrals of the square are calculated and compared to statistics assembled by numerical simulations of the eigenfunctions. Also point statistics both near the focus and away from it are discussed. Finally use of the frequency difference between the cavity eigenvalues and the scar modes is used to determine the random phase reflection coefficient for several scar realizations in the stadium. Normalization of a single point value along the orbit allows a quantitative comparison of the spatial distribution of the scar mode constructions with the numerical simulations. These comparisons show agreement between the matched three regions (with focal point region shift) and the numerical constructions.

# 2 CONVEX MIRRORS AND BOW TIE CAVITY

The bow tie cavity has been used as a canonical shape for an unstable ray geometry with convex boundaries [30].

## 2.1 Geometry

One quarter of this cavity is shown in Figure 1.

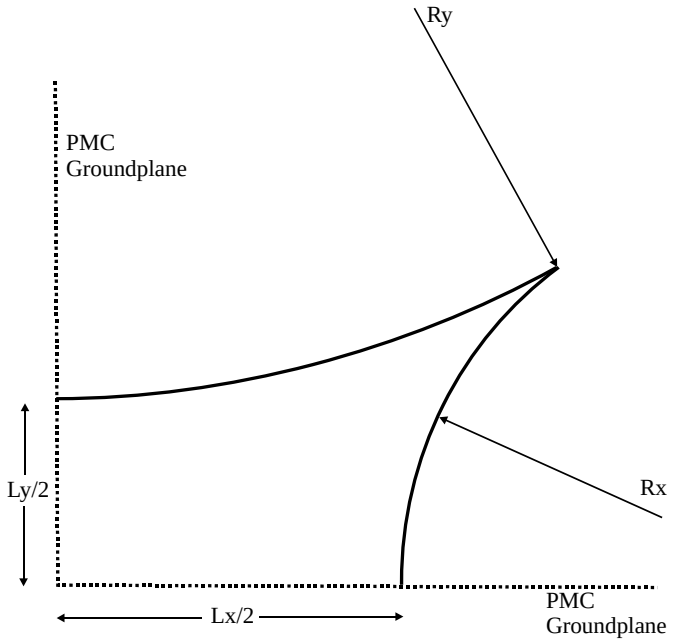


Figure 1. Quarter bowtie cavity geometry.

The cavity boundaries are described by the intersection of circles. Ray analysis leads to foci outside the cavity. Note that the bow tie cavity area is needed and is given in the Appendix. The length of the orbit is taken as $L$ and, in general, is set equal to $L_x$ or $L_y$ depending on which direction is being considered (in this report these are both equal).

## 2.2 Previous Bow Tie Scar Model

Antonsen [30] introduced a Fourier expansion for the field along the scar (the $x$ direction in this case) orbit (for the even case in $x$)

$$u = \frac{2}{L} \sum_p V_p(y) \cos(k_p x)$$

where

$$k_p = (p - 1/2)\,\pi/\ell\,,\; p = 1, 2, 3, ...$$

and the orbit length $L = 2\ell$. The Fourier amplitudes were then solved from a modal equation which resulted from the approximation of very large radius of curvature $R$ of the mirrors

$$V_p''(y) + \left[k^2 - k_p^2\left(1 - \frac{x^2}{R\ell}\right)\right] V_p(y) \approx 0$$

This form leads to a parabolic cylinder function for the field local to the scarred orbit. Unlike typical Gaussian beam modes [18], the propagation here takes place in both the axial and transverse directions because of the unstable mirror geometry. The transverse differential equation therefore has two solutions which must both be considered. Antonsen [30] introduced a random phase reflection coefficient with unit magnitude to represent the reflection from the chaotic region of the cavity (the problem was taken to be

even in $y$ also). The amplitude becomes

$$V_p^2(0) = V_p^2 = v^2 L^2 G_1(\lambda_1, \Lambda) / \left(A\sqrt{kL}\right)$$

where $A$ is the cavity area (including all four quarters of the cavity),

$$G_1(\lambda_1, \Lambda) = \frac{2(\Lambda-1)^{-1/2}}{\left|U_+'(\lambda_1, 0)\right|^2} = \frac{1}{\pi}(\Lambda-1)^{-1/2} \exp[\pi\lambda_1/2] 2^{1/2} \left|\Gamma(1/4 - i\lambda_1/2)\right|^2$$

where $U_+$ is a parabolic cylinder function discussed below ($\Gamma(z)$ is the gamma function [31]), $v$ is a unit Gaussian random variable of unit variance with density

$$f(v) = \frac{1}{\sqrt{2\pi}} e^{-v^2/2}$$

the variable

$$\lambda_1 = \left(k^2 - k_p^2\right) L / [k(\Lambda - 1)]$$

measures the difference in frequency between the operating wavenumber $k$ and the scar wavenumber $k_p$, and

$$\Lambda - 1 = \sqrt{8L/R}$$

Note from $\Gamma(z) \sim e^{-z} z^{z-1/2}\sqrt{2\pi}$, $z \to \infty$ that

$$\left|\Gamma(1/4 - i\lambda_1/2)\right| \sim e^{-\pi\lambda_1/4} (\lambda_1/2)^{-1/4} \sqrt{2\pi}\ ,\ \lambda_1 \to \infty$$

$$G_1(\lambda_1, \Lambda) \sim 4/\sqrt{(\Lambda-1)\lambda_1} \sim 4/\sqrt{2(k-k_p)L}\ ,\ \lambda_1 \to \infty$$

and with $\Gamma(1/4) \approx 3.62561$

$$G_1(0, \Lambda) = \frac{1}{\pi}(\Lambda-1)^{-1/2} 2^{1/2} \Gamma^2(1/4) \approx 5.9(\Lambda-1)^{-1/2}$$

The solid curve of Figure 2 shows the projection amplitude versus the random plane wave projection [30]

$$G_s(\lambda) = \frac{2}{\pi} \int_{-\infty}^{\infty} \frac{\sin^2\left(\lambda/4 - \zeta^2\right)}{\left(\lambda/4 - \zeta^2\right)^2} d\zeta$$

$$\lambda = 2(k - k_p) L$$

shown as the dashed curve (the factor of four from the even symmetry about the $x$ and $y$ axes is included in this definition). Note from the Appendix that

$$G_s(\lambda) = \frac{4}{\sqrt{|\lambda|}} \left\{ \left(1 - \frac{1}{\lambda}\right) C\left(\sqrt{|\lambda|/\pi}\right) + \mathrm{sgn}(\lambda) \left(1 + \frac{1}{\lambda}\right) S\left(\sqrt{|\lambda|/\pi}\right) \right\} - \frac{4}{\lambda\sqrt{\pi}} \{\sin(\lambda/2) - \cos(\lambda/2)\}$$

$$\sim \frac{4}{\sqrt{\lambda}}\ ,\ \lambda >> 1$$

$$\sim \frac{4}{(-\lambda)^{3/2}} \ , \ \ -\lambda >> 1$$

where

$$C(z) = \int_0^z \cos\left(\pi t^2/2\right) dt$$

$$S(z) = \int_0^z \sin\left(\pi t^2/2\right) dt$$

are the Fresnel integrals [31]. The value at zero is

$$G_s(0) = \frac{8}{3\sqrt{\pi}}$$

and thus at $\lambda = 0$ for these parameters ($L = 2$ m, $A \approx 4.6771$ m$^2$) we have

$$\left\langle \sqrt{kL} V_p^2 \right\rangle_r = L^2 G_s(0)/A \approx 1.3$$

As shown in the Appendix, the peak of the solid curve is near

$$\lambda_{1pk} \approx 0.17$$

with the value

$$G_1(\lambda_{1pk}, \Lambda) \approx 6.8 \ \ (\Lambda - 1)^{-1/2}$$

The peak of the quantity on the graph for these parameters is thus

$$\left\langle \sqrt{kL} V_p^2 \right\rangle = L^2 G_1(\lambda_{1pk}, \Lambda)/A \approx 5.2$$

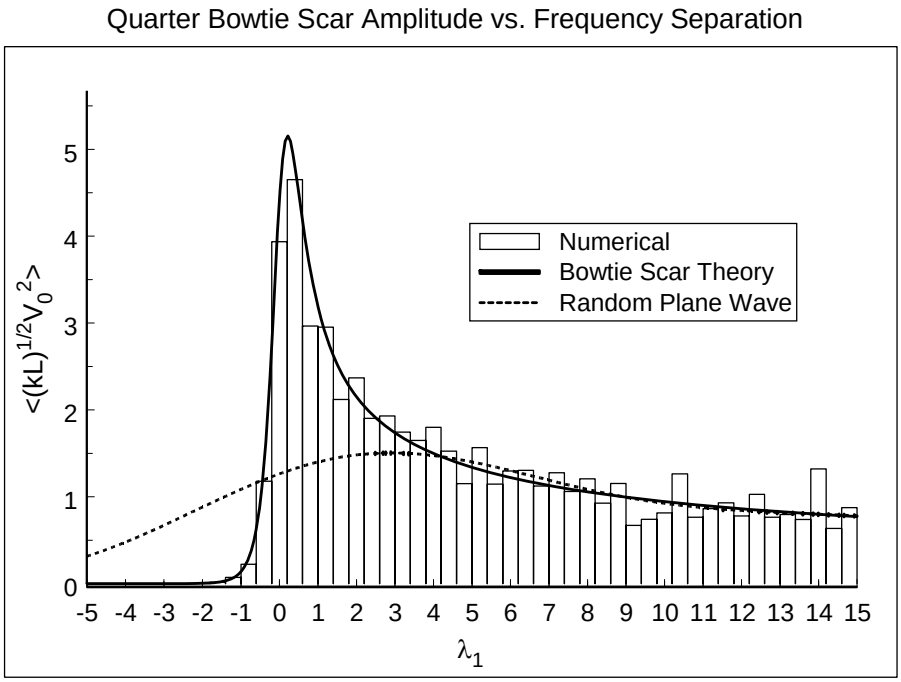


Figure 2. Comparison of bow tie scar projection, random plane wave projection, and numerical histogram from a boundary element moment method solution.

Figure 2 also shows a comparison of the model results with a histogram made from the numerical solution of the bow tie cavity.

Note that stability exponents for this geometry are given by [32] (this is also derived in the Appendix)

$$\Lambda_{\pm} = \left[1 + L/R \pm \sqrt{(1+L/R)^2 - 1}\right]^2 = 2\,(L/R)\,(2 + L/R) + 1 \pm 2\,(1 + L/R)\,\sqrt{(L/R)\,(2 + L/R)}$$

The plus sign $\Lambda_+$ becomes the same as $\Lambda$ in the limit $L/R \to 0$, however it does not produce the same value for the given geometry $\Lambda_+ = 3.47$ versus $\Lambda = 2.26$. This is a consequence of the simplifying limit of large radii taken in the Fourier expansion approach. The next section gives an alternative derivation of the results using a description involving curved trajectories, which gives a feel for the accuracy of the preceding model and allows the generalization in the following sections to the case involving unstable concave mirrors and interior foci.

## 2.3 Elliptical High Frequency Analysis

Vaynshteyn [18] discusses high frequency approximations for stable modes between concave mirrors. Here we wish to consider the generalization to unstable modes between convex mirrors. For two dimensions,

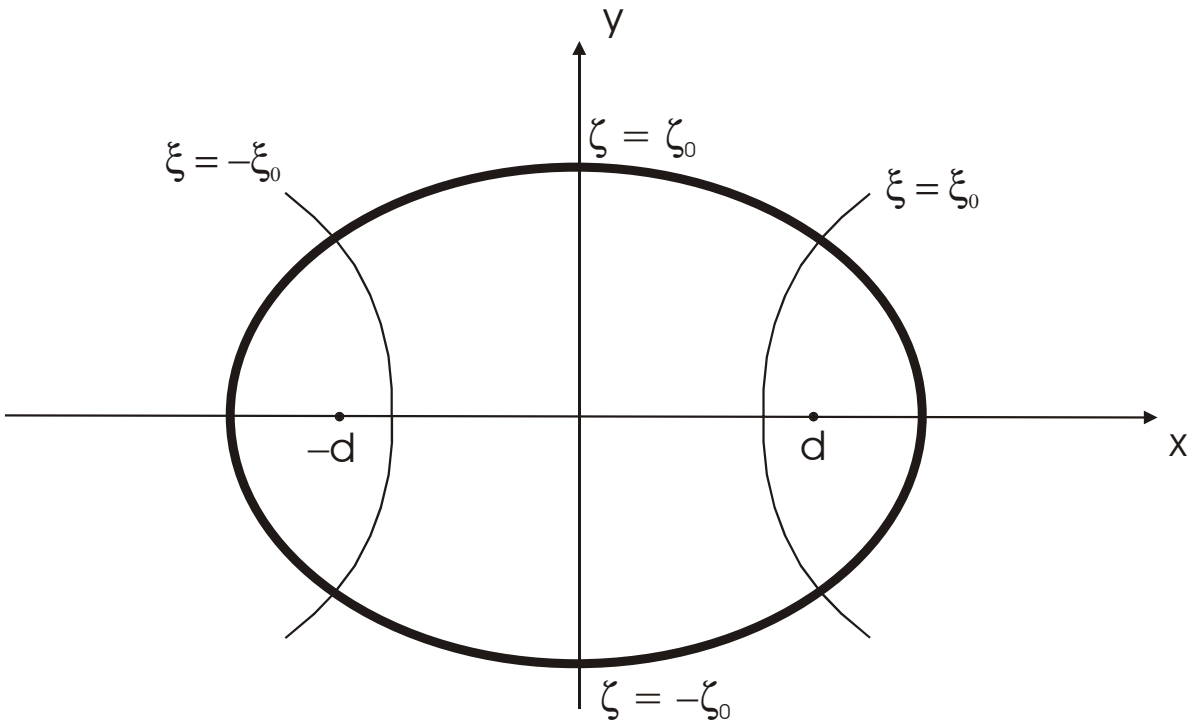


Figure 3. Ellitical geometry applied to bow tie cavity along horizontal bouncing ball orbit.

the elliptic cylinder is fit to the local boundaries at the ends of the unstable orbit $\xi = \xi_0$ as shown in Figure 3. The elliptic cylinder coordinates are related to the Cartesian system by means of

$$x = d \cosh\zeta \sin\xi$$

$$y = d \sinh\zeta \cos\xi$$

where

$$-\infty < \zeta < \infty$$

$$-\pi/2 < \xi < \pi/2$$

To match the local radius of curvature $R$ at the ends of the orbit we take the focal positions (which in this case are exterior to the region) to be

$$d = \ell\sqrt{1 + R/\ell} \tag{1}$$

### 2.3.1 high frequency approximation

The modes of the Helmholtz equation

$$\nabla^2 u + k^2 u = 0$$

are now investigated. This equation can be written in these two-dimensions as

$$\frac{\partial^2 u}{\partial \xi^2} + \frac{\partial^2 u}{\partial \zeta^2} + \gamma^2 \left( \cosh^2 \zeta - \sin^2 \xi \right) u = 0$$

where

$$\gamma = kd = k\ell\sqrt{1 + R/\ell}$$

On the mirror we want

$$u = 0\,,\ \xi = \pm\xi_0\,,\ -\zeta_0 < \zeta < \zeta_0$$

We assume $\gamma >> 1$ and that $\sinh^2 \zeta << 1$. We take the function $u$ to be even about the $x$ and $y$ axes. We seek a solution of the form [18]

$$u = W\left(\xi, \zeta\right) e^{i\gamma \sin \xi} + W\left(-\xi, \zeta\right) e^{-i\gamma \sin \xi}$$

Substituting into the Helmholtz equation gives

$$\frac{\partial^2 W}{\partial \xi^2} + \frac{\partial^2 W}{\partial \zeta^2} + 2i\gamma \cos \xi \frac{\partial W}{\partial \xi} + \left( \gamma^2 \sinh^2 \zeta - i\gamma \sin \xi \right) W = 0$$

Now ignoring the $\partial^2 W/\partial \xi^2$ term [18] (note that these approximations are shown in the Appendix to be consistent with the leading approximation) and using $\sinh^2 \zeta \approx \zeta^2$, we have

$$\frac{\partial^2 W}{\partial \zeta^2} + 2i\gamma \cos \xi \frac{\partial W}{\partial \xi} + \left( \gamma^2 \zeta^2 - i\gamma \sin \xi \right) W \approx 0$$

Next taking

$$W = \frac{1}{\sqrt{\cos \xi}} \Psi$$

$$\tau = \sqrt{2\gamma}\zeta$$

$$\sigma = \int_0^{\xi} \frac{d\xi}{\cos \xi} = \operatorname{arcsinh}\left(\tan \xi\right)$$

gives

$$\frac{\partial^2 \Psi}{\partial \tau^2} + i\frac{\partial \Psi}{\partial \sigma} + \frac{\tau^2}{4} \Psi = 0$$

Letting

$$\Psi\left(\sigma, \tau\right) = e^{-is\sigma} \psi\left(s, \tau\right)$$

gives

$$\frac{\partial^2\psi}{\partial\tau^2}+\left(\frac{\tau^2}{4}+s\right)\psi=0$$

This is a form of the equation of the parabolic cylinder functions. The solution that is outgoing in $\tau$ is [30]

$$U_+(s,\tau)=e^{-\pi(s+i/2)/4}U\left(-is,\tau e^{-i\pi/4}\right)$$

where $U(a,z)$ is the standard solution [31]. The parabolic cylinder function is related to other standard definitions by [31] $U(a,z)=D_{-a-1/2}(z)$. Following [30] the total transverse solution is taken as the incident plus reflected form

$$\psi(s,\tau)=c\,\mathrm{Re}\left[U_+(s,\tau)+e^{i\Phi_0}U_+^*(s,\tau)\right]$$

The transverse boundary condition in $\tau$ is a reflection with a random phase $\Phi_0\left(k^2\right)$ which was introduced by Antonsen to match to the chaotic region of the cavity. The boundary conditions at the mirrors imply

$$u(\pm\xi_0,\zeta)=W(\xi_0,\zeta)\,e^{i\gamma\sin\xi_0}+W(-\xi_0,\zeta)\,e^{-i\gamma\sin\xi_0}=0\,,\ -\zeta_0<\zeta<\zeta_0$$

or

$$\Psi(\sigma_0,\tau)\,e^{i\gamma\sin\xi_0}+\Psi(-\sigma_0,\tau)\,e^{-i\gamma\sin\xi_0}=\psi(s,\tau)\cos(\gamma\sin\xi_0-s\sigma_0)=0\,,\ -\zeta_0<\tau/\sqrt{2\gamma}<\zeta_0$$

with

$$\sigma_0=\mathrm{arcsinh}(\tan\xi_0)=\ln[\tan\xi_0+\sec\xi_0]$$

Thus we take

$$\gamma\sin\xi_0-s\sigma_0=k\ell-s\sigma_0=(p-1/2)\,\pi=k_p\ell\,,\ p=1,2,3,...$$

Note that

$$\sigma_0=\frac{1}{2}\ln\left(\frac{d+\ell}{d-\ell}\right)=\mathrm{Arcsinh}\left(\sqrt{\ell/R}\right)$$

This can also be written in terms of the stability exponents as

$$\sigma_0=\frac{1}{2}\ln\left[(\lambda_+-1)/(1-\lambda_-)\right]=\frac{1}{2}\ln(\lambda_+)=\frac{1}{4}\ln(\Lambda_+)$$

where (see the Appendix) $\lambda_\pm^2=\Lambda_\pm$ and $\pm(\lambda_\pm-1)/2=(d\pm\ell)/R$.

The separation constant $s$ is then

$$s_p=(k-k_p)\,\ell/\sigma_0=\frac{(k-k_p)\,L/2}{\mathrm{Arcsinh}\left[\sqrt{L/(2R)}\right]}=2(k-k_p)\,L/\ln(\Lambda_+)$$

Now if $\sqrt{L/(2R)}<<1$, and assuming $k>>|k-k_p|$ this becomes $s_p\sim(k-k_p)\sqrt{LR/2}\approx\left(k^2-k_p^2\right)\sqrt{LR/(8k^2)}=\lambda_1$ in agreement with the previous Fourier analysis [30].

In summary the solution is

$$u_p = \psi\left(s_p, \zeta\sqrt{2kd}\right)\cos\left[kd\sin\xi - s_p\mathrm{Arcsinh}\left(\tan\xi\right)\right]/\sqrt{\cos\xi}$$

where

$$\psi\left(s_p,\tau\right) = c\,\mathrm{Re}\left[U_+\left(s_p,\tau\right) + e^{i\Phi_0}U_+^*\left(s_p,\tau\right)\right]$$

and the phase phase $\Phi_0\left(k^2\right)$ describes the phase relation between a wave leaving the vicinity of the unstable periodic orbit and one returning [30] with the variation of the $p$th component along the orbit. Reducing the form of this solution to the horizontal orbit $\tau = 0 = \zeta$ we have $x = d\sin\xi$ and

$$u_p = \psi\left(s_p,0\right)\cos\left[kx - \frac{1}{2}s_p\ln\left(\frac{d+x}{d-x}\right)\right]/\sqrt{1-x^2/d^2}$$

or

$$u_p = \psi\left(s_p,0\right)\cos\left[k_p x + p_0\left(x\right)\right]/\sqrt{1-x^2/d^2}$$

where

$$p_0\left(x\right) = \frac{1}{2}s_p\left\{\ln\left(\frac{d+\ell}{d-\ell}\right)\left(x/\ell\right) - \ln\left(\frac{d+x}{d-x}\right)\right\}$$

## 2.4 Spatial Variations of Eigenfunctions

It is instructive to compare the variation of the eigenfunctions on the axes with the sinusoidal distributions and the preceding scar constructions when $k \to k_p$ and $s_p \to 0$. The bow tie has $\ell = 1$ m in both the $x$ and $y$ directions and has $R = 10$ m in the $y$ direction and $R = 1.5$ m in the $x$ direction. Figure 4 shows a scar along the $y$ axis for $k\ell \approx 67.625$ and $k_p\ell \approx 67.544$ for $p = 22$ and $s_p \approx 0.260$.

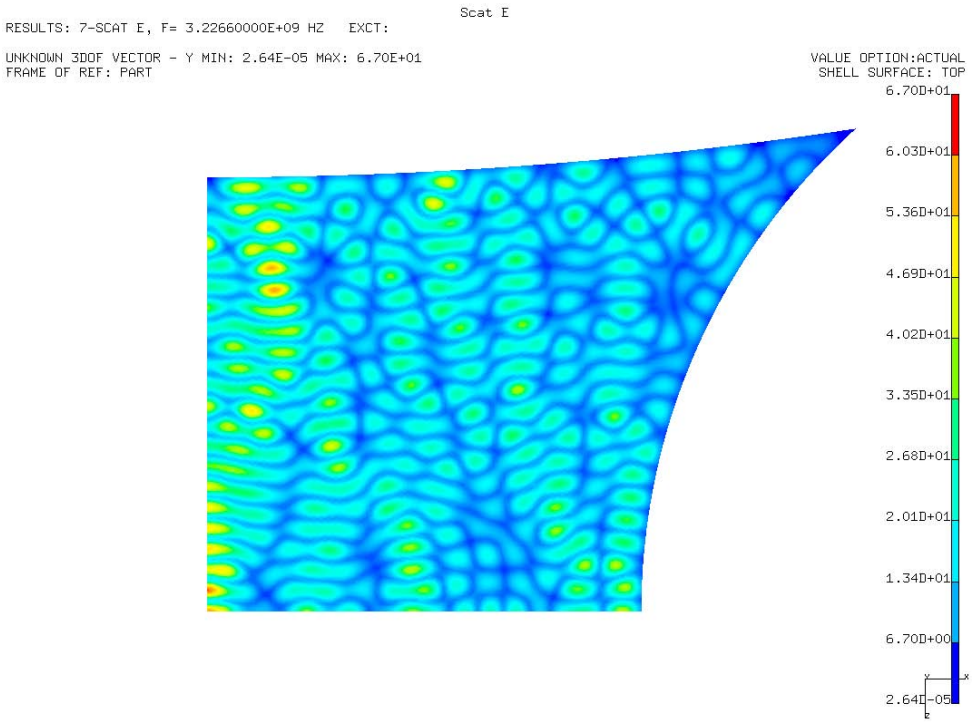


Figure 4. Electric field intensity plot for quarter bow tie cavity at a frequency of 3.2266 GHz, which is near a vertical scar frequency.

The vertical distribution of the electric field is compared to the cosine $\cos(k_p y)$ and to $\cos[k_p y + p_0(y)] / \left(1 - y^2/d^2\right)^{-1/4}$ in Figure 5.

Figure 6 shows a scar along the $x$ axis for $k\ell \approx 61.138$ and $k_p \ell \approx 61.261$ for $p = 20$ and $s_p \approx -0.165$.

The horizontal distribution of the electric field is compared to the cosine $\cos(k_p x)$ and to $\cos[k_p x + p_0(x)] / \left(1 - x^2/d^2\right)^{-1/4}$ in Figure 7.

It is clear from the above comparisons that more than one $p$ component is present in the spatial distributions even when $k$ is very near to a particular value of $k_p$. We expect this since at high frequencies there are high angle rays crossing the orbits from the outer chaotic regions of the cavity.

## 2.5 Normalization of Eigenfunctions

The method used for normalization of the eigenfunction components by Antonsen [30] is now put into the framework of the electromagnetic energy theorem [33]

$$\nabla \cdot \left( \frac{\partial \underline{E}}{\partial \omega} \times \underline{H}^* + \underline{E}^* \times \frac{\partial \underline{H}}{\partial \omega} \right) = i \left[ \frac{\partial(\omega\mu)}{\partial \omega} \underline{H} \cdot \underline{H}^* + \frac{\partial(\omega\varepsilon)}{\partial \omega} \underline{E} \cdot \underline{E}^* \right] - \frac{\partial \underline{E}}{\partial \omega} \cdot \underline{J}^* - \underline{E}^* \cdot \frac{\partial \underline{J}}{\partial \omega}$$

Integrating over the cavity volume and using the divergence theorem

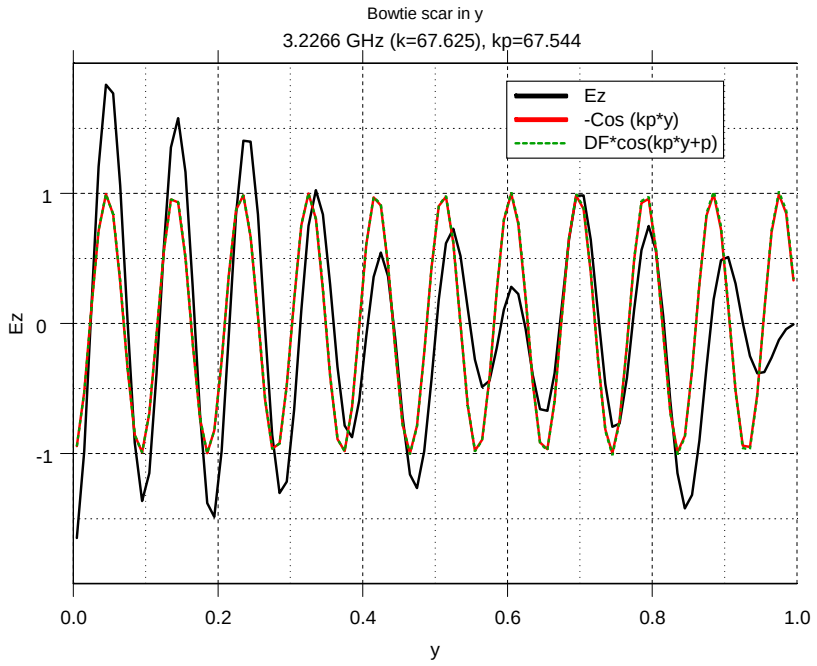


Figure 5. Spatial distribution of electric field along vertical scarred orbit compared to the simple sinusoid and scar construction.

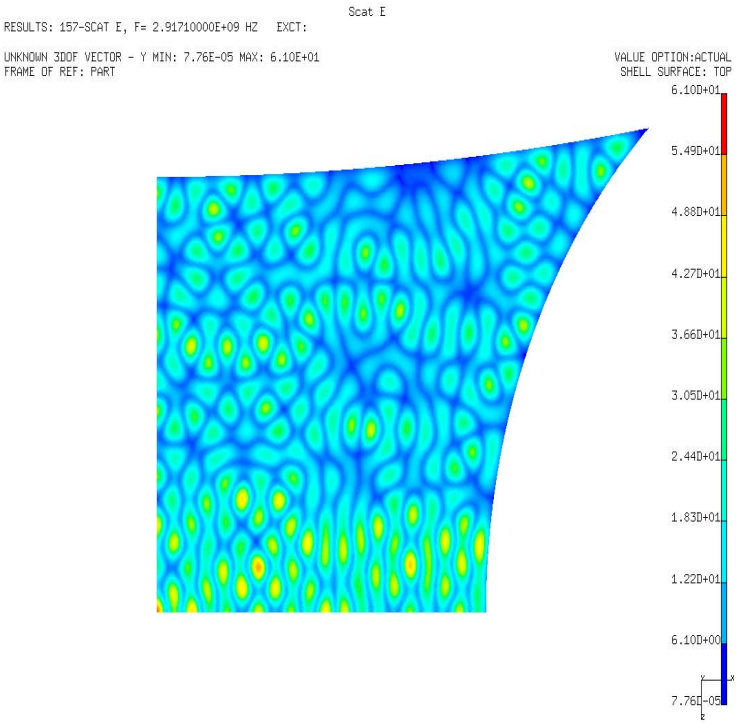


Figure 6. Electric field intensity plot for quarter bow tie cavity at a frequency of 2.9171 GHz, which is near a horizontal scar frequency.

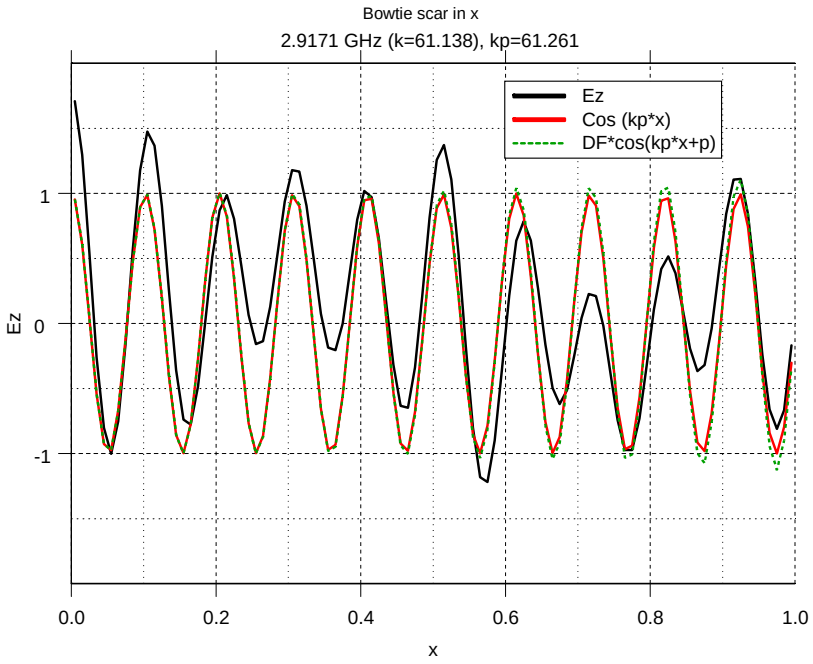


Figure 7. Spatial distribution of electric field along horizontal scarred orbit compared to the simple sinusoid and scar construction.

$$\oint_S \left( \frac{\partial \underline{E}}{\partial \omega} \times \underline{H}^* + \underline{E}^* \times \frac{\partial \underline{H}}{\partial \omega} \right) \cdot \underline{n} dS = i \int_V \left( \mu_0 \underline{H} \cdot \underline{H}^* + \varepsilon_0 \underline{E} \cdot \underline{E}^* \right) dV - \int_V \left( \frac{\partial \underline{E}}{\partial \omega} \cdot \underline{J}^* + \underline{E}^* \cdot \frac{\partial \underline{J}}{\partial \omega} \right) dV$$

where the unit vector $\underline{n}$ in the divergence theorem points out of the cavity region. Using $\underline{n} \times \underline{E} = 0$ on the walls we find

$$\underline{n} \cdot \left( \underline{E}^* \times \frac{\partial \underline{H}}{\partial \omega} \right) = \frac{\partial \underline{H}}{\partial \omega} \cdot (\underline{n} \times \underline{E}) = 0$$

$$\underline{n} \cdot \left( \frac{\partial \underline{E}}{\partial \omega} \times \underline{H}^* \right) = \underline{H}^* \cdot \left( \underline{n} \times \frac{\partial \underline{E}}{\partial \omega} \right) = \underline{H}^* \cdot \frac{\partial}{\partial \omega} (\underline{n} \times \underline{E}) = 0$$

Then

$$i \int_V \left( \mu_0 \underline{H} \cdot \underline{H}^* + \varepsilon_0 \underline{E} \cdot \underline{E}^* \right) dV = \int_V \left( \frac{\partial \underline{E}}{\partial \omega} \cdot \underline{J}^* + \underline{E}^* \cdot \frac{\partial \underline{J}}{\partial \omega} \right) dV$$

Noting that

$$\mu_0 \underline{H} \cdot \underline{H}^* = \frac{\varepsilon_0}{k^2} (\nabla \times \underline{E}) \cdot (\nabla \times \underline{E}^*)$$

and here that

$$\underline{E} = u \underline{e}_z$$

$$\underline{J} = J_z \underline{e}_z$$

so that

$$\nabla \times \underline{E} = \nabla \times (u \underline{e}_z) = \nabla u \times \underline{e}_z$$

and

$$\varepsilon \underline{E} \cdot \underline{E}^* = \varepsilon |u|^2$$

$$\mu \underline{H} \cdot \underline{H}^* = \frac{\varepsilon_0}{k^2} |\nabla u|^2$$

$$\underline{e}_z \times (\nabla u \times \underline{e}_z) = \nabla u$$

so that

$$i \frac{\varepsilon_0}{k^2} \int_V \left( |\nabla u|^2 + k^2 |u|^2 \right) dV = \int_V \left( \frac{\partial u}{\partial \omega} J_z^* + u^* \frac{\partial J_z}{\partial \omega} \right) dV$$

Now using

$$|\nabla u|^2 = \nabla u \cdot \nabla u^* = \nabla \cdot (u^* \nabla u) - u^* \nabla^2 u = \nabla \cdot (u^* \nabla u) + k^2 |u|^2$$

gives

$$i2\varepsilon_0 \int_V |u|^2 \, dV = \int_V \left( \frac{\partial u}{\partial \omega} J_z^* + u^* \frac{\partial J_z}{\partial \omega} \right) dV$$

In two dimensions

$$i2\varepsilon_0 \int_A |u|^2 \, dS = \int_A \left( \frac{\partial u}{\partial \omega} J_z^* + u^* \frac{\partial J_z}{\partial \omega} \right) dS$$

We now select the current to produce the $p$th component of the normal derivative (magnetic field) on $y = 0$ when $k$ is not an eigenvalue of the cavity [30]. From Maxwell's equation

$$\nabla \times \underline{E} = \nabla u \times \underline{e}_z = i\omega\mu_0 \underline{H}$$

we have

$$\underline{H} = \frac{i}{\omega\mu_0} \underline{e}_z \times \nabla u$$

Now for convenience we take $\underline{n}$ to point from the horizontal periodic orbit into the upper cavity region or $\underline{e}_y$

$$\underline{n} \times \underline{H} = \frac{i}{\omega\mu_0} \underline{n} \times (\underline{e}_z \times \nabla u)$$

$$\underline{e}_z \cdot (\underline{n} \times \underline{H}) = \frac{i}{\omega\mu_0} \underline{e}_z \cdot [\underline{n} \times (\underline{e}_z \times \nabla u)] = -\frac{i}{\omega\mu_0} \underline{n} \cdot [\underline{e}_z \times (\underline{e}_z \times \nabla u)] = \frac{i}{\omega\mu_0} \underline{n} \cdot \nabla u = \frac{i}{\omega\mu_0} \frac{\partial u}{\partial n}$$

and thus we take

$$J_z = \frac{i2}{\omega\mu_0} \frac{\partial u_p}{\partial n} \delta(n) \ , \ y = 0$$

where $u_p$ denotes the $p$th scarred eigenfunction component

$$i2\varepsilon_0 \int_A |u|^2 \, dS = \frac{i2}{\mu_0} \int_A \left[ -\frac{\partial u}{\partial \omega} \frac{1}{\omega} \frac{\partial u_p^*}{\partial n} + u^* \frac{\partial}{\partial \omega} \left( \frac{1}{\omega} \frac{\partial u_p}{\partial n} \right) \right] \delta(n) \, dS$$

$$= \frac{i2}{\mu_0} \int_C \left[ -\frac{\partial u}{\partial \omega} \frac{1}{\omega} \frac{\partial u_p^*}{\partial n} + u^* \frac{\partial}{\partial \omega} \left( \frac{1}{\omega} \frac{\partial u_p}{\partial n} \right) \right] d\ell$$

where $C$ is a path along the scarred orbit. In our case the function is taken to be real

$$\mu_0\varepsilon_0 \int_A |u|^2 \, dS = \int_C \left[ -\frac{\partial u}{\partial \omega} \frac{1}{\omega} \frac{\partial u_p}{\partial n} + u \frac{\partial}{\partial \omega} \left( \frac{1}{\omega} \frac{\partial u_p}{\partial n} \right) \right] d\ell$$

If we assume that for high frequencies the components of the eigenfunction are approximately orthogonal along the orbit (as shown in the Appendix)

$$\mu_0\varepsilon_0 \int_A |u|^2 \, dS \sim \int_C \left[ -\frac{\partial u_p}{\partial \omega} \frac{1}{\omega} \frac{\partial u_p}{\partial n} + u_p \frac{1}{\omega} \frac{\partial}{\partial \omega} \left( \frac{\partial u_p}{\partial n} \right) - \frac{1}{\omega^2} u_p \frac{\partial u_p}{\partial n} \right] d\ell$$

Now

$$u_p = \psi\left(s_p, \zeta\sqrt{2kd}\right)\cos\left[kd\sin\xi - s_p\text{Arcsinh}\left(\tan\xi\right)\right]/\sqrt{\cos\xi}$$

$$\frac{\partial u_p}{\partial n} = \frac{\sqrt{2kd}}{h_\zeta}\psi'\left(s_p, \zeta\sqrt{2kd}\right)\cos\left[kd\sin\xi - s_p\text{Arcsinh}\left(\tan\xi\right)\right]/\sqrt{\cos\xi}$$

$$u_p\left(\xi, 0\right) = \psi\left(s_p, 0\right)\cos\left[kd\sin\xi - s_p\text{Arcsinh}\left(\tan\xi\right)\right]/\sqrt{\cos\xi}$$

$$\frac{\partial u_p}{\partial n}\left(\xi, 0\right) = \frac{\sqrt{2kd}}{d\cos\xi}\psi'\left(s_p, 0\right)\cos\left[kd\sin\xi - s_p\text{Arcsinh}\left(\tan\xi\right)\right]/\sqrt{\cos\xi}$$

where

$$\psi\left(s_p, \tau\right) = c\,\text{Re}\left[U_+\left(s_p, \tau\right) + e^{i\Phi_0}U_+^*\left(s_p, \tau\right)\right]$$

If we let $k$ approach an eigenvalue then the normal derivative of $u_p$ vanishes on the scar $\psi'\left(s_p, 0\right) = 0$ (because we have selected the even modes across the scarred orbit). Therefore it is only the operation of taking the $\omega$ derivative of these terms which prevents their vanishing

$$\mu_0\varepsilon_0\int_A |u|^2\, dS = \int_C u_p\frac{1}{\omega}\frac{\partial}{\partial\omega}\left(\frac{\partial u_p}{\partial n}\right)d\ell$$

Thus

$$\mu_0\varepsilon_0\int_A |u|^2\, dS = \int_{-\xi_0}^{\xi_0} u_p\frac{1}{\omega}\frac{\partial}{\partial\omega}\left(\frac{\partial u_p}{\partial\zeta}\right)\frac{h_\xi}{h_\zeta}d\xi$$

$$\frac{\partial u_p}{\partial\zeta} = \sqrt{2\gamma}\psi'\left(s_p, 0\right)\cos\left[kd\sin\xi - s_p\text{Arcsinh}\left(\tan\xi\right)\right]/\sqrt{\cos\xi}$$

where the metric coefficients are

$$h_\zeta = h_\xi = d\sqrt{\sinh^2\zeta + \cos^2\xi}$$

It is only the $\omega$ derivative operation on $\psi'\left(s_p, 0\right)$ which contributes so that

$$\mu_0\varepsilon_0\int_A |u|^2\, dS$$

$$= \sqrt{2\gamma}\int_{-\xi_0}^{\xi_0}\psi\left(s_p, 0\right)\frac{1}{\omega}\,\frac{\partial}{\partial\omega}\psi'\left(s_p, \tau\right)\Big|_{\tau=0}\cos^2\left[kd\sin\xi - s_p\text{Arcsinh}\left(\tan\xi\right)\right]\frac{d\xi}{\cos\xi}$$

Now taking the normalization to be

$$\int_A |u|^2\, dS = 1$$

and transforming to

$$\sigma = \text{Arcsinh}\left(\tan\xi\right)$$

$$d\sigma = \sec\xi d\xi$$

$$\sigma_0 = \frac{1}{2}\ln\left(\frac{d+\ell}{d-\ell}\right) = \text{Arcsinh}\left(\sqrt{\ell/R}\right)$$

$$\sin\xi = \tanh\sigma$$

$$\mu_0\varepsilon_0 = \sqrt{2\gamma}\psi\left(s_p,0\right)\frac{1}{\omega}\left.\frac{\partial}{\partial\omega}\psi'\left(s_p,\tau\right)\right|_{\tau=0} 2\int_0^{\sigma_0}\cos^2\left(kd\tanh\sigma - s_p\sigma\right)d\sigma$$

The Appendix has some comments on the simultaneous choice of normalization and current source strength relative to a source free form of the energy theorem. If we average over the rapidly varying cosine we find

$$\mu_0\varepsilon_0 \sim \sqrt{2\gamma}\psi\left(s_p,0\right)\frac{1}{\omega}\left.\frac{\partial}{\partial\omega}\psi'\left(s_p,\tau\right)\right|_{\tau=0}\sigma_0$$

We approximate this derivative as Antonsen suggested [30] with the outer region phase derivative

$$\left.\frac{\partial}{\partial\omega}\psi'\left(s_p,\tau\right)\right|_{\tau=0} \sim c\,\text{Re}\left[i\frac{\partial\Phi_0}{\partial\omega}e^{i\Phi_0}U_+^{*\prime}\left(s_p,0\right)\right]$$

Since we are choosing only the even eigenfunctions we must have the normal derivative vanish on the scar orbit. This implies the resonance condition

$$2\,\text{Re}\left[U_+'\left(s_p,0\right) + e^{i\Phi_0}U_+^{*\prime}\left(s_p,0\right)\right] = 0$$

or

$$U_+'\left(s_p,0\right) + e^{i\Phi_0}U_+^{*\prime}\left(s_p,0\right) + U_+^{*\prime}\left(s_p,0\right) + e^{-i\Phi_0}U_+'\left(s_p,0\right) = 0$$

$$\left(1+e^{i\Phi_0}\right)U_+^{*\prime}\left(s_p,0\right) + \left(1+e^{-i\Phi_0}\right)U_+'\left(s_p,0\right) = 0$$

$$-\frac{1+e^{i\Phi_0}}{1+e^{-i\Phi_0}} = -e^{i\Phi_0} = \frac{U_+'\left(s_p,0\right)}{U_+^{*\prime}\left(s_p,0\right)}$$

or

$$-\frac{U_+'\left(s_p,0\right)}{U_+^{*\prime}\left(s_p,0\right)} = e^{i\Phi_0}$$

Using this with the Wronskian [30]

$$U_+'U_+^* - U_+^{*\prime}U_+ = i$$

gives

$$\mathrm{Re}\left[U_+\left(s_p,0\right)+e^{i\Phi_0}U_+^*\left(s_p,0\right)\right]=\frac{\mathrm{Im}\left[U_+'\left(s_p,0\right)\right]}{\left|U_+'\left(s_p,0\right)\right|^2}$$

Therefore

$$\mu_0\varepsilon_0\sim c\,\mathrm{Re}\left[U_+\left(s_p,0\right)+e^{i\Phi_0}U_+^*\left(s_p,0\right)\right]\frac{1}{\omega}c\,\mathrm{Re}\left[i\frac{\partial\Phi_0}{\partial\omega}e^{i\Phi_0}U_+^{*\prime}\left(s_p,0\right)\right]\sqrt{2\gamma}\sigma_0$$

$$=-c\frac{\mathrm{Im}\left[U_+'\left(s_p,0\right)\right]}{\left|U_+'\left(s_p,0\right)\right|^2}\frac{1}{\omega}c\,\mathrm{Re}\left[i\frac{\partial\Phi_0}{\partial\omega}U_+'\left(s_p,0\right)\right]\sqrt{2\gamma}\sigma_0$$

or

$$\omega\mu_0\varepsilon_0=c^2k\frac{\partial k}{\partial\omega}\left(\frac{d\Phi_0}{dk^2}\right)\frac{\mathrm{Im}^2\left[U_+'\left(s_p,0\right)\right]}{\left|U_+'\left(s_p,0\right)\right|^2}\sqrt{2\gamma}\ln\left(\frac{d+\ell}{d-\ell}\right)$$

and thus

$$1=c^2\left(\frac{d\Phi_0}{dk^2}\right)\frac{\mathrm{Im}^2\left[U_+'\left(s_p,0\right)\right]}{\left|U_+'\left(s_p,0\right)\right|^2}\sqrt{2\gamma}\ln\left(\frac{d+\ell}{d-\ell}\right)$$

The phase $\Phi_0$ indicates the reflection phase of the $p$th component. Following Antonsen [30] the average derivative is set by taking $\Delta\Phi_0=2\pi$ and the spacing between eigenvalues to be given by the Weyl asymptotic result $\Delta k\sim\pi^2/\left(k^2V\right)$, or in two-dimensions $\Delta k^2=2k\Delta k\sim 4\pi/A$ [5]. In this case the even-even eigenvalues are spaced as if the cavity had one quarter the total area [30].

$$\Delta k^2\sim 16\pi/A$$

Thus we take [30]

$$\left(\frac{d\Phi_0}{dk^2}\right)^{-1}=\frac{8}{A}v^2$$

where $v$ is the Gaussian random variable with unit variance discussed previously. Now introducing this outer phase derivative gives the normalization constant

$$c^2=v^2 8/\left[A\sqrt{2\gamma}\frac{\mathrm{Im}^2\left[U_+'\left(s_p,0\right)\right]}{\left|U_+'\left(s_p,0\right)\right|^2}\ln\left(\frac{d+\ell}{d-\ell}\right)\right]$$

Thus we have the solution

$$u_p\left(x,0\right)=\frac{2v\sqrt{2}}{\left|U_+'\left(s_p,0\right)\right|\sqrt{A\sqrt{2\gamma}\ln\left(\frac{d+\ell}{d-\ell}\right)}}\cos\left[kx-\frac{1}{2}s_p\ln\left(\frac{d+x}{d-x}\right)\right]\left(1-x^2/d^2\right)^{-1/4}$$

## 2.6 Projections Along Orbit

We now consider projections along the scarred orbit and compare scar projections with projections of the random plane wave form of the field.

### 2.6.1 fourier projection

The Fourier expansion of the $p$th eigenfunction component is

$$u_p(x,0) = \frac{2}{L}\sum_{p'} V_{p'p}\cos(k_{p'}x)$$

Now taking the projection

$$V_{p'p} = 2\int_0^\ell \cos(k_{p'}x)\,u_p(x,0)\,dx = \frac{2v\sqrt{2}}{\left|U'_+(s_p,0)\right|\sqrt{A\sqrt{2\gamma}\ln\left(\frac{d+\ell}{d-\ell}\right)}}$$

$$\int_0^\ell \left(1-x^2/d^2\right)^{-1/4}\left\{\cos\left(\left(k_p+k_{p'}\right)x+p_0(x)\right)+\cos\left(\left(k_p-k_{p'}\right)x+p_0(x)\right)\right\}dx$$

where

$$p_0(x) = \frac{1}{2}s_p\left\{\ln\left(\frac{d+\ell}{d-\ell}\right)(x/\ell)-\ln\left(\frac{d+x}{d-x}\right)\right\}$$

Now dropping the first term (which will depend on $O\left(1/\left(k_p+k_{p'}\right)^2\right)$ and will consequently be small for high frequencies)

$$V_{p'p} \sim \frac{2v\sqrt{2}}{\left|U'_+(s_p,0)\right|\sqrt{A\sqrt{2\gamma}\ln\left(\frac{d+\ell}{d-\ell}\right)}}\int_0^\ell \left(1-x^2/d^2\right)^{-1/4}\cos\left(\left(k_p-k_{p'}\right)x+p_0(x)\right)dx$$

$$\sim \frac{2v\sqrt{2}\ell}{\left|U'_+(s_p,0)\right|\sqrt{A\sqrt{2\gamma}\ln\left(\frac{d+\ell}{d-\ell}\right)}}$$

$$\int_0^1 \left(1-x^2\ell^2/d^2\right)^{-1/4}\cos\left[\left(k_p-k_{p'}\right)\ell x+\left(k-k_p\right)\ell\left\{x-\ln\left(\frac{d+x\ell}{d-x\ell}\right)/\ln\left(\frac{d+\ell}{d-\ell}\right)\right\}\right]dx$$

Let us expand the term in braces for $d >> \ell$

$$\left\{x-\ln\left(\frac{1+x\ell/d}{1-x\ell/d}\right)/\ln\left(\frac{1+\ell/d}{1-\ell/d}\right)\right\} \sim x\left(1-x^2\right)\left(\ell/d\right)^2/3+\cdots$$

and

$$V_{p'p} \sim \frac{2v\sqrt{2}\ell}{\left|U'_+\left(s_p,0\right)\right|\sqrt{A\sqrt{2\gamma}\ln\left(\frac{d+\ell}{d-\ell}\right)}}$$

$$\int_0^1 \left(1-x^2\ell^2/d^2\right)^{-1/4}\cos\left[\left(k_p-k_{p'}\right)\ell x+\left(k-k_p\right)\ell\left\{x\left(1-x^2\right)\left(\ell/d\right)^2/3\right\}\right]dx$$

If we drop the terms for $(\ell/d)^2 \to 0$ we see that

$$V_{p'p} \sim \frac{2v\sqrt{2}\ell}{\left|U'_+\left(s_p,0\right)\right|\sqrt{A\sqrt{2\gamma}\ln\left(\frac{d+\ell}{d-\ell}\right)}}\int_0^1 \cos\left[\left(p-p'\right)\pi x\right]dx$$

$$\sim \frac{\delta_{p'p}2v\sqrt{2}\ell}{\left|U'_+\left(s_p,0\right)\right|\sqrt{A\sqrt{2\gamma}\ln\left(\frac{d+\ell}{d-\ell}\right)}}$$

### 2.6.2 scar projection

Instead of representing the eigenfunction in terms of Fourier components suppose we define the projection operator as

$$V_p = 2\int_0^\ell \left(1-x^2/d^2\right)^{-1/4}\cos\left[k_p x+p_0\left(x\right)\right]u\left(x,0\right)dx$$

As shown in the Appendix, the $p$th components are asymptotically orthogonal, so that if the eigenfunction is made up of a sum

$$u\left(x,0\right) \sim \sum_p u_p\left(x,0\right)$$

this projection is

$$V_p \sim 2\frac{2v\sqrt{2}}{\left|U'_+\left(s_p,0\right)\right|\sqrt{A\sqrt{2\gamma}\ln\left(\frac{d+\ell}{d-\ell}\right)}}\int_0^\ell \left(1-x^2/d^2\right)^{-1/2}\cos^2\left[k_p x+p_0\left(x\right)\right]dx$$

where again

$$p_0\left(x\right) = \frac{1}{2}s_p\left\{\ln\left(\frac{d+\ell}{d-\ell}\right)\left(x/\ell\right)-\ln\left(\frac{d+x}{d-x}\right)\right\}$$

Now averaging over the rapidly varying $k_p x$ we find

$$V_p \sim \frac{2vd\sqrt{2}}{\left|U'_+\left(s_p,0\right)\right|\sqrt{A\sqrt{2\gamma}\ln\left(\frac{d+\ell}{d-\ell}\right)}}\int_0^{\ell/d}\left(1-x^2\right)^{-1/2}dx$$

$$\sim \frac{2vd\sqrt{2}}{\left|U'_+\left(s_p,0\right)\right|\sqrt{A\sqrt{2\gamma}\ln\left(\frac{d+\ell}{d-\ell}\right)}}\text{Arcsin}\left(\ell/d\right)$$

Taking the average of the square yields

$$\left\langle \sqrt{kL}V_p^2 \right\rangle \sim L^2 G_1\left(s_p\right)/A$$

where

$$G_1\left(s_p\right) = \frac{4\sqrt{\ell/d}\left(d/\ell\right)^2 \text{Arcsin}^2\left(\ell/d\right)}{\left|U'_+\left(s_p,0\right)\right|^2 \ln\left(\frac{d+\ell}{d-\ell}\right)}$$

and

$$\frac{2^{1/2}\pi}{\left|U'_+\left(s_p,0\right)\right|^2} = \exp\left[\pi s_p/2\right]\left|\Gamma\left(1/4 - is_p/2\right)\right|^2$$

$$\frac{1}{\left|U'_+\left(s_p,0\right)\right|^2} \sim \frac{2}{\sqrt{s_p}}\ ,\ s_p \to \infty$$

and again $s_p = \left(k-k_p\right)\left(L/2\right)/\text{Arcsinh}\left[\sqrt{L/\left(2R\right)}\right]$ and $d = \ell\sqrt{1+R/\ell}$. Note that in terms of the stability exponent

$$G_1\left(s_p\right) = \frac{\left(\sqrt{\Lambda_+ - 1}\right)\left(d/\ell\right)^2 \text{Arcsin}^2\left(\ell/d\right)}{\left(\sqrt{\Lambda_+}+1\right)\left|U'_+\left(s_p,0\right)\right|^2 \ln\left(\Lambda_+\right)}$$

$$\ell/d = \frac{\lambda_+ - 1}{\lambda_+ + 1} = \frac{\sqrt{\Lambda_+}-1}{\sqrt{\Lambda_+}+1} = \frac{\Lambda_+ - 1}{\left(\sqrt{\Lambda_+}+1\right)^2}$$

$$s_p = 2\left(k-k_p\right)L/\ln\left(\Lambda_+\right)$$

Now if we examine the limit $R/\ell \to \infty$

$$\left\langle \sqrt{kL}V_p^2 \right\rangle \to \frac{L^2\left(2R/L\right)^{1/4}}{\left|U'_+\left\{\left(k^2-k_p^2\right)\sqrt{LR/\left(8k^2\right)},0\right\}\right|^2 A}$$

which is the same as Antonsen's result [30].

### 2.6.3 elliptic system projection

It is instructive to carry out the projection in elliptic cylinder coordinates. Transforming the projection operators gives

$$V_p = 2\int_0^{\xi_0} \cos\left[kd\sin\xi - s_p \text{Arcsinh}\left(\tan\xi\right)\right] u_p h_\xi \frac{d\xi}{\sqrt{\cos\xi}}$$

$$h_\xi = d\sqrt{\sinh^2\zeta + \cos^2\xi} \to d\cos\xi$$

with $p$th eigenfunction

$$u_p = \psi\left(s_p, \zeta\sqrt{2kd}\right)\cos\left[kd\sin\xi - s_p\text{Arcsinh}\left(\tan\xi\right)\right]/\sqrt{\cos\xi}$$

or

$$u_p = \frac{v2\sqrt{2}}{\left|U'_+\left(s_p,0\right)\right|\sqrt{A\sqrt{2\gamma}\ln\left(\frac{d+\ell}{d-\ell}\right)}}\cos\left[kd\sin\xi - s_p\text{Arcsinh}\left(\tan\xi\right)\right]/\sqrt{\cos\xi}$$

Thus

$$V_p = \frac{v2d\sqrt{2}}{\left|U'_+\left(s_p,0\right)\right|\sqrt{A\sqrt{2\gamma}\ln\left(\frac{d+\ell}{d-\ell}\right)}}2\int_0^{\xi_0}\cos^2\left[kd\sin\xi - s_p\text{Arcsinh}\left(\tan\xi\right)\right]d\xi$$

Now for $kd$ large we average over the cosine function and find

$$V_p = \frac{v2d\sqrt{2}\xi_0}{\left|U'_+\left(s_p,0\right)\right|\sqrt{A\sqrt{2\gamma}\ln\left(\frac{d+\ell}{d-\ell}\right)}}$$

$$\xi_0 = \text{Arcsin}\left(\ell/d\right)$$

which is the same answer as obtained previously.

### 2.6.4 random plane wave projection

Let us first consider the random plane wave projection with the simplifying assumption of $d$ large

$$V_{pr} = \int_{-\ell}^{\ell}\cos\left(k_p x\right)u_r\left(x,0\right)dx$$

with [30]

$$u_r = \lim_{N\to\infty}\sqrt{2/\left(AN\right)}\,\text{Re}\left[\sum_{j=1}^{N}a_j e^{i\alpha_j + i\underline{k}\cdot\underline{r}}\right]$$

where $a_j$ are real random numbers with $\left\langle a_j^2\right\rangle = 1$, $|\underline{k}| = k$ are random vectors uniformly distributed in angle, and the random phases $\alpha_j$ are uniformly distributed on a $2\pi$ interval. Thus

$$V_{pr} = \int_{-\ell}^{\ell}\cos\left(k_p x\right)\lim_{N\to\infty}\sqrt{2/\left(AN\right)}\,\text{Re}\left[\sum_{j=1}^{N}a_j e^{i\alpha_j + ikx\cos\theta}\right]dx$$

$$= \int_{-\ell}^{\ell} \cos(k_p x) \lim_{N\to\infty} \sqrt{2/(AN)} \left[ \sum_{j=1}^{N} a_j \cos(\alpha_j + kx\cos\theta) \right] dx$$

$$V_{pr}^2 = \lim_{N\to\infty} \sqrt{2/(AN)} \sum_{j=1}^{N}$$

$$\lim_{N'\to\infty} \sqrt{2/(AN')} \sum_{j'=1}^{N'} a_j a_{j'} \int_{-\ell}^{\ell}\int_{-\ell}^{\ell} \cos(k_p x)\cos(k_p x')\cos(\alpha_j + kx\cos\theta)\cos(\alpha_{j'} + kx'\cos\theta)\, dx dx'$$

If we average over the amplitudes $a_j$ and regard different $j$ values as independent the cross terms vanish

$$\left\langle V_{pr}^2 \right\rangle_{a_j,\alpha_j} = \lim_{N\to\infty} \frac{2}{AN} \sum_{j=1}^{N} \int_{-\ell}^{\ell}\int_{-\ell}^{\ell} \cos(k_p x)\cos(k_p x') \left\langle \cos(\alpha_j + kx\cos\theta)\cos(\alpha_j + kx'\cos\theta) \right\rangle_{\alpha_j} dx dx'$$

$$\left\langle \cos(\alpha_j + kx\cos\theta)\cos(\alpha_j + kx'\cos\theta) \right\rangle_{\alpha_j} = \frac{1}{2\pi}\frac{1}{2}\int_0^{2\pi} \left[ \cos(k(x-x')\cos\theta) + \cos(2\alpha_j + k(x+x')\cos\theta) \right] d\alpha_j$$

$$= \frac{1}{2}\cos(k(x-x')\cos\theta) = \frac{1}{2}\cos(kx\cos\theta)\cos(kx'\cos\theta) + \frac{1}{2}\sin(kx\cos\theta)\sin(kx'\cos\theta)$$

$$\left\langle V_{pr}^2 \right\rangle_{a_j,\alpha_j} = \lim_{N\to\infty} \frac{1}{AN} \sum_{j=1}^{N} \int_{-\ell}^{\ell} \cos(k_p x)\cos(kx\cos\theta)\, dx \int_{-\ell}^{\ell} \cos(k_p x')\cos(kx'\cos\theta)\, dx'$$

$$= \lim_{N\to\infty} \frac{1/4}{AN} \sum_{j=1}^{N} \int_{-\ell}^{\ell} \left[ \cos(k_p x - kx\cos\theta) + \cos(k_p x + kx\cos\theta) \right] dx$$

$$\int_{-\ell}^{\ell} \left[ \cos(k_p x' - kx'\cos\theta) + \cos(k_p x' + kx'\cos\theta) \right] dx'$$

or

$$\left\langle V_{pr}^2 \right\rangle = \lim_{N\to\infty} \frac{1}{AN} \sum_{j=1}^{N} \left[ \frac{\sin(k_p - k\cos\theta)\,\ell}{k_p - k\cos\theta} + \frac{\sin(k_p + k\cos\theta)\,\ell}{k_p + k\cos\theta} \right]^2$$

$$= \frac{1}{2\pi A} \int_0^{2\pi} \left[ \frac{\sin(k_p - k\cos\theta)\,\ell}{k_p - k\cos\theta} + \frac{\sin(k_p + k\cos\theta)\,\ell}{k_p + k\cos\theta} \right]^2 d\theta$$

Now when $k \to k_p$ the first term peaks for $\theta \to 0, 2\pi$ and the second term peaks for $\theta \to \pi$. Thus we find (and $\theta = \zeta/\sqrt{k\ell/2}$)

$$\left\langle V_{pr}^2 \right\rangle = \frac{1}{2\pi A}\int_{-\infty}^{\infty}\left[\frac{\sin\left(k_p - k + k\theta^2/2\right)\ell}{k_p - k + k\theta^2/2}\right]^2 d\theta + \frac{1}{2\pi A}\int_{-\infty}^{\infty}\left[\frac{\sin\left(k_p - k + k\left(\theta-\pi\right)^2/2\right)\ell}{k_p - k + k\left(\theta-\pi\right)^2/2}\right]^2 d\theta$$

$$= \frac{\ell^2}{\pi A\sqrt{k\ell/2}}\int_{-\infty}^{\infty}\left[\frac{\sin\left(\left(k_p-k\right)\ell + \zeta^2\right)}{\left(k_p-k\right)\ell+\zeta^2}\right]^2 d\zeta$$

Letting

$$\lambda = 2\left(k - k_p\right)L$$

$$\left\langle V_{pr}^2 \right\rangle = \frac{L^2}{2\pi A\sqrt{kL}}\int_{-\infty}^{\infty}\frac{\sin^2\left(\lambda/4-\zeta^2\right)}{\left(\lambda/4-\zeta^2\right)^2}d\zeta$$

$$\left\langle \sqrt{kL}V_p^2 \right\rangle_r = L^2 G\left(\lambda\right)/A$$

$$G\left(\lambda\right) = \frac{1}{2\pi}\int_{-\infty}^{\infty}\frac{\sin^2\left(\lambda/4-\zeta^2\right)}{\left(\lambda/4-\zeta^2\right)^2}d\zeta$$

Noting from symmetry that [30]

$$\left\langle \sqrt{kL}V_p^2 \right\rangle_r = L^2 G_s\left(\lambda\right)/A$$

with

$$G_s\left(\lambda\right) = 4G\left(\lambda\right)$$

we obtain the previous result.

### 2.6.5 random plane wave projection with elliptical projection operator

Suppose we use the random plane wave form of the field and take the projection with

$$V_{pr} = 2\int_0^{\ell}\left(1 - x^2/d^2\right)^{-1/4}\cos\left[k_p x + p_0\left(x\right)\right]u_r\left(x,0\right)dx$$

with

$$p_0\left(x\right) = \frac{1}{2}s_p\left\{\ln\left(\frac{d+\ell}{d-\ell}\right)\left(x/\ell\right) - \ln\left(\frac{d+x}{d-x}\right)\right\}$$

$$s_p \mathrm{Arcsinh}\left[\sqrt{L/\left(2R\right)}\right] = \lambda/4$$

Then

$$V_{pr} = 2\int_0^\ell \left(1 - x^2/d^2\right)^{-1/4} \cos\left[k_p x + p_0\left(x\right)\right] \lim_{N\to\infty} \sqrt{2/\left(AN\right)}\, \mathrm{Re}\left[\sum_{j=1}^{N} a_j e^{i\alpha_j + ikx\cos\theta}\right] dx$$

The variance of this random variable is then [30]

$$\left\langle V_p^2 \right\rangle_r = \frac{1}{2\pi A}\int_0^{2\pi} \left[F_+\left(\theta\right) + F_-\left(\theta\right)\right]^2 d\theta$$

$$F_+\left(\theta\right) + F_-\left(\theta\right) = 2\int_0^\ell \left(1 - x^2/d^2\right)^{-1/4} \cos\left[k_p x + p_0\left(x\right)\right] \cos\left(kx\cos\theta\right) dx$$

$$= \int_0^\ell \left(1 - x^2/d^2\right)^{-1/4} \left[\cos\left\{k_p x + p_0\left(x\right) + kx\cos\theta\right\} + \cos\left\{k_p x + p_0\left(x\right) - kx\cos\theta\right\}\right] dx$$

Now for large $k$ and $k_p$ we can take $k \to k_p$ and the first term peaks for $\theta \to \pi$ and the second term peaks for $\theta \to 0, 2\pi$ (and $\theta = \zeta/\sqrt{k\ell/2}$)

$$k_p - k\cos\theta \approx \left(k_p - k\right) + k\theta^2/2$$

$$k_p + k\cos\theta \approx \left(k_p - k\right) + k\left(\theta - \pi\right)^2/2$$

and

$$F_+\left(\theta\right) + F_-\left(\theta\right) \approx$$

$$\int_0^\ell \left(1 - x^2/d^2\right)^{-1/4} \left[\cos\left\{\left(\left(k_p - k\right) + k\left(\theta - \pi\right)^2/2\right)x + p_0\left(x\right)\right\} + \cos\left\{\left(\left(k_p - k\right) + k\theta^2/2\right)x + p_0\left(x\right)\right\}\right] dx$$

The contributions from the two points combine (outside the integral there is a factor of two)

$$\left\langle V_p^2 \right\rangle_r \approx \frac{1}{\pi A}\int_{-\infty}^{\infty} \left[\int_0^\ell \left(1 - x^2/d^2\right)^{-1/4} \cos\left\{\left(\left(k_p - k\right) + k\theta^2/2\right)x + p_0\left(x\right)\right\} dx\right]^2 d\theta$$

$$\approx \frac{1}{\pi A\sqrt{k\ell/2}}\int_{-\infty}^{\infty} \left[\int_0^\ell \left(1 - x^2/d^2\right)^{-1/4} \cos\left\{\left(\left(k_p - k\right) + \zeta^2/\ell\right)x + p_0\left(x\right)\right\} dx\right]^2 d\zeta$$

$$\approx \frac{2}{\pi A\sqrt{k\ell/2}}\int_0^{\infty} \left[\int_0^\ell \left(1 - x^2/d^2\right)^{-1/4} \cos\left\{\left(\lambda/4 - \zeta^2\right)x/\ell - p_0\left(x\right)\right\} dx\right]^2 d\zeta$$

$$\lambda = 2\left(k - k_p\right)L$$

or

$$\left\langle \sqrt{kL}\, V_p^2 \right\rangle_r = L^2 G\left(\lambda\right)/A$$

with

$$G(\lambda) = \frac{1}{\pi}\int_0^\infty \left[\int_0^\ell \left(1 - x^2/d^2\right)^{-1/4} \cos\left\{\left(\lambda/4 - \zeta^2\right) x/\ell - p_0(x)\right\} dx/\ell\right]^2 d\zeta$$

$$= \frac{1}{\pi}\int_0^\infty \left[\int_0^1 \left(1 - x^2\ell^2/d^2\right)^{-1/4} \cos\left\{\left(\lambda/4 - \zeta^2\right) x - p_0(x\ell)\right\} dx\right]^2 d\zeta$$

If we take the limit $\ell << d$ then the inner integral becomes

$$\int_0^\ell \left(1 - x^2/d^2\right)^{-1/4} \cos\left\{\left(\lambda/4 - \zeta^2\right) x/\ell - p_0(x)\right\} dx/\ell \to \int_0^\ell \cos\left\{\left(\lambda/4 - \zeta^2\right) x/\ell\right\} dx/\ell = \frac{\sin\left(\lambda/4 - \zeta^2\right)}{\left(\lambda/4 - \zeta^2\right)}$$

and thus

$$G(\lambda) \to \frac{1}{\pi}\int_0^\infty \frac{\sin^2\left(\lambda/4 - \zeta^2\right)}{\left(\lambda/4 - \zeta^2\right)^2} d\zeta$$

which, except for a factor of four, is the same as the result in [30]. Noting the factor of four, we have [30]

$$\left\langle \sqrt{kL} V_p^2 \right\rangle_r = L^2 G_s(\lambda)/A$$

$$G_s(\lambda) = 4G(\lambda) = \frac{4}{\pi}\int_0^\infty \left[\int_0^1 \left(1 - x^2\ell^2/d^2\right)^{-1/4} \cos\left\{\left(\lambda/4 - \zeta^2\right) x - p_0(x\ell)\right\} dx\right]^2 d\zeta$$

#### 2.6.6 projection comparisons

We have already shown the comparison between the numerical solution histogram and the existing scar theory for the case where $\Lambda \sim 1 + \sqrt{8L/R} \approx 2.265$. Figure 8 shows a comparison of the scar theory projections (using the preceding Vaynshteyn constructed formulas, without taking the limit as $\ell/d \to 0$) and the Fourier projections (with the Fourier series solutions) for both the scar theory and the random plane wave fields.

Figure 9 shows the same comparison for the case where $L = 2$ m and $R = 2$ m or $\Lambda \sim 1 + \sqrt{8L/R} \approx 3.83$ (with $A \approx 4.76429$ m$^2$). Note that the actual stability exponent in this case is $\Lambda_+ = \left[1 + L/R + \sqrt{(1 + L/R)^2 - 1}\right]^2 \approx 13.93$. The main reason for the discrepancy in this plot is the approximation of $d = \ell\sqrt{1 + R/\ell} = 1.732$ m versus the asymptotic form $d \sim \sqrt{R\ell} = 1.414$ m. Nevertheless, even for such small values of the radius of curvature, the Fourier approach yields very close answers.

### 2.7 Integral Of Square Along Scar

The integral of the square of the field along the scar is a quantity of interest [30]

$$P = \frac{1}{L}\int_{-\ell}^{\ell} u^2(x, 0)\, dx$$

If we insert the Fourier series for the eigenfunction [30]

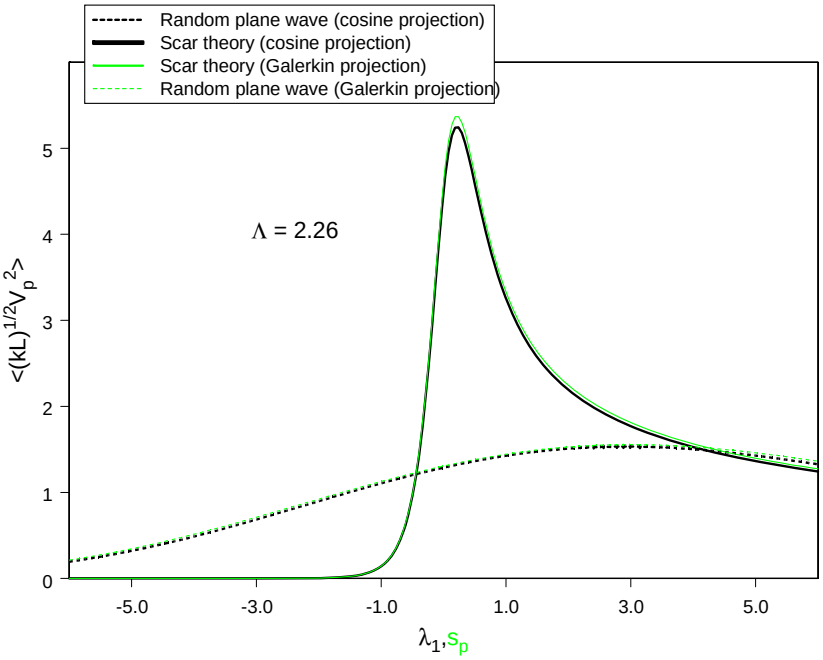


Figure 8. Comparison of scar projections and previous Fourier projections (using Fourier series solution) for both scar theory and random plane wave field for $L = 2$ m and $R = 10$ m.

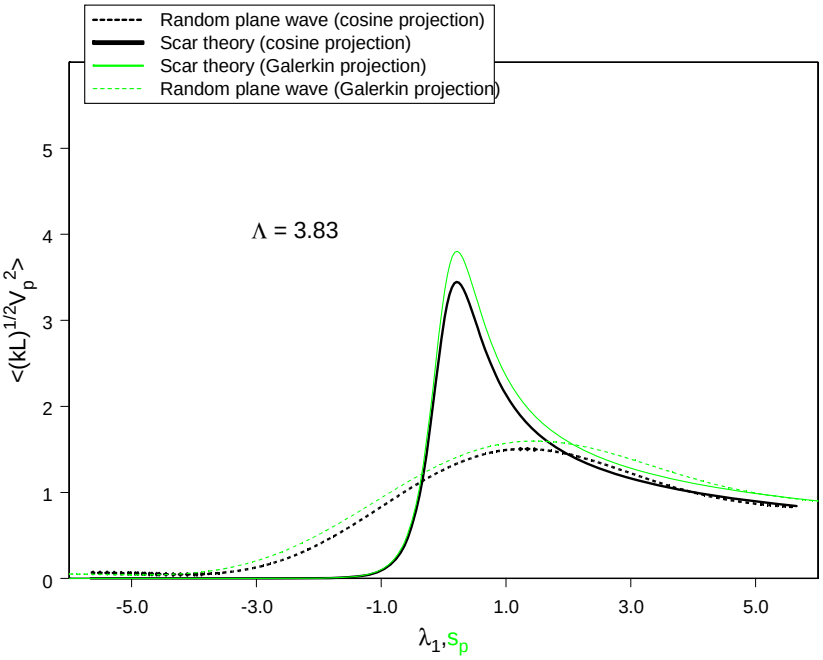


Figure 9. Comparison of scar projections and previous Fourier projections (using Fourier series solution) for both scar theory and random plane wave field for $L = 2$ m and $R = 2$ m.

$$P = \frac{1}{L}\int_{-\ell}^{\ell} u^2(x,0)\,dx = \frac{1}{L}\frac{2}{L}\sum_p \frac{2}{L}\sum_{p'} V_p V_{p'}\int_{-\ell}^{\ell}\cos(k_p x)\cos(k_{p'}x)\,dx$$

$$= \frac{2}{L^2}\sum_p V_p^2$$

and

$$\left\langle \sqrt{kL}P\right\rangle = \frac{2}{L^2}\sum_p \left\langle \sqrt{kL}V_p^2\right\rangle = \frac{2}{A}\sum_p G_1(\lambda_{1p})$$

Because of the summation over $p$, and the repetition of the value of this sum, it is convenient to use the abscissa

$$\mu = (k - k_p)\,\ell/\pi$$

where we do not give the value of $p$ [30].

Alternatively if we use the elliptic system construction and the expansion

$$u(x,0) \sim \sum_p u_p(x,0)$$

the asymptotic orthogonality in the Appendix gives similar results

$$\left\langle \sqrt{kL}P\right\rangle = \frac{2}{L^2}\sum_p \left\langle \sqrt{kL}V_p^2\right\rangle = \frac{2}{A}\sum_p G_1(s_p)$$

The acceleration scheme involving the random plane wave contribution [30] is useful. It involves the subtraction of $G_s(\lambda)$ from the summand and addition of the average of the random plane wave contribution to $P$

$$\left\langle \sqrt{kL}P\right\rangle = \frac{2}{A}\sum_p \left[G_1(s_p) - G_s(\lambda_p)\right] + \left\langle \sqrt{kL}P_r\right\rangle$$

### 2.7.1 average of random plane wave over interval

Let us consider the integral

$$P_r = \frac{1}{L}\int_{-\ell}^{\ell} u_r^2 dx$$

Using the random plane wave representation

$$u_r = \lim_{N\to\infty}\sqrt{2/(AN)}\,\mathrm{Re}\left[\sum_{j=1}^{N} a_j e^{i\alpha_j + i\underline{k}\cdot\underline{r}}\right]$$

where $a_j$ are real random numbers with $\left\langle a_j^2\right\rangle = 1$, $|\underline{k}| = k$ are random vectors uniformly distributed in angle, and the random phases $\alpha_j$ are uniformly distributed on a $2\pi$ interval we have

$$LP_r = \int_{-\ell}^{\ell} \lim_{N\to\infty} \sqrt{2/\left(AN\right)} \left[\sum_{j=1}^{N} a_j \cos\left(\alpha_j + kx\cos\theta\right)\right] \lim_{N'\to\infty} \sqrt{2/\left(AN'\right)} \left[\sum_{j'=1}^{N'} a_{j'} \cos\left(\alpha_{j'} + kx\cos\theta\right)\right] dx$$

$$= \int_{-\ell}^{\ell} \lim_{N\to\infty} \sqrt{2/\left(AN\right)} \sum_{j=1}^{N} \lim_{N'\to\infty} \sqrt{2/\left(AN'\right)} \sum_{j'=1}^{N'} a_j a_{j'} \cos\left(\alpha_j + kx\cos\theta\right) \cos\left(\alpha_{j'} + kx\cos\theta\right) dx$$

If we average over the amplitudes $a_j$ and regard different $j$ values as independent the cross terms vanish

$$L\left\langle P_r\right\rangle_{a_j,\alpha_j} = \lim_{N\to\infty} \frac{2}{AN} \sum_{j=1}^{N} \int_{-\ell}^{\ell} \left\langle \cos^2\left(\alpha_j + kx\cos\theta\right)\right\rangle_{\alpha_j} dx$$

$$\left\langle \cos^2\left(\alpha_j + kx\cos\theta\right)\right\rangle_{\alpha_j} = \frac{1}{2\pi}\frac{1}{2}\int_0^{2\pi} \left[1 + \cos\left(2\alpha_j + 2kx\cos\theta\right)\right] d\alpha_j = \frac{1}{2}$$

$$L\left\langle P_r\right\rangle_{a_j,\alpha_j} = \lim_{N\to\infty} \frac{2}{AN} \sum_{j=1}^{N} L/2$$

$$\left\langle P_r\right\rangle_{a_j,\alpha_j} = 1/A$$

However if we average only the even part with respect to $x$ (since we are considering only the even solution here)

$$LP_r = \int_{-\ell}^{\ell} \lim_{N\to\infty} \sqrt{2/\left(AN\right)} \left[\sum_{j=1}^{N} a_j \cos\left(\alpha_j\right) \cos\left(kx\cos\theta\right)\right] \lim_{N'\to\infty} \sqrt{2/\left(AN'\right)} \left[\sum_{j'=1}^{N'} a_{j'} \cos\left(\alpha_{j'}\right) \cos\left(kx\cos\theta\right)\right] dx$$

$$= \int_{-\ell}^{\ell} \lim_{N\to\infty} \sqrt{2/\left(AN\right)} \sum_{j=1}^{N} \lim_{N'\to\infty} \sqrt{2/\left(AN'\right)} \sum_{j'=1}^{N'} a_j a_{j'} \cos\left(\alpha_j\right) \cos\left(\alpha_{j'}\right) \cos\left(\alpha_j + kx\cos\theta\right) \cos\left(\alpha_{j'} + kx\cos\theta\right) dx$$

If we average over the amplitudes $a_j$ and regard different $j$ values as independent the cross terms vanish

$$L\left\langle P_r\right\rangle_{a_j,\alpha_j} = \lim_{N\to\infty} \frac{2}{AN} \sum_{j=1}^{N} \int_{-\ell}^{\ell} \left\langle \cos^2\left(\alpha_j\right) \cos^2\left(\alpha_j + kx\cos\theta\right)\right\rangle_{\alpha_j} dx$$

where

$$\left\langle \cos^2\left(\alpha_j\right) \cos^2\left(\alpha_j + kx\cos\theta\right)\right\rangle_{\alpha_j}$$

$$= \frac{1}{2\pi}\frac{1}{4}\int_0^{2\pi} \left[1 + \cos\left(2\alpha_j\right)\right] \left[1 + \cos\left(2\alpha_j\right)\cos\left(2kx\cos\theta\right)\right] d\alpha_j = \frac{1}{4}\left[1 + \cos\left(2kx\cos\theta\right)\right]$$

Now averaging over $\theta$

$$L\left\langle P_r\right\rangle = \lim_{N\to\infty}\frac{2}{AN}\sum_{j=1}^{N}\int_{-\ell}^{\ell}\frac{1}{4}\frac{1}{2\pi}\int_0^{2\pi}\left[1+\cos\left(2kx\cos\theta\right)\right]d\theta dx = \lim_{N\to\infty}\frac{2}{AN}\sum_{j=1}^{N}\int_{-\ell}^{\ell}\frac{1}{4}dx$$

$$L\left\langle P_r\right\rangle = \lim_{N\to\infty}\frac{2}{AN}\sum_{j=1}^{N}L/4$$

$$\left\langle P_r\right\rangle = 1/\left(2A\right)$$

Symmetries as in $G_s\left(\lambda\right)$ thus give [30]

$$\left\langle P_r\right\rangle = 2/A$$

Therefore

$$\left\langle\sqrt{kL}\left(P-P_r\right)\right\rangle = \left\langle\sqrt{kL}P\right\rangle - \frac{2}{A}\left\langle\sqrt{kL}\right\rangle = \frac{2}{A}\sum_p\left[G_1\left(s_p\right)-G_s\left(\lambda_p\right)\right]$$

where

$$\mu = \left(k-k_p\right)\ell/\pi = \lambda/\left(4\pi\right) = s_p\frac{1}{\pi}\mathrm{Arcsinh}\sqrt{\ell/R} = \frac{s_p}{4\pi}\ln\left(\Lambda_+\right)$$

### 2.7.2 comparison of integral of square

We now compare calculations of the mean of the integral of the square of the eigenfunction along the orbit for the case where $L = 2$ m and $R = 10$ m. Figure 10 shows the original Fourier form of the terms in the summation with various numbers of terms included. This shows that very few terms are needed; near the peak only a single term is required to achieve reasonable accuracy.

Figure 11 shows a comparison of the Fourier trigonometric calculation versus the elliptical calculation with a single term in the summation. They are nearly identical for this case.

Figure 12 shows the calculated histogram from the numerical calculation for the difference versus $\mu$. Notice that the height of the difference is overestimated by the theory by nearly a factor of two. This is also true in the previous work [30].

It should be noted that the total integral of the square over the orbit is dominated by the level of the random plane wave average as shown by the histogram in Figure 13.

## 2.8 Alternative Eigenfunction Representation and Integral Along Scar

It is instructive to consider the approximation of the eigenfunction as

$$u \sim \sum_p u_p + u_r - \sum_p c'_{rp}u_p$$

where $u_p$ are the scar components (and might be a single term or a truncated sum) and $u_r$ is the random plane wave symmetrized field. The projections of $u_r$ on the $u_p$ are removed by the final terms so we do not double count these contributions (where we assume asymptotic orthogonality approximately holds)

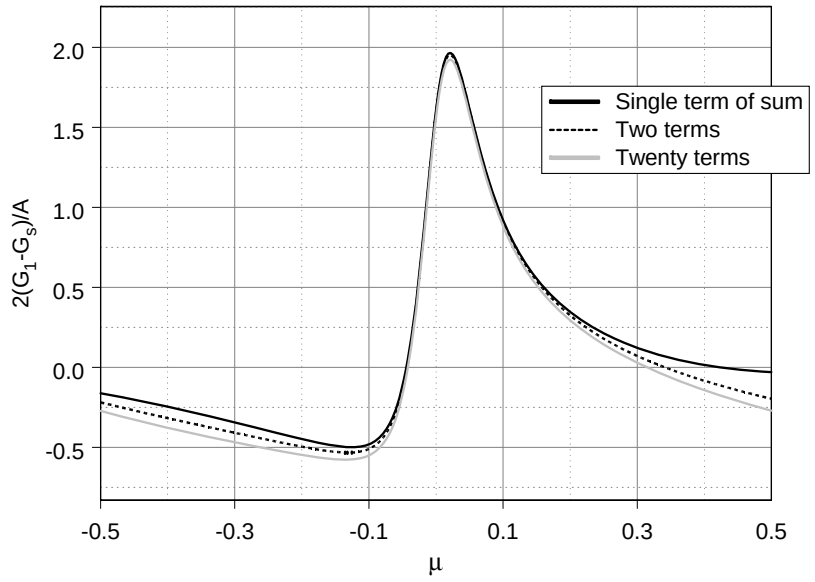


Figure 10. Comparison of the mean of the integral of square of eigenfunction minus the square of the random plane wave for various numbers of terms included in the summation. The Fourier expansion is used here.

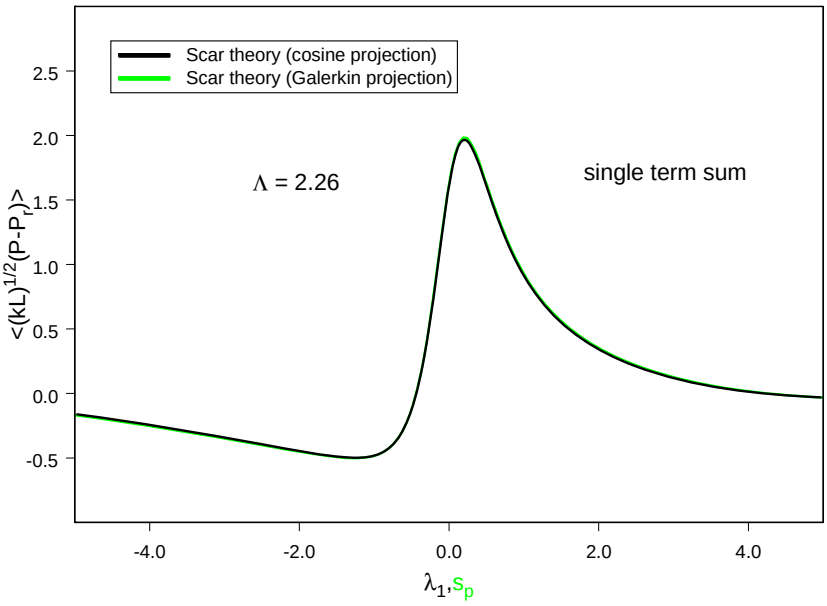


Figure 11. Comparison of trigonometric functions versus elliptical functions.

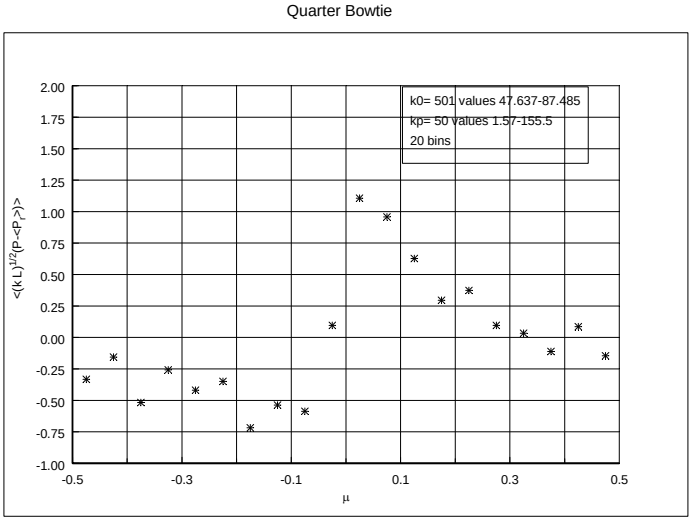


Figure 12. Histogram for the mean integral of the square of the eigenfunction minus the random plane wave from numerical simulation of quarter bow tie cavity with $L = 2$ m and $R = 10$ m as a function of $\mu = (k - k_p)\,\ell/\pi$.

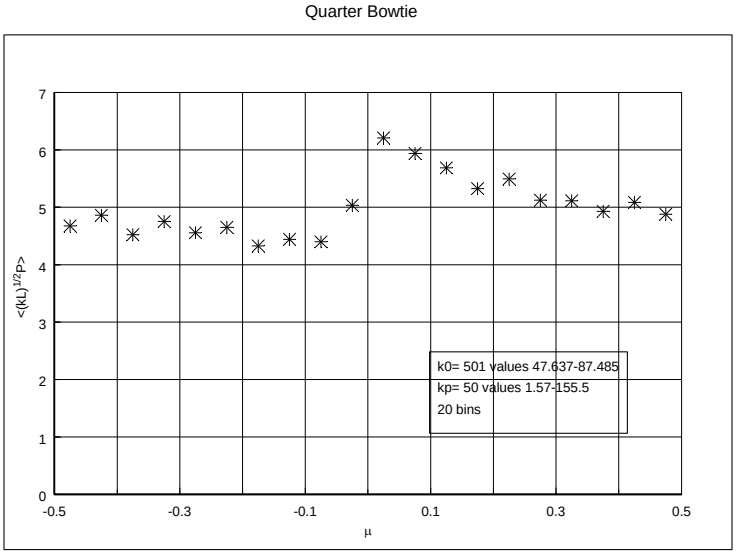


Figure 13. Histogram for the mean integral of the square of the eigenfunction over the scarred orbit from the numerical simulation of the quarter bow tie cavity with $L = 2$ m and $R = 10$ m as a function of $\mu = (k - k_p)\,\ell/\pi$.

$$c'_{rp}\int_{-\ell}^{\ell}u_p^2dx\sim\int_{-\ell}^{\ell}u_ru_pdx$$

Now taking the integral of the square along the orbit gives

$$\int_{-\ell}^{\ell}u^2dx\sim\sum_p\int_{-\ell}^{\ell}u_p^2dx+\int_{-\ell}^{\ell}\left(u_r-\sum_p c'_{rp}u_p\right)^2dx$$

$$\sim\sum_p\int_{-\ell}^{\ell}u_p^2dx+\int_{-\ell}^{\ell}u_r\left(u_r-\sum_p c'_{rp}u_p\right)dx$$

$$\sim\sum_p\int_{-\ell}^{\ell}u_p^2dx+\int_{-\ell}^{\ell}u_r^2dx-\sum_p c'_{rp}\int_{-\ell}^{\ell}u_ru_pdx$$

$$\sim\sum_p\int_{-\ell}^{\ell}\left(1-c'^2_{rp}\right)u_p^2dx+\int_{-\ell}^{\ell}u_r^2dx$$

and

$$\int_{-\ell}^{\ell}u^2dx-\int_{-\ell}^{\ell}u_r^2dx\sim\sum_p\left[1-\left(\int_{-\ell}^{\ell}u_ru_pdx/\int_{-\ell}^{\ell}u_p^2dx\right)^2\right]\int_{-\ell}^{\ell}u_p^2dx$$

where the cross terms do not appear as a result of the definition of the constants. Then taking the mean

$$\langle P\rangle-\langle P_r\rangle\approx\frac{1}{2\ell}\sum_p\left[\int_{-\ell}^{\ell}\left\langle u_p^2\right\rangle dx-\int_{-\ell}^{\ell}\left\langle c'^2_{rp}u_p^2\right\rangle dx\right]$$

with

$$\left\langle c'^2_{rp}u_p^2\right\rangle=\left\langle\left(u_p\int_{-\ell}^{\ell}u_ru_pdx/\int_{-\ell}^{\ell}u_p^2dx\right)^2\right\rangle$$

$$=\left\langle u_p^2(x)\int_{-\ell}^{\ell}u_r(x'')u_p(x'')dx''\int_{-\ell}^{\ell}u_r(x')u_p(x')dx'/\left(\int_{-\ell}^{\ell}u_p^2(x)dx\right)^2\right\rangle$$

$$=u_p^2(x)\int_{-\ell}^{\ell}\int_{-\ell}^{\ell}\langle u_r(x')u_r(x'')\rangle u_p(x'')u_p(x')dx''dx'/\left(\int_{-\ell}^{\ell}u_p^2(x)dx\right)^2$$

where the averages do not apply to $u_p^2$ simply because the expression is homogeneous in the random variable $v^2$ (which cancelled out in the previous line). Using the two dimensional correlation function [5]

$$\langle Au_r(\underline{r})u_r(\underline{r}')\rangle=J_0\left(k\sqrt{(x-x')^2+(y-y')^2}\right)$$

but adding the image on the symmetry line $y=0$, we have

$$\langle A u_r(x,0)\, u_r(x',0)\rangle = 4J_0(k|x-x'|)$$

and thus

$$\left\langle c_{rp}'^2 u_p^2\right\rangle = \frac{4}{A}u_p^2(x)\int_{-\ell}^{\ell}\int_{-\ell}^{\ell} J_0(k(x-x'))\, u_p(x)\, u_p(x')\, dxdx' / \left(\int_{-\ell}^{\ell} u_p^2 dx\right)^2$$

Then (we can insert averages due to the homogeneous nature of the expression)

$$\langle P\rangle - \langle P_r\rangle \approx \sum_p \left[1 - \frac{4}{A}\int_{-\ell}^{\ell}\int_{-\ell}^{\ell} J_0(k(x-x'))\langle u_p(x)\, u_p(x')\rangle\, dxdx' / \left(\int_{-\ell}^{\ell}\langle u_p^2\rangle\, dx\right)^2\right]\frac{1}{2\ell}\int_{-\ell}^{\ell}\langle u_p^2\rangle\, dx$$

Now inserting the scar function

$$u_p(x,0) = \frac{2v\sqrt{2}}{\left|U_+'(s_p,0)\right|\sqrt{A\sqrt{2\gamma}\ln\left(\frac{d+\ell}{d-\ell}\right)}}\cos^2\left[k_p x + p_0(x)\right]\left(1 - x^2/d^2\right)^{-1/4}$$

with mean square

$$\left\langle u_p^2(x,0)\right\rangle = \frac{8}{\left|U_+'(s_p,0)\right|^2 A\sqrt{2\gamma}\ln\left(\frac{d+\ell}{d-\ell}\right)}\cos^2\left[k_p x + p_0(x)\right]\left(1 - x^2/d^2\right)^{-1/2}$$

$$p_0(x) = \frac{1}{2}s_p\left\{\ln\left(\frac{d+\ell}{d-\ell}\right)(x/\ell) - \ln\left(\frac{d+x}{d-x}\right)\right\}$$

$$\int_{-\ell}^{\ell}\left\langle u_p^2(x,0)\right\rangle dx \approx \frac{8d}{\left|U_+'(s_p,0)\right|^2 A\sqrt{2\gamma}\ln\left(\frac{d+\ell}{d-\ell}\right)}\mathrm{Arcsin}(\ell/d)$$

and

$$\langle P\rangle - \langle P_r\rangle \approx \frac{1}{\ell A}\sum_p \left[\frac{4d}{\left|U_+'(s_p,0)\right|^2\sqrt{2\gamma}\ln\left(\frac{d+\ell}{d-\ell}\right)}\mathrm{Arcsin}(\ell/d) -\right.$$

$$\left. 2\int_{-\ell}^{\ell}\int_{-\ell}^{\ell} J_0(k(x-x'))\cos\left[k_p x + p_0(x)\right]\left(1 - x^2/d^2\right)^{-1/4}\cos\left[k_p x' + p_0(x')\right]\left(1 - x'^2/d^2\right)^{-1/4} dxdx'\right.$$

$$\left. / \left(d\mathrm{Arcsin}(\ell/d)\right)\right]$$

If we take the limit $\ell << d$ (with $s_p$ not too large) we return to the Fourier form of the scar function (and $s_p \to \lambda_1$)

$$\langle P - P_r\rangle \approx \frac{1}{\ell A}\sum_p \left[\frac{2d}{\left|U_+'(s_p,0)\right|^2\sqrt{2\gamma}} -\right.$$

$$\frac{1}{\ell}\int_{-\ell}^{\ell}\int_{-\ell}^{\ell} J_0\left(k\left(x-x'\right)\right)\left\{\cos k_p\left(x-x'\right)+\cos k_p\left(x+x'\right)\right\}dxdx'\Bigg]$$

Letting $u = x - x'$ and $v = x + x'$ (and including 1/2 for the Jacobian of the transformation) gives

$$\langle P - P_r\rangle \approx \frac{1}{\ell A}\sum_p \Bigg[\frac{2d}{\left|U_+'\left(s_p,0\right)\right|^2\sqrt{2\gamma}} - \frac{1}{2\ell}\int_{-2\ell}^{2\ell}\int_{-2\ell+|u|}^{2\ell-|u|} J_0\left(ku\right)\cos\left(k_p u\right)dvdu$$

$$-\frac{1}{2\ell}\int_{-2\ell}^{2\ell}\int_{-2\ell+|u|}^{2\ell-|u|} J_0\left(ku\right)\cos\left(k_p v\right)dvdu\Bigg]$$

$$\approx \frac{1}{\ell A}\sum_p \Bigg[\frac{2d}{\left|U_+'\left(s_p,0\right)\right|^2\sqrt{2\gamma}} - \frac{2}{\ell}\int_0^{2\ell} J_0\left(ku\right)\cos\left(k_p u\right)\left(2\ell-|u|\right)du$$

$$-\frac{2}{k_p\ell}\int_0^{2\ell} J_0\left(ku\right)\sin\left\{k_p\left(2\ell-|u|\right)\right\}du\Bigg]$$

To approximate

$$\langle P - P_r\rangle \approx \frac{8}{A}\sum_p \Bigg[\frac{d/\left(4\ell\right)}{\left|U_+'\left(s_p,0\right)\right|^2\sqrt{2\gamma}} - \int_0^1 \left(1-u\right)J_0\left(2k\ell u\right)\cos\left(2k_p\ell u\right)du$$

$$-\frac{1}{2k_p\ell}\int_0^1 J_0\left(2k\ell u\right)\sin\left\{2k_p\ell\left(1-u\right)\right\}du\Bigg]$$

for high frequencies we drop the second term and approximate the Bessel function as

$$J_0\left(2k\ell u\right) \sim \frac{1}{\sqrt{k\ell u}}\cos\left(2k\ell u - \pi/4\right)$$

to find

$$\langle P - P_r\rangle \sim \frac{8}{A}\sum_p \Bigg[\frac{d/\left(4\ell\right)}{\left|U_+'\left(s_p,0\right)\right|^2\sqrt{2\gamma}} - \frac{1}{2\sqrt{2\pi k\ell}}\int_0^1 \left(1-u\right)\left\{\cos\left(2\left(k-k_p\right)\ell u\right)+\sin\left(2\left(k-k_p\right)\ell u\right)\right\}du\Bigg]$$

$$\sim \frac{8}{A}\sum_p \Bigg[\frac{d/\left(4\ell\right)}{\left|U_+'\left(s_p,0\right)\right|^2\sqrt{2\gamma}} - \frac{1}{2\sqrt{\pi k\ell}}\int_0^1 \left(1-u\right)\cos\left(2\left(k-k_p\right)\ell u - \pi/4\right)\frac{du}{\sqrt{u}}\Bigg]$$

$$\sim \frac{2}{A}\sum_p \Bigg[\frac{d/\ell}{\left|U_+'\left(s_p,0\right)\right|^2\sqrt{2\gamma}} - \frac{2}{\sqrt{\pi k\ell}}\int_0^1 \left(1-u\right)\cos\left(\lambda_p u/2 - \pi/4\right)\frac{du}{\sqrt{u}}\Bigg]$$

where

$$\lambda_p = 4\left(k-k_p\right)\ell$$

Now it turns out that

$$G_s(\lambda_p) \approx \sqrt{kL}\frac{1}{L}\int_{-\ell}^{\ell}\int_{-\ell}^{\ell} 2J_0(k(x-x'))\langle u_p(x,0)\,u_p(x',0)\rangle\,dxdx' / \int_{-\ell}^{\ell}\left\langle u_p^2(x,0)\right\rangle dx$$

or

$$G_s(\lambda_p) = \frac{4}{\sqrt{2\pi}}\int_0^1 (1-u)\cos(\lambda_p u/2-\pi/4)\frac{du}{\sqrt{u}} = \frac{4}{\pi}\int_0^\infty \frac{\sin^2\left(\lambda_p/4-\zeta^2\right)}{\left(\lambda_p/4-\zeta^2\right)^2}d\zeta$$

$$\sim \frac{4}{\sqrt{\lambda_p}}\ ,\ \lambda_p\to\infty$$
$$\sim \frac{4}{(-\lambda_p)^{3/2}}\ ,\ \lambda_p\to-\infty$$

where this is summed in the Appendix in terms of Fresnel integrals. Therefore

$$\left\langle\sqrt{kL}(P-P_r)\right\rangle \sim \frac{2}{A}\sum_p\left[\frac{\sqrt{d/\ell}}{\left|U_+'(\lambda_{1p},0)\right|^2}-G_s(\lambda_p)\right] \sim \frac{2}{A}\sum_p\left[G_1(\lambda_{1p},\Lambda)-G_s(\lambda_p)\right]$$

where

$$G_1(\lambda_1,\Lambda) = \frac{2(\Lambda-1)^{-1/2}}{\left|U_+'(\lambda_1,0)\right|^2}$$

and we have used

$$\sqrt{\ell/d} = \frac{\sqrt{\Lambda_+-1}}{\sqrt{\Lambda_+}+1} \sim \frac{1}{2}\sqrt{\Lambda-1}$$

$$\langle P_r\rangle = 2/A$$

Thus with this direct inclusion of the random plane wave component in the eigenfunction we obtain the same result [30]. This approach will prove useful in the stadium cavity in the second part of the report.

We have seen that cancellation of $G_1-G_s$ occurs for $p\to 0$ and $\lambda_{1p},\lambda_p\to\infty$. For $p\to\infty$ and $\lambda_{1p},\lambda_p\to-\infty$, we do not see cancellation, but $G_1$ decays exponentially. The random plane wave contribution also converges. For example if we use the asymptotic form of $G_s$ for $p\geq 1$ with $k=k_p$ we find

$$\frac{2}{A}\sum_{p=1}^{\infty}G_s(\lambda_p) \sim \frac{2}{A}\sum_{p=1}^{\infty}\frac{4}{(4\pi p)^{3/2}} = \frac{2.6124}{A\pi^{3/2}} \approx 0.1$$

Note that we have dropped the length units here and in the graphs. The $p=0$ term in this case, where $k=k_p$, is

$$\frac{2}{A}G_s(0) = \frac{16}{3A\sqrt{\pi}} \approx 0.64335$$

and the peak of the scar function (which is also near $k=k_p$ and is more rapidly varying than the rest of the summation) is

$$\frac{2}{A} G_1 \left(\lambda_{1pk}, \Lambda\right) \approx 2.6$$

Thus near the peak

$$\left\langle \sqrt{kL} \left(P - P_r\right) \right\rangle \approx 2.6 - 0.6 - 0.1 \approx 1.9$$

## 2.9 Point Value Statistics

It is of interest to examine the statistics of some point values of the field in the cavity. It is convenient to plot the quantity $A \left\langle u^2 \right\rangle = A \left\langle E^2 \right\rangle$ as a function of $s_p \sim \lambda_1$. We note that this quantity from the random plane wave contribution alone is expected to approach unity for the random plane wave field out in the volume of the cavity (away from the axis symmetry lines), approach two on the axes, and approach four at the origin. These values agree with general trends shown on Figures 14, 15, 16, and 17.

There is no clear enhancement near zero. To get a feel for the scar enhancement of the point values let us take

$$u \sim \sum_p u_p + u_r - \sum_p c'_{rp} u_p$$

with

$$c'_{rp} \int_{-\ell}^{\ell} u_p^2 dx \sim \int_{-\ell}^{\ell} u_r u_p dx$$

Now taking the average of the square along the orbit gives

$$\left\langle u^2 \right\rangle \sim \sum_p \left\langle u_p^2 \right\rangle + \left\langle \left( u_r - \sum_p c'_{rp} u_p \right)^2 \right\rangle$$

$$\sim \sum_p \left\langle u_p^2 \right\rangle + \left\langle u_r \left( u_r - \sum_p c'_{rp} u_p \right) \right\rangle$$

$$\sim \sum_p \left\langle u_p^2 \right\rangle + \left\langle u_r^2 \right\rangle - \sum_p \left\langle u_r c'_{rp} u_p \right\rangle$$

$$\sim \sum_p \left\langle u_p^2 \right\rangle + \left\langle u_r^2 \right\rangle - \sum_p \left\langle \int_{-\ell}^{\ell} u_r \left(x, 0\right) u_r \left(x', 0\right) u_p \left(x, 0\right) u_p \left(x', 0\right) dx' / \int_{-\ell}^{\ell} u_p^2 dx \right\rangle$$

$$\sim \sum_p \left\langle u_p^2 \right\rangle + \left\langle u_r^2 \right\rangle - \sum_p \int_{-\ell}^{\ell} \left\langle u_r \left(x, 0\right) u_r \left(x', 0\right) \right\rangle u_p \left(x, 0\right) u_p \left(x', 0\right) dx' / \int_{-\ell}^{\ell} u_p^2 dx$$

$$\sim \sum_p \left\langle u_p^2 \right\rangle + \left\langle u_r^2 \right\rangle - \sum_p \int_{-\ell}^{\ell} \frac{4}{A} J_0 \left(k \left|x - x'\right|\right) \left\langle u_p \left(x, 0\right) u_p \left(x', 0\right) \right\rangle dx' / \int_{-\ell}^{\ell} \left\langle u_p^2 \right\rangle dx$$

The final integration can be carried out approximately, noting that we are eventually interested in averaging

over local oscillations on the orbit

$$4\int_{-\ell}^{\ell} J_0\left(k\left|x-x'\right|\right)\left\langle u_p\left(x,0\right)u_p\left(x',0\right)\right\rangle dx' / \int_{-\ell}^{\ell}\left\langle u_p^2\right\rangle dx \sim \cos\left[k_p x+p_0\left(x\right)\right]\left(1-x^2/d^2\right)^{-1/4} 4\sqrt{\frac{2}{\pi k}}$$

$$\int_{-\ell}^{\ell}\frac{\cos\left(k\left|x-x'\right|-\pi/4\right)}{\sqrt{\left|x-x'\right|}}\cos\left[k_p x'+p_0\left(x'\right)\right]\left(1-x'^2/d^2\right)^{-1/4}dx' / \int_{-\ell}^{\ell}\cos^2\left[k_p x'+p_0\left(x'\right)\right]\left(1-x'^2/d^2\right)^{-1/2}dx'$$

$$\approx 2\sqrt{\frac{2}{\pi k}}\int_{-\ell}^{\ell}\frac{\cos\left(k\left|x-x'\right|-\pi/4\right)}{\sqrt{\left|x-x'\right|}}\left[\cos\left(k_p\left|x-x'\right|\right)+\cos\left(k_p\left(x+x'\right)\right)\right]dx' / \int_{-\ell}^{\ell}\cos^2\left(k_p x'\right)dx'$$

$$\approx \frac{1}{\ell}\sqrt{\frac{2}{\pi k}}\int_{-\ell}^{\ell}\frac{\cos\left(\left(k-k_p\right)\left|x-x'\right|-\pi/4\right)}{\sqrt{\left|x-x'\right|}}dx'$$

$$\approx \frac{1}{\ell}\sqrt{\frac{2}{\pi k}}\int_{-\ell}^{\ell}\frac{\cos\left(\lambda\left|x-x'\right|/\left(4\ell\right)-\pi/4\right)}{\sqrt{\left|x-x'\right|}}dx'$$

where we dropped the phase and amplitude variation in the final expressions. Suppose we examine the integral for $k=k_p$

$$\int_{-\ell}^{\ell}\frac{\cos\left(\pi/4\right)}{\sqrt{\left|x-x'\right|}}dx' = \frac{1}{\sqrt{2}}\int_{-\ell}^{x}\frac{dx'}{\sqrt{x-x'}}+\frac{1}{\sqrt{2}}\int_{x}^{\ell}\frac{dx'}{\sqrt{x'-x}} = \sqrt{2}\left(\sqrt{\ell+x}+\sqrt{\ell-x}\right)$$

The first term in the summand is

$$\left\langle Au_p^2\left(x,0\right)\right\rangle = \frac{2}{\left|U_+'\left(s_p,0\right)\right|^2\sqrt{2kd}\frac{1}{4}\ln\left(\frac{d+\ell}{d-\ell}\right)}\cos^2\left[k_p x+p_0\left(x\right)\right]\left(1-x^2/d^2\right)^{-1/2}$$

$$= \frac{\exp\left[\pi s_p/2\right]\left|\Gamma\left(1/4-is_p/2\right)\right|^2}{\pi\sqrt{kd}\ln\left(\Lambda_+\right)}\cos^2\left[k_p x+p_0\left(x\right)\right]\left(1-x^2/d^2\right)^{-1/2}$$

and if we average over the oscillations of the cosine in $x$

$$\left\langle Au_p^2\left(x,0\right)\right\rangle_x = \frac{1}{\left|U_+'\left(s_p,0\right)\right|^2\sqrt{2kd}\frac{1}{4}\ln\left(\frac{d+\ell}{d-\ell}\right)}\left(1-x^2/d^2\right)^{-1/2}$$

Therefore

$$\left\langle Au^2\left(x,0\right)\right\rangle_x \approx \sum_p\left\langle Au_p^2\left(x,0\right)\right\rangle_x+\left\langle Au_r^2\left(x,0\right)\right\rangle$$

$$-\sum_p\int_{-\ell}^{\ell}4J_0\left(k\left|x-x'\right|\right)\left\langle u_p\left(x,0\right)u_p\left(x',0\right)\right\rangle dx' / \int_{-\ell}^{\ell}\left\langle u_p^2\right\rangle dx$$

Thus

$$\left\langle Au^2(x,0)\right\rangle_x - \left\langle Au_r^2(x,0)\right\rangle \approx \sum_p \left[\left\langle Au_p^2(x,0)\right\rangle_x - \frac{1}{\ell}\sqrt{\frac{2}{\pi k}}\int_{-\ell}^{\ell}\frac{\cos\left(\lambda\left|x-x'\right|/(4\ell)-\pi/4\right)}{\sqrt{\left|x-x'\right|}}dx'\right]$$

If we keep only the term for $k \to k_p$, and (from the Appendix) use the peak value as $s_p \to 0$

$$\left|U_+'(s_{pk},0)\right|^{-2} \approx 3.4$$

as well as use the stability exponent

$$\sqrt{\ell/d} = \frac{\sqrt{\Lambda_+ - 1}}{\left(\sqrt{\Lambda_+}+1\right)}$$

we find

$$\left\langle Au_p^2(x,0)\right\rangle_x \le \frac{3.4\sqrt{\Lambda_+ - 1}}{\sqrt{kL}\left(\sqrt{\Lambda_+}+1\right)\ln(\Lambda_+)}\left(1-x^2/d^2\right)^{-1/2}$$

and

$$\left\langle Au^2(x,0)\right\rangle_x - \left\langle Au_r^2(x,0)\right\rangle \approx \frac{1}{\sqrt{kL}}\left[\frac{3.4\sqrt{\Lambda_+ - 1}}{\left(\sqrt{\Lambda_+}+1\right)\ln(\Lambda_+)}\left(1-x^2/d^2\right)^{-1/2} - 2\sqrt{\frac{2}{\pi}}\left(\sqrt{1+x/\ell}+\sqrt{1-x/\ell}\right)\right]$$

If the stability exponent approaches unity (with $\ell << d$) we drop the function of $x$ and expand the logarithm to obtain

$$\left\langle Au_p^2(x,0)\right\rangle_x \le \frac{1.7}{\sqrt{kL(\Lambda_+ - 1)}}$$

Thus the first term will dominate for stability exponents very near unity. We would also expect that these formulas give an indication of the form of the amplitude as a focus is approached, but fail to be accurate within several wavelengths of the location. Thus taking a half wavelength distance $(d-x) = d_f \ge O(\pi/k)$ gives

$$\left(1-x^2/d^2\right)^{-1/2} \sim 1/\sqrt{2(d-x)/d} = \sqrt{\frac{d}{2d_f}} \le O\left(\sqrt{\frac{kd}{2\pi}}\right) = O\left[\frac{1}{2}\left(\sqrt{\Lambda_+}+1\right)\sqrt{\frac{kL}{\pi(\Lambda_+ - 1)}}\right]$$

$$\left\langle Au_p^2(x,0)\right\rangle_x \le O\left[\frac{1.7}{\pi\ln(\Lambda_+)}\right]$$

This behavior with stability exponent is the same as given recently by a different method [29]. Note that the size of the stability exponent in the bow tie cavity is connected with how close the focal point $d$ comes to the interior cavity region (and how small $d_f$ can be). The random plane wave level on the symmetry axis is

$$\left\langle Au_r^2(x,0)\right\rangle = 2$$

In our particular bow tie cavity, we are away from the focus and can drop $\left(1-x^2/d^2\right)^{-1/2}$, with stability exponent $\Lambda_+ \approx 3.47$, leading to

$$\left\langle Au_p^2(x,0)\right\rangle_x \leq \frac{3.4\sqrt{\Lambda_+ - 1}}{\sqrt{kL}\left(\sqrt{\Lambda_+}+1\right)\ln\left(\Lambda_+\right)} \approx \frac{1.5}{\sqrt{kL}} \approx 0.13$$

Thus we see that there is little effect from the scar. There is doubling of the random plane wave level on the symmetry axis. We have chosen to regard this symmetry doubling as separate from the scar enhancement, as Antonsen did.

### 2.9.1 point statistics from simulations

Several plots are given both out in the volume of the cavity as well as on the $y$ axis (where $L = 2$ m and $R = 10$ m). Figure 14 shows the value of $\left\langle Au^2(0,0)\right\rangle$. This is showing a trend near four.

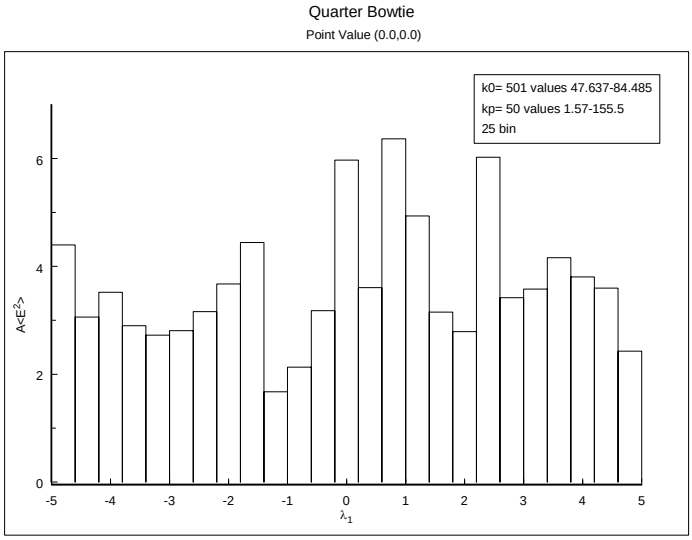


Figure 14. Point histogram of the electric field at the center of the bow tie cavity (on both $x$ and $y$ symmetry planes).

Figure 15 shows $\left\langle Au^2\left(0, 0.2 \text{ m}\right)\right\rangle$ and a trend toward the value two.

Figure 16 shows $\left\langle Au^2\left(0, 0.6 \text{ m}\right)\right\rangle$ and a trend toward the value two.

Figure 17 shows the field out in the cavity $\left\langle Au^2\left(0.5 \text{ m}, 0. \text{ m}\right)\right\rangle$, with a trend toward unity.

## 2.10 Odd Symmetry Along Orbit

The case where the eigenfunction exhibits odd symmetry along the scar orbit is now examined.

### 2.10.1high frequency elliptical solution

We take the function $u$ to be even with respect to the $y$ axis but odd with respect to the $x$ axis. We seek a solution of the form

$$u = W\left(\xi, \zeta\right) e^{i\gamma \sin \xi} - W\left(-\xi, \zeta\right) e^{-i\gamma \sin \xi}$$

The boundary conditions at the mirrors imply

$$\pm u\left(\pm\xi_0, \zeta\right) = W\left(\xi_0, \zeta\right) e^{i\gamma \sin \xi_0} - W\left(-\xi_0, \zeta\right) e^{-i\gamma \sin \xi_0} = 0\,,\ -\zeta_0 < \zeta < \zeta_0$$

or with

$$\Psi\left(\sigma, \tau\right) = e^{-is\sigma} \psi\left(s, \tau\right)$$

we have

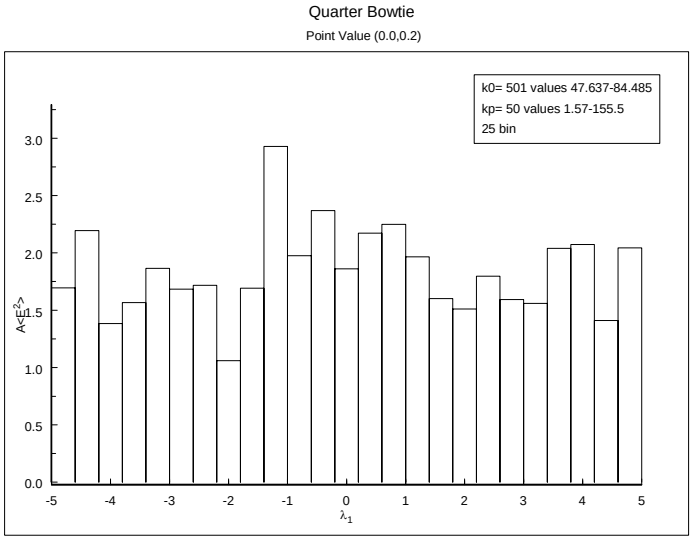


Figure 15. Point histogram of the electric field along $y$ axis at $y = 0.2$ m where $L = 2$ m and $R = 10$ m.

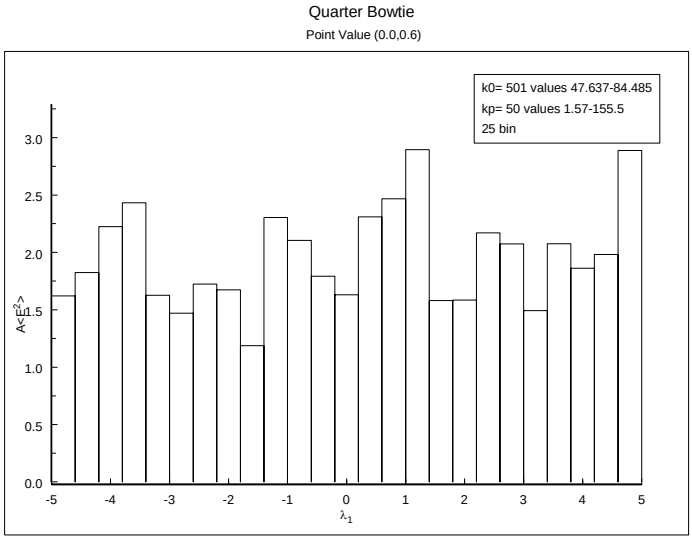


Figure 16. Point histogram of electric field along $y$ axis at $y = 0.6$ m, with $L = 2$ m and $R = 10$ m.

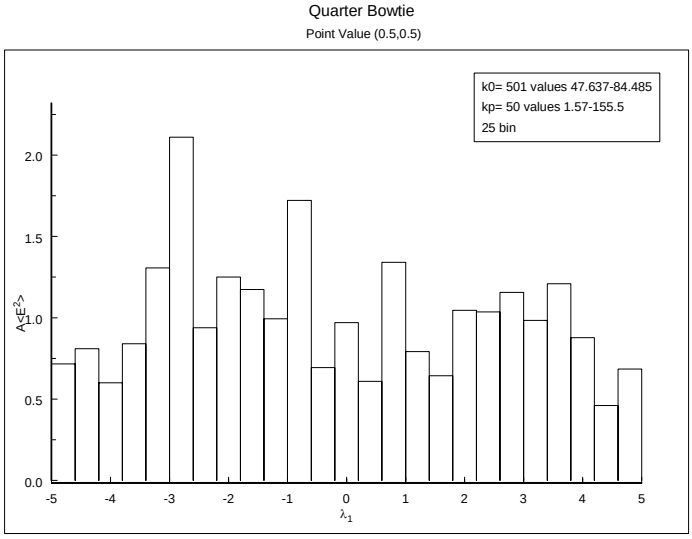


Figure 17. Point histogram of electric field out in the volume with $x = y = 0.5$ m.

$$\Psi\left(\sigma_0,\tau\right)e^{i\gamma\sin\xi_0}-\Psi\left(-\sigma_0,\tau\right)e^{-i\gamma\sin\xi_0}=\psi\left(s,\tau\right)\sin\left(\gamma\sin\xi_0-s\sigma_0\right)=0\,,\,-\zeta_0<\tau/\sqrt{2\gamma}<\zeta_0$$

with

$$\sigma_0=\operatorname{arcsinh}\left(\tan\xi_0\right)=\ln\left[\tan\xi_0+\sec\xi_0\right]$$

Thus we take

$$\gamma\sin\xi_0-s\sigma_0=k\ell-s\sigma_0=p\pi=k_p\ell\,,\,p=0,1,2,3,...$$

Note that

$$\sigma_0=\frac{1}{2}\ln\left(\frac{d+\ell}{d-\ell}\right)=\operatorname{Arcsinh}\left(\sqrt{\ell/R}\right)=\frac{1}{4}\ln\left(\Lambda_+\right)$$

The separation constant $s$ is then

$$s_p=\left(k-k_p\right)\ell/\sigma_0=\frac{\left(k-k_p\right)L/2}{\operatorname{Arcsinh}\left[\sqrt{L/\left(2R\right)}\right]}=2\left(k-k_p\right)L/\ln\left(\Lambda_+\right)$$

In summary the solution is

$$u=\psi\left(s_p,\zeta\sqrt{2kd}\right)\sin\left[kd\sin\xi-s_p\operatorname{Arcsinh}\left(\tan\xi\right)\right]/\sqrt{\cos\xi}$$

where

$$\psi\left(s_p,\tau\right)=c\,\mathrm{Re}\left[U_+\left(s_p,\tau\right)+e^{i\Phi_0}U_+^*\left(s_p,\tau\right)\right]$$

and the phase phase $\Phi_0\left(k^2\right)$ describes the phase relation between a wave leaving the vicinity of the unstable periodic orbit and one returning [30].

### 2.10.2energy theorem normalization

If we let $k$ approach an eigenvalue then the normal derivative of $u_p$ vanishes on the scar $\psi'\left(s_p,0\right)=0$ (because we have selected the even modes across the scarred orbit). Therefore it is only the operation of taking the $\omega$ derivative of these terms in the energy theorem which prevents their vanishing. We thus find

$$\mu_0\varepsilon_0\int_A\left|u\right|^2dS=\int_C u_p\frac{1}{\omega}\frac{\partial}{\partial\omega}\left(\frac{\partial u_p}{\partial n}\right)d\ell$$

The metric coefficients in this system are

$$h_\zeta=h_\xi=d\sqrt{\sinh^2\zeta+\cos^2\xi}$$

Thus

$$\mu_0\varepsilon_0\int_A\left|u\right|^2dS=\int_{-\xi_0}^{\xi_0}u_p\frac{1}{\omega}\frac{\partial}{\partial\omega}\left(\frac{\partial u_p}{\partial\zeta}\right)\frac{h_\xi}{h_\zeta}d\xi$$

where

$$\frac{\partial u_p}{\partial \zeta} = \sqrt{2\gamma}\psi'\left(s_p,0\right)\sin\left[kd\sin\xi - s_p\mathrm{Arcsinh}\left(\tan\xi\right)\right]/\sqrt{\cos\xi}$$

It is only the $\omega$ derivative operation on $\psi'\left(s_p,0\right)$ which contributes

$$\mu_0\varepsilon_0\int_A |u|^2\,dS$$

$$= \sqrt{2\gamma}\int_{-\xi_0}^{\xi_0}\psi\left(s_p,0\right)\frac{1}{\omega}\,\frac{\partial}{\partial\omega}\psi'\left(s_p,\tau\right)\Big|_{\tau=0}\sin^2\left[kd\sin\xi - s_p\mathrm{Arcsinh}\left(\tan\xi\right)\right]\frac{d\xi}{\cos\xi}$$

Now taking the normalization to be

$$\int_A |u|^2\,dS = 1$$

and transforming to

$$\sigma = \mathrm{Arcsinh}\left(\tan\xi\right)$$

$$d\sigma = \sec\xi d\xi$$

$$\sin\xi = \tanh\sigma$$

gives

$$\mu_0\varepsilon_0 = \sqrt{2\gamma}\psi\left(s_p,0\right)\frac{1}{\omega}\,\frac{\partial}{\partial\omega}\psi'\left(s_p,\tau\right)\Big|_{\tau=0}\,2\int_0^{\sigma_0}\sin^2\left(kd\tanh\sigma - s_p\sigma\right)d\sigma$$

If we average over the rapidly varying sine we find

$$\mu_0\varepsilon_0 \sim \sqrt{2\gamma}\psi\left(s_p,0\right)\frac{1}{\omega}\,\frac{\partial}{\partial\omega}\psi'\left(s_p,\tau\right)\Big|_{\tau=0}\sigma_0$$

We approximate this derivative as Antonsen suggested [30] with the outer region phase derivative

$$\frac{\partial}{\partial\omega}\psi'\left(s_p,\tau\right)\Big|_{\tau=0} \sim c\,\mathrm{Re}\left[i\frac{\partial\Phi_0}{\partial\omega}e^{i\Phi_0}U_+^{*\prime}\left(s_p,0\right)\right]$$

Since we are choosing only the even eigenfunctions we must have the normal derivative vanish on the scar orbit. This implies the resonance condition

$$2\,\mathrm{Re}\left[U_+'\left(s_p,0\right) + e^{i\Phi_0}U_+^{*\prime}\left(s_p,0\right)\right] = 0$$

or

$$U_+'\left(s_p,0\right) + e^{i\Phi_0}U_+^{*\prime}\left(s_p,0\right) + U_+^{*\prime}\left(s_p,0\right) + e^{-i\Phi_0}U_+'\left(s_p,0\right) = 0$$

$$\left(1+e^{i\Phi_0}\right)U_+^{*\prime}\left(s_p,0\right)+\left(1+e^{-i\Phi_0}\right)U_+^{\prime}\left(s_p,0\right)=0$$

$$-\frac{1+e^{i\Phi_0}}{1+e^{-i\Phi_0}}=-e^{i\Phi_0}=\frac{U_+^{\prime}\left(s_p,0\right)}{U_+^{*\prime}\left(s_p,0\right)}$$

or

$$-\frac{U_+^{\prime}\left(s_p,0\right)}{U_+^{*\prime}\left(s_p,0\right)}=e^{i\Phi_0}$$

Using this with the Wronskian

$$U_+^{\prime}U_+^{*}-U_+^{*\prime}U_+=i$$

gives

$$\mathrm{Re}\left[U_+\left(s_p,0\right)+e^{i\Phi_0}U_+^{*}\left(s_p,0\right)\right]=\frac{\mathrm{Im}\left[U_+^{\prime}\left(s_p,0\right)\right]}{\left|U_+^{\prime}\left(s_p,0\right)\right|^2}$$

Therefore

$$\mu_0\varepsilon_0\sim c\,\mathrm{Re}\left[U_+\left(s_p,0\right)+e^{i\Phi_0}U_+^{*}\left(s_p,0\right)\right]\frac{1}{\omega}c\,\mathrm{Re}\left[i\frac{\partial\Phi_0}{\partial\omega}e^{i\Phi_0}U_+^{*\prime}\left(s_p,0\right)\right]\sqrt{2\gamma}\sigma_0$$

$$=-c\frac{\mathrm{Im}\left[U_+^{\prime}\left(s_p,0\right)\right]}{\left|U_+^{\prime}\left(s_p,0\right)\right|^2}\frac{1}{\omega}c\,\mathrm{Re}\left[i\frac{\partial\Phi_0}{\partial\omega}U_+^{\prime}\left(s_p,0\right)\right]\sqrt{2\gamma}\sigma_0$$

or

$$\omega\mu_0\varepsilon_0=c^2k\frac{\partial k}{\partial\omega}\left(\frac{d\Phi_0}{dk^2}\right)\frac{\mathrm{Im}^2\left[U_+^{\prime}\left(s_p,0\right)\right]}{\left|U_+^{\prime}\left(s_p,0\right)\right|^2}\sqrt{2\gamma}\ln\left(\frac{d+\ell}{d-\ell}\right)$$

or

$$1=c^2\left(\frac{d\Phi_0}{dk^2}\right)\frac{\mathrm{Im}^2\left[U_+^{\prime}\left(s_p,0\right)\right]}{\left|U_+^{\prime}\left(s_p,0\right)\right|^2}\sqrt{2\gamma}\ln\left(\frac{d+\ell}{d-\ell}\right)$$

or

$$c^2=v^2 8/\left[A\sqrt{2\gamma}\frac{\mathrm{Im}^2\left[U_+^{\prime}\left(s_p,0\right)\right]}{\left|U_+^{\prime}\left(s_p,0\right)\right|^2}\ln\left(\frac{d+\ell}{d-\ell}\right)\right]$$

where we have again used [30]

$$v^2=\frac{A}{8}\left(\frac{d\Phi_0}{dk^2}\right)^{-1}$$

Thus we have the solution

$$u_p(x,0) = \frac{2v\sqrt{2}}{\left|U'_+(s_p,0)\right|\sqrt{A\sqrt{2\gamma}\ln\left(\frac{d+\ell}{d-\ell}\right)}}\sin\left[kx - \frac{1}{2}s_p\ln\left(\frac{d+x}{d-x}\right)\right]\left(1-x^2/d^2\right)^{-1/4}$$

$$= \frac{2v\sqrt{2}}{\left|U'_+(s_p,0)\right|\sqrt{A\sqrt{2\gamma}\ln\left(\frac{d+\ell}{d-\ell}\right)}}\sin\left[k_p x + p_0(x)\right]\left(1-x^2/d^2\right)^{-1/4}$$

where again

$$p_0(x) = \frac{1}{2}s_p\left\{\ln\left(\frac{d+\ell}{d-\ell}\right)(x/\ell) - \ln\left(\frac{d+x}{d-x}\right)\right\}$$

### 2.10.3projection operation

Let us take the projection operator to be defined by

$$V_p = 2\int_0^\ell \left(1-x^2/d^2\right)^{-1/4}\sin\left[k_p x + p_0(x)\right]u(x,0)\,dx$$

$$\sim 2\frac{2v\sqrt{2}}{\left|U'_+(s_p,0)\right|\sqrt{A\sqrt{2\gamma}\ln\left(\frac{d+\ell}{d-\ell}\right)}}\int_0^\ell \left(1-x^2/d^2\right)^{-1/2}\sin^2\left[k_p x + p_0(x)\right]dx$$

Suppose we transform the projection to elliptic cylinder coordinates

$$V_p = 2\int_0^{\xi_0}\sin\left[kd\sin\xi - s_p\mathrm{Arcsinh}(\tan\xi)\right]u_p h_\xi\frac{d\xi}{\sqrt{\cos\xi}}$$

$$h_\xi = d\sqrt{\sinh^2\zeta + \cos^2\xi} \to d\cos\xi$$

with $p$th component

$$u_p = \psi\left(s_p, \zeta\sqrt{2kd}\right)\sin\left[kd\sin\xi - s_p\mathrm{Arcsinh}(\tan\xi)\right]/\sqrt{\cos\xi}$$

$$\psi(s_p,\tau) = c\,\mathrm{Re}\left[U_+(s_p,\tau) + e^{i\Phi_0}U_+^*(s_p,\tau)\right]$$

On axis $\zeta = 0$

$$u_p = \frac{v2\sqrt{2}}{\left|U'_+(s_p,0)\right|\sqrt{A\sqrt{2\gamma}\ln\left(\frac{d+\ell}{d-\ell}\right)}}\sin\left[kd\sin\xi - s_p\mathrm{Arcsinh}(\tan\xi)\right]/\sqrt{\cos\xi}$$

so that

$$V_p = \frac{v2d\sqrt{2}}{\left|U'_+(s_p,0)\right|\sqrt{A\sqrt{2\gamma}\ln\left(\frac{d+\ell}{d-\ell}\right)}} 2\int_0^{\xi_0} \sin^2\left[kd\sin\xi - s_p \mathrm{Arcsinh}\left(\tan\xi\right)\right] d\xi$$

Now for $kd$ large we average over the sine function and find

$$V_p = \frac{v2d\sqrt{2}\xi_0}{\left|U'_+(s_p,0)\right|\sqrt{A\sqrt{2\gamma}\ln\left(\frac{d+\ell}{d-\ell}\right)}}$$

where

$$\xi_0 = \mathrm{Arcsin}\left(\ell/d\right)$$

which is the same answer as obtained previously in the case where the solution had even symmetry along the orbit, except that here

$$k_p\ell = p\pi$$

### 2.10.4random plane wave projection

Let us first consider the random plane wave projection with the simplifying assumption of $d$ large and projection

$$V_{pr} = \int_{-\ell}^{\ell} \sin\left(k_p x\right) u_r\left(x,0\right) dx$$

with [30]

$$u_r = \lim_{N\to\infty} \sqrt{2/\left(AN\right)}\,\mathrm{Re}\left[\sum_{j=1}^{N} a_j e^{i\alpha_j + i\underline{k}\cdot\underline{r}}\right]$$

where $a_j$ are real random numbers with $\left\langle a_j^2\right\rangle = 1$, $|\underline{k}| = k$ are random vectors uniformly distributed in angle, and the random phases $\alpha_j$ are uniformly distributed on a $2\pi$ interval. Thus

$$V_{pr} = \int_{-\ell}^{\ell} \sin\left(k_p x\right) \lim_{N\to\infty} \sqrt{2/\left(AN\right)}\,\mathrm{Re}\left[\sum_{j=1}^{N} a_j e^{i\alpha_j + ikx\cos\theta}\right] dx$$

$$= \int_{-\ell}^{\ell} \sin\left(k_p x\right) \lim_{N\to\infty} \sqrt{2/\left(AN\right)}\left[\sum_{j=1}^{N} a_j \cos\left(\alpha_j + kx\cos\theta\right)\right] dx$$

$$V_{pr}^2 = \lim_{N\to\infty} \sqrt{2/\left(AN\right)} \sum_{j=1}^{N}$$

$$\lim_{N'\to\infty}\sqrt{2/\left(AN'\right)}\sum_{j'=1}^{N'}a_j a_{j'}\int_{-\ell}^{\ell}\int_{-\ell}^{\ell}\sin\left(k_p x\right)\sin\left(k_p x'\right)\cos\left(\alpha_j+kx\cos\theta\right)\cos\left(\alpha_{j'}+kx'\cos\theta\right)dxdx'$$

If we average over the amplitudes $a_j$ and regard different $j$ values as independent the cross terms vanish

$$\left\langle V_{pr}^2\right\rangle_{a_j,\alpha_j}=\lim_{N\to\infty}\frac{2}{AN}\sum_{j=1}^{N}\int_{-\ell}^{\ell}\int_{-\ell}^{\ell}\sin\left(k_p x\right)\sin\left(k_p x'\right)\left\langle\cos\left(\alpha_j+kx\cos\theta\right)\cos\left(\alpha_j+kx'\cos\theta\right)\right\rangle_{\alpha_j}dxdx'$$

with

$$\left\langle\cos\left(\alpha_j+kx\cos\theta\right)\cos\left(\alpha_j+kx'\cos\theta\right)\right\rangle_{\alpha_j}=\frac{1}{2\pi}\frac{1}{2}\int_0^{2\pi}\left[\cos\left(k\left(x-x'\right)\cos\theta\right)+\cos\left(2\alpha_j+k\left(x+x'\right)\cos\theta\right)\right]d\alpha_j$$

$$=\frac{1}{2}\cos\left(k\left(x-x'\right)\cos\theta\right)=\frac{1}{2}\cos\left(kx\cos\theta\right)\cos\left(kx'\cos\theta\right)+\frac{1}{2}\sin\left(kx\cos\theta\right)\sin\left(kx'\cos\theta\right)$$

and

$$\left\langle V_{pr}^2\right\rangle_{a_j,\alpha_j}=\lim_{N\to\infty}\frac{1}{AN}\sum_{j=1}^{N}\int_{-\ell}^{\ell}\sin\left(k_p x\right)\sin\left(kx\cos\theta\right)dx\int_{-\ell}^{\ell}\sin\left(k_p x'\right)\sin\left(kx'\cos\theta\right)dx'$$

$$=\lim_{N\to\infty}\frac{1/4}{AN}\sum_{j=1}^{N}\int_{-\ell}^{\ell}\left[\cos\left(k_p x-kx\cos\theta\right)-\cos\left(k_p x+kx\cos\theta\right)\right]dx$$

$$\int_{-\ell}^{\ell}\left[\cos\left(k_p x'-kx'\cos\theta\right)-\cos\left(k_p x'+kx'\cos\theta\right)\right]dx'$$

or

$$\left\langle V_{pr}^2\right\rangle=\lim_{N\to\infty}\frac{1}{AN}\sum_{j=1}^{N}\left[\frac{\sin\left(k_p-k\cos\theta\right)\ell}{k_p-k\cos\theta}-\frac{\sin\left(k_p+k\cos\theta\right)\ell}{k_p+k\cos\theta}\right]^2$$

$$=\frac{1}{2\pi A}\int_0^{2\pi}\left[\frac{\sin\left(k_p-k\cos\theta\right)\ell}{k_p-k\cos\theta}-\frac{\sin\left(k_p+k\cos\theta\right)\ell}{k_p+k\cos\theta}\right]^2d\theta$$

Now when $k\to k_p$ the first term peaks for $\theta\to 0,2\pi$ and the second term peaks for $\theta\to\pi$. Thus we find (and $\theta=\zeta/\sqrt{k\ell/2}$)

$$\left\langle V_{pr}^2\right\rangle=\frac{1}{2\pi A}\int_{-\infty}^{\infty}\left[\frac{\sin\left(k_p-k+k\theta^2/2\right)\ell}{k_p-k+k\theta^2/2}\right]^2d\theta+\frac{1}{2\pi A}\int_{-\infty}^{\infty}\left[\frac{\sin\left(k_p-k+k\left(\theta-\pi\right)^2/2\right)\ell}{k_p-k+k\left(\theta-\pi\right)^2/2}\right]^2d\theta$$

$$=\frac{\ell^2}{\pi A\sqrt{k\ell/2}}\int_{-\infty}^{\infty}\left[\frac{\sin\left(\left(k_p-k\right)\ell+\zeta^2\right)}{\left(k_p-k\right)\ell+\zeta^2}\right]^2d\zeta$$

Letting

$$\lambda = 2\left(k - k_p\right) L$$

$$\left\langle V_{pr}^2 \right\rangle = \frac{L^2}{2\pi A\sqrt{kL}} \int_{-\infty}^{\infty} \frac{\sin^2\left(\lambda/4 - \zeta^2\right)}{\left(\lambda/4 - \zeta^2\right)^2} d\zeta$$

or

$$\left\langle \sqrt{kL} V_p^2 \right\rangle_r = L^2 G\left(\lambda\right)/A$$

$$G\left(\lambda\right) = \frac{1}{2\pi} \int_{-\infty}^{\infty} \frac{\sin^2\left(\lambda/4 - \zeta^2\right)}{\left(\lambda/4 - \zeta^2\right)^2} d\zeta$$

Introduction of the symmetries gives

$$G_s\left(\lambda\right) = 4G\left(\lambda\right)$$

the same as the even case.

Suppose we use the random plane waves and take the projection with

$$V_{pr} = 2\int_0^{\ell} \left(1 - x^2/d^2\right)^{-1/4} \sin\left[k_p x + p_0\left(x\right)\right] u_r\left(x, 0\right) dx$$

with

$$u_r = \lim_{N\to\infty} \sqrt{2/\left(AN\right)}\, \mathrm{Re}\left[\sum_{j=1}^{N} a_j e^{i\alpha_j + i\underline{k}\cdot\underline{r}}\right]$$

where $a_j$ are real random numbers with $\left\langle a_j^2 \right\rangle = 1$, $|\underline{k}| = k$ are random vectors uniformly distributed in angle, and the random phases $\alpha_j$ are uniformly distributed on a $2\pi$ interval.

$$V_{pr} = 2\int_0^{\ell} \left(1 - x^2/d^2\right)^{-1/4} \sin\left[k_p x + p_0\left(x\right)\right] \lim_{N\to\infty} \sqrt{2/\left(AN\right)}\, \mathrm{Re}\left[\sum_{j=1}^{N} a_j e^{i\alpha_j + ikx\cos\theta}\right] dx$$

The variance of this random variable is

$$\left\langle V_p^2 \right\rangle_r = \frac{1}{2\pi A} \int_0^{2\pi} \left[F_+\left(\theta\right) + F_-\left(\theta\right)\right]^2 d\theta$$

$$F_+\left(\theta\right) + F_-\left(\theta\right) = 2\int_0^{\ell} \left(1 - x^2/d^2\right)^{-1/4} \sin\left[k_p x + p_0\left(x\right)\right] \sin\left(kx\cos\theta\right) dx$$

$$= \int_0^{\ell} \left(1 - x^2/d^2\right)^{-1/4} \left[\cos\left\{k_p x + p_0\left(x\right) - kx\cos\theta\right\} - \cos\left\{k_p x + p_0\left(x\right) + kx\cos\theta\right\}\right] dx$$

Now for large $k$ and $k_p$ we can take $k \to k_p$ and $\theta \to 0, \pi$ (and $\theta = \zeta/\sqrt{k\ell/2}$)

$$k_p - k\cos\theta \approx (k_p - k) + k\theta^2/2$$

$$k_p + k\cos\theta \approx (k_p - k) + k\left(\theta - \pi\right)^2/2$$

and

$$F'_+(\theta) + F'_-(\theta) \approx$$

$$\int_0^\ell \left(1 - x^2/d^2\right)^{-1/4} \left[\cos\left\{\left((k_p - k) + k\theta^2/2\right)x + p_0(x)\right\} - \cos\left\{\left((k_p - k) + k\left(\theta - \pi\right)^2/2\right)x + p_0(x)\right\}\right] dx$$

$$\left\langle V_p^2 \right\rangle_r \approx \frac{1}{2\pi A}\int_0^{2\pi} \left[\int_0^\ell \left(1 - x^2/d^2\right)^{-1/4} \cos\left\{\left((k_p - k) + k\theta^2/2\right)x + p_0(x)\right\} dx\right.$$

$$\left. - \int_0^\ell \left(1 - x^2/d^2\right)^{-1/4} \cos\left\{\left((k_p - k) + k\left(\theta - \pi\right)^2/2\right)x + p_0(x)\right\} dx\right]^2 d\theta$$

$$\approx \frac{1}{\pi A\sqrt{k\ell/2}}\int_{-\infty}^{\infty} \left[\int_0^\ell \left(1 - x^2/d^2\right)^{-1/4} \cos\left\{\left((k_p - k) + \zeta^2/\ell\right)x + p_0(x)\right\} dx\right]^2 d\zeta$$

$$\approx \frac{2}{\pi A\sqrt{k\ell/2}}\int_0^{\infty} \left[\int_0^\ell \left(1 - x^2/d^2\right)^{-1/4} \cos\left\{\left(\lambda/4 - \zeta^2\right)x/\ell - p_0(x)\right\} dx\right]^2 d\zeta$$

$$\lambda = 2\left(k - k_p\right)L$$

$$p_0(x) = \frac{1}{2}s_p\left\{\ln\left(\frac{d+\ell}{d-\ell}\right)(x/\ell) - \ln\left(\frac{d+x}{d-x}\right)\right\}$$

$$s_p \mathrm{Arcsinh}\left[\sqrt{L/(2R)}\right] = \lambda/4$$

the same as the even case.

Thus the odd symmetry along the orbit results in the same statistics but with resonances at $k_p\ell = p\pi$ instead of at $k_p\ell = (p - 1/2)\pi$.

## 2.11 Odd Symmetry Perpendicular To Orbit

The case where the electric field is odd with respect to the normal direction to the orbit is now considered. This will be useful to consider before treating the case where the bow tie cavity is asymmetric with respect to the normal direction to the orbit. To start this problem we first require a form of the normalization condition that can be used for this parity (as well as in the asymmetric case).

### 2.11.1second normalization condition

A second normalization condition can be arrived at by looking at the magnetic current

$$J_{mx} = \left(u_p^+ - u_p^-\right)\delta\left(n\right)$$

where $u_p^+$ is the $p$th component of the eigenfunction immediately above the orbit and $u_p^-$ is the $p$th component immediately below the orbit. The energy theorem [33] with magnetic currents is found from Maxwell's equations

$$\nabla \times \underline{E} = -\underline{J}_m + i\omega\mu_0\underline{H}$$

$$\nabla \times \underline{H} = -i\omega\varepsilon_0\underline{E}$$

by taking

$$\nabla \cdot \left(\frac{\partial \underline{E}}{\partial \omega} \times \underline{H}^* + \underline{E}^* \times \frac{\partial \underline{H}}{\partial \omega}\right)$$

$$= \underline{H}^* \cdot \nabla \times \frac{\partial \underline{E}}{\partial \omega} - \frac{\partial \underline{E}}{\partial \omega} \cdot \nabla \times \underline{H}^* + \frac{\partial \underline{H}}{\partial \omega} \cdot \nabla \times \underline{E}^* - \underline{E}^* \cdot \nabla \times \frac{\partial \underline{H}}{\partial \omega}$$

Next we can write

$$\nabla \times \frac{\partial \underline{E}}{\partial \omega} = \frac{\partial}{\partial \omega}\left(\nabla \times \underline{E}\right) = -\frac{\partial \underline{J}_m}{\partial \omega} + i\omega\mu_0\frac{\partial \underline{H}}{\partial \omega} + i\frac{\partial\left(\omega\mu_0\right)}{\partial \omega}\underline{H}$$

$$\nabla \times \frac{\partial \underline{H}}{\partial \omega} = \frac{\partial}{\partial \omega}\left(\nabla \times \underline{H}\right) = -i\omega\varepsilon_0\frac{\partial \underline{E}}{\partial \omega} - i\frac{\partial\left(\omega\varepsilon_0\right)}{\partial \omega}\underline{E}$$

and thus

$$\nabla \cdot \left(\frac{\partial \underline{E}}{\partial \omega} \times \underline{H}^* + \underline{E}^* \times \frac{\partial \underline{H}}{\partial \omega}\right)$$

$$= -\underline{H}^* \cdot \frac{\partial \underline{J}_m}{\partial \omega} - \frac{\partial \underline{H}}{\partial \omega} \cdot \underline{J}_m^* + i\frac{\partial\left(\omega\varepsilon_0\right)}{\partial \omega}\underline{E} \cdot \underline{E}^* + i\frac{\partial\left(\omega\mu_0\right)}{\partial \omega}\underline{H} \cdot \underline{H}^*$$

Integration over the volume and application of the divergence theorem yields

$$\oint_S \left(\frac{\partial \underline{E}}{\partial \omega} \times \underline{H}^* + \underline{E}^* \times \frac{\partial \underline{H}}{\partial \omega}\right) \cdot \underline{n} dS = i\int_V \left(\mu_0\underline{H} \cdot \underline{H}^* + \varepsilon_0\underline{E} \cdot \underline{E}^*\right) dV - \int_V \left(\frac{\partial \underline{H}}{\partial \omega} \cdot \underline{J}_m^* + \underline{H}^* \cdot \frac{\partial \underline{J}_m}{\partial \omega}\right) dV$$

Using $\underline{n} \times \underline{E} = 0$ on the walls we find

$$\underline{n} \cdot \left(\underline{E}^* \times \frac{\partial \underline{H}}{\partial \omega}\right) = \frac{\partial \underline{H}}{\partial \omega} \cdot \left(\underline{n} \times \underline{E}\right) = 0$$

$$\underline{n}\cdot\left(\frac{\partial\underline{E}}{\partial\omega}\times\underline{H}^*\right)=\underline{H}^*\cdot\left(\underline{n}\times\frac{\partial\underline{E}}{\partial\omega}\right)=\underline{H}^*\cdot\frac{\partial}{\partial\omega}\left(\underline{n}\times\underline{E}\right)=0$$

and

$$i\int_V\left(\mu_0\underline{H}\cdot\underline{H}^*+\varepsilon_0\underline{E}\cdot\underline{E}^*\right)dV=\int_V\left(\frac{\partial\underline{H}}{\partial\omega}\cdot\underline{J}_m^*+\underline{H}^*\cdot\frac{\partial\underline{J}_m}{\partial\omega}\right)dV$$

Noting that

$$\mu_0\underline{H}\cdot\underline{H}^*=\frac{\varepsilon_0}{k^2}\left(\nabla\times\underline{E}\right)\cdot\left(\nabla\times\underline{E}^*\right)$$

and here that

$$\underline{E}=u\underline{e}_z$$

$$\underline{J}_m=J_{mx}\underline{e}_x$$

so that

$$\nabla\times\underline{E}=\nabla\times\left(u\underline{e}_z\right)=\nabla u\times\underline{e}_z$$

and

$$\nabla\times\underline{E}=\nabla u\times\underline{e}_z=i\omega\mu_0\underline{H}$$

$$\underline{e}_x\cdot\left(\nabla u\times\underline{e}_z\right)=\underline{e}_y\cdot\nabla u=\frac{\partial u}{\partial n}$$

$$\varepsilon\underline{E}\cdot\underline{E}^*=\varepsilon\left|u\right|^2$$

$$\mu\underline{H}\cdot\underline{H}^*=\frac{\varepsilon_0}{k^2}\left|\nabla u\right|^2$$

$$\underline{e}_z\times\left(\nabla u\times\underline{e}_z\right)=\nabla u$$

so that

$$i\frac{\varepsilon_0}{k^2}\int_V\left(\left|\nabla u\right|^2+k^2\left|u\right|^2\right)dV=\int_V\left[\frac{\partial}{\partial\omega}\left(\frac{-i}{\omega\mu_0}\frac{\partial u}{\partial n}\right)J_{mx}^*+\frac{i}{\omega\mu_0}\frac{\partial u^*}{\partial n}\frac{\partial J_{mx}}{\partial\omega}\right]dV$$

Now using

$$\left|\nabla u\right|^2=\nabla u\cdot\nabla u^*=\nabla\cdot\left(u^*\nabla u\right)-u^*\nabla^2u=\nabla\cdot\left(u^*\nabla u\right)+k^2\left|u\right|^2$$

gives

$$2\varepsilon_0\mu_0\int_V |u|^2\,dV = \int_V \left[-\frac{\partial}{\partial\omega}\left(\frac{1}{\omega}\frac{\partial u}{\partial n}\right)J^*_{mx} + \frac{1}{\omega}\frac{\partial u^*}{\partial n}\frac{\partial J_{mx}}{\partial\omega}\right]dV$$

In two dimensions

$$2\varepsilon_0\mu_0\int_A |u|^2\,dS = \int_A \left[-\frac{\partial}{\partial\omega}\left(\frac{1}{\omega}\frac{\partial u}{\partial n}\right)J^*_{mx} + \frac{1}{\omega}\frac{\partial u^*}{\partial n}\frac{\partial J_{mx}}{\partial\omega}\right]dS$$

Now inserting the magnetic current excitation

$$J_{mx} = \left(u_p^+ - u_p^-\right)\delta\left(n\right)$$

and assuming asymptotic orthogonality along the scarred orbit

$$2\varepsilon_0\mu_0\int_A |u|^2\,dS = \int_C \left[-\frac{\partial}{\partial\omega}\left(\frac{1}{\omega}\frac{\partial u_p}{\partial n}\right)\left(u_p^+ - u_p^-\right) + \frac{1}{\omega}\frac{\partial u_p}{\partial n}\frac{\partial}{\partial\omega}\left(u_p^+ - u_p^-\right)\right]d\ell$$

Now in this case we regard the magnetic field $\partial u_p/\partial n$ as continuous across the scar and the electric field $u_p$ as discontinuous, when the magnetic current drive is present. As resonance is approached, the discontinuity will disappear and $u_p^+ - u_p^- \to 0$. Thus we keep only the derivative term in frequency

$$2\varepsilon_0\mu_0\int_A |u|^2\,dS \to \int_C \frac{1}{\omega}\frac{\partial u_p}{\partial n}\frac{\partial}{\partial\omega}\left(u_p^+ - u_p^-\right)d\ell$$

This form will clearly provide a normalization on the odd amplitude coefficient. Let us transform to the elliptical system

$$2\varepsilon_0\mu_0\int_A |u|^2\,dS = -\int_C \frac{1}{\omega}\frac{\partial u_p}{\partial\zeta}\frac{\partial}{\partial\omega}\left(u_p^+ - u_p^-\right)\frac{h_\xi}{h_\zeta}d\xi$$

$$= -\int_{-\xi_0}^{\xi_0} \frac{1}{\omega}\frac{\partial u_p}{\partial\zeta}\frac{\partial}{\partial\omega}\left(u_p^+ - u_p^-\right)d\xi$$

where $n$ points in from the upper region. Now taking the area integral equal to unity gives

$$2\varepsilon_0\mu_0 = -\frac{1}{\omega}\sqrt{2\gamma}\int_{-\xi_0}^{\xi_0} \frac{\partial u_p}{\partial\tau}\frac{\partial}{\partial\omega}\left(u_p^+ - u_p^-\right)d\xi$$

### 2.11.2odd normal scar problem

Suppose we have geometric symmetry but we focus on the odd problem. The high frequency solution is taken as

$$u_p = \pm c\,\mathrm{Re}\left[U_+\left(s_p,\tau\right) + e^{i\Phi_0}U_+^*\left(s_p,\tau\right)\right]\cos\left[kd\sin\xi - s_p\mathrm{Arcsinh}\left(\tan\xi\right)\right]/\sqrt{\cos\xi}$$

using the energy theorem

$$2\varepsilon_0\mu_0 = -\frac{1}{\omega}\sqrt{2\gamma}\int_{-\xi_0}^{\xi_0} \frac{\partial u_p}{\partial\tau}\frac{\partial}{\partial\omega}\left(u_p^+ - u_p^-\right)d\xi$$

to determine the normalization. The resonance condition is

$$u_p(\tau = 0) = 0$$

or

$$2\,\mathrm{Re}\left[U_+(s_p,0) + e^{i\Phi_0}U_+^*(s_p,0)\right] = 0$$

$$= \left(1 + e^{-i\Phi_0}\right)U_+(s_p,0) + \left(1 + e^{i\Phi_0}\right)U_+^*(s_p,0)$$

or

$$-\frac{U_+(s_p,0)}{U_+^*(s_p,0)} = e^{i\Phi_0}$$

Now taking the derivatives with the outer phase derivative dominant

$$\frac{\partial}{\partial\omega}\left(u_p^+ - u_p^-\right) = 2c\frac{\partial\Phi_0}{\partial\omega}\,\mathrm{Re}\left[ie^{i\Phi_0}U_+^*(s_p,0)\right]\cos\left[kd\sin\xi - s_p\mathrm{Arcsinh}(\tan\xi)\right]/\sqrt{\cos\xi}$$

$$= 2c\frac{\partial\Phi_0}{\partial\omega}\,\mathrm{Im}\left[U_+(s_p,0)\right]\cos\left[kd\sin\xi - s_p\mathrm{Arcsinh}(\tan\xi)\right]/\sqrt{\cos\xi}$$

$$\frac{\partial u_p}{\partial\tau} = c\,\mathrm{Re}\left[U_+'(s_p,0) + e^{i\Phi_0}U_+^{*\prime}(s_p,0)\right]\cos\left[kd\sin\xi - s_p\mathrm{Arcsinh}(\tan\xi)\right]/\sqrt{\cos\xi}$$

$$= -\frac{c}{\left|U_+(s_p,0)\right|^2}\,\mathrm{Im}\left[U_+(s_p,0)\right]\cos\left[kd\sin\xi - s_p\mathrm{Arcsinh}(\tan\xi)\right]/\sqrt{\cos\xi}$$

and the Wronskian

$$U_+'U_+^* - U_+^{*\prime}U_+ = i$$

Then the energy theory gives

$$\varepsilon_0\mu_0 = \frac{1}{\omega}c^2\sqrt{2\gamma}\frac{\mathrm{Im}^2\left[U_+(s_p,0)\right]}{\left|U_+(s_p,0)\right|^2}\frac{\partial\Phi_0}{\partial\omega}\int_{-\xi_0}^{\xi_0}\cos^2\left[kd\sin\xi - s_p\mathrm{Arcsinh}(\tan\xi)\right]d\xi/\cos\xi$$

Transforming to

$$\sigma = \mathrm{Arcsinh}(\tan\xi)$$

$$d\sigma = \sec\xi d\xi$$

$$\sigma_0 = \frac{1}{2}\ln\left(\frac{d+\ell}{d-\ell}\right) = \mathrm{Arcsinh}\left(\sqrt{\ell/R}\right) = \frac{1}{4}\ln(\Lambda_+)$$

$$\sin\xi = \tanh\sigma$$

gives

$$\mu_0\varepsilon_0 = \frac{1}{\omega}c^2\sqrt{2\gamma}\frac{\mathrm{Im}^2\left[U_+\left(s_p,0\right)\right]}{\left|U_+\left(s_p,0\right)\right|^2}\frac{\partial\Phi_0}{\partial\omega}2\int_0^{\sigma_0}\cos^2\left(kd\tanh\sigma - s_p\sigma\right)d\sigma$$

If we approximate the integral for large $kd$ by averaging over the cosine we find

$$\mu_0\varepsilon_0 \approx \frac{1}{\omega}c^2\sqrt{2\gamma}\frac{\mathrm{Im}^2\left[U_+\left(s_p,0\right)\right]}{\left|U_+\left(s_p,0\right)\right|^2}\frac{\partial\Phi_0}{\partial\omega}\sigma_0 = 2c^2\sqrt{2\gamma}\frac{\mathrm{Im}^2\left[U_+\left(s_p,0\right)\right]}{\left|U_+\left(s_p,0\right)\right|^2}\mu_0\varepsilon_0\frac{d\Phi_0}{dk^2}\sigma_0$$

or

$$1 \approx c^2\sqrt{2\gamma}\frac{\mathrm{Im}^2\left[U_+\left(s_p,0\right)\right]}{\left|U_+\left(s_p,0\right)\right|^2}\frac{d\Phi_0}{dk^2}\ln\left(\frac{d+\ell}{d-\ell}\right)$$

Now using [30]

$$\nu^2 = \frac{A}{8}\left(\frac{d\Phi_0}{dk^2}\right)^{-1}$$

gives

$$\frac{\left|U_+\left(s_p,0\right)\right|^2}{\mathrm{Im}^2\left[U_+\left(s_p,0\right)\right]}\frac{8}{\sqrt{2\gamma}A\ln\left(\frac{d+\ell}{d-\ell}\right)}v^2 \approx c^2$$

The only difference between this amplitude for the odd case and the amplitude in the even case is that the derivatives are missing. The normal derivative on the scar is then

$$\frac{\partial u_p}{\partial\tau} = \frac{1}{\sqrt{2\gamma}}\frac{\partial u_p}{\partial\zeta} = -\frac{v}{\left|U_+\left(s_p,0\right)\right|}\sqrt{\frac{8}{\sqrt{2\gamma}A\ln\left(\frac{d+\ell}{d-\ell}\right)}}\cos\left[kd\sin\xi - s_p\mathrm{Arcsinh}\left(\tan\xi\right)\right]/\sqrt{\cos\xi}$$

Now let us find the projection

$$V_p' = -2\int_0^{\ell}\left(1-x^2/d^2\right)^{-1/4}\cos\left[k_p x + p_0\left(x\right)\right]\frac{1}{k}\frac{\partial u}{\partial y}\left(x,0\right)dx$$

where

$$p_0\left(x\right) = \frac{1}{2}s_p\left\{\ln\left(\frac{d+\ell}{d-\ell}\right)\left(x/\ell\right) - \ln\left(\frac{d+x}{d-x}\right)\right\}$$

Transforming to elliptic cylinder coordinates

$$V_p' = -2\int_0^{\xi_0}\cos\left[kd\sin\xi - s_p\mathrm{Arcsinh}\left(\tan\xi\right)\right]\frac{1}{k}\frac{\partial u}{\partial\zeta}\frac{h_\xi}{h_\zeta}\frac{d\xi}{\sqrt{\cos\xi}}$$

$$= -2\sqrt{2\gamma}\int_0^{\xi_0}\cos\left[kd\sin\xi - s_p\mathrm{Arcsinh}\left(\tan\xi\right)\right]\frac{1}{k}\frac{\partial u}{\partial\tau}\frac{d\xi}{\sqrt{\cos\xi}}$$

$$= \frac{v}{|U_+(s_p,0)|}\sqrt{\frac{8}{\sqrt{2\gamma}A\ln\left(\frac{d+\ell}{d-\ell}\right)}}\frac{2}{k}\sqrt{2\gamma}\int_0^{\xi_0}\cos^2\left[kd\sin\xi - s_p\text{Arcsinh}\left(\tan\xi\right)\right]\frac{d\xi}{\cos\xi}$$

If we average over the cosine for large $kd$ we have

$$V_p' \approx \frac{v}{|U_+(s_p,0)|}\sqrt{\frac{8}{\sqrt{2\gamma}A\ln\left(\frac{d+\ell}{d-\ell}\right)}}\frac{1}{k}\sqrt{2\gamma}\int_0^{\xi_0}\sec\xi d\xi$$

$$= \frac{v/k}{|U_+(s_p,0)|}\sqrt{\frac{8\sqrt{2\gamma}}{A\ln\left(\frac{d+\ell}{d-\ell}\right)}}\ln\left(\sec\xi_0+\tan\xi_0\right)$$

$$\sinh\sigma_0 = \tan\xi_0$$

$$\sec\xi_0 = \cosh\sigma_0$$

$$\ln\left(\sec\xi_0+\tan\xi_0\right) = \sigma_0$$

Alternatively transforming to $\sigma = \text{Arcsinh}(\tan\xi)$ gives

$$V_p' = \frac{v}{|U_+(s_p,0)|}\sqrt{\frac{8}{\sqrt{2\gamma}A\ln\left(\frac{d+\ell}{d-\ell}\right)}}\frac{2}{k}\sqrt{2\gamma}\int_0^{\sigma_0}\cos^2\left(kd\tanh\sigma - s_p\sigma\right)d\sigma$$

Now for large $kd$

$$V_p' = \frac{v\sigma_0/k}{|U_+(s_p,0)|}\sqrt{\frac{8\sqrt{2\gamma}}{A\ln\left(\frac{d+\ell}{d-\ell}\right)}} = \frac{v/k}{|U_+(s_p,0)|}\sqrt{\frac{2\sqrt{2\gamma}}{A}\ln\left(\frac{d+\ell}{d-\ell}\right)}$$

Thus we find

$$\left\langle kL\sqrt{kL}V_p'^2\right\rangle = \frac{1}{|U_+(s_p,0)|^2}\frac{2L\sqrt{2Ld}}{A}\ln\left(\frac{d+\ell}{d-\ell}\right)$$

where

$$U_+(s,\tau) = e^{-\pi(s+i/2)/4}U\left(-is,\tau e^{-i\pi/4}\right)$$

and $U$ is the standard parabolic cylinder function [31], with limit

$$U_+(s,0) = e^{-\pi(s+i/2)/4}2^{is_p/2-1/4}\frac{\sqrt{\pi}}{\Gamma\left(3/4-is/2\right)}$$

Thus

$$\left\langle kL\sqrt{kL}V_p'^2\right\rangle = e^{\pi s_p/2}\left|\Gamma\left(3/4-is_p/2\right)\right|^2\frac{4L\sqrt{Ld}}{\pi A}\ln\left(\frac{d+\ell}{d-\ell}\right)$$

or in terms of stability exponent

$$\left\langle kL\sqrt{kL}V_p'^2\right\rangle = \frac{1}{\pi}2^{1/2}e^{\pi s_p/2}\left|\Gamma\left(3/4-is_p/2\right)\right|^2\frac{L^2}{A}\left(\sqrt{\Lambda_+}+1\right)\frac{\ln\left(\Lambda_+\right)}{\sqrt{\Lambda_+-1}}$$

$$\sqrt{\ell/d} = \frac{\sqrt{\Lambda_+-1}}{\left(\sqrt{\Lambda_+}+1\right)}$$

$$s_p = 2\left(k-k_p\right)L/\ln\left(\Lambda_+\right)$$

Noting the asymptotic form

$$\frac{1}{\pi}2^{-1/2}e^{\pi s_p/2}\left|\Gamma\left(3/4-is_p/2\right)\right|^2 \sim \sqrt{s_p}\ ,\ s_p\to\infty$$

we see that this projection grows as $\sqrt{s_p}$

$$\left\langle kL\sqrt{kL}V_p'^2\right\rangle \sim \frac{4L\sqrt{2Lds_p}}{A}\ln\left(\frac{d+\ell}{d-\ell}\right)\ ,\ s_p\to\infty$$

### 2.11.3random plane wave odd projection

Suppose we use the random plane wave representation and take the projection with

$$V_{pr}' = -2\int_0^\ell\left(1-x^2/d^2\right)^{-1/4}\cos\left[k_px+p\left(x\right)\right]\frac{1}{k}\frac{\partial u_r}{\partial y}\left(x,0\right)dx$$

where

$$u_r = \lim_{N\to\infty}\sqrt{2/\left(AN\right)}\,\mathrm{Re}\left[\sum_{j=1}^N a_j e^{i\alpha_j+i\underline{k}\cdot\underline{r}}\right]$$

where $a_j$ are real random numbers with $\left\langle a_j^2\right\rangle = 1$, $|\underline{k}| = k$ are random vectors uniformly distributed in angle, and the random phases $\alpha_j$ are uniformly distributed on a $2\pi$ interval. The normal derivative is then

$$\frac{1}{k}\frac{\partial u_r}{\partial y} = \lim_{N\to\infty}\sqrt{2/\left(AN\right)}\,\mathrm{Re}\left[\sum_{j=1}^N a_j\frac{k_y}{k}e^{i\alpha_j+i\underline{k}\cdot\underline{r}}\right]$$

The variance of this random variable is

$$\left\langle V_p'^2\right\rangle_r = \frac{1}{2\pi A}\int_0^{2\pi}\left[F_+'\left(\theta\right)+F_-'\left(\theta\right)\right]^2 d\theta$$

$$F_+'\left(\theta\right)+F_-'\left(\theta\right) = 2\int_0^\ell\left(1-x^2/d^2\right)^{-1/4}\cos\left[k_px+p_0\left(x\right)\right]\sin\theta\cos\left(kx\cos\theta\right)dx$$

$$= \int_0^\ell \left(1 - x^2/d^2\right)^{-1/4} \left[\cos\left\{k_p x + p_0(x) + kx\cos\theta\right\} + \cos\left\{k_p x + p_0(x) - kx\cos\theta\right\}\right] \sin\theta dx$$

Now for large $k$ and $k_p$ we can take $k \to k_p$ and $\theta \to 0, \pi$ (and $\theta = \zeta/\sqrt{k\ell/2}$)

$$k_p - k\cos\theta \approx (k_p - k) + k\theta^2/2$$

$$k_p + k\cos\theta \approx (k_p - k) + k(\theta - \pi)^2/2$$

and

$$F'_+(\theta) + F'_-(\theta) \approx \int_0^\ell \left(1 - x^2/d^2\right)^{-1/4}$$

$$\left[(\pi - \theta)\cos\left\{\left((k_p - k) + k(\theta - \pi)^2/2\right)x + p_0(x)\right\} + \theta\cos\left\{\left((k_p - k) + k\theta^2/2\right)x + p_0(x)\right\}\right] dx$$

$$\left\langle V_p^2 \right\rangle_r \approx \frac{1}{2\pi A} \int_0^{2\pi} \left[\int_0^\ell \left(1 - x^2/d^2\right)^{-1/4} (\pi - \theta)\cos\left\{\left((k_p - k) + k(\theta - \pi)^2/2\right)x + p_0(x)\right\} dx\right.$$

$$\left. + \int_0^\ell \left(1 - x^2/d^2\right)^{-1/4} \theta\cos\left\{\left((k_p - k) + k\theta^2/2\right)x + p_0(x)\right\} dx\right]^2 d\theta$$

$$\approx \frac{1}{\pi A (k\ell/2)^{3/2}} \int_{-\infty}^\infty \left[\int_0^\ell \left(1 - x^2/d^2\right)^{-1/4} \zeta\cos\left\{\left((k_p - k) + \zeta^2/\ell\right)x + p_0(x)\right\} dx\right]^2 d\zeta$$

$$\approx \frac{2}{\pi A (k\ell/2)^{3/2}} \int_0^\infty \left[\int_0^\ell \left(1 - x^2/d^2\right)^{-1/4} \zeta\cos\left\{\left(\lambda/4 - \zeta^2\right)x/\ell - p_0(x)\right\} dx\right]^2 d\zeta$$

$$\lambda = 2(k - k_p)L$$

$$p_0(x) = \frac{1}{2} s_p \left\{\ln\left(\frac{d + \ell}{d - \ell}\right)(x/\ell) - \ln\left(\frac{d + x}{d - x}\right)\right\}$$

$$s_p \text{Arcsinh}\left[\sqrt{L/(2R)}\right] = \lambda/4$$

or

$$\left\langle (kL)^{3/2} V_p^2 \right\rangle_r = L^2 G'(\lambda)/A$$

with

$$G'(\lambda) = \frac{4}{\pi} \int_0^\infty \left[\int_0^\ell \left(1 - x^2/d^2\right)^{-1/4} \zeta\cos\left\{\left(\lambda/4 - \zeta^2\right)x/\ell - p_0(x)\right\} dx/\ell\right]^2 d\zeta$$

Now due to the symmetries we take

$$\left\langle (kL)^{3/2} V_p^2 \right\rangle_r = L^2 G_s'(\lambda)/A$$

$$G_s'(\lambda) = 4G' = \frac{16}{\pi}\int_0^\infty \left[\int_0^\ell \left(1 - x^2/d^2\right)^{-1/4} \zeta \cos\left\{\left(\lambda/4 - \zeta^2\right) x/\ell - p_0(x)\right\} dx/\ell\right]^2 d\zeta$$

$$= \frac{16}{\pi}\int_0^\infty \left[\int_0^1 \left(1 - x^2\ell^2/d^2\right)^{-1/4} \zeta \cos\left\{\left(\lambda/4 - \zeta^2\right) x - p_0(x\ell)\right\} dx\right]^2 d\zeta$$

If we take the limit $\ell << d$ then the inner integral becomes

$$\int_0^\ell \left(1 - x^2/d^2\right)^{-1/4} \zeta \cos\left\{\left(\lambda/4 - \zeta^2\right) x/\ell - p_0(x)\right\} dx/\ell \to \int_0^\ell \zeta \cos\left\{\left(\lambda/4 - \zeta^2\right) x/\ell\right\} dx/\ell = \zeta \frac{\sin\left(\lambda/4 - \zeta^2\right)}{\left(\lambda/4 - \zeta^2\right)}$$

and thus

$$G_s'(\lambda) \to \frac{16}{\pi}\int_0^\infty \frac{\sin^2\left(\lambda/4 - \zeta^2\right)}{\left(\lambda/4 - \zeta^2\right)^2}\zeta^2 d\zeta$$

$$s_p = \lambda/\ln(\Lambda_+)$$

Figure 18 shows a comparison of the odd scar projection (solid curve) and the random plane wave projection (dashed curve is the preceding simplified expression). The dotted curve is the large $s_p$ form of the odd scar theory (it is set to zero for negative $s_p$). There is no enhancement of the field relative to the random plane wave projection but there is a reduction (antiscar) for $s_p < 5$. However because the scaling here is $(kL)^{3/2}$ versus $(kL)^{1/2}$ in the even case, the contribution from the odd case is correspondingly smaller.

Figure 19 shows the comparison between the histogram generated along the $L = 2$ m and $R = 10$ m orbit in the symmetric bow tie for the odd problem (normal derivative of the field) along with the odd scar theory projection and the random plane wave projection.

## 2.12 Asymmetric Bow Tie Cavity

The case where the outer regions are not symmetrical is now considered. We first generalize the original energy theorem to the case where the function is not even on the orbit.

### 2.12.1first normalization condition

From the energy theorem

$$i2\varepsilon_0 \int_A |u|^2 dS = \int_A \left(\frac{\partial u}{\partial \omega} J_z^* + u^* \frac{\partial J_z}{\partial \omega}\right) dS$$

with in this case

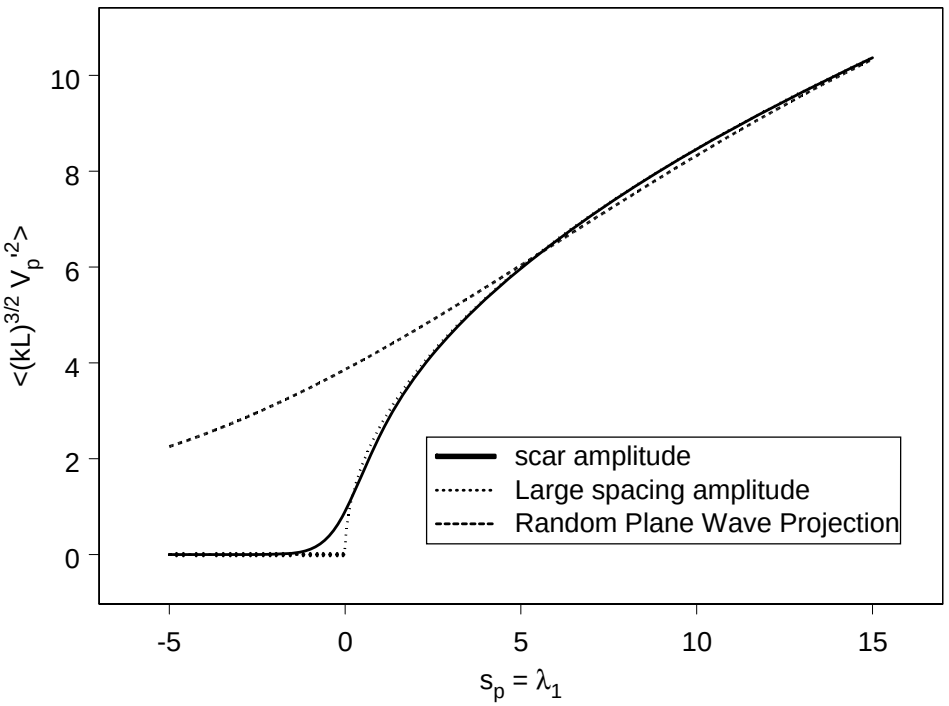


Figure 18. Comparison of scar projection and random plane wave projection for electric field which is odd with respect to the normal of the orbit. Geometry is $L = 2$ m and $R = 10$ m. The dotted curve is the asymptotic scar projection for large $s_p$.

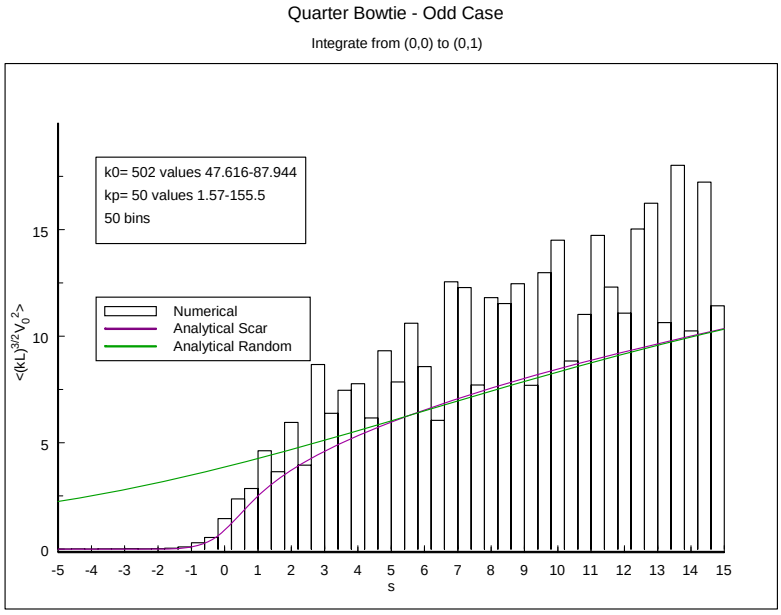


Figure 19. Odd problem in symmetric bow tie cavity. Histogram is for the projection of the normal derivative of the field on orbit (magnetic field). Theory is odd scar mode projection and odd random plane wave projection.

$$J_z = \frac{i}{\omega\mu_0}\left(\frac{\partial u_p^+}{\partial n} - \frac{\partial u_p^-}{\partial n}\right)\delta(n)\ ,\ y = 0$$

we have (we take $u$ to be continuous at $y = 0$)

$$i2\varepsilon_0 \int_A |u|^2\, dS = \frac{i}{\mu_0}\int_C \left[-\frac{\partial u}{\partial\omega}\frac{1}{\omega}\left(\frac{\partial u_p^+}{\partial n} - \frac{\partial u_p^-}{\partial n}\right)^* + u^*\frac{\partial}{\partial\omega}\frac{1}{\omega}\left(\frac{\partial u_p^+}{\partial n} - \frac{\partial u_p^-}{\partial n}\right)\right] d\ell$$

Taking the eigenfunction as real and assuming the integrals along the scar produce approximate orthogonality (we take $u_p$ to be continuous at $y = 0$)

$$2\varepsilon_0 \int_A |u|^2\, dS = \frac{1}{\mu_0}\int_C \left[-\frac{\partial u_p}{\partial\omega}\frac{1}{\omega}\left(\frac{\partial u_p^+}{\partial n} - \frac{\partial u_p^-}{\partial n}\right) + u_p\frac{\partial}{\partial\omega}\frac{1}{\omega}\left(\frac{\partial u_p^+}{\partial n} - \frac{\partial u_p^-}{\partial n}\right)\right] d\ell$$

Now in the elliptic system

$$2\varepsilon_0 \int_A |u|^2\, dS = \frac{1}{\mu_0}\int_C \left[-\frac{\partial u_p}{\partial\omega}\frac{1}{\omega}\left(\frac{\partial u_p^+}{\partial\zeta} - \frac{\partial u_p^-}{\partial\zeta}\right) + u_p\frac{\partial}{\partial\omega}\frac{1}{\omega}\left(\frac{\partial u_p^+}{\partial\zeta} - \frac{\partial u_p^-}{\partial\zeta}\right)\right]\frac{h_\xi}{h_\zeta} d\xi$$

Setting

$$\int_A |u|^2\, dS = 1$$

gives

$$2\varepsilon_0\mu_0 = \int_{-\xi_0}^{\xi_0}\left[-\frac{\partial u_p}{\partial\omega}\frac{1}{\omega}\left(\frac{\partial u_p^+}{\partial\zeta} - \frac{\partial u_p^-}{\partial\zeta}\right) + u_p\frac{\partial}{\partial\omega}\frac{1}{\omega}\left(\frac{\partial u_p^+}{\partial\zeta} - \frac{\partial u_p^-}{\partial\zeta}\right)\right] d\xi$$

Now noting that we eventually want to take the limit as the eigenfunction derivative becomes continuous across $y = 0$

$$2\varepsilon_0\mu_0 = \int_{-\xi_0}^{\xi_0} u_p\frac{1}{\omega}\frac{\partial}{\partial\omega}\left(\frac{\partial u_p^+}{\partial\zeta} - \frac{\partial u_p^-}{\partial\zeta}\right) d\xi$$

$$= \frac{1}{\omega}\sqrt{2\gamma}\int_{-\xi_0}^{\xi_0} u_p\frac{\partial}{\partial\omega}\left(\frac{\partial u_p^+}{\partial\tau} - \frac{\partial u_p^-}{\partial\tau}\right) d\xi$$

### 2.12.2even and odd decomposition

Suppose we decompose the general field by writing

$$u_p = \psi(s_p, \tau)\cos\left[kd\sin\xi - s_p\mathrm{Arcsinh}(\tan\xi)\right]/\sqrt{\cos\xi}$$

and

$$\psi = \psi_e + \psi_o$$

with the even and odd functions defined as

$$\psi_e = c_e \,\mathrm{Re}\left[U_+\left(s_p,|\tau|\right) + e^{i\Phi_0}U_+^*\left(s_p,|\tau|\right)\right]$$

$$\psi_o = c_o \,\mathrm{Re}\left[U_+\left(s_p,|\tau|\right) + e^{i\Phi_1}U_+^*\left(s_p,|\tau|\right)\right]\mathrm{sgn}\left(\tau\right)$$

where in the asymmetric case we have two random phase functions. Note that the even solution is continuous at $\tau = 0$, whereas the odd solution has continuous normal derivative at $\tau = 0$. Thus the scar continuity conditions apply separately to these two. Continuity of the normal derivative only involves the even part

$$2\,\mathrm{Re}\left[U_+'\left(s_p,0\right) + e^{i\Phi_0}U_+^{*\prime}\left(s_p,0\right)\right] = 0$$

$$= \left(1 + e^{-i\Phi_0}\right)U_+'\left(s_p,0\right) + \left(1 + e^{i\Phi_0}\right)U_+^{*\prime}\left(s_p,0\right)$$

or

$$e^{i\Phi_0} = -\frac{U_+'\left(s_p,0\right)}{U_+^{*\prime}\left(s_p,0\right)} = \frac{\left[U_+'\left(s_p,0\right)\right]^2}{\left|U_+'\left(s_p,0\right)\right|^2}$$

whereas continuity of the field only involves the odd part

$$2\,\mathrm{Re}\left[U_+\left(s_p,0\right) + e^{i\Phi_1}U_+^*\left(s_p,0\right)\right] = 0$$

$$= \left(1 + e^{-i\Phi_1}\right)U_+\left(s_p,0\right) + \left(1 + e^{i\Phi_1}\right)U_+^*\left(s_p,0\right)$$

or

$$e^{i\Phi_1} = -\frac{U_+\left(s_p,0\right)}{U_+^*\left(s_p,0\right)} = -\frac{\left[U_+\left(s_p,0\right)\right]^2}{\left|U_+\left(s_p,0\right)\right|^2}$$

The normalization conditions are

$$2\varepsilon_0\mu_0 = \frac{1}{\omega}\sqrt{2\gamma}\int_{-\xi_0}^{\xi_0} u_p \frac{\partial}{\partial\omega}\left(\frac{\partial u_p^+}{\partial\tau} - \frac{\partial u_p^-}{\partial\tau}\right)d\xi$$

$$2\varepsilon_0\mu_0 = \frac{1}{\omega}\sqrt{2\gamma}\int_{-\xi_0}^{\xi_0} \frac{\partial u_p}{\partial\tau}\frac{\partial}{\partial\omega}\left(u_p^+ - u_p^-\right)d\xi$$

where we write

$$2u_p = u_p^+ + u_p^-$$

$$2\frac{\partial u_p}{\partial\tau} = \frac{\partial u_p^+}{\partial\tau} + \frac{\partial u_p^-}{\partial\tau}$$

Using these relations, the even and odd normalization conditions also separate as

$$2\varepsilon_0\mu_0 = \frac{1}{\omega}\sqrt{2\gamma}\int_0^{\xi_0}\left(u_p^+ + u_p^-\right)\frac{\partial}{\partial\omega}\left(\frac{\partial u_p^+}{\partial\tau} - \frac{\partial u_p^-}{\partial\tau}\right)d\xi$$

$$2\varepsilon_0\mu_0 = \frac{1}{\omega}\sqrt{2\gamma}\int_0^{\xi_0}\left(\frac{\partial u_p^+}{\partial\tau} + \frac{\partial u_p^-}{\partial\tau}\right)\frac{\partial}{\partial\omega}\left(u_p^+ - u_p^-\right)d\xi$$

where only the even condition shows up in the first and only the odd shows up in the second. Thus we end up with two separate two-by-two systems for the coefficients and for the resonant frequencies. Since we have assumed that the local geometry is completely symmetric, this splitting is not too surprising. The question is if and how the random phases are connected (should even and odd resonant frequencies be degenerate?). We anticipate that as $k \to k_p$ the coupling between even and odd problems is reduced, since the local geometry is symmetric and the ray "spends large amounts of time" in the region of the scar. If the phases are not correlated, then the even and odd scar modes will in general resonate at different eigenfrequencies. There could be accidental degeneracies if the two phases are realized in a certain way to make the two resonant frequencies the same, but in general they will be distinct. This means that statistics along the scarred orbit in the general case will be the same as the even case for $E_z$ and the same as the odd case for $H_x$ (assuming the area is maintained the same). Note that the frequency derivatives of the phase functions will be approximately the same as in the symmetric cavity since the average modal spacing for each set of modes is expected to be the same.

### 2.12.3 comparisons of even-odd theory with asymmetric simulations

The asymmetric bow tie cavity has $L = 2$ m and $R = 10$ m along the orbit. The other two radii are $R = 1.5$ m and $R = 2$ m, creating the asymmetry. Figure 20 shows the projection of the electric field along the orbit compared to the even scar theory. The agreement looks similar to the symmetric cavity results.

Figure 21 shows a comparison of the asymmetric cavity histogram for the projection of the normal derivative of the electric field on the orbit with the odd theory. The results look similar to the symmetric cavity for the odd case.

Figure 22 shows electric field intensity for a typical eigenmode in the top half of the asymmetric bow tie cavity. The chaotic nature of the field for typical eigenfunctions is apparent.

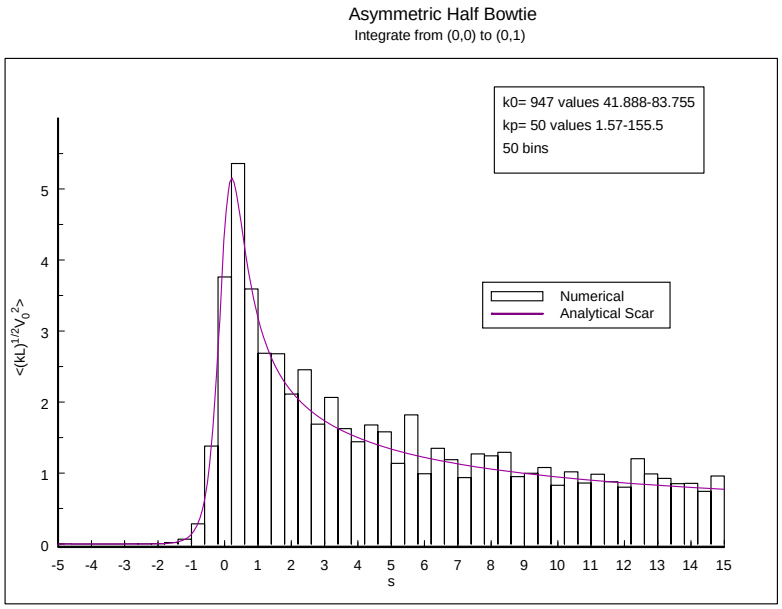


Figure 20. Comparison of histogram for the projection of the electric field along the orbit in the asymmetrical bow tie cavity with the even theory and random plane wave projection.

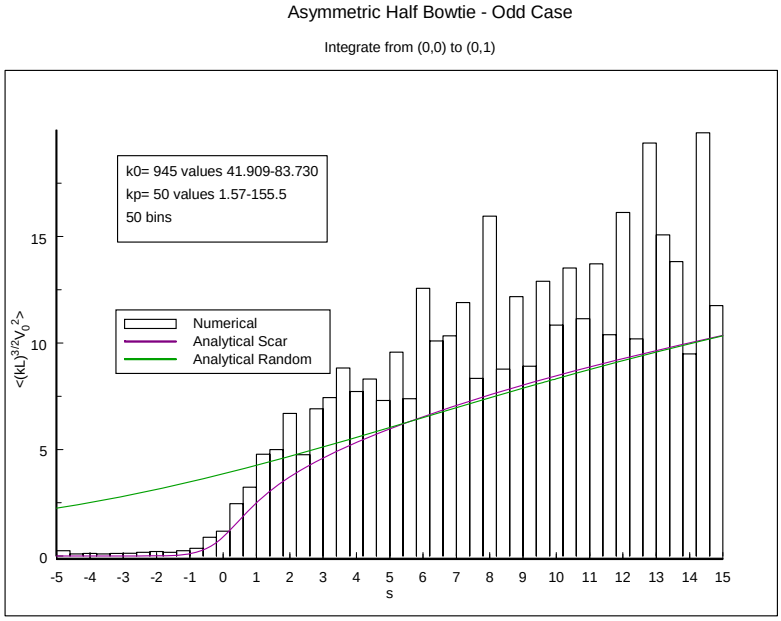


Figure 21. Histogram is for the projection of the normal derivative of the field on the orbit (magnetic field) in the asymmetric bow tie cavity. Theory is odd scar mode projection and odd random plane wave projection.

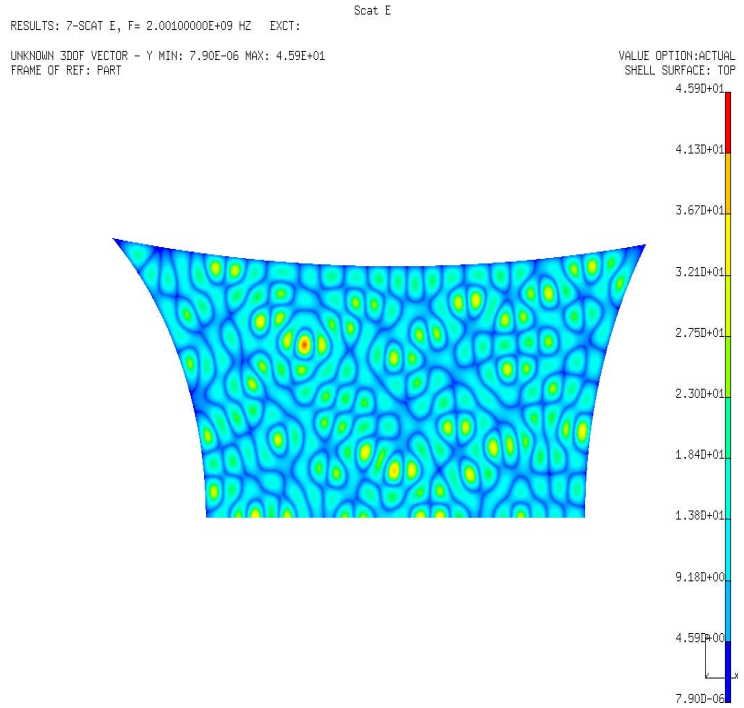


Figure 22. The electric field intensity of a typical eigenfunction in the asymmetric bow tie cavity showing random behavior.

Figure 23 shows electric field intensity for a vertical scar $p = 15$ in the top half of the asymmetric bow tie cavity.

Figure 24 shows electric field intensity for another vertical scar $p = 19$ in the top half of the asymmetric bow tie cavity.

Figure 25 shows electric field intensity for a horizontal scar along the symmetry line in the top half of the asymmetric bow tie cavity.

# 3 CONCAVE MIRRORS AND STADIUM CAVITY

The stadium cavity will be used as a canonical example of an unstable cavity with concave walls. The application of the scar theory of Antonsen to the stadium cavity with a bouncing ball mode between the concave walls is now considered.

## 3.1 Geometry

Taking the wall radius of curvature to be $R$ and the path across the major axis to be $L > 2R$, we write the stability exponents as (here we reverse the sign of $R$ for the concave mirror from the formulas above in the bow tie cavity for the convex mirror)

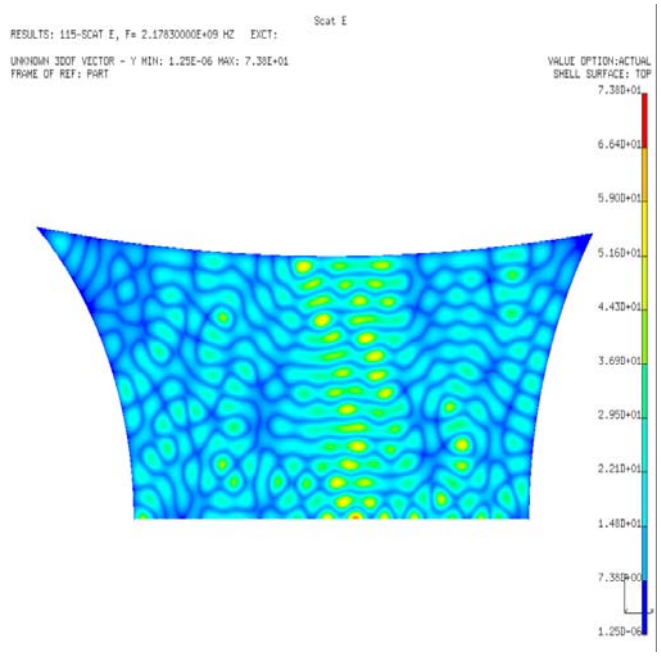


Figure 23. Vertical scar electric field intensity in asymmetric bow tie cavity $k\ell \approx 45.654$ and with $p = 15$, $k_p\ell \approx 45.5531$.

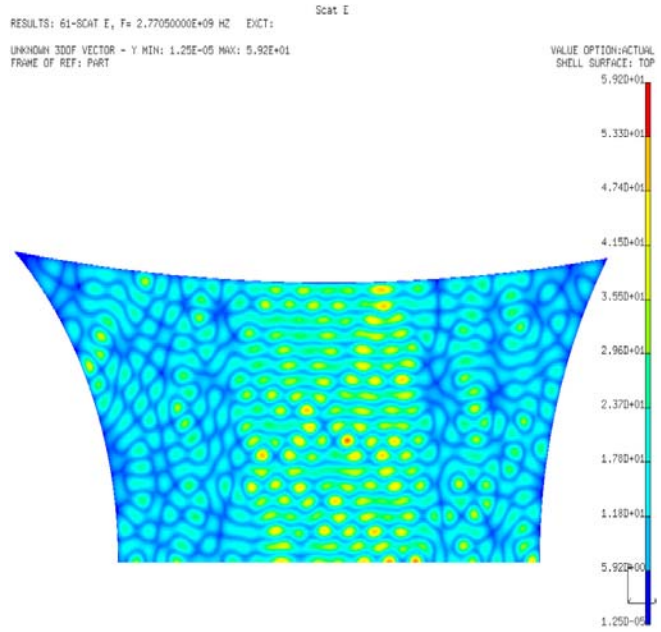


Figure 24. Another vertical scar electric field intensity plot with $k\ell \approx 58.065$ and with $p = 19$, $k_p\ell \approx 58.12$.

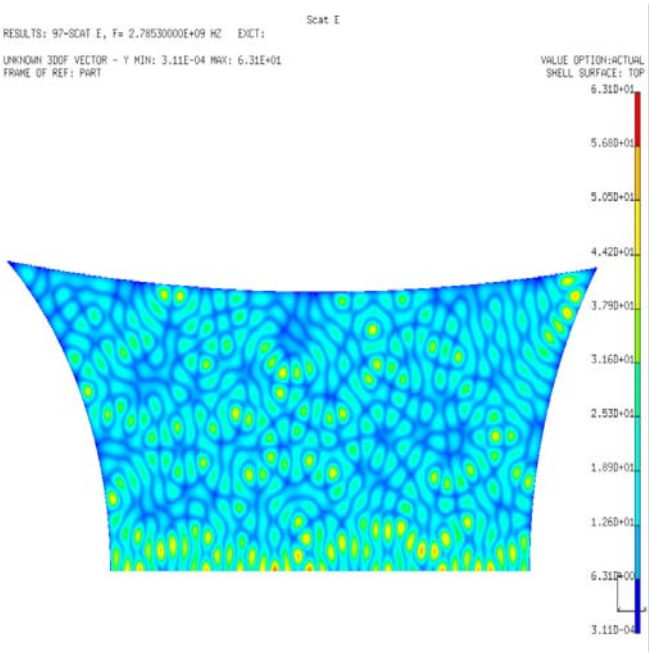


Figure 25. Horizontal scar electric field intensity in asymmetric bow tie cavity.

$$\Lambda_{\pm} = \lambda_{\pm}^2 = \left[ (L/R - 1) \pm \sqrt{(L/R - 1)^2 - 1} \right]^2$$

$$\Lambda_{+} = 2\,(L/R - 2)\,(L/R) + 1 + 2\,(L/R - 1)\,\sqrt{(L/R - 2)\,(L/R)}$$

If we take $L = 2.2R$ (we are using $L = 0.55$ m and $R = 0.25$ m in these short stadium examples) then

$$\Lambda_{+} = 3.472$$

For this geometry we chose the value of $\Lambda_{+}$ to be the same as in the bow tie cavity and intended to apply the same scar theory results. However it is clear from a picture of the fields in Figure 26 that more is going on (for example, the hot spot at the focus).

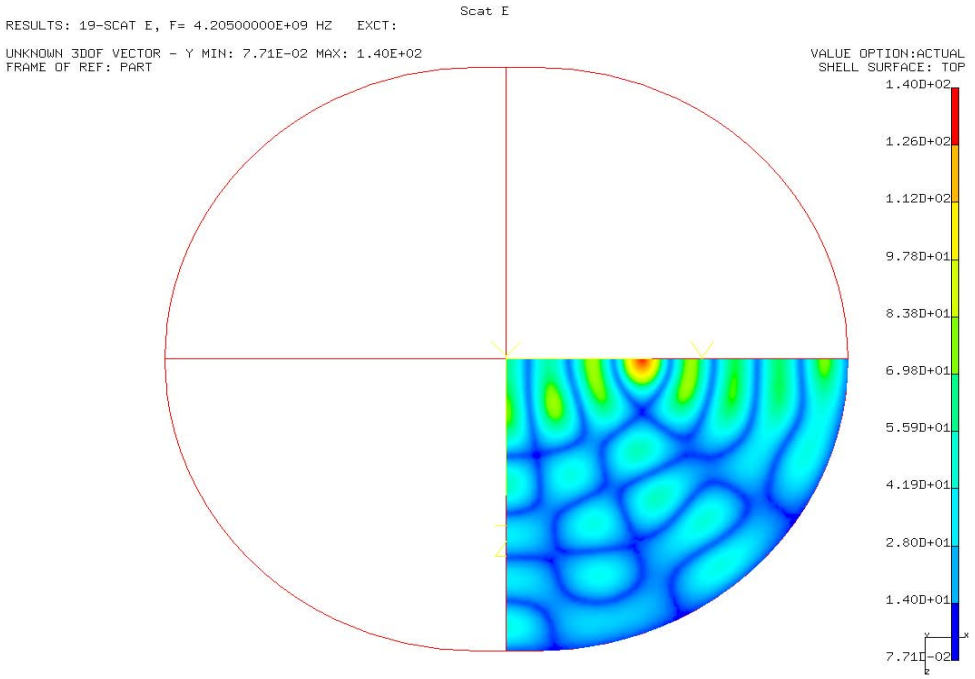


Figure 26. Bouncing ball mode along horizontal axis in stadium cavity at 4.205 GHz. The geometry has $L = 0.55$ m and $R = 0.25$ m.

The resonance condition can be easily found by tracing a ray along the orbit. Starting at the origin using time dependence $e^{-i\omega t}$, we reflect off the mirror at $x = \ell$ with a $\pi$ phase shift, then pass through the right focal point with a $-\pi/2$ phase shift [34], and back to the origin with $2p\pi$ total phase accumulation (required at the symmetry line).

$$2k_p\ell + \pi - \pi/2 = 2p\pi \ , \ p = 1, 2, ...$$

Because of the foci, the simple Fourier expansion of the field used in the convex case is not justified. We break up the cavity into three regions and assume evenness of the field. Region 1 is between foci and Region 2 is outside the foci. Region 3 is in the vicinity of the foci. We now want to solve the problem between concave mirrors containing two foci. Here we will apply Vaynshteyn's method along the major axis of the elliptical cavity. We can adjust the ellipse to match local curvature and separation distances of the stadium.

## 3.2 Elliptical High Frequency Analysis In Outer Two Regions

Vaynshteyn has treatments for stable modes between concave mirrors. Here we wish to consider the generalization to unstable modes between concave mirrors. Following Vaynshteyn [18] we have Figure 27 where

$$x = d \cosh\zeta \sin\xi$$

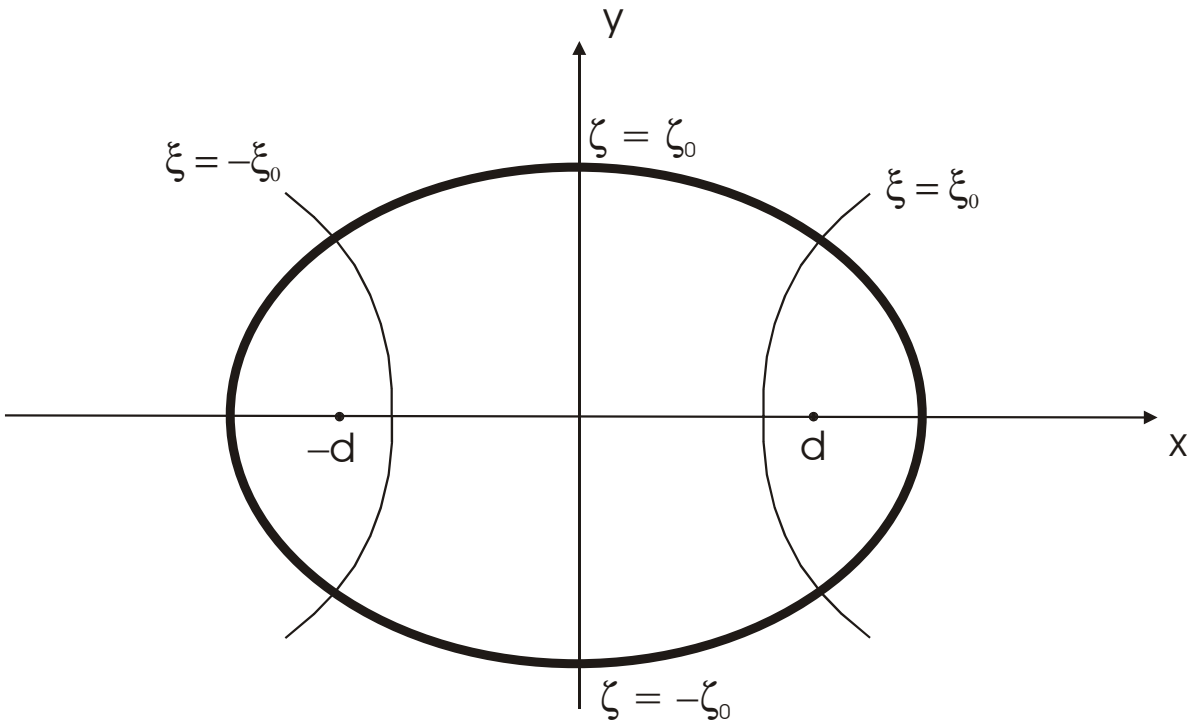


Figure 27. Elliptic cylinder geometry for modeling stadium horizontal scar.

$$y = d \sinh\zeta \cos\xi$$

$$-\infty < \zeta < \infty$$

$$-\pi/2 < \xi < \pi/2$$

We take

$$L = 2\ell$$

where

$$\ell = d \cosh\zeta_0$$

On the mirror we have

$$x = d \cosh\zeta_0 \sin\xi$$

$$y = d \sinh\zeta_0 \cos\xi$$

$$\sqrt{1-\left[y/\left(d\sinh\zeta_0\right)\right]^2}=\sin\xi$$

As $y\to 0$ we have

$$\sin\xi\sim 1-\frac{1}{2}\left[y/\left(d\sinh\zeta_0\right)\right]^2$$

and

$$x\sim d\cosh\zeta_0-\frac{y^2}{2d}\frac{\cosh\zeta_0}{\sinh^2\zeta_0}$$

On a circle of radius $R$, centered at $(x_0,0)$ where $x_0=d\cosh\zeta_0-R$, we can write

$$\left(x-x_0\right)^2+y^2=R^2$$

$$x=d\cosh\zeta_0-R+\sqrt{R^2-y^2}\sim d\cosh\zeta_0-\frac{y^2}{2R}$$

Thus

$$R=d\sinh^2\zeta_0/\cosh\zeta_0$$

Also

$$R=d\left(\cosh\zeta_0-1/\cosh\zeta_0\right)$$

$$\ell=d\cosh\zeta_0$$

and

$$R=\ell-d^2/\ell$$

$$d=\sqrt{\ell\left(\ell-R\right)}=\ell\sqrt{1-R/\ell}$$

### 3.2.1 modal description in region one: between foci

Figure 28 shows the regions near the scarred orbit on the major axis.

The modes of the Helmholtz equation

$$\nabla^2u+k^2u=0$$

are now investigated. This can be written in these two-dimensions as [18]

$$\frac{\partial^2u}{\partial\xi^2}+\frac{\partial^2u}{\partial\zeta^2}+\gamma^2\left(\cosh^2\zeta-\sin^2\xi\right)u=0$$

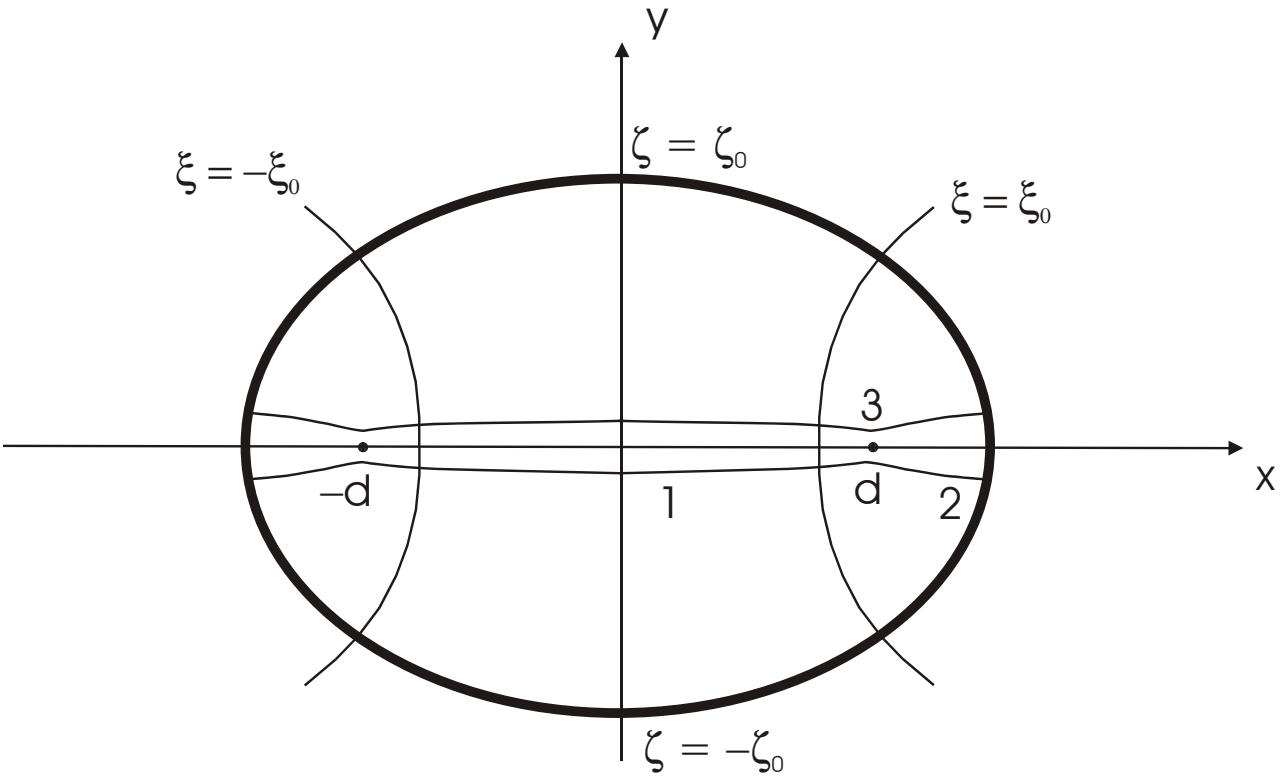


Figure 28. Elliptical cylinder geometry showing the three regions about the focal point used in modeling the horizontal scar.

where

$$\gamma = kd = k\ell\sqrt{1 - R/\ell}$$

We assume $\gamma >> 1$. On the mirror we want

$$u = 0\,,\ \zeta = \pm\zeta_0\,,\ \xi_0 < |\xi| < \pi/2$$

We will solve the problem separately in the several regions of the stadium cavity. We assume in the first region that we are inside the foci with $-\xi_0 < \xi < \xi_0$ and that near the orbit we have $\sinh^2\zeta << 1$. We take the function $u$ to be even about the $x$ and $y$ axes. We seek a solution of the form [18]

$$u = W(\xi,\zeta)\, e^{i\gamma\sin\xi} + W(-\xi,\zeta)\, e^{-i\gamma\sin\xi}\ ,\ \ |\xi| < \xi_0$$

Substituting into the Helmholtz equation

$$\frac{\partial^2 W}{\partial\xi^2} + \frac{\partial^2 W}{\partial\zeta^2} + 2i\gamma\cos\xi\frac{\partial W}{\partial\xi} + \left(\gamma^2\sinh^2\zeta - i\gamma\sin\xi\right)W = 0$$

Now ignoring the $\partial^2 W/\partial\xi^2$ term [18] and using $\sinh^2\zeta \approx \zeta^2$, we have (this is the first term of an asymptotic series as discussed in the appendix)

$$\frac{\partial^2 W}{\partial\zeta^2} + 2i\gamma\cos\xi\frac{\partial W}{\partial\xi} + \left(\gamma^2\zeta^2 - i\gamma\sin\xi\right)W \approx 0$$

Now we take

$$W = \frac{1}{\sqrt{\cos\xi}}\Psi$$

$$\tau = \sqrt{2\gamma}\zeta$$

$$\sigma = \int_0^\xi \frac{d\xi}{\cos\xi} = \operatorname{arcsinh}(\tan\xi)$$

$$\sigma_0 = \operatorname{arcsinh}(\tan\xi_0) = \ln\left[\tan\xi_0 + \sec\xi_0\right]$$

gives

$$\frac{\partial^2\Psi}{\partial\tau^2} + i\frac{\partial\Psi}{\partial\sigma} + \frac{\tau^2}{4}\Psi = 0$$

Letting

$$\Psi(\sigma,\tau) = e^{-is\sigma}\psi(s,\tau)$$

gives

$$\frac{\partial^2 \psi}{\partial \tau^2} + \left( \frac{\tau^2}{4} + s \right) \psi = 0$$

This is a form of the equation of the parabolic cylinder functions. The solutions are (we are using notation and normalization consistent with Antonsen [30])

$$\psi(s,\tau) = c\,\mathrm{Re}\left[ U_+(s,\tau) + e^{i\Phi_0} U_+^*(s,\tau) \right]$$

$$U_+(s,\tau) = e^{-\pi(s+i/2)/4} U\left( -is, \tau e^{-i\pi/4} \right)$$

where $U(a,z)$ is the parabolic cylinder function in Abramowitz [31]. The transverse boundary condition in $\tau$ is a reflection with a random phase $\Phi_0\left(k^2\right)$ which was introduced by Antonsen to match to the chaotic region of the cavity. The asymptotic form of the parabolic cylinder function gives

$$U_+(s,\tau) \sim e^{i\tau^2/4 - (1/2 - is)\ln\tau} = e^{i\tau^2/4} \tau^{is-1/2}\ ,\ \tau \to +\infty$$

### 3.2.2 modal description in region two: outside foci

In the second region outside the foci we assume that $-\zeta_0 < \zeta < \zeta_0$ and that $\cos^2\xi << 1$. We seek a second solution of the form

$$u = W(\xi,\zeta)\, e^{i\gamma\cosh\zeta} + W(-\xi,\zeta)\, e^{-i\gamma\cosh\zeta}\ ,\ \ |\xi| > \xi_0$$

$$x = d\cosh\zeta\sin\xi$$

$$y = d\sinh\zeta\cos\xi$$

Note that the sign change in the exponential goes with the sign change of $\xi$ before the limit $\xi \to \pi/2$ is applied. The parity in $\xi$ is actually required since the Region 1 matching (which is even in $\xi$) will make the disjoint region two's have even parity also. The fact that this introduces the standing wave in Region 2 is comforting.

In this second region we could also change the coordinate system to have, $-\pi < \xi < \pi$, and $0 < \zeta < \infty$. This makes the coordinates continuous across $y = 0$. Substituting into the Helmholtz equation

$$\frac{\partial^2 u}{\partial \xi^2} + \frac{\partial^2 u}{\partial \zeta^2} + \gamma^2 \left( \cosh^2\zeta - \sin^2\xi \right) u = 0$$

$$\frac{\partial^2 W}{\partial \xi^2} + \frac{\partial^2 W}{\partial \zeta^2} + 2i\gamma\sinh\zeta\frac{\partial W}{\partial \zeta} + \left( i\gamma\cosh\zeta + \gamma^2\cos^2\xi \right) W = 0$$

Let us now substitute the second term $W(-\xi,\zeta)\, e^{-i\gamma\cosh\zeta}$ into the Helmholtz equation

$$\frac{\partial^2 W}{\partial \xi^2} + \frac{\partial^2 W}{\partial \zeta^2} - 2i\gamma\sinh\zeta\frac{\partial W}{\partial \zeta} + \left( -i\gamma\cosh\zeta + \gamma^2\cos^2\xi \right) W = 0$$

The original equation is not recovered by choosing a change in sign of $\xi$. It can be recovered by a $\pm i\pi$ shift

in $\zeta$ where $\cosh(\zeta \pm i\pi) = -\cosh\zeta$ and $\sinh(\zeta \pm i\pi) = -\sinh\zeta$. Let us take

$$u = W(\xi,\zeta)\, e^{i\gamma\cosh\zeta} + W(\xi,\zeta - i\pi)\, e^{-i\gamma\cosh\zeta} \ , \ \ |\xi| > \xi_0$$

Now ignoring the $\partial^2 W/\partial\zeta^2$ term and using $\cos^2\xi = \cos^2(\pi/2 - |\xi| - \pi/2) = \sin^2(\pi/2 - |\xi|) \approx (\pi/2 - |\xi|)^2$, we have

$$\frac{\partial^2 W}{\partial \xi^2} + 2i\gamma\sinh\zeta\frac{\partial W}{\partial\zeta} + \left[i\gamma\cosh\zeta + \gamma^2(\pi/2 - |\xi|)^2\right] W \approx 0$$

We will focus on the $\xi > 0$ side so we can define $\xi' = \pi/2 - \xi$, $|\xi'| < \pi/2 - \xi_0$. To generalize to both sides of Region 2 we can take $\xi' = \pm\pi/2 - \xi$

$$\frac{\partial^2 W}{\partial \xi'^2} + 2i\gamma\sinh\zeta\frac{\partial W}{\partial\zeta} + \left(i\gamma\cosh\zeta + \gamma^2\xi'^2\right) W \approx 0$$

(If we avoided the focal region, should we connect the region with $y > 0$ interior to the focus to the region $y < 0$ outside the focus? Does this lead to a more symmetrical looking transverse solution? In other words we could take $\xi' = \xi - \pi/2 > 0$ and $\cos\xi = \cos\left(\xi' + \pi/2\right) = -\sin\xi' \approx -\xi'$.) Now letting

$$W = \frac{1}{\sqrt{\sinh\zeta}}\Psi$$

$$\tau' = \sqrt{2\gamma}\xi'$$

$$\sigma' = \int_\infty^\zeta \frac{d\zeta}{\sinh\zeta} = \ln\left[\tanh(\zeta/2)\right]$$

gives

$$\sinh\zeta\frac{\partial}{\partial\zeta} = \sinh\zeta\frac{\partial\sigma'}{\partial\zeta}\frac{\partial}{\partial\sigma'} = \frac{\partial}{\partial\sigma'}$$

$$\frac{\partial^2}{\partial\tau'^2}\Psi + i\frac{\partial\Psi}{\partial\sigma'} + \frac{1}{4}\tau'^2\Psi \approx 0$$

Note that

$$\sigma' = \int_\infty^{\zeta - i\pi} \frac{d\zeta}{\sinh\zeta} = -\int_\infty^\zeta \frac{d\zeta}{\sinh\zeta}$$

$$\sigma'_0 = \ln\left[\tanh(\zeta_0/2)\right]$$

$$\sqrt{\sinh(\zeta - i\pi)} \to -i\sqrt{\sinh\zeta}$$

Note that this sign of the square root agrees with that used in the ray tracing phase shift through the focus. Because of the mirror boundary condition this equation must be integrated under the restriction that

$$\Psi\left(\sigma_0', \tau'\right) = \Psi\left(-\sigma_0', \tau'\right) e^{i\chi}$$

$$\chi = -2\gamma \cosh\zeta_0 + \pi\left(2n-1\right) + \pi/2 = -kL + \pi\left(2n-1\right) + \pi/2$$

Letting

$$\Psi\left(\sigma', \tau'\right) = e^{-is'\sigma'} \psi\left(s', \tau'\right)$$

gives

$$\frac{\partial^2 \psi}{\partial \tau'^2} + \left(\frac{\tau'^2}{4} + s'\right)\psi = 0$$

The mirror condition gives

$$1 = e^{i2s'\sigma_0' + i\chi}$$

$$2s'\sigma_0' + \chi = 2m\pi$$

$$2s'\sigma_0' = 2m\pi + kL - \pi\left(2n-1\right) - \pi/2 = 2\left(m-n\right)\pi + \pi/2 + kL$$

$$= -\left(2p - 1/2\right)\pi + kL = \left(k - k_p\right) L$$

where

$$k_p L = \pi\left(2p - 1/2\right)$$

$$p = 1, 2, ...$$

We take the real part at the end of the Region 2 construction.

### 3.2.3 more symmetrical version of region two solution

It turns out to be convenient to take the solution in Region 2 as

$$u = e^{-i\pi/4}\left[W\left(\xi,\zeta\right) e^{i\gamma\cosh\zeta} + W\left(\xi, \zeta - i\pi\right) e^{-i\gamma\cosh\zeta}\right] \ , \ \ |\xi| > \xi_0$$

This choice eliminates a factor $e^{i\pi/4}$ that would appear in subsequent sections.

### 3.2.4 more general version of region two solution

To make sure we have not missed any choices in the second solution, suppose we take the solution in Region 2 to be more generally

$$u = e^{-i\pi/4 - i\Phi_1/2}\left[W\left(\xi,\zeta\right) e^{i\gamma\cosh\zeta} + e^{i\Phi_1} W\left(\xi, \zeta - i\pi\right) e^{-i\gamma\cosh\zeta}\right] \ , \ \ |\xi| > \xi_0$$

$$= \frac{1}{\sqrt{\sinh\zeta}}\left[\Psi\left(\sigma',\tau'\right)e^{i\gamma\cosh\zeta - i\pi/4 - i\Phi_1/2} + \Psi\left(-\sigma',\tau'\right)e^{-i\gamma\cosh\zeta + i\pi/4 + i\Phi_1/2}\right]$$

$$= \frac{2}{\sqrt{\sinh\zeta}}\psi\left(s',\tau'\right)\cos\left(\gamma\cosh\zeta - s'\sigma' - \pi/4 - \Phi_1/2\right)$$

where

$$\psi\left(s',\tau'\right) = c\,\mathrm{Re}\left[U_+\left(s',\tau'\right) + e^{i\Phi_0'}U_+^*\left(s',\tau'\right)\right]$$

$$U_+\left(s,\tau\right) = e^{-\pi(s+i/2)/4}U\left(-is,\tau e^{-i\pi/4}\right)$$

$$\tau' = \sqrt{2\gamma}\xi'$$

$$\xi' = \pm\pi/2 - \xi$$

$$2s'\sigma_0' = 2s'\ln\left[\tanh\left(\zeta_0/2\right)\right] = \left(k - k_p\right)L$$

$$\sigma' = \int_\infty^\zeta \frac{d\zeta}{\sinh\zeta} = \ln\left[\tanh\left(\zeta/2\right)\right]$$

The mirror condition gives

$$\cos\left(\gamma\cosh\zeta_0 - s'\sigma_0' - \pi/4 - \Phi_1/2\right) = \cos\left(k_p\ell - \pi/4 - \Phi_1/2\right) = 0$$

or

$$k_p\ell - \pi/4 - \Phi_1/2 = \pi\left(p - 1/2\right)$$

At this point we can think of $k_p$ and hence $s'$ as still arbitrary ($k_p$ and $s'$ are directly related). The introduced phase $\Phi_1$ is selected to match the mirror boundary condition.

### 3.2.5 modified region one solution

Because the solution must be even in $\xi$ we can write in Region 1

$$u = C\left[W\left(\xi,\zeta\right)e^{i\gamma\sin\xi} + W\left(-\xi,\zeta\right)e^{-i\gamma\sin\xi}\right]\ ,\ \ |\xi| < \xi_0$$

$$= C\frac{1}{\sqrt{\cos\xi}}\left[\Psi\left(\sigma,\tau\right)e^{i\gamma\sin\xi} + \Psi\left(-\sigma,\tau\right)e^{-i\gamma\sin\xi}\right]$$

$$= 2\frac{\psi\left(s,\tau\right)}{\sqrt{\cos\xi}}\cos\left(\gamma\sin\xi - s\sigma\right)$$

$$= 2C\frac{\psi(s,\tau)}{\sqrt{\sin\xi'}}\cos\left(\gamma\cos\xi' - s\sigma\right)\ ,\ \xi' = \pi/2 - \xi$$

For matching purposes (with Region 2) it is convenient to take

$$\psi(s,\tau) = c\,\mathrm{Re}\left[e^{-i\pi/4}U_+(s,\tau) + e^{i\pi/4}e^{i\Phi_0}U_+^*(s,\tau)\right]$$

$$\sigma = \int_0^\xi \frac{d\xi}{\cos\xi} = \mathrm{arcsinh}\left(\tan\xi\right)$$

$$= \ln\left(\tan\xi + \sec\xi\right) = \ln\left\{\tan\frac{1}{2}\left(\xi + \pi/2\right)\right\} = -\ln\left\{\tan\left(\xi'/2\right)\right\}$$

$$\tau = \sqrt{2\gamma}\zeta$$

$$U_+(s,\tau) = e^{-\pi(s+i/2)/4}U\left(-is, \tau e^{-i\pi/4}\right)$$

## 3.3 Behavior Near Focal Region And Matching

We now consider matching through the focal region.

### 3.3.1 approach of focal point

We first take the limits of the outer two regions as the focal region is approached. However to allow flexibility in phase matching at the focus, we will allow the focal point to shift by a small amount in the Region 1 and Region 2 solutions (this is somewhat similar to matching done in a nonlinear shock problem [35] where the matching boundary is allowed to vary to first order in position) relative to the Region 3 solution

$$d \to d + \delta$$

$$\gamma \to \gamma + k\delta$$

where $\delta << d$ is a geometrically small shift. Thus in Region 1 we find

$$u \sim 2Cc\,\mathrm{Re}\left[e^{-i\pi/4}U_+\left(s, \sqrt{2\gamma}\zeta\right) + e^{i\pi/4}e^{i\Phi_0}U_+^*\left(s, \sqrt{2\gamma}\zeta\right)\right]$$

$$\xi'^{-1/2}\cos\left[\gamma\left(1 - \xi'^2/2\right) + k\delta + s\ln\left(\xi'/2\right)\right]\ ,\ \xi' \to 0$$

In Region 2 we find

$$u \sim 2c\,\mathrm{Re}\left[U_+\left(s', \sqrt{2\gamma}\xi'\right) + e^{i\Phi_0'}U_+^*\left(s', \sqrt{2\gamma}\xi'\right)\right]$$

$$\zeta^{-1/2}\cos\left[\gamma\left(1+\zeta^2/2\right)+k\delta-s'\ln\left(\zeta/2\right)-\pi/4-\Phi_1/2\right]\,,\,\zeta\to 0$$

where

$$s'\ln\left[\tanh\left(\zeta_0/2\right)\right]=\left(k-k_p\right)\ell$$

$$k_p\ell-\pi/4-\Phi_1/2=\pi\left(p-1/2\right)$$

### 3.3.2 small shift in focal position

We can also view this shift as a change in the original coordinate system $(x,y)$ or $(\xi,\zeta)$ or $\left(\xi',\zeta\right)$

$$x=d\cosh\zeta\sin\xi=d\cosh\zeta\cos\xi'\sim d\left(1+\zeta^2/2-\xi'^2/2\right)$$

$$y=d\sinh\zeta\cos\xi=d\sinh\zeta\sin\xi'\sim d\zeta\xi'$$

to the focal coordinate system $(x',y')$ or $\left(\widehat{\xi}',\widehat{\zeta}\right)$ with

$$x-\delta=x'=d\cosh\widehat{\zeta}\cos\widehat{\xi}'\sim d\left(1+\widehat{\zeta}^2/2-\widehat{\xi}'^2/2\right)$$

$$y=y'=d\sinh\widehat{\zeta}\sin\widehat{\xi}'\sim d\widehat{\zeta}\widehat{\xi}'$$

Thus the small shift $\delta$ enters as an additive correction as in the preceding section.

### 3.3.3 focal region three

Near the focus $\xi=\pi/2$ and $\zeta=0$ we approximate the Helmholtz equation

$$\frac{\partial^2 u}{\partial\xi^2}+\frac{\partial^2 u}{\partial\zeta^2}+\gamma^2\left(\cosh^2\zeta-\sin^2\xi\right)u=0$$

or

$$\frac{\partial^2 u}{\partial\xi^2}+\frac{\partial^2 u}{\partial\zeta^2}+\gamma^2\left(\sinh^2\zeta+\cos^2\xi\right)u=0$$

as $\xi'=\pi/2-\xi$ (we are assuming that $\zeta^4<<1$ and that $\xi'^4<<1$)

$$\frac{\partial^2 u}{\partial\xi^2}+\frac{\partial^2 u}{\partial\zeta^2}+\gamma^2\left(\sinh^2\zeta+\sin^2\xi'\right)u=0$$

or

$$\frac{\partial^2 u}{\partial\xi'^2}+\frac{\partial^2 u}{\partial\zeta^2}+\gamma^2\left(\zeta^2+\xi'^2\right)u=0$$

Separating variables

$$u = X\left(\xi'\right) Z\left(\zeta\right)$$

$$\left(\frac{1}{X}\frac{\partial^2 X}{\partial \xi'^2} + \gamma^2 \xi'^2\right) + \left(\frac{1}{Z}\frac{\partial^2 Z}{\partial \zeta^2} + \gamma^2 \zeta^2\right) = 0$$

Taking the separation constant to be $2\gamma g$ we find

$$\frac{\partial^2 X}{\partial \xi'^2} + \left(-2\gamma g + \gamma^2 \xi'^2\right) X = 0$$

$$\frac{\partial^2 Z}{\partial \zeta^2} + \left(2\gamma g + \gamma^2 \zeta^2\right) Z = 0$$

Thus we find parabolic cylinder equations in both directions. Letting

$$\xi' \sqrt{2\gamma} = \tau'$$

in the first and

$$\zeta \sqrt{2\gamma} = \tau$$

in the second, gives

$$\frac{\partial^2 X}{\partial \tau'^2} + \left(-g + \frac{1}{4}\tau'^2\right) X = 0$$

$$\frac{\partial^2 Z}{\partial \tau^2} + \left(g + \frac{1}{4}\tau^2\right) Z = 0$$

$$u = XZ = C_0 c \,\mathrm{Re}\left[U_+\left(-g, \tau'\right) + B' U_+^*\left(-g, \tau'\right)\right] \mathrm{Re}\left[U_+\left(g, \tau\right) + B U_+^*\left(g, \tau\right)\right]$$

$$= C_0 c \,\mathrm{Re}\left[U_+\left(-g, \xi'\sqrt{2\gamma}\right) + B' U_+^*\left(-g, \xi'\sqrt{2\gamma}\right)\right] \mathrm{Re}\left[e^{-i\pi/4} U_+\left(g, \zeta\sqrt{2\gamma}\right) + e^{i\pi/4} B U_+^*\left(g, \zeta\sqrt{2\gamma}\right)\right]$$

For purposes of matching we take $g = s = -s'$ and $B = e^{i\Phi_0}$ and $B' = e^{i\Phi_0'}$

$$u = C_0 c \,\mathrm{Re}\left[U_+\left(s', \xi'\sqrt{2\gamma}\right) + e^{i\Phi_0'} U_+^*\left(s', \xi'\sqrt{2\gamma}\right)\right] \mathrm{Re}\left[e^{-i\pi/4} U_+\left(-s', \zeta\sqrt{2\gamma}\right) + e^{i\pi/4} e^{i\Phi_0} U_+^*\left(-s', \zeta\sqrt{2\gamma}\right)\right]$$

Expanding as we leave the focal region

$$U_+\left(s, \tau\right) \sim e^{i\tau^2/4 - (1/2 - is)\ln\tau} = e^{i\tau^2/4} \tau^{is - 1/2} \ , \ \tau \to +\infty$$

$$u \sim 2C_0 \cos\left(\Phi_0'/2\right) c \,\mathrm{Re}\left[e^{-i\pi/4} U_+\left(-s', \zeta\sqrt{2\gamma}\right) + e^{i\pi/4} e^{i\Phi_0} U_+^*\left(-s', \zeta\sqrt{2\gamma}\right)\right]$$

$$\left(\xi'\sqrt{2\gamma}\right)^{-1/2} \cos\left[\xi'^2\gamma/2 + s'\ln\left(\xi'/2\right) + s'\ln\left(2\sqrt{2\gamma}\right) - \Phi_0'/2\right] \text{, Region } 3 \to 1$$

$$u \sim 2C_0 \cos\left(\Phi_0/2\right) c \,\mathrm{Re}\left[U_+\left(s', \xi'\sqrt{2\gamma}\right) + e^{i\Phi_0'} U_+^*\left(s', \xi'\sqrt{2\gamma}\right)\right]$$

$$\left(\zeta\sqrt{2\gamma}\right)^{-1/2} \cos\left[\zeta^2\gamma/2 - s'\ln\left(\zeta/2\right) - s'\ln\left(2\sqrt{2\gamma}\right) - \pi/4 - \Phi_0/2\right] \text{ , Region } 3 \to 2$$

These must match to the limiting forms of the outer solutions from the preceding sections

$$u \sim 2Cc\,\mathrm{Re}\left[e^{-i\pi/4} U_+\left(-s', \sqrt{2\gamma}\zeta\right) + e^{i\pi/4} e^{i\Phi_0} U_+^*\left(-s', \sqrt{2\gamma}\zeta\right)\right]$$

$$\xi'^{-1/2} \cos\left[\gamma\left(1 - \xi'^2/2\right) + k\delta - s'\ln\left(\xi'/2\right)\right] \text{ , } \xi' \to 0$$

in Region 1, and to

$$u \sim 2c\,\mathrm{Re}\left[U_+\left(s', \sqrt{2\gamma}\xi'\right) + e^{i\Phi_0'} U_+^*\left(s', \sqrt{2\gamma}\xi'\right)\right]$$

$$\zeta^{-1/2} \cos\left[\gamma\left(1 + \zeta^2/2\right) + k\delta - s'\ln\left(\zeta/2\right) - \pi/4 - \Phi_1/2\right] \text{ , } \zeta \to 0$$

in Region 2, where

$$s'\ln\left[\tanh\left(\zeta_0/2\right)\right] = \left(k - k_p\right)\ell$$

$$k_p\ell - \pi/4 - \Phi_1/2 = \pi\left(p - 1/2\right)$$

The functional behaviors are identical, but the phases only match if

$$s'\ln\left(2\sqrt{2\gamma}\right) - \Phi_0'/2 = -\gamma - k\delta + n\pi$$

$$-s'\ln\left(2\sqrt{2\gamma}\right) - \Phi_0/2 = \gamma + k\delta - \Phi_1/2 + n'\pi$$

and the amplitudes match if

$$C_0\left(2\gamma\right)^{-1/4}\cos\left(\Phi_0'/2\right) = C\left(-1\right)^n$$

$$C_0\left(2\gamma\right)^{-1/4}\cos\left(\Phi_0/2\right) = \left(-1\right)^{n'}$$

### 3.3.4 evenness conditions on scar

Because we have selected the even functions with respect to the normal to the scarred orbit, we must have the normal derivatives vanish on the scar center

$$\mathrm{Re}\left[U_+'\left(s', 0\right) + e^{i\Phi_0'} U_+^{*\prime}\left(s', 0\right)\right] = 0 = \mathrm{Re}\left[e^{-i\pi/4} U_+'\left(s, 0\right) + e^{i\pi/4} e^{i\Phi_0} U_+^{*\prime}\left(s, 0\right)\right]$$

where the left side is the Region 2 form and the right side is the Region 1 form. If we write the real part as one half the sum of the function and its conjugate, we see that these conditions imply

$$e^{i\Phi_0'} = -\frac{U_+'(s',0)}{U_+^{*\prime}(s',0)}$$

and

$$e^{i\Phi_0} = i\frac{U_+'(s,0)}{U_+^{*\prime}(s,0)}$$

Using the properties of the parabolic cylinder functions and $s = -s'$

$$U_+'(s,\tau) = e^{-\pi(s+i3/2)/4}U'\left(-is, \tau e^{-i\pi/4}\right)$$

$$e^{-i\pi/4}U_+'(s,0) = e^{-\pi(s+i5/2)/4}U'(-is,0) = -\left[e^{-\pi(s+i3/2)/4}U'(is,0)\right]^*$$

$$= -e^{\pi s'/2}\left[e^{-\pi\left(s'+i3/2\right)/4}U'(-is',0)\right]^* = -e^{\pi s'/2}\left[e^{-\pi\left(s'+i3/2\right)/4}U'(-is',0)\right]^* = -e^{\pi s'/2}U_+^{*\prime}(s',0)$$

Taking negative the ratio of this to its conjugate gives

$$e^{i\Phi_0} = i\frac{U_+'(s,0)}{U_+'^*(s,0)} = -\frac{U_+^{*\prime}(s',0)}{U_+'(s',0)} = e^{-i\Phi_0'}$$

Thus

$$\Phi_0' = -\Phi_0 + 2j\pi\,,\ j = 0, \pm 1, \pm 2, ...$$

but the multiple of $2\pi$ does not seem to add anything and thus we take

$$\Phi_0' = -\Phi_0$$

The single remaining condition then determines $s' = -s$ given a value of the reflection phase $\Phi_0$. Note that this choice of reflection phase conjugate implies that the incoming wave from the outer region travels toward the scarred orbit in one region, but on the other side of the focus travels away from the scarred orbit. This construction of the transverse dependence has thus allowed a consistent solution between the two regions to be found.

### 3.3.5 summary of conditions

The summary of conditions is now given. The first is the evenness across the scar

$$\mathrm{Re}\left[U_+'(s',0) + e^{-i\Phi_0}U_+^{*\prime}(s',0)\right] = 0 = \mathrm{Re}\left[e^{-i\pi/4}U_+'(-s',0) + e^{i\pi/4}e^{i\Phi_0}U_+^{*\prime}(-s',0)\right]$$

(the two conditions are now consistent) determines $s'$ given $\Phi_0$. From the mirror condition

$$\Phi_1/2 = k_p\ell - \pi(p - 1/4)$$

where $k_p$ and $s'$ are related by

$$s' \ln\left[\tanh\left(\zeta_0/2\right)\right] = \left(k - k_p\right)\ell$$

This can also be written in terms of the stability exponents as

$$-s' = s = 2\left(k - k_p\right)\ell / \ln\left(\frac{\ell + d}{\ell - d}\right) = 2\left(k - k_p\right) L / \ln\left(\Lambda_+\right)$$

where

$$\sigma_0' = \ln\left[\tanh\left(\zeta_0/2\right)\right] = -\frac{1}{2}\ln\left(\frac{\ell + d}{\ell - d}\right) = -\frac{1}{2}\ln\left(\frac{\lambda_+ + 1}{\lambda_- + 1}\right) = -\frac{1}{2}\ln\left(\lambda_+\right) = -\frac{1}{4}\ln\left(\Lambda_+\right)$$

and

$$\sqrt{d/\ell} = \frac{\sqrt{\Lambda_+ - 1}}{\left(\sqrt{\Lambda_+} + 1\right)}$$

and where $\lambda_\pm^2 = \Lambda_\pm$, $\lambda_+\lambda_- = 1 = \Lambda_+\Lambda_-$ and $\left(\lambda_\pm + 1\right)/2 = \left(\ell \pm d\right)/R$. The phase matching conditions can be written as

$$\Phi_1/2 = \pi\left(n + n'\right)$$

$$k\delta = -\gamma - s' \ln\left(2\sqrt{2\gamma}\right) - \Phi_0/2 + n\pi$$

and the amplitude conditions give the coefficients as

$$C = (-1)^{n'-n}$$

$$C_0 = (-1)^{n'} \left(2\gamma\right)^{1/4} \sec\left(\Phi_0/2\right)$$

It appears like the phase $\Phi_1/2$ adds nothing since it must be a multiple of $\pi$ and sign changes in the Region 2 solution due to this phase are accompanied by sign changes in $C$ and in the Region 1 solution (which thus can be absorbed into the amplitude coefficients). Furthermore the factor $\sec\left(\Phi_0/2\right)$ only enters because we failed to set the problem up with symmetrical factors $\exp\left(\pm\Phi_0/2\right)$ in the combinations of parabolic cylinder functions.

### 3.3.6 final set of conditions

Thus if we set $\Phi_1$ to zero we have the evenness condition across the scar orbit to determine the allowed values of the separation constant $s'$ in terms of the chaotic phase $\Phi_0$

$$\mathrm{Re}\left[U_+'\left(s', 0\right) + e^{-i\Phi_0} U_+^{*\prime}\left(s', 0\right)\right] = 0$$

We have the mirror conditions which connect the separation constant values and the resonant frequencies $k$

$$k_p \ell = \pi\left(p - 1/4\right)$$

$$s' \ln\left[\tanh\left(\zeta_0/2\right)\right] = \left(k - k_p\right)\ell$$

We also have the focal point shift $\delta$

$$k\delta = -\gamma - s' \ln\left(2\sqrt{2\gamma}\right) - \Phi_0/2 + n\pi$$

and the amplitude constants (here we note that if $n$ and $n'$ are both even or odd $C$ is one, but if they have opposite parities, then $C = -1$ which cancels the phase shift $\Phi_1/2$ then an odd multiple of $\pi$)

$$C = 1$$

$$C_0 = (-1)^n \left(2\gamma\right)^{1/4} \sec\left(\Phi_0/2\right)$$

The transcendental equation for $s'$ can be written as

$$e^{-i\Phi_0} + e^{-i\pi 3/4} 2^{is'} \frac{\Gamma\left(is'/2 + 1/4\right)}{\Gamma\left(-is'/2 + 1/4\right)} = 0$$

or by use of the duplication theorem

$$e^{-i\Phi_0} + \frac{e^{-i\pi 3/4}\sqrt{\pi}}{\Gamma\left(-is' + 1/2\right)\left\{\cosh\left(\pi s'/2\right) + i\sinh\left(\pi s'/2\right)\right\}} = 0$$

To get a feel for the connection with $\Phi_0$ for small $s'$ we can expand as

$$\frac{\Gamma\left(is'/2 + 1/4\right)}{\Gamma\left(-is'/2 + 1/4\right)} \sim$$

$$\frac{1 + \psi\left(is'/2 + 1/4\right)\left(is'/2\right) + \left[\left\{\psi\left(is'/2 + 1/4\right)\right\}^2 + \psi'\left(is'/2 + 1/4\right)\right]\left(is'/2\right)^2/2}{1 + \psi\left(-is'/2 + 1/4\right)\left(-is'/2\right) + \left[\left\{\psi\left(-is'/2 + 1/4\right)\right\}^2 + \psi'\left(-is'/2 + 1/4\right)\right]\left(-is'/2\right)^2/2}$$

$$\sim \frac{1 + \psi\left(1/4\right)\left(is'/2\right) + \left[\left\{\psi\left(1/4\right)\right\}^2 + \psi'\left(1/4\right)\right]\left(is'/2\right)^2/2}{1 + \psi\left(1/4\right)\left(-is'/2\right) + \left[\left\{\psi\left(1/4\right)\right\}^2 + \psi'\left(1/4\right)\right]\left(-is'/2\right)^2/2}$$

$$\sim \left[1 + \psi\left(1/4\right)\left(is'/2\right)\right]\left[1 - \psi\left(1/4\right)\left(-is'/2\right) + \left\{\psi\left(1/4\right)\left(-is'/2\right)\right\}^2\right]$$

$$\sim 1 + is'\psi\left(1/4\right) - \frac{1}{2}s'^2\left\{\psi\left(1/4\right)\right\}^2$$

where $\psi\left(z\right)$ is the digamma function [31].

### 3.3.7 focal shift in simulations

In the calculations of the focal point shift we use

$$k_p\ell = \pi\left(p - 1/4\right)$$

$$s' = 2\left(k_p - k\right)\ell / \ln\left(\frac{\ell + d}{\ell - d}\right)$$

and the focal point shift $\delta$

$$k\left(d + \delta\right) = -s' \ln\left(2\sqrt{kd}\right) - \left(\Phi_0 + \pi/4 + s' \ln 2\right)/2 + \left(n + 1/8\right)\pi$$

The transcendental equation for $s'$ can be written as

$$e^{-i\left(\Phi_0 + \pi/4 + s' \ln 2\right)} = \frac{\Gamma\left(is'/2 + 1/4\right)}{\Gamma\left(-is'/2 + 1/4\right)}$$

giving

$$k\left(d + \delta\right) = -s' \ln\left(2\sqrt{kd}\right) + \arg\Gamma\left(1/4 + is'/2\right) + \left(n + 1/8\right)\pi$$

### 3.3.8 focal shift examples

We now look at several examples of focal shift that are used in spatial comparisons between the theory and the numerical simulations in the next section.

Note that if $k \to k_p$, and therefore $s' \to 0$, the chaotic phase becomes

$$e^{-i\Phi_0} + e^{-i\pi 3/4} = 0$$

or

$$\Phi_0 \sim 3\pi/4 + \left(2m - 1\right)\pi$$

The focal shift in this case becomes

$$k_p\delta \sim -k_p d - \Phi_0/2 + n\pi \sim -k_p d + \left(n - m + 1/8\right)\pi$$

Thus in this case denoting the shift by $\delta_0$

$$k_p\left(d + \delta_0\right) \sim \left(n - m + 1/8\right)\pi$$

Note that we can set $m = 0$

$$\Phi_0 = -\pi/4$$

$$k_p\delta_0 \sim -k_p d + \left(n + 1/8\right)\pi$$

$$C_0 = \left(-1\right)^n \left(2\gamma\right)^{1/4} \sec\left(\Phi_0/2\right)$$

Let us examine the reflected phases below when we do not have $k = k_p$ (or $s' = 0$ and $\Phi_0 = -\pi/4$) to see what the evenness conditions look like. The values of $k$ near $k_p$ are found from the numerical simulations of the eigenvalues in each of these examples. This wave number eigenvalue is used to determine $s'$. Next, $\Phi_0$ is found from the transcendental equation; we first use the small $s'$ expansion to do this, followed by the

exact transcendental equation relation. These values are then used to determine the shifted focal point location. Because we used a phase matching condition for the focal point shift, there is a set of discrete choices possible for this focal point location. We explore these and examine which one seems to agree with the spatial distribution from the simulations. The choice that agrees with the numerical simulation is listed and the comparison it gives to the spatial variations of these scars with the numerical eigenfunctions are illustrated in the next section. It appears in these examples that the focal point selection is the first one to the right of the geometrical location $d = \ell\sqrt{1 - R/\ell}$.

Using the resonant frequency

$$k_p \ell = (p - 1/4)\,\pi$$

we find

$$(d + \delta_0)/\ell \sim (n + 1/8)/(p - 1/4)$$

$$\delta_0/\ell = \frac{n + 1/8}{p - 1/4} - d/\ell = \frac{n + 1/8}{p - 1/4} - \sqrt{1 - R/\ell} = \frac{n + 1/8 - (p - 1/4)\sqrt{1 - R/\ell}}{p - 1/4}$$

For $p = 8$ (note that $d/\ell = 0.3015$, and from the simulation $f = 4.205$ GHz, $k = 0.9955 k_p$ so that from $(k - k_p)\,L = s'_m \ln\left(\frac{\ell - d}{\ell + d}\right)$ we find $s'_m = 0.3520$, and from the expansion $\Phi_0 = -\pi/4 + 1.2441$, whereas an exact evaluation of the transcendental equation yields $\Phi_0 = -\pi/4 + 1.0743$) with varying $n$ we have

$$(d + \delta_0)/\ell \approx 0.2742, 0.4032, 0.5323, 0.6613$$

The approximate form of the transcendental equation

$$e^{-i\Phi_0} + e^{-i\pi 3/4}\left[1 + is'\left(\ln 2 + \psi\left(1/4\right)\right)\right] = 0$$

with

$$\psi\left(1/2\right) = \psi\left(1/4\right) + \ln 2 + \pi/2 = -\gamma' - 2\ln 2$$

$$\gamma' = 0.5772$$

gives

$$e^{-i\Phi_0} + e^{-i\pi 3/4}\left[1 - is'\left(\gamma' + 2\ln 2 + \pi/2\right)\right] \approx e^{-i\Phi_0} + e^{-i\pi 3/4}\left[1 - is' 3.5343\right]$$

$$\approx e^{-i\Phi_0} + e^{-i\pi 3/4 - is' 3.5343} = 0$$

and thus

$$\Phi_0 = -\pi/4 + s'\left(\gamma' + 2\ln 2 + \pi/2\right)$$

Therefore plugging this expansion into the actual shift formula

$$k\left(d+\delta\right)=-s'\ln\left(2\sqrt{2\gamma}\right)-\Phi_0/2+n\pi$$

$$k_p\ell=\pi\left(p-1/4\right)$$

$$s'=2\left(k_p-k\right)\ell/\ln\left(\frac{\ell+d}{\ell-d}\right)$$

gives (we ignore terms of order $\left(k-k_p\right)\delta$)

$$k_p\left(d+\delta\right)\sim\left(k_p-k\right)d-\left[\ln\left(4\sqrt{2k_pd}\right)+\left(\gamma'+\pi/2\right)/2\right]2\left(k_p-k\right)\ell/\ln\left(\frac{\ell+d}{\ell-d}\right)+\left(n+1/8\right)\pi$$

$$d+\delta\sim-\left[2\ln\left(4\sqrt{2k_pd}\right)+\gamma'+\pi/2-\frac{d}{\ell}\ln\left(\frac{\ell+d}{\ell-d}\right)\right]\left(\frac{k_p-k}{k_p}\right)\ell/\ln\left(\frac{\ell+d}{\ell-d}\right)+\frac{n+1/8}{p-1/4}\ell$$

or

$$d+\delta\sim-\left[\ln\left(4\sqrt{2k_pd}\right)+\frac{1}{2}\gamma'+\pi/4-\frac{d}{2\ell}\ln\left(\frac{\ell+d}{\ell-d}\right)\right]s'/k_p+\frac{n+1/8}{p-1/4}\ell$$

$$k_p\left(d+\delta\right)\sim-\left[\ln\left(4\sqrt{2k_pd}\right)+\frac{1}{2}\gamma'+\pi/4-\frac{d}{2\ell}\ln\left(\frac{\ell+d}{\ell-d}\right)\right]s'+\pi\left(n+1/8\right)$$

$$k_p\delta\sim-\left[\ln\left(4\sqrt{2k_pd}\right)+\frac{1}{2}\gamma'+\pi/4-\frac{d}{2\ell}\ln\left(\frac{\ell+d}{\ell-d}\right)\right]s'+\pi\left(n+1/8\right)-\pi\left(p-1/4\right)d/\ell$$

Alternatively if we use the exact form

$$e^{-i\Phi_0}=e^{i\pi/4}2^{is'}\frac{\Gamma\left(is'/2+1/4\right)}{\Gamma\left(-is'/2+1/4\right)}$$

$$\Phi_0/2=-\pi/8-\frac{1}{2}s'\ln 2-\arg\Gamma\left(1/4+is'/2\right)$$

$$2\arg\Gamma\left(1/4+is'/2\right)=\ln\left[\frac{\Gamma\left(1/4+is'/2\right)}{\Gamma\left(1/4-is'/2\right)}\right]$$

$$k_p\left(d+\delta\right)\sim\left(k_p-k\right)d-s'\ln\left(2\sqrt{\gamma}\right)+\arg\Gamma\left(1/4+is'/2\right)+\left(n+1/8\right)\pi$$

$$\left(d+\delta\right)/\ell\sim\frac{1}{k_p\ell}\left[s'\left\{\frac{d}{2\ell}\ln\left(\frac{\ell+d}{\ell-d}\right)-\ln\left(2\sqrt{k_pd}\right)\right\}+\arg\Gamma\left(1/4+is'/2\right)\right]+\frac{\left(n+1/8\right)\pi}{\left(p-1/4\right)\pi}$$

Thus

$$-s'\ln\left(2\sqrt{2\gamma}\right)-\Phi_0/2=-0.717-0.622$$

and

$$(d+\delta)/\ell \approx 0.2192, 0.3482, 0.4773, 0.6063$$

$$d+\delta \approx 0.06028, 0.09576^*, 0.1313, 0.1667$$

or using the exact transcendental equation values for the phase

$$(d+\delta)/\ell \approx 0.2227, 0.3517, 0.4808, 0.6098$$

$$d+\delta \approx 0.06124, 0.09672^*, 0.1322, 0.16769$$

The entry with the asterisk corresponding to $n = 3$ is the one immediately to the right of the geometric focal point and the one used in the simulation comparison. Note that the coefficient of the Region 3 solution has a factor of $(-1)^n = -1$ for all cases where $n$ is odd.

The second example $p = 9$ ($f = 4.768$ GHz, $k = 0.9997k_p$ and $s' = 0.02641$, $\Phi_0 = -\pi/4 + 0.09336$, and exact evaluation of the transcendental equation yields $\Phi_0 = -\pi/4 + 0.09321$)

$$(d+\delta_0)/\ell \sim (n+1/8)/(p-1/4)$$

$$(d+\delta_0)/\ell \approx 0.24286, 0.35714, 0.47143, 0.58571$$

$$(d+\delta)/\ell \approx 0.2385, 0.35275, 0.46704, 0.57635$$

$$d+\delta \approx 0.06558, 0.097006^*, 0.12844, 0.1585$$

or using the exact transcendental equation values for the phase

$$(d+\delta)/\ell \approx 0.2385, 0.35275, 0.46704, 0.57635$$

$$d+\delta \approx 0.06558, 0.097006^*, 0.12844, 0.1585$$

where $n = 3$ for the solution with the asterisk. The simulation yielded a focus at 0.0986 m.

The third example $p = 10$ ($f = 5.276$ GHz, $k = 0.99276k_p$ and $s' = 0.71313$, $\Phi_0 = -\pi/4 + 2.5204$, and exact evaluation of the transcendental equation yields $\Phi_0 = -\pi/4 + 1.5672$, the error being caused by the large size of $s'$ in this case) and

$$(d+\delta_0)/\ell \approx 0.21795, 0.32051, 0.42308, 0.52564$$

$$(d+\delta)/\ell \approx 0.1267, 0.2293, 0.33185, 0.4344$$

$$d+\delta \approx 0.03485, 0.06305, 0.09126^*, 0.1195$$

or using the the exact transcendental equation values for the phase

$$(d+\delta)/\ell \approx 0.1423, 0.24484, 0.34741, 0.4500$$

$$d+\delta \approx 0.03913, 0.06733, 0.09554^*, 0.12374$$

where $n = 4$ for the solution with the asterisk. Another scar associated with $p = 10$ is at $k > k_p$. This has ($f = 5.3307$ GHz, $k = 1.003048k_p$ and $s' = -0.3000$, $\Phi_0 = -\pi/4 - 1.06024$, and exact evaluation of the transcendental equation yields $\Phi_0 = -\pi/4 - 0.93965$)

$$(d+\delta_0)/\ell \approx 0.21795, 0.32051, 0.42308, 0.52564$$

$$(d+\delta)/\ell \approx 0.2563, 0.3589, 0.46146, 0.5640$$

$$d+\delta \approx 0.07049, 0.09869^*, 0.1269, 0.1551$$

or using the the exact transcendental equation values for the phase

$$(d+\delta)/\ell \approx 0.25436, 0.35692, 0.4595, 0.5620$$

$$d+\delta \approx 0.06995, 0.09815^*, 0.12636, 0.1546$$

where $n = 3$ for the solution with the asterisk.

The fourth example $p = 11$ ($f = 5.843$ GHz, $k = 0.9971k_p$ and $s' = 0.3148$, $\Phi_0 = -\pi/4 + 1.1126$, and exact evaluation of the transcendental equation yields $\Phi_0 = -\pi/4 + 0.95695$)

$$(d+\delta_0)/\ell \approx 0.1977, 0.2907, 0.3837, 0.4767$$

$$(d+\delta)/\ell \approx 0.1607, 0.2537, 0.3467, 0.4397$$

$$d+\delta \approx 0.04420, 0.06977, 0.09535^*, 0.1209$$

or using the exact transcendental equation values for the phase

$$(d+\delta)/\ell \approx 0.1630, 0.2560, 0.3490, 0.4420$$

$$d+\delta \approx 0.04483, 0.07041, 0.095982^*, 0.12156$$

where $n = 4$ for the solution with the asterisk.

The fifth example $p = 12$ ($f = 6.406$ GHz, $k = 1.00027k_p$ and $s' = -0.0320$, $\Phi_0 = -\pi/4 - 0.1131$, and exact evaluation of the transcendental equation yields $\Phi_0 = -\pi/4 - 0.1139$)

$$(d+\delta_0)/\ell \approx 0.18085, 0.26596, 0.35106, 0.43617$$

$$(d+\delta)/\ell \approx 0.1843, 0.2694, 0.3545, 0.4414$$

$$d+\delta \approx 0.0507, 0.0741, 0.09750^*, 0.1214$$

where $n = 4$ for the solution with the asterisk.

The sixth example $p = 13$ ($f = 6.914$ GHz, $k = 0.994858k_p$ and $s' = 0.66188$, $\Phi_0 = -\pi/4 + 2.3393$, and exact evaluation of the transcendental equation yields $\Phi_0 = -\pi/4 + 1.523898$)

$$(d+\delta_0)/\ell \approx 0.16666, 0.245098, 0.32353, 0.40196, 0.48039, 0.558823$$

and using the the exact transcendental equation values for the phase

$$(d+\delta)/\ell \approx 0.1099, 0.1883, 0.26674, 0.34517, 0.4236, 0.50204$$

$$d+\delta \approx 0.0302, 0.05178, 0.07335, 0.09492^*, 0.1165, 0.1381$$

where $n = 5$ for the solution with the asterisk.

The seventh example $p = 14$ ($f = 7.482$ GHz, $k = 0.99829k_p$ and $s' = 0.23731$, $\Phi_0 = -\pi/4 + 0.83872$, and exact evaluation of the transcendental equation yields $\Phi_0 = -\pi/4 + 0.7749667$)

$$(d+\delta_0)/\ell \approx 0.15454, 0.22727, 0.300000, 0.37272, 0.445454, 0.51818$$

$$(d+\delta)/\ell \approx 0.13207, 0.2048, 0.27753, 0.35025, 0.42298, 0.4957$$

$$d+\delta \approx 0.03632, 0.05632, 0.07632, 0.09632^*, 0.11632, 0.13632$$

and using the the exact transcendental equation values for the phase

$$(d+\delta)/\ell \approx 0.1328, 0.2055, 0.2783, 0.3510, 0.4237, 0.4964$$

$$d+\delta \approx 0.03652, 0.05652, 0.07652, 0.09652^*, 0.1165, 0.1365$$

where $n = 5$ for the solution with the asterisk.

The eighth example $p = 15$ ($f = 8.042$ GHz, $k = 1.000262k_p$ and $s' = -0.039085$, $\Phi_0 = -\pi/4 - 0.138137$, and exact evaluation of the transcendental equation yields $\Phi_0 = -\pi/4 - 0.13789$)

$$(d+\delta_0)/\ell \approx 0.144068, 0.211864, 0.279661, 0.347458, 0.415254, 0.48305$$

$$(d+\delta)/\ell \approx 0.14755, 0.21534, 0.28314, 0.35094, 0.41873, 0.4865$$

$$d+\delta \approx 0.04057, 0.05922, 0.077864, 0.096508^*, 0.115152, 0.13379$$

where $n = 5$ for the solution with the asterisk.

The ninth example $p = 16$ ($f = 8.557$ GHz, $k = 0.996742k_p$ and $s' = 0.517994$, $\Phi_0 = -\pi/4 + 1.83075$, and exact evaluation of the transcendental equation yields $\Phi_0 = -\pi/4 + 1.35735$)

$$(d + \delta_0)/\ell \approx 0.198412, 0.261905, 0.325397, 0.388888, 0.452381, 0.515873$$

and using the exact transcendental equation values for the phase

$$(d + \delta)/\ell \approx 0.15966, 0.22316, 0.2866, 0.35013, 0.41363, 0.47713$$

$$d + \delta \approx 0.04391, 0.06137, 0.07883, 0.09629^*, 0.11375, 0.1312$$

where $n = 6$ for the solution with the asterisk.

The tenth example $p = 17$ ($f = 9.051$ GHz, $k = 0.991342k_p$ and $s' = 1.46402$, $\Phi_0 = -\pi/4 + 5.17423$, and exact evaluation of the transcendental equation yields $\Phi_0 = -\pi/4 + 1.65189$)

$$(d + \delta_0)/\ell \approx 0.30597, 0.365672, 0.425373, 0.4850746, 0.544776$$

$$(d + \delta)/\ell \approx 0.1894, 0.24913, 0.30883, 0.36853, 0.42823$$

$$d + \delta \approx 0.05209, 0.06851, 0.08493, 0.101346^*, 0.11776$$

or using the the exact transcendental equation values for the phase

$$(d + \delta)/\ell \approx 0.222895, 0.28260, 0.342298, 0.402000, 0.4617$$

$$d + \delta \approx 0.0613, 0.07771, 0.094132^*, 0.11055, 0.126968$$

where $n = 7$ for the solution with the asterisk.

Another $p = 17$ case has $k > k_p$. Thus we have ($f = 9.1735$ GHz, $k = 1.00476k_p$ and $s' = -0.804868$, $\Phi_0 = -\pi/4 - 2.844647$, and exact evaluation of the transcendental equation yields $\Phi_0 = -\pi/4 - 1.62756$)

$$(d + \delta_0)/\ell \approx 0.186567, 0.246269, 0.30597$$

and using the the exact transcendental equation values for the phase

$$(d + \delta)/\ell \approx 0.23887, 0.29857, 0.358276$$

$$d + \delta \approx 0.06567, 0.08211^*, 0.098526$$

where $n = 4$ for the solution with the asterisk.

The eleventh example $p = 18$ ($f = 9.627$ GHz, $k = 0.9950263k_p$ and $s' = 0.8913$, $\Phi_0 = -\pi/4 + 3.1501$, and exact evaluation of the transcendental equation yields $\Phi_0 = -\pi/4 + 1.66713$)

$$(d+\delta_0)/\ell \approx 0.2887324, 0.3450704, 0.4014085, 0.4577465, 0.5140845$$

and using the the exact transcendental equation values for the phase

$$(d+\delta)/\ell \approx 0.2346, 0.29095, 0.3473, 0.4036, 0.45996$$

$$d+\delta \approx 0.064517, 0.08001, 0.09550^*, 0.1110, 0.1265$$

where $n = 7$ for the solution with the asterisk.

Thus we see in all but one of these cases (where the solution was almost exactly the geometrical focus) that the first choice outside the geometrical point is the one that agrees well with the simulation. The generality of this selection is not clear (other stadium geometries). Higher order terms in the solution (as discussed in the Appendix) may allow the amplitude to play a role in the choice.

### 3.4 Field Comparisons On Axis

The field on axis is now compared. The field on axis, in Region 1

$$u_p \sim c_2 e^{-\pi s'/2}\sqrt{2d}\left(d^2-x^2\right)^{-1/4}\cos\left[kx - s'\frac{1}{2}\ln\left(\frac{d-x}{d+x}\right)\right] \text{ , Region 1}$$

$$\approx c_2 e^{-\pi s'/2}\sqrt{2d}\left(d^2-x^2\right)^{-1/4}\cos\left(k_p x\right) \text{ , Region 1}$$

and in Region 2

$$u_p \sim c_2\sqrt{2d}\left(x^2-d^2\right)^{-1/4}\cos\left[kx - s'\frac{1}{2}\ln\left(\frac{x-d}{x+d}\right) - \pi/4\right] \text{ , Region 2}$$

$$\approx c_2\sqrt{2d}\left(x^2-d^2\right)^{-1/4}\cos\left(k_p x - \pi/4\right) \text{ , Region 2}$$

where we have used

$$\frac{\left|U_+'\left(s',0\right)\right|}{\left|U_+'\left(-s',0\right)\right|} = e^{-\pi s'/2}$$

$$s'\ln\left(\frac{\ell+d}{\ell-d}\right) = 2\left(k_p-k\right)\ell$$

$$d = \ell\sqrt{1-R/\ell}$$

$$k_p\ell = \pi\left(p-1/4\right)$$

Near the focus

$$u_p = C_0 c\,\mathrm{Re}\left[U_+\left(s',\xi'\sqrt{2\gamma}\right) + e^{-i\Phi_0}U_+^*\left(s',\xi'\sqrt{2\gamma}\right)\right]$$

$$\mathrm{Re}\left[e^{-i\pi/4}U_+\left(-s',\zeta\sqrt{2\gamma}\right)+e^{i\pi/4}e^{i\Phi_0}U_+^*\left(-s',\zeta\sqrt{2\gamma}\right)\right]$$

where

$$x=d\cosh\zeta\cos\xi'\sim d\left(1+\zeta^2/2\right)\left(1-\xi'^2/2\right)\sim d\left(1+\zeta^2/2-\xi'^2/2\right)$$

$$y=d\sinh\zeta\sin\xi'\sim d\zeta\xi'\left(1+\zeta^2/6\right)\left(1-\xi'^2/6\right)\sim d\zeta\xi'\left(1+\zeta^2/6-\xi'^2/6\right)$$

The coefficient is found by using

$$e^{i\Phi_0}=-\frac{U_+^{*\prime}\left(s',0\right)}{U_+'\left(s',0\right)}$$

and

$$\cos\left(\Phi_0/2\right)=\pm\sqrt{\frac{1+\cos\left(\Phi_0\right)}{2}}=\frac{\mathrm{Im}\left[U_+'\left(s',0\right)\right]}{\left|U_+'\left(s',0\right)\right|}$$

where the plus sign was selected by taking the limiting case $s'=0$ and $\Phi_0=-\pi/4$ with [31]

$$U_+'\left(s',0\right)=e^{-\pi\left(s'+i3/2\right)/4}U'\left(-is',0\right)=-\frac{e^{-\pi\left(s'+i3/2\right)/4}\sqrt{\pi}}{2^{-is'/2-1/4}\Gamma\left(-is'/2+1/4\right)}$$

and

$$U_+'\left(0,0\right)=-\frac{e^{-i\pi3/8}2^{1/4}\sqrt{\pi}}{\Gamma\left(1/4\right)}$$

so that

$$\frac{\mathrm{Im}\left[U_+'\left(0,0\right)\right]}{\left|U_+'\left(0,0\right)\right|}=\cos\left(\pi/8\right)$$

Thus

$$C_0=\left(-1\right)^n\left(2\gamma\right)^{1/4}\sec\left(\Phi_0/2\right)=\left(-1\right)^n\left(2\gamma\right)^{1/4}\frac{\left|U_+'\left(s',0\right)\right|}{\mathrm{Im}\left[U_+'\left(s',0\right)\right]}$$

$$=-\left(-1\right)^n\left(2\gamma\right)^{1/4}\frac{\left|\Gamma\left(is'/2+1/4\right)\right|}{\mathrm{Im}\left\{2^{is'/2}e^{-i3\pi/8}\Gamma\left(is'/2+1/4\right)\right\}}$$

Now from the definition of the new amplitude $c_2$ in Regions 1 and 2

$$c_2=\sqrt{2}c\,\mathrm{Re}\left[U_+\left(s',0\right)+e^{-i\Phi_0}U_+^*\left(s',0\right)\right]$$

$$c_2e^{-\pi s'/2}=\sqrt{2}c\,\mathrm{Re}\left[e^{-i\pi/4}U_+\left(-s',0\right)+e^{i\pi/4}e^{i\Phi_0}U_+^*\left(-s',0\right)\right]$$

Thus in Region 3 we can write

$$u_p(x,0) = -(-1)^n (\gamma/2)^{1/4} \frac{|\Gamma(is'/2+1/4)|}{\mathrm{Im}\left\{2^{is'/2}e^{-i3\pi/8}\Gamma(is'/2+1/4)\right\}}$$

$$c_2 \,\mathrm{Re}\left[e^{-i\pi/4}U_+\left(-s',\zeta\sqrt{2\gamma}\right) - e^{-i\pi/4}\frac{U'_+(-s',0)}{U'^*_+(-s',0)}U^*_+\left(-s',\zeta\sqrt{2\gamma}\right)\right]$$

$$= -(-1)^n (\gamma/2)^{1/4} \frac{|\Gamma(is'/2+1/4)|}{\mathrm{Im}\left\{2^{is'/2}e^{-i3\pi/8}\Gamma(is'/2+1/4)\right\}}$$

$$c_2 \,\mathrm{Re}\left[e^{-i\pi/4}U_+\left(-s',\zeta\sqrt{2\gamma}\right) + 2^{-is'}\frac{\Gamma(-is'/2+1/4)}{\Gamma(is'/2+1/4)}U^*_+\left(-s',\zeta\sqrt{2\gamma}\right)\right]$$

$$\zeta \approx \sqrt{2(x-d-\delta)/d}$$

for $x > d+\delta$ and

$$u_p(x,0) = -(-1)^n (\gamma/2)^{1/4} \frac{|\Gamma(is'/2+1/4)|}{\mathrm{Im}\left\{2^{is'/2}e^{-i3\pi/8}\Gamma(is'/2+1/4)\right\}}$$

$$c_2 e^{-\pi s'/2} \,\mathrm{Re}\left[U_+\left(s',\xi'\sqrt{2\gamma}\right) - \frac{U'_+(s',0)}{U'^*_+(s',0)}U^*_+\left(s',\xi'\sqrt{2\gamma}\right)\right]$$

$$= -(-1)^n (\gamma/2)^{1/4} \frac{|\Gamma(is'/2+1/4)|}{\mathrm{Im}\left\{2^{is'/2}e^{-i3\pi/8}\Gamma(is'/2+1/4)\right\}}$$

$$c_2 e^{-\pi s'/2} \,\mathrm{Re}\left[U_+\left(s',\xi'\sqrt{2\gamma}\right) + 2^{is'}e^{i\pi/4}\frac{\Gamma(is'/2+1/4)}{\Gamma(-is'/2+1/4)}U^*_+\left(s',\xi'\sqrt{2\gamma}\right)\right]$$

$$\xi' \approx \sqrt{2(d+\delta-x)/d}$$

for $x < d+\delta$. Note that the square root relation between the elliptical coordinates and the $x$ coordinate means that the derivative (or slope) in $x$ is not zero at the focus! These distributions are compared to the scarred eigenfunctions found from numerical simulations of the stadium cavity. Because of the random variable $v$ involved in the amplitude coefficient $c$, and hence in $c_2$, we adjusted the amplitude $c_2$ of the scar distribution to match the simulation at one point (at one of the peaks, usually on the right side, and not at the focus).

Figure 29 shows a comparison between the numerical simulation of the eigenfunction (red curve) and $p = 8$ scar theory. The black curves are Region 1 and Region 2 formulas (the green curves are the same with $k = k_p$ or $s' = 0$ in the sinusoidal distributions, not in the amplitudes, as given in the approximate expressions at the top of this subsection). The tan curve is the Region 3 focal point region, shifted by the theoretical focal point shift with $n = 3$. The electric field intensity plot in Figure 26 corresponds to this scar.

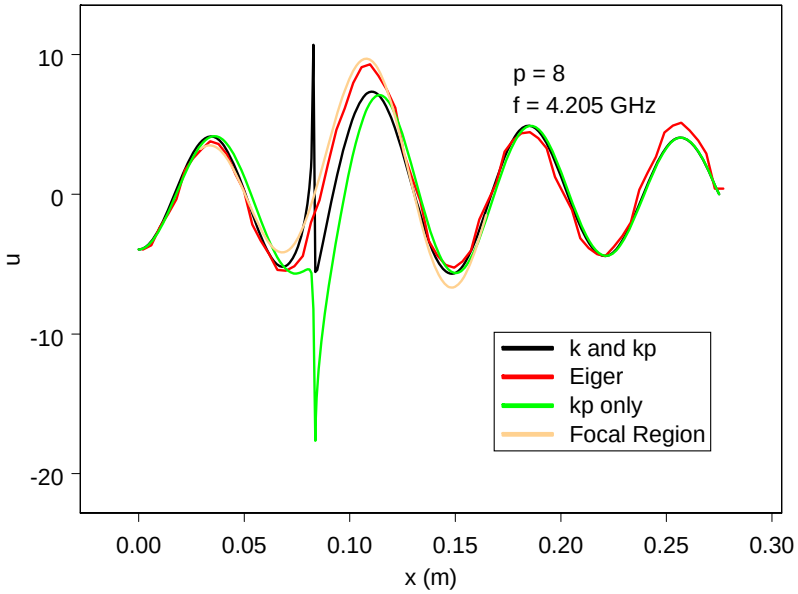


Figure 29. Comparison between simulation of eigenfunction (red curve) and $p = 8$ scar. The black curves are Region 1 and Region 2 formulas (the green curves are the same with $k = k_p$ in the cosine distributions). The tan curve is the Region 3 focal point region, shifted by the theoretical focal point shift.

Figure 30 shows a comparison between the numerical simulation of the eigenfunction (red curve) and $p = 9$ scar theory. The black curves are Region 1 and Region 2 formulas (the green curves are the same with $k = k_p$ or $s' = 0$ in the sinusoidal distributions, not in the amplitudes). The tan curve is the Region 3 focal point region, shifted by the theoretical focal point shift with $n = 3$. Figure 31 shows the corresponding electric field intensity.

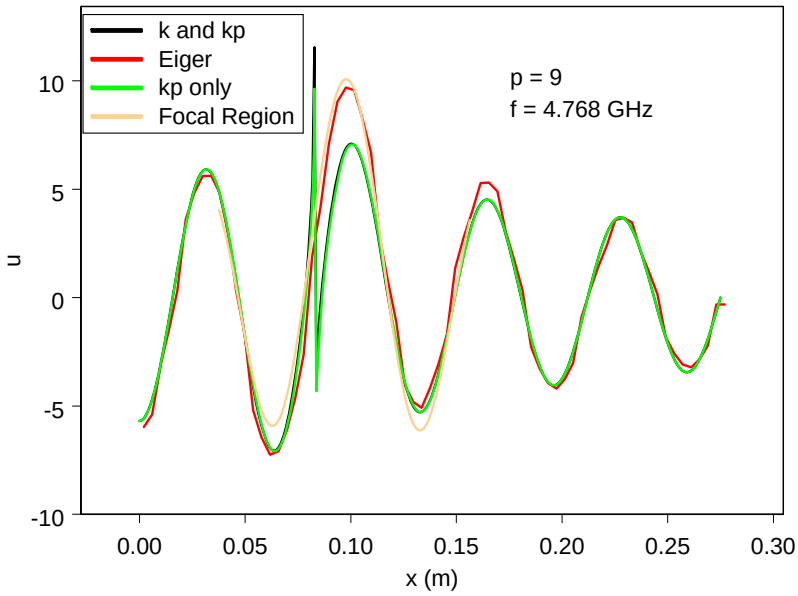


Figure 30. Comparison between simulation of eigenfunction (red curve) and $p = 9$ scar. The black curves are Region 1 and Region 2 formulas (the green curves are the same with $k = k_p$ in the cosine distributions). The tan curve is the Region 3 focal point region, shifted by the theoretical focal point shift.

Figure 32 shows a simplified comparison, with the curves in truncated to their regions of validity, of the simulation and $p = 9$ scar theory.

Figure 33 shows a comparison between the numerical simulation of the eigenfunction (red curve) and $p = 10$ scar theory. The black curves are Region 1 and Region 2 formulas (the green curves are the same with $k = k_p$ or $s' = 0$ in the sinusoidal distributions, not in the amplitudes). The tan curve is the Region 3 focal point region, shifted by the theoretical focal point shift with $n = 4$.

Figure 34 shows a comparison between the numerical simulation of another eigenfunction (red curve) and $p = 10$ scar theory. The black curves are Region 1 and Region 2 formulas (the green curves are the same with $k = k_p$ or $s' = 0$ in the sinusoidal distributions, not in the amplitudes). The tan curve is the Region 3 focal point region, shifted by the theoretical focal point shift with $n = 3$. Figure 35 shows the corresponding electric field intensity.

Figure 36 shows a comparison between the numerical simulation of the eigenfunction (red curve) and $p = 11$ scar theory. The black curves are Region 1 and Region 2 formulas (the green curves are the same with $k = k_p$ or $s' = 0$ in the sinusoidal distributions, not in the amplitudes). The tan curve is the Region 3 focal point region, shifted by the theoretical focal point shift with $n = 4$.

Figure 37 shows a comparison between the numerical simulation of the eigenfunction (red curve) and $p = 12$ scar theory. The black curves are Region 1 and Region 2 formulas (the green curves are the same with $k = k_p$ or $s' = 0$ in the sinusoidal distributions, not in the amplitudes). The tan curve is the Region 3 focal point region, shifted by the theoretical focal point shift with $n = 4$. The dashed tan curve is the unshifted Region 3 focal point spatial distribution, which is misaligned with the Region 1 and Region 2

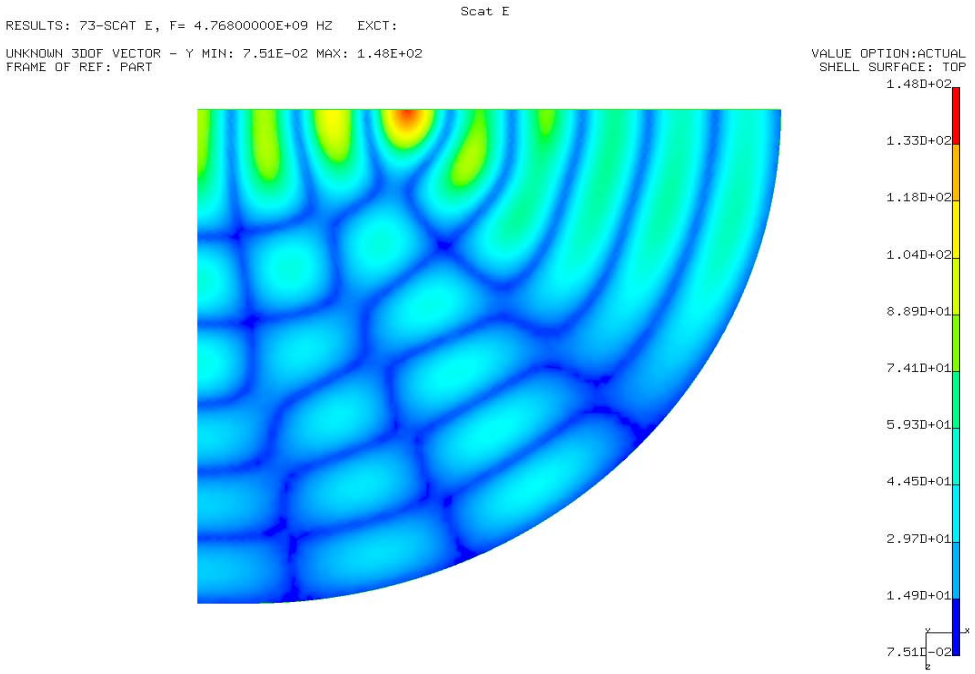


Figure 31. Bouncing ball mode along horizontal axis in stadium cavity at 4.768 GHz. The geometry has $L = 0.55$ m and $R = 0.25$ m.

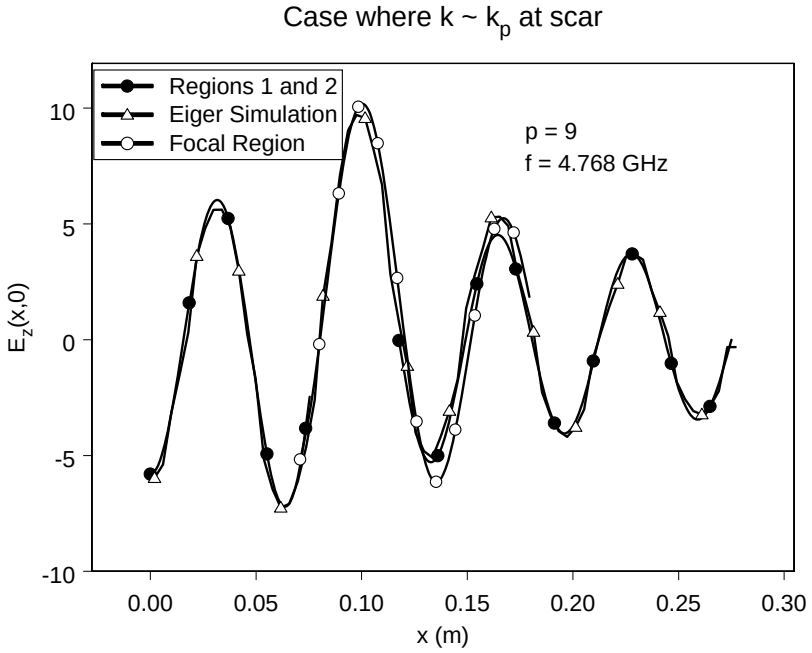


Figure 32. Black and white simplified comparison between simulation of eigenfunction (diamonds) and $p = 9$ scar. The solid dot curves are Region 1 and Region 2 formulas. The open dot curve is the Region 3 focal point region, shifted by the theoretical focal point shift.

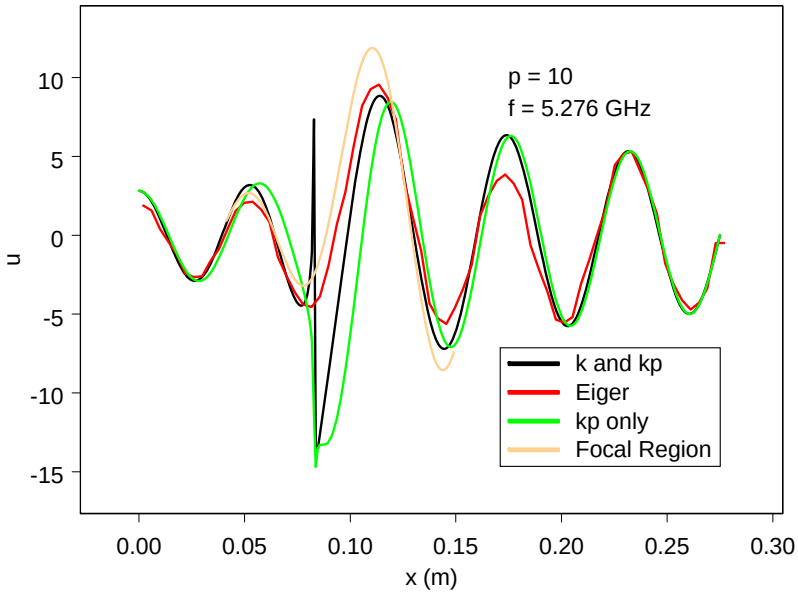


Figure 33. Comparison between simulation of eigenfunction (red curve) and $p = 10$ scar. The black curves are Region 1 and Region 2 formulas (the green curves are the same with $k = k_p$ in the cosine distributions). The tan curve is the Region 3 focal point region, shifted by the theoretical focal point shift.

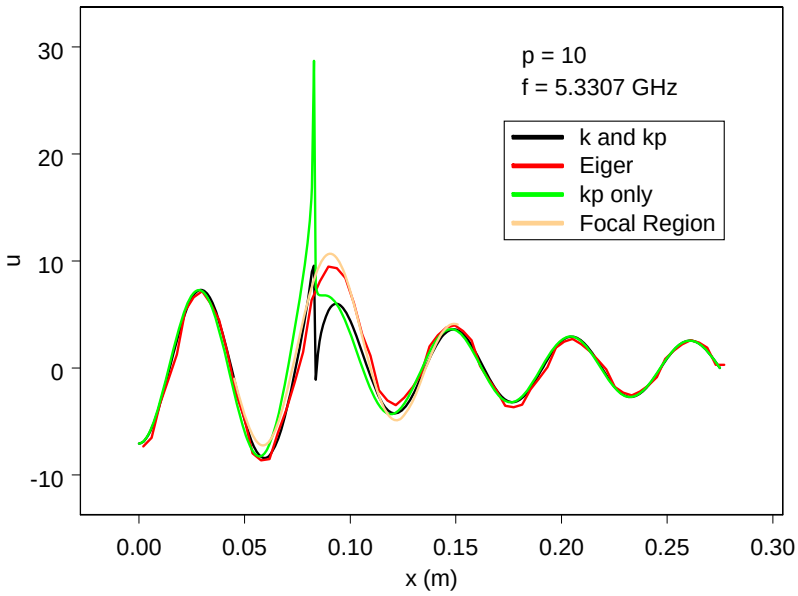


Figure 34. Comparison between simulation of another eigenfunction (red curve) and $p = 10$ scar. The black curves are Region 1 and Region 2 formulas (the green curves are the same with $k = k_p$ in the cosine distributions). The tan curve is the Region 3 focal point region, shifted by the theoretical focal point shift.

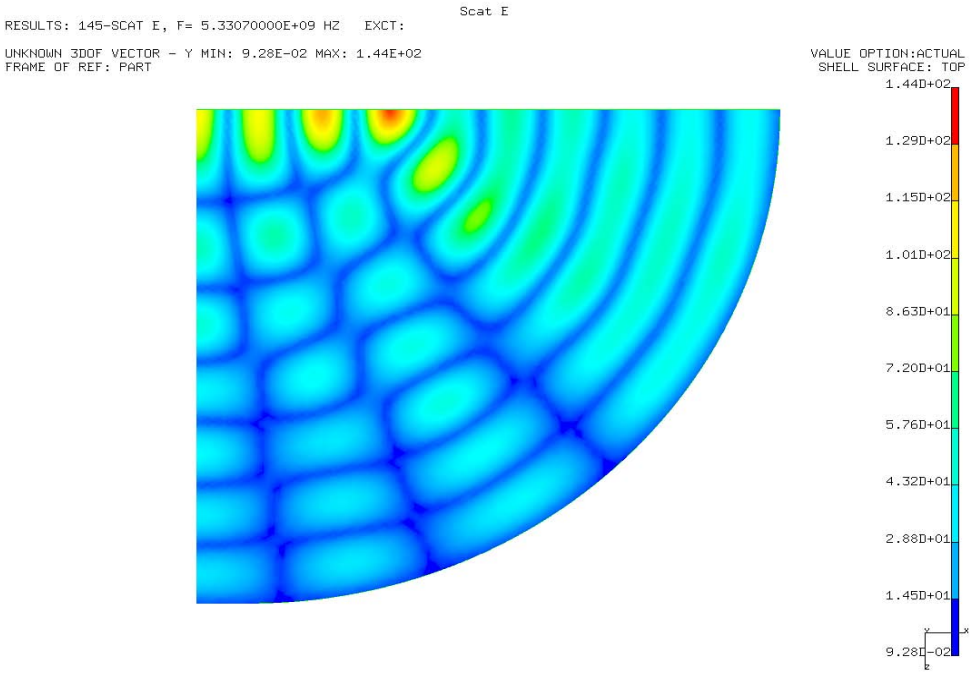


Figure 35. Bouncing ball mode along horizontal axis in stadium cavity at 5.3307 GHz. The geometry has $L = 0.55$ m and $R = 0.25$ m.

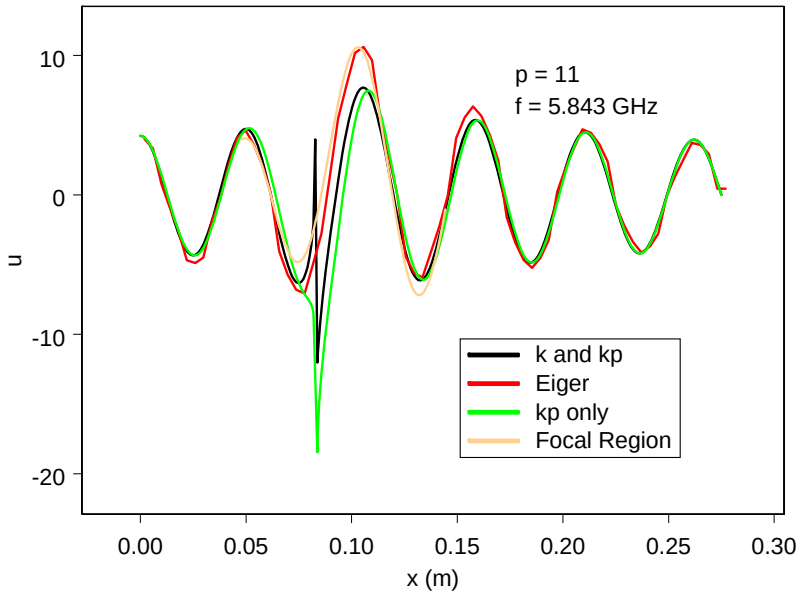


Figure 36. Comparison between simulation of eigenfunction (red curve) and $p = 11$ scar. The black curves are Region 1 and Region 2 formulas (the green curves are the same with $k = k_p$ in the cosine distributions). The tan curve is the Region 3 focal point region, shifted by the theoretical focal point shift.

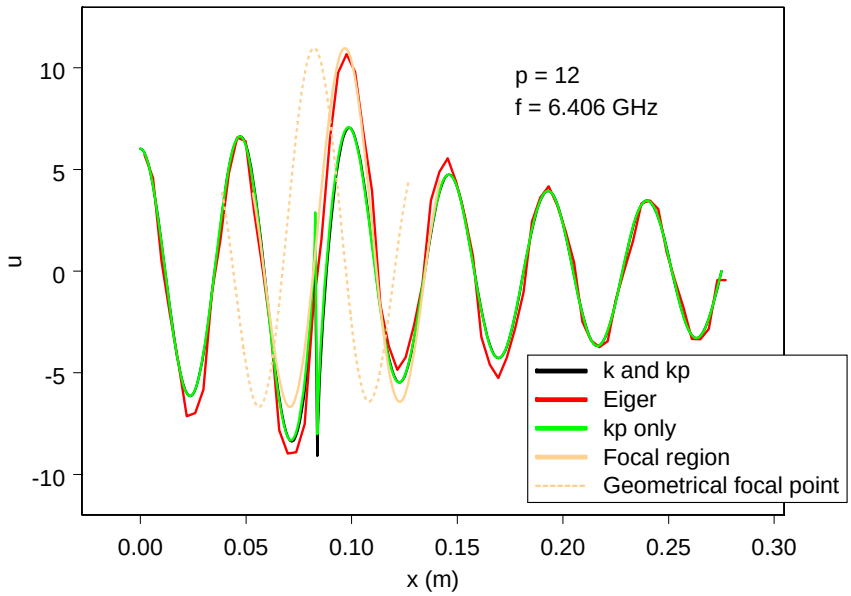


Figure 37. Comparison between simulation of eigenfunction (red curve) and $p = 12$ scar. The black curves are Region 1 and Region 2 formulas (the green curves are the same with $k = k_p$ in the cosine distributions). The tan curve is the Region 3 focal point region, shifted by the theoretical focal point shift.

distributions.

Figure 38 shows a comparison between the numerical simulation of the eigenfunction (red curve) and $p = 13$ scar theory. The black curves are Region 1 and Region 2 formulas (the green curves are the same with $k = k_p$ or $s' = 0$ in the sinusoidal distributions, not in the amplitudes). The tan curve is the Region 3 focal point region, shifted by the theoretical focal point shift with $n = 5$. Figure 39 shows the corresponding electric field intensity.

Figure 40 shows a comparison between the numerical simulation of the eigenfunction (red curve) and $p = 14$ scar theory. The black curves are Region 1 and Region 2 formulas (the green curves are the same with $k = k_p$ or $s' = 0$ in the sinusoidal distributions, not in the amplitudes). The tan curve is the Region 3 focal point region, shifted by the theoretical focal point shift with $n = 5$.

Figure 41 shows a comparison between the numerical simulation of the eigenfunction (red curve) and $p = 15$ scar theory. The black curves are Region 1 and Region 2 formulas (the green curves are the same with $k = k_p$ or $s' = 0$ in the sinusoidal distributions, not in the amplitudes). The tan curve is the Region 3 focal point region, shifted by the theoretical focal point shift with $n = 5$.

Figure 42 shows a comparison between the numerical simulation of the eigenfunction (red curve) and $p = 16$ scar theory. The black curves are Region 1 and Region 2 formulas (the green curves are the same with $k = k_p$ or $s' = 0$ in the sinusoidal distributions, not in the amplitudes). The tan curve is the Region 3 focal point region, shifted by the theoretical focal point shift with $n = 6$.

Figure 43 shows a comparison between the numerical simulation of the eigenfunction (red curve) and

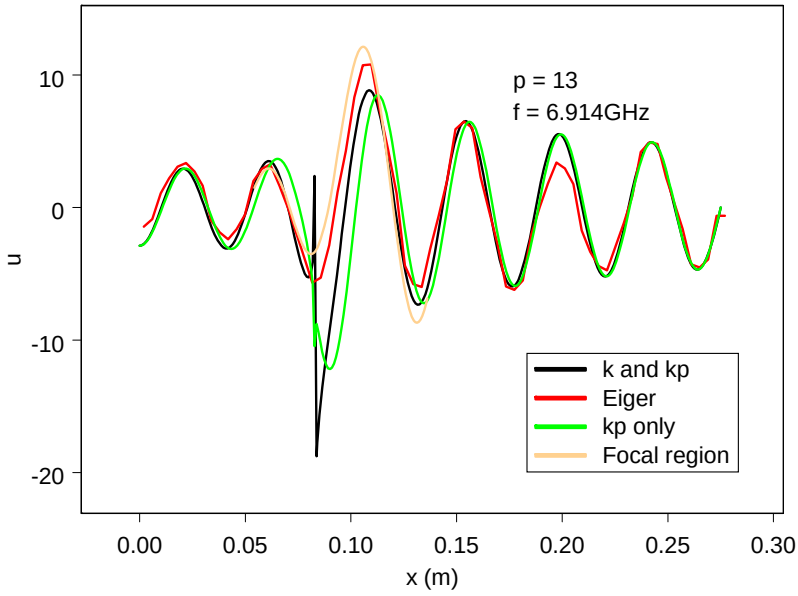


Figure 38. Comparison between simulation of eigenfunction (red curve) and $p = 13$ scar. The black curves are Region 1 and Region 2 formulas (the green curves are the same with $k = k_p$ in the cosine distributions). The tan curve is the Region 3 focal point region, shifted by the theoretical focal point shift.

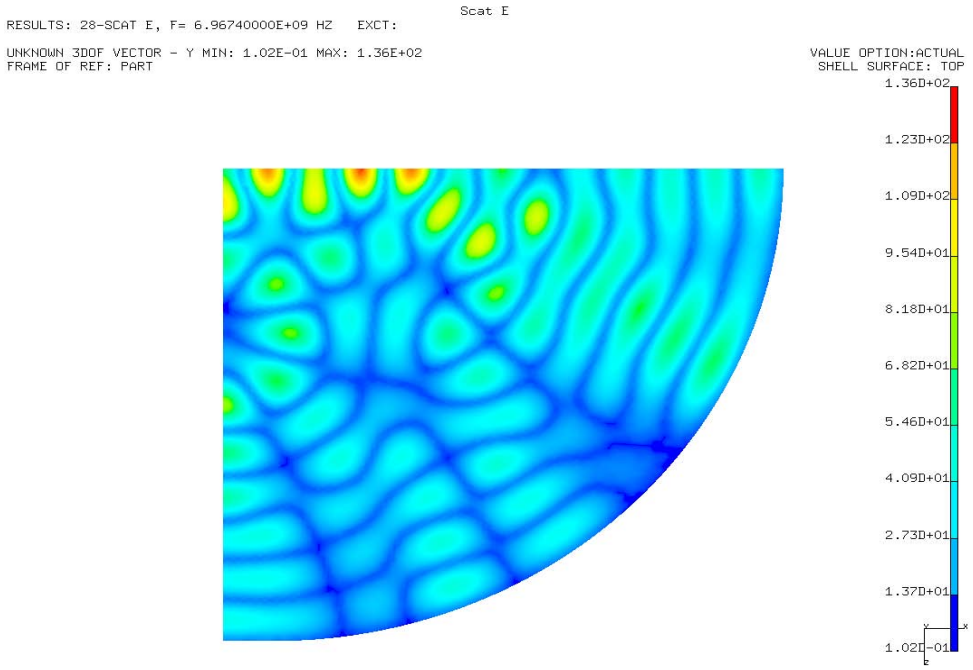


Figure 39. Bouncing ball mode along horizontal axis in stadium cavity at 6.9674 GHz. The geometry has $L = 0.55$ m and $R = 0.25$ m.

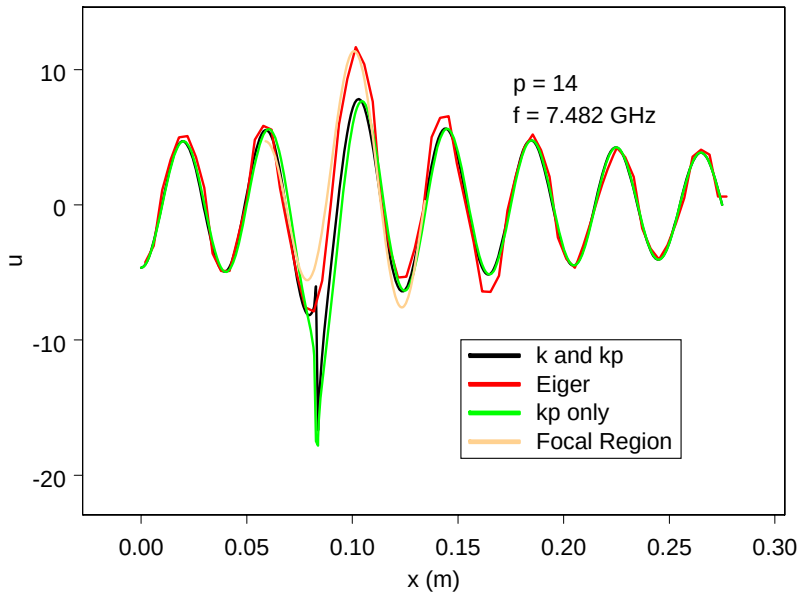


Figure 40. Comparison between simulation of eigenfunction (red curve) and $p = 14$ scar. The black curves are Region 1 and Region 2 formulas (the green curves are the same with $k = k_p$ in the cosine distributions). The tan curve is the Region 3 focal point region, shifted by the theoretical focal point shift.

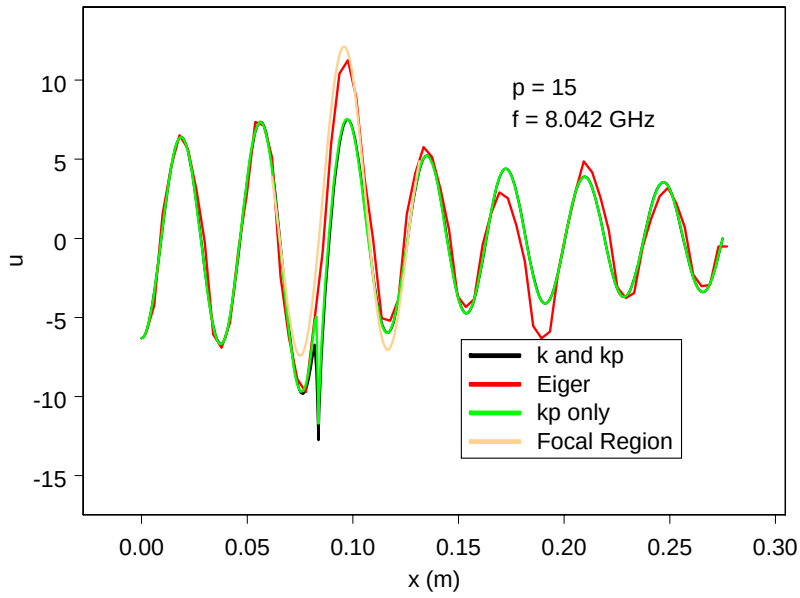


Figure 41. Comparison between simulation of eigenfunction (red curve) and $p = 15$ scar. The black curves are Region 1 and Region 2 formulas (the green curves are the same with $k = k_p$ in the cosine distributions). The tan curve is the Region 3 focal point region, shifted by the theoretical focal point shift.

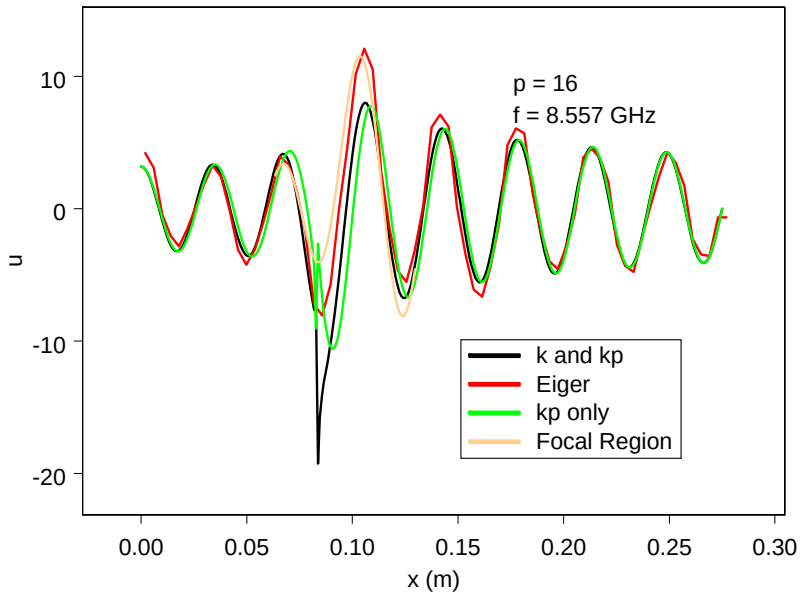


Figure 42. Comparison between simulation of eigenfunction (red curve) and $p = 16$ scar. The black curves are Region 1 and Region 2 formulas (the green curves are the same with $k = k_p$ in the cosine distributions). The tan curve is the Region 3 focal point region, shifted by the theoretical focal point shift.

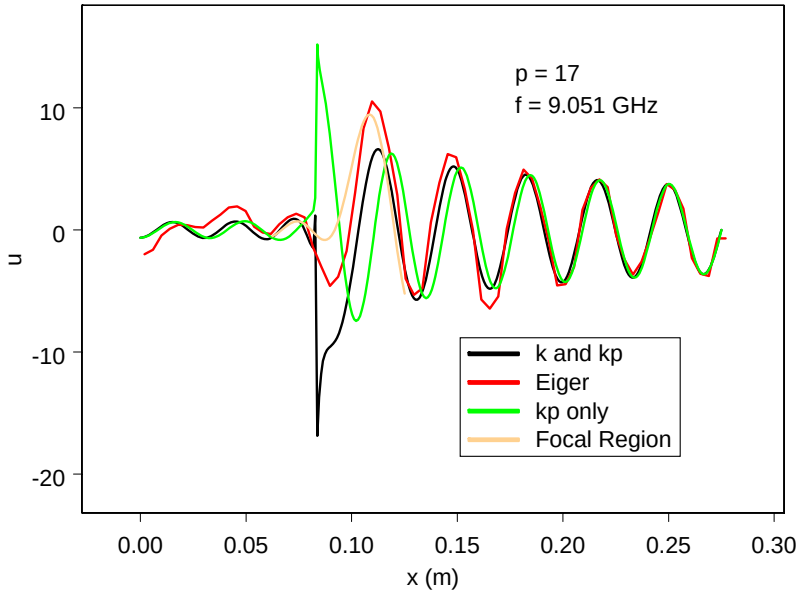


Figure 43. Comparison between simulation of eigenfunction (red curve) and $p = 17$ scar. The black curves are Region 1 and Region 2 formulas (the green curves are the same with $k = k_p$ in the cosine distributions). The tan curve is the Region 3 focal point region, shifted by the theoretical focal point shift.

$p = 17$ scar theory. The black curves are Region 1 and Region 2 formulas (the green curves are the same with $k = k_p$ or $s' = 0$ in the sinusoidal distributions, not in the amplitudes). The tan curve is the Region 3 focal point region, shifted by the theoretical focal point shift with $n = 7$. Figure 44 shows the corresponding electric field intensity.

Figure 45 shows a simplified comparison, with the curves truncated to their regions of validity, of the simulation and $p = 17$ scar theory.

Figure 46 shows a comparison between the numerical simulation of another eigenfunction (red curve) and $p = 17$ scar theory. The black curves are Region 1 and Region 2 formulas (the green curves are the same with $k = k_p$ or $s' = 0$ in the sinusoidal distributions, not in the amplitudes). The tan curve is the Region 3 focal point region, shifted by the theoretical focal point shift with $n = 4$. Figure 47 shows the corresponding electric field intensity.

Figure 48 shows a comparison between the numerical simulation of the eigenfunction (red curve) and $p = 18$ scar theory. The black curves are Region 1 and Region 2 formulas (the green curves are the same with $k = k_p$ or $s' = 0$ in the sinusoidal distributions, not in the amplitudes). The tan curve is the Region 3 focal point region, shifted by the theoretical focal point shift with $n = 7$.

From examination of these comparisons we see that the scar theory produces quite good agreement with the simulations for the form of the spatial distributions, including the focal point regions. From examination of the field intensity plots and the corresponding values of $s = -s'$ in the preceding section, for each of the $p$ and $k$ values, we see that the region of scar intensity is between foci (Region 1) when $s \geq 0$, but is outside the foci (Region 2) when $s \leq 0$. The behavior between foci is consistent with the behavior

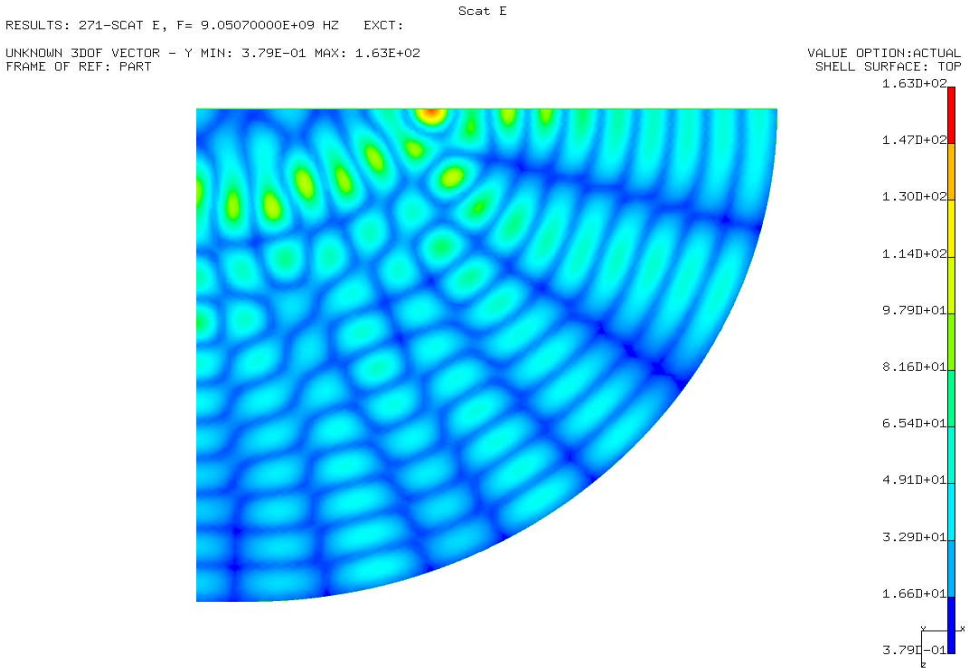


Figure 44. Bouncing ball mode along horizontal axis in stadium cavity at 9.0707 GHz. The geometry has $L = 0.55$ m and $R = 0.25$ m.

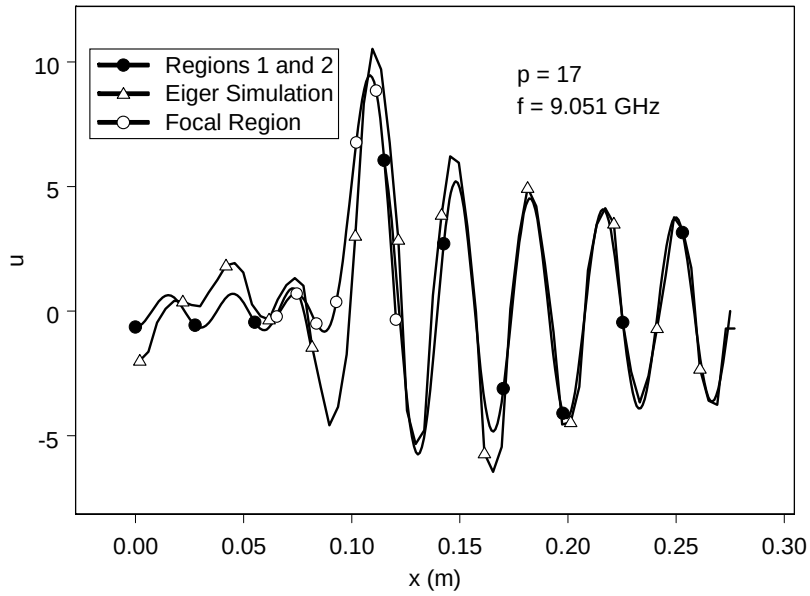


Figure 45. Black and white simplified comparison between simulation of eigenfunction (diamonds) and $p = 17$ scar. The solid dot curves are Region 1 and Region 2 formulas. The open dot curve is the Region 3 focal point region, shifted by the theoretical focal point shift.

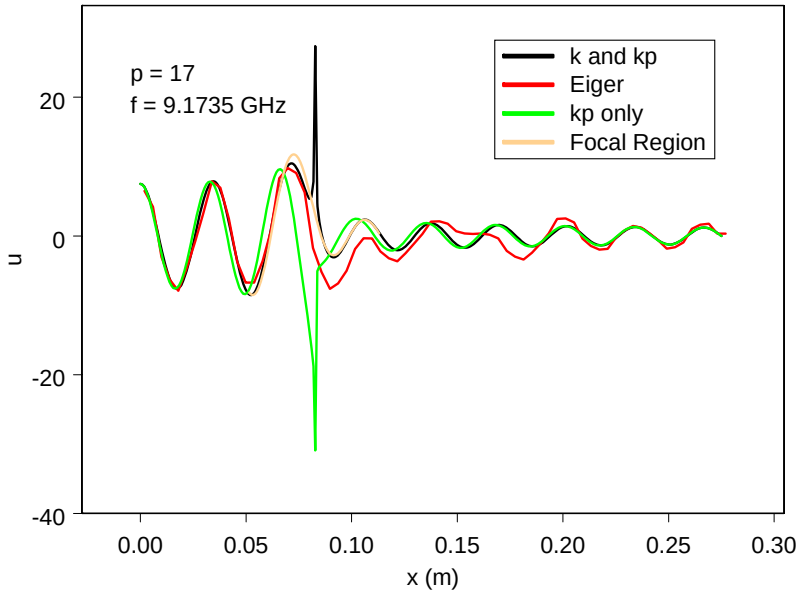


Figure 46. Comparison between simulation of another eigenfunction (red curve) and $p = 17$ scar. The black curves are Region 1 and Region 2 formulas (the green curves are the same with $k = k_p$ in the cosine distributions). The tan curve is the Region 3 focal point region, shifted by the theoretical focal point shift.

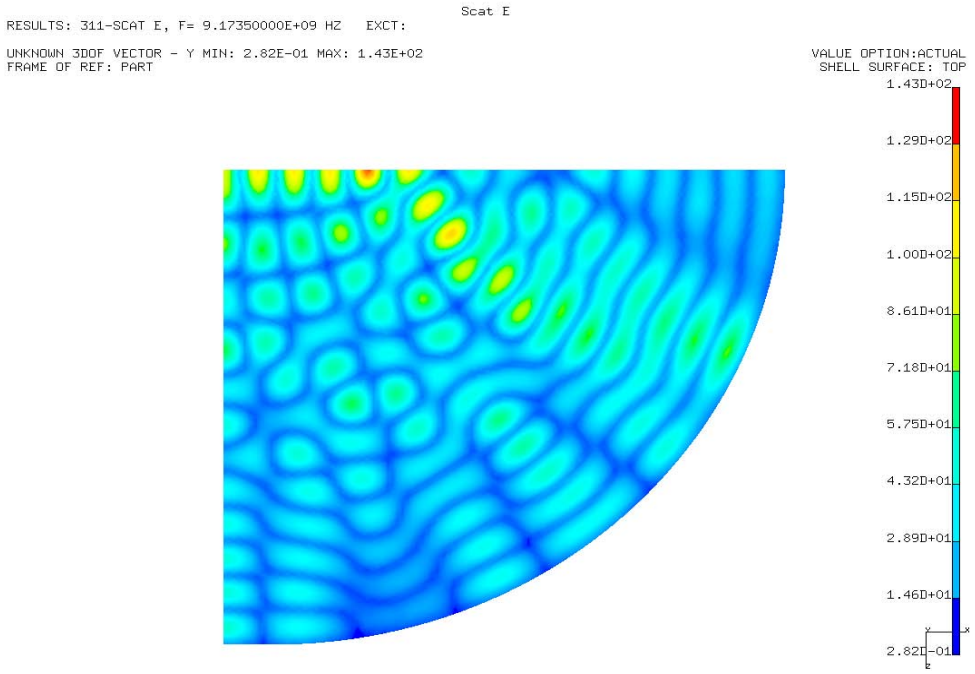


Figure 47. Bouncing ball mode along horizontal axis in stadium cavity at 9.1735 GHz. The geometry has $L = 0.55$ m and $R = 0.25$ m.

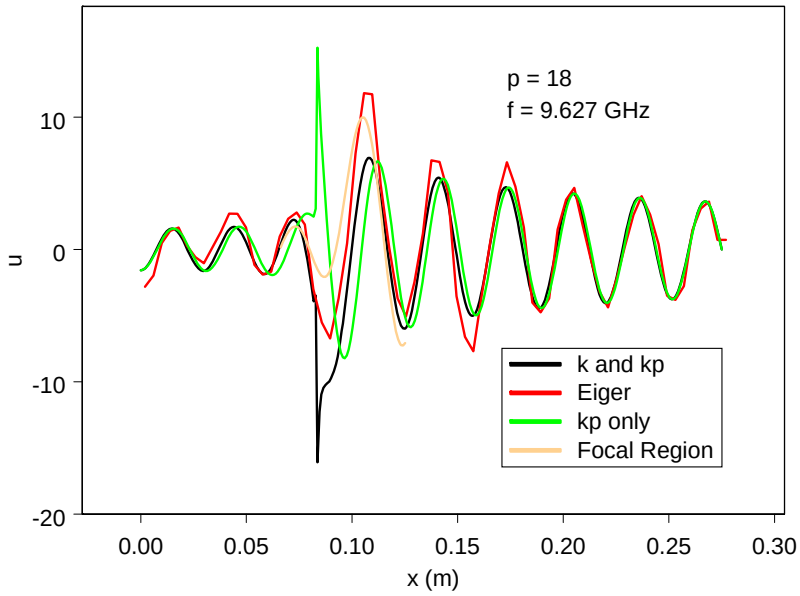


Figure 48. Comparison between simulation of eigenfunction (red curve) and $p = 18$ scar. The black curves are Region 1 and Region 2 formulas (the green curves are the same with $k = k_p$ in the cosine distributions). The tan curve is the Region 3 focal point region, shifted by the theoretical focal point shift.

in the bow tie cavity where the intensity on the orbit decays exponentially when $s_p < 0$. The behavior in Region 1 makes sense for $k\ell < k_p\ell$ since one would expect a slightly longer orbital length would be required to achieve resonance along the elliptical path.

### 3.4.1 distribution of shifts

Let us attempt to find a distribution function for the shifts in focal point position. The normalized shift function, without corrections ($s' = 0$), is

$$\delta_0/\ell = \frac{n+1/8}{p-1/4} - d/\ell = \frac{n+1/8}{p-1/4} - \sqrt{1-R/\ell} = \frac{n+1/8-(p-1/4)\sqrt{1-R/\ell}}{p-1/4} \geq 0$$

If we define

$$n_c = (p-1/4)\, d/\ell - 1/8$$

then

$$\delta_0/\ell = (n-n_c)\,/\,(p-1/4) = (n-n_c)\,/\,(k_p\ell/\pi)$$

Now suppose we take $n - n_c$ to be uniformly distributed between 0 and 1. Then $k_p\delta_0/\pi$ will be distributed the same way. If we consider the mean value

$$k_p\,\langle\delta_0\rangle\,/\pi \approx 1/2$$

we note that for the range $p = 8-36$ we might expect (using $p = 20$ as an average) $\langle\delta_0\rangle\,/\ell \approx 1/\,(2p-1/2) \rightarrow 0.0253$ or $\langle d+\delta_0\rangle = 0.090$ m with a maximum of about 0.097 m.

The correction resulting from the phase is

$$k_p\delta \sim \left[\frac{d}{2\ell}\ln\left(\frac{\ell+d}{\ell-d}\right) - \ln\left(2\sqrt{k_pd}\right)\right] s' + \arg\Gamma\left(1/4+is'/2\right) + \pi\,(n-n_c)$$

and for small $s'$

$$k_p\delta \sim -\left[\ln\left(4\sqrt{2k_pd}\right) + \frac{1}{2}\gamma' + \pi/4 - \frac{d}{2\ell}\ln\left(\frac{\ell+d}{\ell-d}\right)\right] s' + \pi\,(n-n_c)$$

The value of the first term is $-3.26$ for $s' = 1$ and $p = 20$ ($-4.18$ from the second expression). This correction for nonzero $s'$ just forces a larger value of $n$ to be chosen for the above geometrical focal point criterion. Figure 49 shows the cumulative distribution for $8 \leq p \leq 36$ (orange curve) and $-5 \leq s \leq 5$ with the correction in $s'$ (blue curves). The preceding uniform distribution seems to fit the rising portion of the distribution in the figure (0.083 m to 0.097 m) quite well. Note that this figure displays a distribution for a uniform set of choices in $p$. For a wide range of $p$, the fact that the density of modes grows linearly with frequency in the two-dimensional cavity, weights the distribution toward higher frequencies and higher values of $p$.

In an attempt to automatically locate the shifted focal locations in the simulations (using all of the eigenfunctions) of the stadium cavity, we calculated the elliptical projection operator (to be discussed in later sections) on the scar with the focal location variable. This projection operator is defined using only Regions 1 and 2. We then maximized its mean square value by varying the focus location. Figure 50 shows the results as a function of $s$, where the size of the symbols are weighted by the value of the maximum projection operator. The central horizontal clustering seems to populate the expected locations. The values

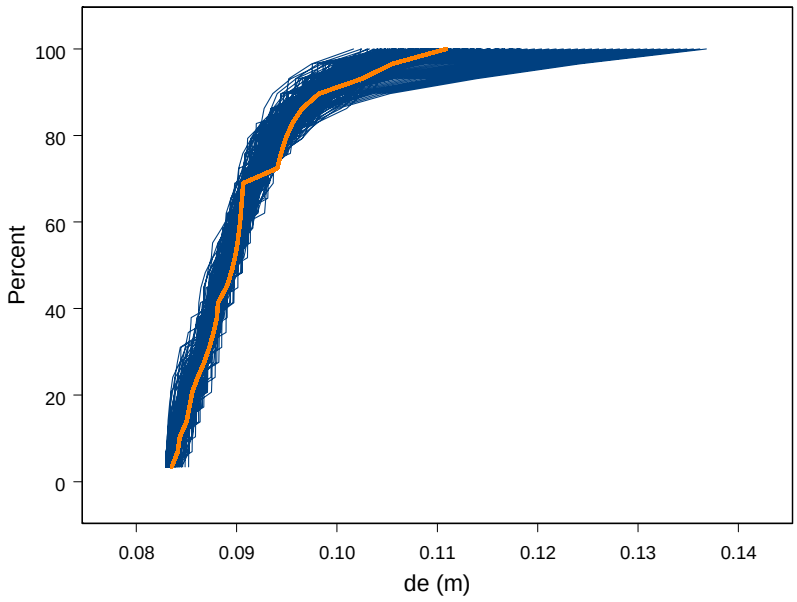


Figure 49. Cumulative distribution of focal point shifts for $8 \leq p \leq 36$ (and $-5 \leq s \leq 5$ for blue curve which includes correction).

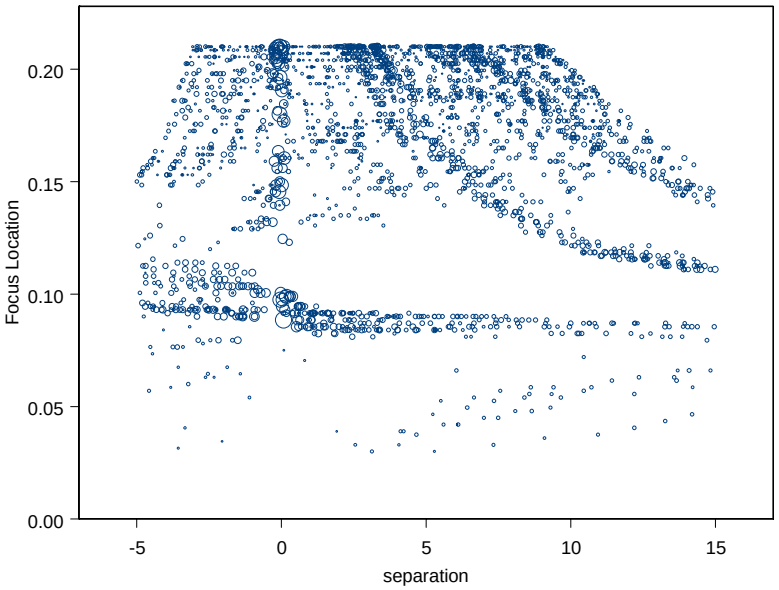


Figure 50. An attempt at locating the shifted focal point locations by maximizing the elliptic projection operator as a function of $d_e$.

below this level have small values and may not represent scarred eigenfunctions. The scattering of values with larger positions above a gap from the horizontal cluster may also not represent scarred eigenfunctions. We have investigated a few near $s = 0$ and observed that some are not scarred eigenfunctions but others have broad projection operator maxima, for which visual observation would put the focal point near the horizontal clustering, but the absolute peak discerned by the software was larger.

### 3.4.2 focal continuity condition when s is zero

It is instructive to let $s = 0$ and look at the effect of the focal shift on the $u_p(x, 0)$ in Regions 1 and 2. In this case we have $k = k_p$ and

$$k_p(d + \delta_0) = (n + 1/8)\pi$$

The $p$th component in Region 1 is

$$u_p \sim \frac{2v\Gamma(1/4)}{\gamma^{1/4}\left|U'_+(0,0)\right|\sqrt{\pi A \ln\left(\frac{\ell+d}{\ell-d}\right)}}\sqrt{d}\left(d^2 - x^2\right)^{-1/4}\cos(k_p x) \text{ , Region 1}$$

and in Region 2 is

$$u_p \sim \frac{2v\Gamma\left(1/4\right)}{\gamma^{1/4}\left|U_+'\left(0,0\right)\right|\sqrt{\pi A \ln\left(\frac{\ell+d}{\ell-d}\right)}}\sqrt{d}\left(x^2-d^2\right)^{-1/4}\cos\left(k_p x-\pi/4\right)\text{ , Region 2}$$

We note that

$$\cos\left(k_p x\right)=\cos\left(k_p x-\pi/4\right)\ ,\ x=d+\delta_0$$

Thus the phase continuity condition actually extends to zero distance from the shifted focal point. In other words the asymptotic forms from the outer two regions are continuous at this point.

### 3.5 Normalization of Eigenfunctions

To apply the method used for normalization by Antonsen [30] to the stadium cavity we again use the energy theorem [33]

$$\nabla\cdot\left(\frac{\partial\underline{E}}{\partial\omega}\times\underline{H}^*+\underline{E}^*\times\frac{\partial\underline{H}}{\partial\omega}\right)=i\left[\frac{\partial\left(\omega\mu\right)}{\partial\omega}\underline{H}\cdot\underline{H}^*+\frac{\partial\left(\omega\varepsilon\right)}{\partial\omega}\underline{E}\cdot\underline{E}^*\right]-\frac{\partial\underline{E}}{\partial\omega}\cdot\underline{J}^*-\underline{E}^*\cdot\frac{\partial\underline{J}}{\partial\omega}$$

Integrating over the cavity volume and using the divergence theorem

$$\oint_S\left(\frac{\partial\underline{E}}{\partial\omega}\times\underline{H}^*+\underline{E}^*\times\frac{\partial\underline{H}}{\partial\omega}\right)\cdot\underline{n}dS=i\int_V\left(\mu_0\underline{H}\cdot\underline{H}^*+\varepsilon_0\underline{E}\cdot\underline{E}^*\right)dV-\int_V\left(\frac{\partial\underline{E}}{\partial\omega}\cdot\underline{J}^*+\underline{E}^*\cdot\frac{\partial\underline{J}}{\partial\omega}\right)dV$$

Using $\underline{n}\times\underline{E}=0$ on the walls we find

$$\underline{n}\cdot\left(\underline{E}^*\times\frac{\partial\underline{H}}{\partial\omega}\right)=\frac{\partial\underline{H}}{\partial\omega}\cdot\left(\underline{n}\times\underline{E}\right)=0$$

$$\underline{n}\cdot\left(\frac{\partial\underline{E}}{\partial\omega}\times\underline{H}^*\right)=\underline{H}^*\cdot\left(\underline{n}\times\frac{\partial\underline{E}}{\partial\omega}\right)=\underline{H}^*\cdot\frac{\partial}{\partial\omega}\left(\underline{n}\times\underline{E}\right)=0$$

Then

$$i\int_V\left(\mu_0\underline{H}\cdot\underline{H}^*+\varepsilon_0\underline{E}\cdot\underline{E}^*\right)dV=\int_V\left(\frac{\partial\underline{E}}{\partial\omega}\cdot\underline{J}^*+\underline{E}^*\cdot\frac{\partial\underline{J}}{\partial\omega}\right)dV$$

Noting that

$$\mu_0\underline{H}\cdot\underline{H}^*=\frac{\varepsilon_0}{k^2}\left(\nabla\times\underline{E}\right)\cdot\left(\nabla\times\underline{E}^*\right)$$

and here that

$$\underline{E}=u\underline{e}_z$$

$$\underline{J}=J_z\underline{e}_z$$

so that

$$\nabla \times \underline{E} = \nabla \times (u\underline{e}_z) = \nabla u \times \underline{e}_z$$

and

$$\varepsilon_0 \underline{E} \cdot \underline{E}^* = \varepsilon_0 |u|^2$$

$$\mu_0 \underline{H} \cdot \underline{H}^* = \frac{\varepsilon_0}{k^2} |\nabla u|^2$$

$$\underline{e}_z \times (\nabla u \times \underline{e}_z) = \nabla u$$

so that

$$i\frac{\varepsilon_0}{k^2} \int_V \left( |\nabla u|^2 + k^2 |u|^2 \right) dV = \int_V \left( \frac{\partial u}{\partial \omega} J_z^* + u^* \frac{\partial J_z}{\partial \omega} \right) dV$$

Now using

$$|\nabla u|^2 = \nabla u \cdot \nabla u^* = \nabla \cdot (u^* \nabla u) - u^* \nabla^2 u = \nabla \cdot (u^* \nabla u) + k^2 |u|^2$$

gives

$$i2\varepsilon_0 \int_V |u|^2 dV = \int_V \left( \frac{\partial u}{\partial \omega} J_z^* + u^* \frac{\partial J_z}{\partial \omega} \right) dV$$

Now we take a single $p$th component for the current on axis

$$J_z = \frac{i}{\omega \mu_0} \left( \frac{\partial u_p^+}{\partial n} - \frac{\partial u_p^-}{\partial n} \right) \delta(n) \ , \ y = 0$$

and (we take $u$ to be continuous at $y = 0$)

$$i2\varepsilon_0 \int_A |u|^2 dS = \frac{i}{\mu_0} \int_C \left[ -\frac{\partial u}{\partial \omega} \frac{1}{\omega} \left( \frac{\partial u_p^+}{\partial n} - \frac{\partial u_p^-}{\partial n} \right)^* + u^* \frac{\partial}{\partial \omega} \frac{1}{\omega} \left( \frac{\partial u_p^+}{\partial n} - \frac{\partial u_p^-}{\partial n} \right) \right] d\ell$$

Taking the eigenfunction as real and assuming the integrals along the scar produce approximate orthogonality as discussed in the Appendix (we take $u_p$ to be continuous at $y = 0$)

$$2\varepsilon_0 \int_A |u|^2 dS = \frac{1}{\mu_0} \int_C \left[ -\frac{\partial u_p}{\partial \omega} \frac{1}{\omega} \left( \frac{\partial u_p^+}{\partial n} - \frac{\partial u_p^-}{\partial n} \right) + u_p \frac{\partial}{\partial \omega} \frac{1}{\omega} \left( \frac{\partial u_p^+}{\partial n} - \frac{\partial u_p^-}{\partial n} \right) \right] d\ell$$

Now in the elliptic system the metric coefficients are

$$h_\zeta = h_\xi = d\sqrt{\sinh^2 \zeta + \cos^2 \xi}$$

and thus

$$2\varepsilon_0 \int_A |u|^2 dS = \frac{1}{\mu_0} \int_{C_1} \left[ -\frac{\partial u_p}{\partial \omega} \frac{1}{\omega} \left( \frac{\partial u_p^+}{\partial \zeta} - \frac{\partial u_p^-}{\partial \zeta} \right) + u_p \frac{\partial}{\partial \omega} \frac{1}{\omega} \left( \frac{\partial u_p^+}{\partial \zeta} - \frac{\partial u_p^-}{\partial \zeta} \right) \right] \frac{h_\xi}{h_\zeta} d\xi$$

$$-\frac{1}{\mu_0}\int_{C_2}\left[-\frac{\partial u_p}{\partial\omega}\frac{1}{\omega}\left(\frac{\partial u_p^+}{\partial\xi}-\frac{\partial u_p^-}{\partial\xi}\right)+u_p\frac{\partial}{\partial\omega}\frac{1}{\omega}\left(\frac{\partial u_p^+}{\partial\xi}-\frac{\partial u_p^-}{\partial\xi}\right)\right]\frac{h_\zeta}{h_\xi}d\zeta$$

Setting

$$\int_A |u|^2\, dS = 1$$

gives

$$\varepsilon_0\mu_0 = \int_0^{\pi/2}\left[-\frac{\partial u_p}{\partial\omega}\frac{1}{\omega}\left(\frac{\partial u_p^+}{\partial\zeta}-\frac{\partial u_p^-}{\partial\zeta}\right)+u_p\frac{\partial}{\partial\omega}\frac{1}{\omega}\left(\frac{\partial u_p^+}{\partial\zeta}-\frac{\partial u_p^-}{\partial\zeta}\right)\right]d\xi$$

$$+\int_0^{\zeta_0}\left[-\frac{\partial u_p}{\partial\omega}\frac{1}{\omega}\left(\frac{\partial u_p^+}{\partial\xi'}-\frac{\partial u_p^-}{\partial\xi'}\right)+u_p\frac{\partial}{\partial\omega}\frac{1}{\omega}\left(\frac{\partial u_p^+}{\partial\xi'}-\frac{\partial u_p^-}{\partial\xi'}\right)\right]d\zeta$$

### 3.5.1 carrying out the integration

The solution in Region 1 is

$$u_p = 2\frac{\psi(s,\tau)}{\sqrt{\cos\xi}}\cos(\gamma\sin\xi - s\sigma)$$

$$= 2\frac{\psi(s,\tau)}{\sqrt{\sin\xi'}}\cos\left(\gamma\cos\xi' - s\sigma\right),\ \xi' = \pi/2 - \xi$$

where

$$\psi(s,\tau) = c\,\mathrm{Re}\left[e^{-i\pi/4}U_+(s,\tau) + e^{i\pi/4}e^{i\Phi_0}U_+^*(s,\tau)\right]$$

$$\sigma = \int_0^\xi \frac{d\xi}{\cos\xi} = \mathrm{arcsinh}(\tan\xi) = \int_{\xi'}^{\pi/2}\frac{d\xi'}{\sin\xi'} = -\ln\left\{\tan\left(\xi'/2\right)\right\}$$

$$\tau = \sqrt{2\gamma}\zeta$$

$$U_+(s,\tau) = e^{-\pi(s+i/2)/4}U\left(-is, \tau e^{-i\pi/4}\right)$$

$$k_p\ell = \pi(p - 1/4)$$

The solution in Region 2 is

$$u_p = \frac{2}{\sqrt{\sinh\zeta}}\psi(s',\tau')\cos(\gamma\cosh\zeta - s'\sigma' - \pi/4)$$

where

$$s' = -s$$

$$\psi\left(s', \tau'\right) = c\,\mathrm{Re}\left[U_+\left(-s, \tau'\right) + e^{-i\Phi_0} U_+^*\left(-s, \tau'\right)\right]$$

$$U_+\left(s, \tau\right) = e^{-\pi(s+i/2)/4} U\left(-is, \tau e^{-i\pi/4}\right)$$

$$\tau' = \sqrt{2\gamma}\xi'$$

$$\xi' = \pm\pi/2 - \xi$$

$$2s'\sigma_0' = 2s' \ln\left[\tanh\left(\zeta_0/2\right)\right] = \left(k - k_p\right) L$$

$$\sigma' = \int_\infty^\zeta \frac{d\zeta}{\sinh\zeta} = \ln\left[\tanh\left(\zeta/2\right)\right]$$

The solution in Region 3 is

$$u_p = (-1)^n \left(2\gamma\right)^{1/4} \frac{\left|U_+'\left(s', 0\right)\right|}{\mathrm{Im}\left[U_+'\left(s', 0\right)\right]} c\,\mathrm{Re}\left[U_+\left(s', \xi'\sqrt{2\gamma}\right) + e^{-i\Phi_0} U_+^*\left(s', \xi'\sqrt{2\gamma}\right)\right]$$

$$\mathrm{Re}\left[e^{-i\pi/4} U_+\left(-s', \zeta\sqrt{2\gamma}\right) + e^{i\pi/4} e^{i\Phi_0} U_+^*\left(-s', \zeta\sqrt{2\gamma}\right)\right]$$

Here we apply the normalization with only Region 1 and Region 2 solutions separated by the coordinate value $\xi = \pi/2$ ($\xi' = 0$) and $\cosh\zeta_0 = \ell/d$. The Appendix discusses the Region 3 contribution. To carry out the integration we introduce a slight displacement $\Delta$ on either side of the focus, so that the integration range is $\xi = 0$ to

$$\xi = \mathrm{Arcsin}\left(1 - \Delta/d\right) \approx \frac{\pi}{2} - \sqrt{2\Delta/d}$$

and from $\zeta$ equal to

$$\zeta = \mathrm{Arccosh}\left(1 + \Delta/d\right) \approx \sqrt{2\Delta/d}$$

to $\zeta_0$. Then in Region 1 we have

$$\frac{\partial u_p^+}{\partial\zeta} - \frac{\partial u_p^-}{\partial\zeta} = 4c\sqrt{2\gamma}\,\mathrm{Re}\left[e^{-i\pi/4} U_+'\left(s, \tau\right) + e^{i\pi/4} e^{i\Phi_0} U_+^{*\prime}\left(s, \tau\right)\right] \frac{1}{\sqrt{\sin\xi'}} \cos\left(\gamma\cos\xi' - s\sigma\right)$$

Now taking the limit as $\tau \to 0$

$$\left(\frac{\partial u_p^+}{\partial\zeta} - \frac{\partial u_p^-}{\partial\zeta}\right) \propto \mathrm{Re}\left[e^{-i\pi/4} U_+'\left(s, 0\right) + e^{i\pi/4} e^{i\Phi_0} U_+^{*\prime}\left(s, 0\right)\right] \to 0$$

or

$$e^{i\Phi_0} = i\frac{U'_+(s,0)}{U^{*\prime}_+(s,0)}$$

$$\frac{\partial}{\partial\omega}\frac{1}{\omega}\left(\frac{\partial u_p^+}{\partial\zeta} - \frac{\partial u_p^-}{\partial\zeta}\right) = 4c\frac{1}{\omega}\sqrt{2\gamma}\frac{\partial\Phi_0}{\partial\omega}\,\mathrm{Im}\left[e^{-i\pi/4}U'_+(s,0)\right]\frac{1}{\sqrt{\cos\xi}}\cos\left(\gamma\sin\xi - s\sigma\right)$$

$$u_p = 2\frac{1}{\sqrt{\cos\xi}}c\frac{\mathrm{Im}\left[e^{-i\pi/4}U'_+(s,0)\right]}{\left|U'_+(s,0)\right|^2}\cos\left(\gamma\sin\xi - s\sigma\right)$$

In Region 2 we have

$$\left(\frac{\partial u_p^+}{\partial\xi'} - \frac{\partial u_p^-}{\partial\xi'}\right) = \sqrt{2\gamma}\frac{4}{\sqrt{\sinh\zeta}}c\,\mathrm{Re}\left[U'_+(-s,\tau') + e^{-i\Phi_0}U^{*\prime}_+(-s,\tau')\right]\cos\left(\gamma\cosh\zeta + s\sigma' - \pi/4\right)$$

$$\left(\frac{\partial u_p^+}{\partial\xi'} - \frac{\partial u_p^-}{\partial\xi'}\right) \propto \mathrm{Re}\left[U'_+(-s,0) + e^{-i\Phi_0}U^{*\prime}_+(-s,0)\right] \to 0$$

or

$$e^{-i\Phi_0} = -\frac{U'_+(-s,0)}{U^{*\prime}_+(-s,0)}$$

$$\frac{\partial}{\partial\omega}\frac{1}{\omega}\left(\frac{\partial u_p^+}{\partial\xi'} - \frac{\partial u_p^-}{\partial\xi'}\right) = -\sqrt{2\gamma}\frac{4}{\sqrt{\sinh\zeta}}c\frac{1}{\omega}\frac{\partial\Phi_0}{\partial\omega}\,\mathrm{Im}\left[U'_+(-s,0)\right]\cos\left(\gamma\cosh\zeta + s\sigma' - \pi/4\right)$$

$$u_p = \frac{2}{\sqrt{\sinh\zeta}}c\frac{\mathrm{Im}\left[U'_+(-s,0)\right]}{\left|U'_+(-s,0)\right|^2}\cos\left(\gamma\cosh\zeta + s\sigma' - \pi/4\right)$$

where we have used the Wronskian

$$U'_+U^*_+ - U^{*\prime}_+U_+ = i$$

Now assembling the normalization condition

$$\varepsilon_0\mu_0 = 16c^2\sqrt{2\gamma}\mu_0\varepsilon_0\frac{\partial\Phi_0}{\partial k^2}\frac{\mathrm{Im}^2\left[e^{-i\pi/4}U'_+(s,0)\right]}{\left|U'_+(s,0)\right|^2}\int_0^{\pi/2-\sqrt{2\Delta/d}}\cos^2\left(\gamma\sin\xi - s\sigma\right)\frac{d\xi}{\cos\xi}$$

$$-16c^2\sqrt{2\gamma}\mu_0\varepsilon_0\frac{\partial\Phi_0}{\partial k^2}\frac{\mathrm{Im}^2\left[U'_+(-s,0)\right]}{\left|U'_+(-s,0)\right|^2}\int_{\sqrt{2\Delta/d}}^{\zeta_0}\cos^2\left(\gamma\cosh\zeta + s\sigma' - \pi/4\right)\frac{d\zeta}{\sinh\zeta}$$

Transforming the first integral to $\xi'$

$$\varepsilon_0\mu_0 = 16c^2\sqrt{2\gamma}\mu_0\varepsilon_0\frac{\partial\Phi_0}{\partial k^2}\frac{\mathrm{Im}^2\left[e^{-i\pi/4}U'_+(s,0)\right]}{\left|U'_+(s,0)\right|^2}\int_{\sqrt{2\Delta/d}}^{\pi/2}\cos^2\left(\gamma\cos\xi' - s\sigma\right)\frac{d\xi'}{\sin\xi'}$$

$$-16c^2\sqrt{2\gamma}\mu_0\varepsilon_0\frac{\partial\Phi_0}{\partial k^2}\frac{\mathrm{Im}^2\left[U_+'(-s,0)\right]}{\left|U_+'(-s,0)\right|^2}\int_{\sqrt{2\Delta/d}}^{\zeta_0}\cos^2\left(\gamma\cosh\zeta+s\sigma'-\pi/4\right)\frac{d\zeta}{\sinh\zeta}$$

Transforming to $\sigma$ and $\sigma''=-\sigma'$, with $\cos\xi'=\tanh\sigma$ and $\cosh\zeta=-\coth\sigma'=\coth\sigma''$ and $d\xi'/\sin\xi'=d\sigma$ and $d\zeta/\sinh\zeta=d\sigma'$ gives

$$\varepsilon_0\mu_0=-16c^2\sqrt{2\gamma}\mu_0\varepsilon_0\frac{\partial\Phi_0}{\partial k^2}\frac{\mathrm{Im}^2\left[e^{-i\pi/4}U_+'(s,0)\right]}{\left|U_+'(s,0)\right|^2}\int_0^{\ln\left(\sqrt{2d/\Delta}\right)}\cos^2\left(\gamma\tanh\sigma-s\sigma\right)d\sigma$$

$$+16c^2\sqrt{2\gamma}\mu_0\varepsilon_0\frac{\partial\Phi_0}{\partial k^2}\frac{\mathrm{Im}^2\left[U_+'(-s,0)\right]}{\left|U_+'(-s,0)\right|^2}\int_{-\ln\left(\sqrt{2d/\Delta}\right)}^{-\sigma_0'}\cos^2\left(\gamma\coth\sigma''+s\sigma''-\pi/4\right)d\sigma''$$

where $\sigma_0'=\ln\left\{\tanh\left(\zeta_0/2\right)\right\}=\frac{1}{2}\ln\left(\frac{\ell-d}{\ell+d}\right)<0$.

Noting that

$$U_+'(-s',0)=e^{\pi s'/2-i3\pi/4}U_+^{*\prime}(s',0)$$

we see that

$$\frac{\mathrm{Im}^2\left[U_+'(-s,0)\right]}{\left|U_+'(-s,0)\right|^2}=\frac{\mathrm{Im}^2\left[e^{-i\pi/4}U_+'(s,0)\right]}{\left|U_+'(s,0)\right|^2}$$

so

$$\varepsilon_0\mu_0=16c^2\sqrt{2\gamma}\mu_0\varepsilon_0\frac{\partial\Phi_0}{\partial k^2}\frac{\mathrm{Im}^2\left[e^{-i\pi/4}U_+'(s,0)\right]}{\left|U_+'(s,0)\right|^2}$$

$$\left[-\int_0^{\ln\left(\sqrt{2d/\Delta}\right)}\cos^2\left(\gamma\tanh\sigma-s\sigma\right)d\sigma+\int_{-\ln\left(\sqrt{2d/\Delta}\right)}^{-\sigma_0'}\cos^2\left(\gamma\coth\sigma''+s\sigma''-\pi/4\right)d\sigma''\right]$$

If we average over the rapidly varying sinusoids

$$\varepsilon_0\mu_0=-8c^2\sqrt{2\gamma}\mu_0\varepsilon_0\frac{\partial\Phi_0}{\partial k^2}\frac{\mathrm{Im}^2\left[e^{-i\pi/4}U_+'(s,0)\right]}{\left|U_+'(s,0)\right|^2}\sigma_0'$$

This evaluation made use of a principal value interpretation of the energy theorem integration (in $\zeta$and $\xi'$) at the focal point. The Appendix discusses how the Region 3 contribution leads to this interpretation.

We now adopt Antonsen's conjecture [30] that

$$v^2=\frac{A}{8}\left|\frac{d\Phi_0}{dk^2}\right|^{-1}$$

is the square of a unit Gaussian random variable and that $v$ is a Gaussian random variable with zero mean and unit variance.

## 3.6 Trigonometric Projection Operator

This section considers simplified definitions of the projection operator, motivated by the $s \to 0$ limit of the preceding scar functions.

### 3.6.1 no amplitude factors

Suppose we use the even trigonometric form

$$u_p^T = c\cos(k_p x) \ , \ \ |x| < d$$

$$= c\cos(k_p |x| - \pi/4)$$

motivated by the $s \to 0$ limit of the high frequency scar functions in the preceding sections (as well as neglecting the amplitude factors $\left|1 - x^2/d^2\right|^{-1/4}$), to define a projection operator

$$V_p^T = 2\int_0^d \cos(k_p x)\, u(x,0)\, dx + 2\int_d^\ell \cos(k_p x - \pi/4)\, u(x,0)\, dx$$

First we insert only the scarred component

$$V_{pp}^T = 2\int_0^d u_p(x,0)\cos(k_p x)\, dx + 2\int_d^\ell u_p(x,0)\cos(k_p x - \pi/4)\, dx$$

where in Region 1

$$u_p(x,0) \sim 2\frac{1}{\sqrt{\cos\xi}} c \frac{\mathrm{Im}\left[e^{-i\pi/4} U_+'(s,0)\right]}{\left|U_+'(s,0)\right|^2} \cos(\gamma\sin\xi - s\sigma)$$

$$\sim \frac{2v}{(2\gamma)^{1/4}\left|U_+'(-s',0)\right|\sqrt{A\ln\left(\frac{\ell+d}{\ell-d}\right)}} \sqrt{2d}\left(d^2 - x^2\right)^{-1/4} \cos\left[k_p x + p_1(x)\right] \text{ , Region 1}$$

and in Region 2

$$u_p(x,0) \sim \frac{2}{\sqrt{\sinh\zeta}} c \frac{\mathrm{Im}\left[U_+'(s',0)\right]}{\left|U_+'(s',0)\right|^2} \cos(\gamma\cosh\zeta - s'\sigma' - \pi/4)$$

$$\sim \frac{2v}{(2\gamma)^{1/4}\left|U_+'(s',0)\right|\sqrt{A\ln\left(\frac{\ell+d}{\ell-d}\right)}} \sqrt{2d}\left(x^2 - d^2\right)^{-1/4} \cos\left[k_p x - \pi/4 + p_2(x)\right] \text{ , Region 2}$$

with

$$U_+'(-s',0) = e^{\pi s'/2 - i3\pi/4} U_+^{*\prime}(s',0)$$

$$\frac{\sqrt{2}v\left|U_{+}'\left(s,0\right)\right|}{\left(2\gamma\right)^{1/4}\operatorname{Im}\left[e^{-i\pi/4}U_{+}'\left(s,0\right)\right]\sqrt{A\ln\left(\frac{\ell+d}{\ell-d}\right)}}=c=\frac{\sqrt{2}v\left|U_{+}'\left(s',0\right)\right|}{\left(2\gamma\right)^{1/4}\operatorname{Im}\left[U_{+}'\left(s',0\right)\right]\sqrt{A\ln\left(\frac{\ell+d}{\ell-d}\right)}}$$

and

$$s'\ln\left(\frac{\ell+d}{\ell-d}\right)=2\left(k_p-k\right)\ell$$

$$s'=-s$$

$$p_1\left(x\right)=\frac{1}{2}s'\left\{\ln\left(\frac{d+x}{d-x}\right)-\ln\left(\frac{\ell+d}{\ell-d}\right)\left(x/\ell\right)\right\}$$

$$p_2\left(x\right)=\frac{1}{2}s'\left\{\ln\left(\frac{x+d}{x-d}\right)-\ln\left(\frac{\ell+d}{\ell-d}\right)\left(x/\ell\right)\right\}$$

Thus

$$V_{pp}^{T}=2\frac{2v}{\left(2\gamma\right)^{1/4}\left|U_{+}'\left(-s',0\right)\right|\sqrt{A\ln\left(\frac{\ell+d}{\ell-d}\right)}}\sqrt{2d}\int_{0}^{d}\left(d^2-x^2\right)^{-1/4}\cos\left[k_px+p_1\left(x\right)\right]\cos\left(k_px\right)dx$$

$$+2\frac{2v}{\left(2\gamma\right)^{1/4}\left|U_{+}'\left(s',0\right)\right|\sqrt{A\ln\left(\frac{\ell+d}{\ell-d}\right)}}\sqrt{2d}\int_{d}^{\ell}\left(x^2-d^2\right)^{-1/4}\cos\left[k_px-\pi/4+p_2\left(x\right)\right]\cos\left(k_px-\pi/4\right)dx$$

$$=2\frac{2v}{\left(2\gamma\right)^{1/4}\left|U_{+}'\left(-s',0\right)\right|\sqrt{A\ln\left(\frac{\ell+d}{\ell-d}\right)}}$$

$$\sqrt{2d}\int_{0}^{d}\left(d^2-x^2\right)^{-1/4}\left\{\cos^2\left(k_px\right)\cos\left(p_1\left(x\right)\right)-\sin\left(k_px\right)\cos\left(k_px\right)\sin\left(p_1\left(x\right)\right)\right\}dx$$

$$+2\frac{2v}{\left(2\gamma\right)^{1/4}\left|U_{+}'\left(s',0\right)\right|\sqrt{A\ln\left(\frac{\ell+d}{\ell-d}\right)}}$$

$$\sqrt{2d}\int_{d}^{\ell}\left(x^2-d^2\right)^{-1/4}\left\{\cos^2\left(k_px-\pi/4\right)\cos\left(p_2\left(x\right)\right)-\cos\left(k_px-\pi/4\right)\sin\left(k_px-\pi/4\right)\sin\left(p_2\left(x\right)\right)\right\}dx$$

Now if we average over the rapidly varying sinusoids

$$V_{pp}^{T}\approx\frac{2v}{\left(2\gamma\right)^{1/4}\left|U_{+}'\left(-s',0\right)\right|\sqrt{A\ln\left(\frac{\ell+d}{\ell-d}\right)}}\sqrt{2d}\int_{0}^{d}\left(d^2-x^2\right)^{-1/4}\cos\left(p_1\left(x\right)\right)dx$$

$$+\frac{2v}{(2\gamma)^{1/4}\left|U_+'(s',0)\right|\sqrt{A\ln\left(\frac{\ell+d}{\ell-d}\right)}}\sqrt{2d}\int_d^{\ell}\left(x^2-d^2\right)^{-1/4}\cos\left(p_2(x)\right)dx$$

or

$$V_{pp}^T\approx\frac{2v\sqrt{2}d}{(2\gamma)^{1/4}\left|U_+'(-s',0)\right|\sqrt{A\ln\left(\frac{\ell+d}{\ell-d}\right)}}\int_0^1\left(1-x^2\right)^{-1/4}\cos\left[\frac{1}{2}s'\left\{\ln\left(\frac{1+x}{1-x}\right)-x\,(d/\ell)\ln\left(\frac{\ell+d}{\ell-d}\right)\right\}\right]dx$$

$$+\frac{2v\sqrt{2}d}{(2\gamma)^{1/4}\left|U_+'(s',0)\right|\sqrt{A\ln\left(\frac{\ell+d}{\ell-d}\right)}}\int_1^{\ell/d}\left(x^2-1\right)^{-1/4}\cos\left[\frac{1}{2}s'\left\{\ln\left(\frac{x+1}{x-1}\right)-x\,(d/\ell)\ln\left(\frac{\ell+d}{\ell-d}\right)\right\}\right]dx$$

### 3.6.2 no amplitude factors and elimination of phase shifts

If we drop the phase shifts $p_1(x)$ and $p_2(x)$ in the integrands of the preceding results we find

$$V_{pp}^T=\frac{2v\sqrt{2}d}{(2\gamma)^{1/4}\sqrt{A\ln\left(\frac{\ell+d}{\ell-d}\right)}}\left[\frac{1}{\left|U_+'(-s',0)\right|}\int_0^1\left(1-x^2\right)^{-1/4}dx+\frac{1}{\left|U_+'(s',0)\right|}\int_1^{\ell/d}\left(x^2-1\right)^{-1/4}dx\right]$$

The first integral is

$$\int_0^1\left(1-x^2\right)^{-1/4}dx=\frac{1}{2}\int_0^1(1-u)^{-1/4}u^{-1/2}=\frac{\Gamma(3/4)\Gamma(1/2)}{2\Gamma(5/4)}=\frac{2^{3/2}\pi^{3/2}}{\Gamma^2(1/4)}$$

$$\approx 1.19814\approx 0.76275\,(\pi/2)$$

The second integral can be evaluated by letting $x^2=u$, followed by the transformations $1-1/u=v$ or $u=1/(1-v)$, $u-1=v/(1-v)$ and $du=dv/(1-v)^2$

$$\int_1^{\ell/d}\left(x^2-1\right)^{-1/4}dx=\frac{1}{2}\int_1^{(\ell/d)^2}(u-1)^{-1/4}u^{-1/2}du=\frac{1}{2}\int_0^{1-(d/\ell)^2}(1-v)^{-5/4}v^{-1/4}dv$$

$$=\frac{1}{2}B_{1-(d/\ell)^2}\left(\frac{3}{4},-\frac{1}{4}\right)\approx 1.919598\approx 1.027319\zeta_0$$

where $B_x(a,b)$ is the incomplete beta function [31] and $\mathrm{Arccosh}(\ell/d)=\zeta_0$. Note that the final equalities are noted because if we had included the amplitude factors $\left|1-x^2/d^2\right|^{-1/4}$ in the projection operator we would have obtained $\pi/2$ in Region 1 and $\zeta_0$ in Region 2 as shown in the next subsubsection.

### 3.6.3 amplitude factors present with no phase shifts

If we include the amplitude factors but no phase shifts

$$V_{pp} = 2\int_0^d u\left(x,0\right)\sqrt{d}\left(d^2-x^2\right)^{-1/4}\cos\left(k_p x\right)dx + 2\int_d^\ell u\left(x,0\right)\sqrt{d}\left(x^2-d^2\right)^{-1/4}\cos\left(k_p x-\pi/4\right)dx$$

Inserting the high frequency solutions

$$V_{pp} = \frac{4v\sqrt{2}d}{\left(2\gamma\right)^{1/4}\left|U_+'\left(-s',0\right)\right|\sqrt{A\ln\left(\frac{\ell+d}{\ell-d}\right)}}\int_0^d\left(d^2-x^2\right)^{-1/2}\cos^2\left(k_p x\right)dx$$

$$+\frac{4v\sqrt{2}d}{\left(2\gamma\right)^{1/4}\left|U_+'\left(s',0\right)\right|\sqrt{A\ln\left(\frac{\ell+d}{\ell-d}\right)}}\int_d^\ell\left(x^2-d^2\right)^{-1/2}\cos^2\left(k_p x-\pi/4\right)dx$$

Now averaging over the cosines gives

$$V_{pp} \sim \frac{2v\sqrt{2}d}{\left(2\gamma\right)^{1/4}\left|U_+'\left(-s',0\right)\right|\sqrt{A\ln\left(\frac{\ell+d}{\ell-d}\right)}}\int_0^1\left(1-x^2\right)^{-1/2}dx$$

$$+\frac{2v\sqrt{2}d}{\left(2\gamma\right)^{1/4}\left|U_+'\left(s',0\right)\right|\sqrt{A\ln\left(\frac{\ell+d}{\ell-d}\right)}}\int_1^{\ell/d}\left(x^2-1\right)^{-1/2}dx$$

$$\sim \frac{2v\sqrt{2}d}{\left(2\gamma\right)^{1/4}\sqrt{A\ln\left(\frac{\ell+d}{\ell-d}\right)}}\left[\frac{\pi/2}{\left|U_+'\left(-s',0\right)\right|}+\frac{\zeta_0}{\left|U_+'\left(s',0\right)\right|}\right]$$

Squaring gives

$$V_{pp}^2 \sim \frac{v^2 8d^2}{\sqrt{2\gamma}A\ln\left(\frac{\ell+d}{\ell-d}\right)}\left[\frac{\pi/2}{\left|U_+'\left(-s',0\right)\right|}+\frac{\zeta_0}{\left|U_+'\left(s',0\right)\right|}\right]^2$$

where

$$\zeta_0 = \operatorname{Arccosh}\left(\ell/d\right) = \ln\left(\ell/d+\sqrt{\ell^2/d^2-1}\right)$$

$$A = \pi R^2 + 2R\left(L-2R\right) = 4R^2\left(\pi/4+\frac{d^2}{\ell R}\right)$$

$$V_{pp}^2 \sim \frac{v^2 8d^2}{\sqrt{2kd}A\ln\left(\frac{\ell+d}{\ell-d}\right)}\frac{1}{\pi\sqrt{2}}\left[\left|\Gamma\left(is'/2+1/4\right)\right|\pi/2+\left|\Gamma\left(-is'/2+1/4\right)\right|\zeta_0\right]^2$$

$$s'\ln\left(\frac{\ell+d}{\ell-d}\right) = \left(k_p-k\right)L = 2\left(k_p-k\right)\ell$$

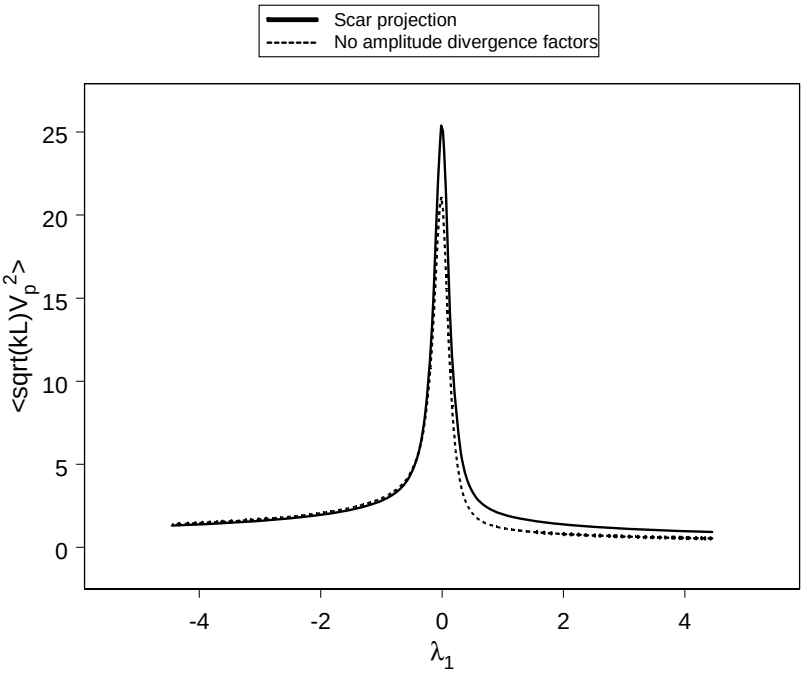


Figure 51. Comparison of projections with and without amplitude factors. The phase shifts are neglected in both regions.

$$d = \ell\sqrt{1 - R/\ell}$$

$$k_p \ell = \pi\left(p - 1/4\right)$$

$$\left\langle \sqrt{kL} V_{pp}^2 \right\rangle \sim \frac{8d^2/\pi}{\sqrt{2d/\ell} A \ln\left(\frac{\ell+d}{\ell-d}\right)} \left[\left|\Gamma\left(is'/2 + 1/4\right)\right| \pi/2 + \left|\Gamma\left(-is'/2 + 1/4\right)\right| \zeta_0\right]^2$$

$$\sim \frac{8d^2/\pi}{\sqrt{2d/\ell} A \ln\left(\frac{\ell+d}{\ell-d}\right)} \left|\Gamma\left(is'/2 + 1/4\right)\right|^2 \left[\pi/2 + \zeta_0\right]^2$$

$$\lambda_1 = \left(k - k_p\right)\sqrt{R\ell} = -s'\frac{1}{2}\ln\left(\frac{\ell+d}{\ell-d}\right)\sqrt{R/\ell}$$

Figure 51 shows the comparison of these projections with and without the amplitude divergence factors, with the phase factors neglected. There is a slight reduction of the peak level without the amplitude factors.

### 3.6.4 no amplitude factors and focal point shift

Because we believe that the focal point in the simulations shifts slightly with realization of the scarred orbits, it is convenient for comparisons with this simplified theory to use a simple modification to capture the average results. We simply replace $d$ in the theory with the the average shift location

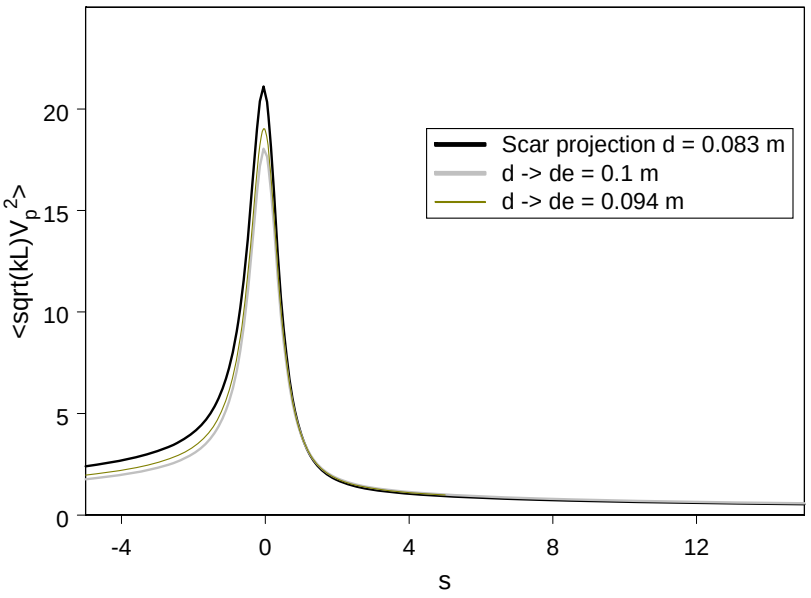


Figure 52. Effect of applying average focal point shift without phase factors or amplitude divergence factors.

$$d \to d_e = d + \langle \delta \rangle$$

where we could select the average discussed previously $\langle \delta_0 \rangle \approx \ell / (2 \langle p \rangle - 1/2)$ or something slightly larger to capture the increases due to $s \neq 0$. Figure 52 shows the variation of the projections with $d$.

### 3.6.5 projection without amplitude factors but with phase factors and focal point shift

Applying the average focal point shift and retaining the phase factors we have

$$V_{pp}^T \approx$$

$$\frac{2v\sqrt{2}d_e}{(2\gamma)^{1/4}\left|U_+'(-s',0)\right|\sqrt{A\ln\left(\frac{\ell+d_e}{\ell-d_e}\right)}}\int_0^1 \left(1-x^2\right)^{-1/4}\cos\left[\frac{1}{2}s'\left\{\ln\left(\frac{1+x}{1-x}\right)-x\left(d_e/\ell\right)\ln\left(\frac{\ell+d_e}{\ell-d_e}\right)\right\}\right]dx$$

$$+\frac{2v\sqrt{2}d_e}{(2\gamma)^{1/4}\left|U_+'(s',0)\right|\sqrt{A\ln\left(\frac{\ell+d_e}{\ell-d_e}\right)}}\int_1^{\ell/d_e}\left(x^2-1\right)^{-1/4}\cos\left[\frac{1}{2}s'\left\{\ln\left(\frac{x+1}{x-1}\right)-x\left(d_e/\ell\right)\ln\left(\frac{\ell+d_e}{\ell-d_e}\right)\right\}\right]dx$$

Figure 53 shows the comparison with a numerical histogram from the boundary element solutions using $d_e \approx 0.094$. Notice that the tails of the scar trigonometric projection decrease rapidly with $s$. This is a consequence of interference in the integrand resulting from the phase factors $p_1$ and $p_2$. Also shown is the projection of the random plane wave representation, which will be given below. Notice that the histogram

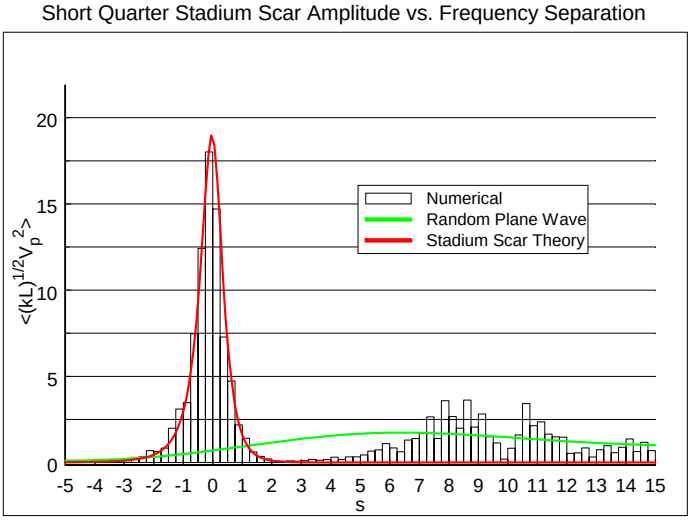


Figure 53. Comparison of trigonometric projection and numerical histogram for short stadium cavity along horizontal bouncing ball scar. The scar theory used an average shifted focal point $d_e \approx 0.094$ m.

seems to show another scar $p'$ component contributing to the trigonometric projection. The amplitude of the next peak does not seem to be too far above the random plane wave projection. The next section looks at an explanation for this next peak.

### 3.6.6 projection of next scar component

The contribution of the other scar components can in general can be written as

$$V_{p,p+m}^{T} = 2\int_0^d u_{p+m}(x,0)\cos(k_p x)\,dx + 2\int_d^\ell u_{p+m}(x,0)\cos(k_p x - \pi/4)\,dx$$

$$= 2\frac{2v}{(2\gamma)^{1/4}\left|U_+'\left(-s_{p+m}',0\right)\right|\sqrt{A\ln\left(\frac{\ell+d}{\ell-d}\right)}}\sqrt{2d}\int_0^d \left(d^2-x^2\right)^{-1/4}\cos\left[k_{p+m}x + p_1^{(p+m)}(x)\right]\cos(k_p x)\,dx$$

$$+2\frac{2v}{(2\gamma)^{1/4}\left|U_+'\left(s_{p+m}',0\right)\right|\sqrt{A\ln\left(\frac{\ell+d}{\ell-d}\right)}}$$

$$\sqrt{2d}\int_d^\ell \left(x^2-d^2\right)^{-1/4}\cos\left[k_{p+m}x - \pi/4 + p_2^{(p+m)}(x)\right]\cos(k_p x - \pi/4)\,dx$$

Averaging over the rapidly varying part (or taking only the difference arguments in the cosines) gives

$$V_{p,p+m}^{T} \approx \frac{2v\sqrt{2}d}{(2\gamma)^{1/4}\left|U_{+}'\left(-s_{p+m}',0\right)\right|\sqrt{A\ln\left(\frac{\ell+d}{\ell-d}\right)}}$$

$$\int_{0}^{1}\left(1-x^{2}\right)^{-1/4}\cos\left[\frac{1}{2}s_{p+m}'\left\{\ln\left(\frac{1+x}{1-x}\right)-x\left(d/\ell\right)\ln\left(\frac{\ell+d}{\ell-d}\right)\right\}+m\pi xd/\ell\right]dx$$

$$+\frac{2v\sqrt{2}d}{(2\gamma)^{1/4}\left|U_{+}'\left(s_{p+m}',0\right)\right|\sqrt{A\ln\left(\frac{\ell+d}{\ell-d}\right)}}$$

$$\int_{1}^{\ell/d}\left(x^{2}-1\right)^{-1/4}\cos\left[\frac{1}{2}s_{p+m}'\left\{\ln\left(\frac{x+1}{x-1}\right)-x\left(d/\ell\right)\ln\left(\frac{\ell+d}{\ell-d}\right)\right\}+m\pi xd/\ell\right]dx$$

where

$$s_{p+m}' = 2\left(k_{p+m}-k\right)\ell/\ln\left(\frac{\ell+d}{\ell-d}\right)$$

$$k_{p+m}\ell = \pi\left(p+m-1/4\right)$$

Figure 54 shows several trigonometric projections, all without amplitude divergence factors. The black curve shows the result without phase factors $p_1$ and $p_2$ and no shift in focal location from the geometrical point. The light grey curve has phase factors $p_1$ and $p_2$ but no shift in focal location. Notice the rapid drop in the tails of the peak due to these phase factors. The dark grey curve is the projection with phase factors $p_1$ and $p_2$ but a shift in average focal location (in this case to $d_e \approx 0.1$ m). This gives a slight drop in peak amplitude. The green curve is again the random plane wave trigonometric projection. The blue curve is the $p$th trigonometric projection of the $(p+1)$th component. The purple curve is the $p$th trigonometric projection of the $(p+2)$th component. Notice that these contributions lie in the region of the second histogram peak and have similar amplitudes. It therefore seems that the reason for the second histogram peak is lack of orthogonality in the trigonometric projection.

### 3.6.7 random plane wave projection

Suppose we use the random plane waves and take the projection with

$$V_{pr}^{T} = \int_{-\ell}^{\ell} u_r\left(x,0\right)\left[\begin{array}{c}\cos\left(k_p x\right),\ |x|<d\\ \cos\left(k_p\left|x\right|-\pi/4\right),\ |x|>d\end{array}\right]dx$$

The variance of this random variable is

$$\left\langle V_{p}^{T2}\right\rangle_{r} = \frac{1}{2\pi A}\int_{0}^{2\pi}\left[F_{+}\left(\theta\right)+F_{-}\left(\theta\right)\right]^{2}d\theta$$

$$F_{+}\left(\theta\right)+F_{-}\left(\theta\right) = 2\int_{0}^{d}\cos\left(k_p x\right)\cos\left(kx\cos\theta\right)dx + 2\int_{d}^{\ell}\cos\left(k_p\left|x\right|-\pi/4\right)\cos\left(kx\cos\theta\right)dx$$

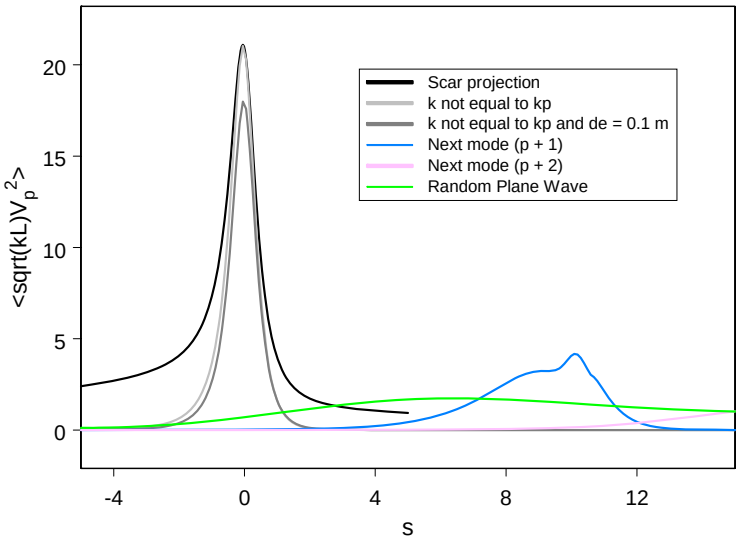


Figure 54. Comparison of various trigonometric projections without amplitude divergence factors. The effect of phase factors reducing the tails of the peak, the reduction of the peak due to the average focal shift, and the lack of othogonality of the trigonometric operator with respect to the scar components are the effects illustrated.

$$= \frac{\sin\left\{\left(k\cos\theta + k_p\right)d\right\}}{\left(k\cos\theta + k_p\right)} + \frac{\sin\left\{\left(k\cos\theta + k_p\right)\ell - \pi/4\right\}}{\left(k\cos\theta + k_p\right)} - \frac{\sin\left\{\left(k\cos\theta + k_p\right)d - \pi/4\right\}}{\left(k\cos\theta + k_p\right)}$$

$$+ \frac{\sin\left\{\left(k\cos\theta - k_p\right)d\right\}}{\left(k\cos\theta - k_p\right)} + \frac{\sin\left\{\left(k\cos\theta - k_p\right)\ell + \pi/4\right\}}{\left(k\cos\theta - k_p\right)} - \frac{\sin\left\{\left(k\cos\theta - k_p\right)d + \pi/4\right\}}{\left(k\cos\theta - k_p\right)}$$

Now suppose we look near the singularities when $k \to k_p$ (and $\theta = \zeta/\sqrt{k\ell/2}$)

$$k_p - k\cos\theta \approx \left(k_p - k\right) + k\theta^2/2$$

$$k_p + k\cos\theta \approx \left(k_p - k\right) + k\left(\theta - \pi\right)^2/2$$

$$\left\langle V_p^2 \right\rangle_r \approx \frac{1}{2\pi A}\int_0^{2\pi} F_+^2\left(\theta\right)d\theta + \frac{1}{2\pi A}\int_0^{2\pi} F_-^2\left(\theta\right)d\theta$$

$$\approx \frac{1}{2\pi A}\int_0^{2\pi} \frac{\left[\sin\left\{\left(k\cos\theta + k_p\right)d\right\} + \sin\left\{\left(k\cos\theta + k_p\right)\ell - \pi/4\right\} - \sin\left\{\left(k\cos\theta + k_p\right)d - \pi/4\right\}\right]^2}{\left(k\cos\theta + k_p\right)^2}d\theta$$

$$+ \frac{1}{2\pi A}\int_0^{2\pi} \frac{\left[\sin\left\{\left(k\cos\theta - k_p\right)d\right\} + \sin\left\{\left(k\cos\theta - k_p\right)\ell - \pi/4\right\} - \sin\left\{\left(k\cos\theta - k_p\right)d - \pi/4\right\}\right]^2}{\left(k\cos\theta - k_p\right)^2}d\theta$$

$$\approx \frac{1}{\pi A}$$

$$\int_{-\infty}^{\infty} \frac{\left[\sin\left\{\left(\left(k_p - k\right) + k\theta^2/2\right)d\right\} + \sin\left\{\left(\left(k_p - k\right) + k\theta^2/2\right)\ell - \pi/4\right\} - \sin\left\{\left(\left(k_p - k\right) + k\theta^2/2\right)d - \pi/4\right\}\right]^2}{\left(\left(k_p - k\right) + k\theta^2/2\right)^2}d\theta$$

$$\approx \frac{1}{\pi A\sqrt{k\ell/2}}\int_{-\infty}^{\infty}$$

$$\frac{\left[\sin\left\{\left(\left(k_p - k\right)\ell + \zeta^2\right)\left(d/\ell\right)\right\} + \sin\left\{\left(\left(k_p - k\right)\ell + \zeta^2\right) - \pi/4\right\} - \sin\left\{\left(\left(k_p - k\right)\ell + \zeta^2\right)\left(d/\ell\right) - \pi/4\right\}\right]^2}{\left(\left(k_p - k\right)\ell + \zeta^2\right)^2/\ell^2}d\zeta$$

$$\approx \frac{L^2}{A\sqrt{kL}}\int_{-\infty}^{\infty} \frac{\left[\sin\left\{\left(\lambda/4 - \zeta^2\right)\left(d/\ell\right)\right\} + \sin\left\{\left(\lambda/4 - \zeta^2\right) + \pi/4\right\} - \sin\left\{\left(\lambda/4 - \zeta^2\right)\left(d/\ell\right) + \pi/4\right\}\right]^2}{\left(\lambda/4 - \zeta^2\right)^2}d\zeta/\left(2\pi\right)$$

where

$$\lambda = 2\left(k - k_p\right)L$$

Thus we can write the ransom plane wave projection as

$$\left\langle \sqrt{kL}V_p^2 \right\rangle_r \approx L^2 G(\lambda)/A$$

where

$$G(\lambda) = \frac{1}{2\pi}\int_{-\infty}^{\infty}$$

$$\frac{\left[\left(1-1/\sqrt{2}\right)\sin\left\{\left(\lambda/4-\zeta^2\right)(d/\ell)\right\}+\sin\left(\lambda/4-\zeta^2\right)/\sqrt{2}+\cos\left(\lambda/4-\zeta^2\right)/\sqrt{2}-\cos\left\{\left(\lambda/4-\zeta^2\right)(d/\ell)\right\}/\sqrt{2}\right]^2}{\left(\lambda/4-\zeta^2\right)^2}d\zeta$$

Introducing the symmetries along the axes we again take

$$G_s(\lambda) = 4G(\lambda)$$

Thus we plotted

$$\left\langle \sqrt{kL}V_p^2 \right\rangle_r \approx L^2 G_s(\lambda)/A$$

on the preceding graphs for the random plane wave trigonometric projection.

### 3.7 Elliptical Projection Operator

It is more useful to set up the projection operator based on the $p$th component field on axis. In Region 1 it is

$$u_p \sim \frac{2v}{(2\gamma)^{1/4}\left|U_+'(s,0)\right|\sqrt{A\ln\left(\frac{\ell+d}{\ell-d}\right)}}\sqrt{2d}\left(d^2-x^2\right)^{-1/4}\cos\left[k_p x + p_1(x)\right], \text{ Region 1}$$

and in Region 2 it is

$$u_p \sim \frac{2v}{(2\gamma)^{1/4}\left|U_+'(s',0)\right|\sqrt{A\ln\left(\frac{\ell+d}{\ell-d}\right)}}\sqrt{2d}\left(x^2-d^2\right)^{-1/4}\cos\left[k_p x - \pi/4 + p_2(x)\right], \text{ Region 2}$$

where

$$s = -s'$$

$$s'\ln\left(\frac{\ell+d}{\ell-d}\right) = \frac{s'}{2}\ln(\Lambda_+) = 2(k_p-k)\ell$$

$$p_1(x) = \frac{1}{2}s'\left\{\ln\left(\frac{d+x}{d-x}\right) - \ln\left(\frac{\ell+d}{\ell-d}\right)(x/\ell)\right\}$$

$$p_2(x) = \frac{1}{2}s'\left\{\ln\left(\frac{x+d}{x-d}\right) - \ln\left(\frac{\ell+d}{\ell-d}\right)(x/\ell)\right\}$$

Noting that

$$\left|U_+'\left(s,0\right)\right| = e^{\pi s'/2}\left|U_+'\left(s',0\right)\right|$$

we define the Galerkin-type projection operator as

$$e^{\pi|s'|/4}V_p = e^{-\pi s'/4}2\sqrt{d}\int_0^d u\left(x,0\right)\left(d^2-x^2\right)^{-1/4}\cos\left[k_p x + p_1\left(x\right)\right]dx$$

$$+e^{\pi s'/4}2\sqrt{d}\int_d^\ell u\left(x,0\right)\left(x^2-d^2\right)^{-1/4}\cos\left[k_p x - \pi/4 + p_2\left(x\right)\right]dx$$

where we have maintained the exponential scaling of the eigenfunction form of the projection operator between the two regions. If we insert a series form

$$u \sim \sum_p u_p$$

assuming asymptotic orthogonality holds, as discussed in the Appendix, we obtain

$$e^{\pi|s'|/4}V_p \sim e^{-\pi s'/4}2\sqrt{d}\int_0^d u_p\left(x,0\right)\left(d^2-x^2\right)^{-1/4}\cos\left[k_p x + p_1\left(x\right)\right]dx$$

$$+e^{\pi s'/4}2\sqrt{d}\int_d^\ell u_p\left(x,0\right)\left(x^2-d^2\right)^{-1/4}\cos\left[k_p x - \pi/4 + p_2\left(x\right)\right]dx$$

Now inserting the high frequency solution gives

$$\exp\left(\pi\left|s'\right|/4\right)V_p = 2\sqrt{d}\frac{2v}{\left(2\gamma\right)^{1/4}\left|U_+'\left(-s',0\right)\right|\sqrt{A\ln\left(\frac{\ell+d}{\ell-d}\right)}}\sqrt{2d}e^{-\pi s'/4}\int_0^d\left(d^2-x^2\right)^{-1/2}\cos^2\left[k_p x + p_1\left(x\right)\right]dx$$

$$+2\sqrt{d}\frac{2v}{\left(2\gamma\right)^{1/4}\left|U_+'\left(s',0\right)\right|\sqrt{A\ln\left(\frac{\ell+d}{\ell-d}\right)}}\sqrt{2d}e^{\pi s'/4}\int_d^\ell\left(x^2-d^2\right)^{-1/2}\cos^2\left[k_p x - \pi/4 + p_2\left(x\right)\right]dx$$

Averaging over the rapidly varying cosine factors gives

$$\exp\left(\pi\left|s'\right|/4\right)V_p \sim \frac{2\sqrt{2}vd}{\left(2\gamma\right)^{1/4}\left|U_+'\left(-s',0\right)\right|\sqrt{A\ln\left(\frac{\ell+d}{\ell-d}\right)}}e^{-\pi s'/4}\int_0^d\left(d^2-x^2\right)^{-1/2}dx$$

$$+\frac{2\sqrt{2}vd}{\left(2\gamma\right)^{1/4}\left|U_+'\left(s',0\right)\right|\sqrt{A\ln\left(\frac{\ell+d}{\ell-d}\right)}}e^{\pi s'/4}\int_d^\ell\left(x^2-d^2\right)^{-1/2}dx$$

$$\sim \frac{2\sqrt{2}vd}{(2\gamma)^{1/4}\sqrt{A\ln\left(\frac{\ell+d}{\ell-d}\right)}}\left[e^{-\pi s'/4}\frac{\pi/2}{\left|U'_+(-s',0)\right|}+e^{\pi s'/4}\frac{\mathrm{Arccosh}\,(\ell/d)}{\left|U'_+(s',0)\right|}\right]$$

$$\sim \frac{2\sqrt{2}vd}{(2\gamma)^{1/4}\sqrt{A\ln\left(\frac{\ell+d}{\ell-d}\right)}}\left[e^{-\pi s'/4}\frac{\pi/2}{\left|U'_+(-s',0)\right|}+e^{\pi s'/4}\frac{\zeta_0}{\left|U'_+(s',0)\right|}\right]$$

or

$$\exp(\pi|s|/4)\,V_p \sim \frac{2\sqrt{2}vd}{(2\gamma)^{1/4}\sqrt{A\left|U'_+(s,0)\,U'_+(s',0)\right|\ln\left(\frac{\ell+d}{\ell-d}\right)}}\left(e^{\pi s/2}\pi/2+e^{\pi s'/2}\zeta_0\right)$$

where

$$\zeta_0 = \ln\left(\ell/d+\sqrt{\ell^2/d^2-1}\right)$$

Note that for $s=-s'=0$

$$V_p \sim \frac{2vd}{\gamma^{1/4}\sqrt{\pi A\ln\left(\frac{\ell+d}{\ell-d}\right)}}\left(\frac{\pi}{2}+\zeta_0\right)\Gamma(1/4)$$

The quantity considered in the bow tie cavity is given in the stadium by

$$\left\langle\sqrt{kL}V_p^2\right\rangle = L^2G_1(s)/A$$

where

$$\exp(\pi|s|/2)\,G_1(s) \sim \frac{2(d/\ell)^{3/2}}{\ln\left(\frac{\ell+d}{\ell-d}\right)}\left[e^{\pi s/4}\frac{\pi/2}{\left|U'_+(s,0)\right|}+e^{\pi s'/4}\frac{\zeta_0}{\left|U'_+(s',0)\right|}\right]^2$$

$$\sim \frac{2(d/\ell)^{3/2}}{\left|U'_+(s,0)\,U'_+(s',0)\right|\ln\left(\frac{\ell+d}{\ell-d}\right)}\left(e^{\pi s/2}\pi/2+e^{\pi s'/2}\zeta_0\right)^2$$

The value at $s=0$, using the geometrical focal point $d$, is

$$\left\langle\sqrt{kL}V_p^2\right\rangle = L^2G_1(0)/A \sim \frac{L^2}{A}\frac{(d/\ell)\sqrt{2d/\ell}}{\pi\ln\left(\frac{\ell+d}{\ell-d}\right)}\left(\frac{\pi}{2}+\zeta_0\right)^2\Gamma^2(1/4)\approx 25.45$$

and the asymptotic forms are

$$\frac{1}{\left|U'_+(s',0)\right|}=\frac{1}{\left|U'_+(-s,0)\right|}=e^{\pi s'/4}\frac{\left|\Gamma(-is'/2+1/4)\right|}{2^{1/4}\sqrt{\pi}}\sim\sqrt{2}s'^{-1/4},\ s'>>1$$

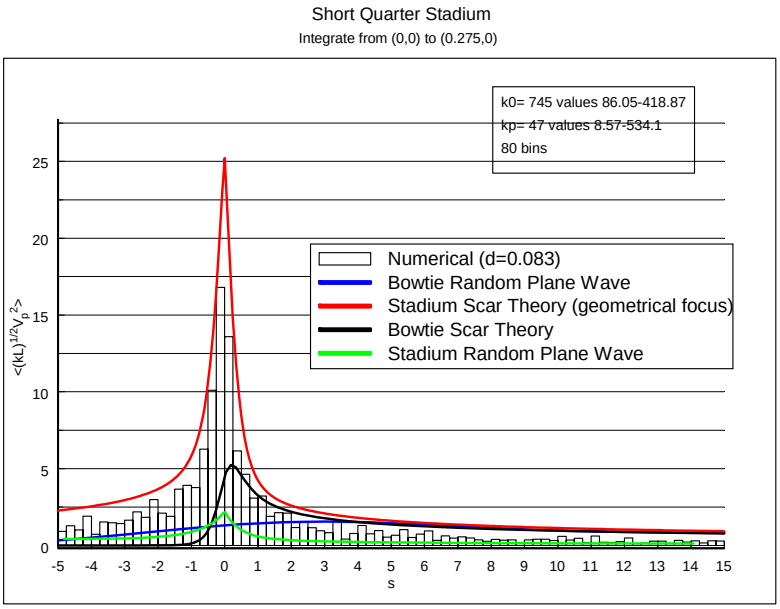


Figure 55. Comparison of scar projection and numerical histogram using geometrical focal location. Also shown for reference is the bow tie scar theory. Finally the random plane wave projection is plotted.

$$\frac{1}{\left|U'_+(-s',0)\right|} = \frac{1}{\left|U'_+(s,0)\right|} \sim e^{-\pi s'/2}\sqrt{2}s'^{-1/4}\,,\; s' >> 1$$

Figure 55 shows a comparison of the scar projection using the geometrical focal location $d \approx 0.083$ m and the numerical histogram data from the boundary element simulation, using the elliptic projection operator and geometrical focal location (this includes amplitude divergence factors and phase factors). Notice that the projection operator with the phase factors widens the tails about the peak (the theory result is similar to the preceding trigonometric result). The theory peak somewhat overestimates the numerical results. The bow tie cavity results are shown for comparison. the random plane wave projection is also given.

Figure 56 shows the comparison when the average shift location is used $d \to d_e = d + \langle\delta\rangle \approx 0.092$ m in the theory as well as in the numerical histogram projection. The random plane wave projection discussed in the subsubsection below is plotted. The bow tie theory is also shown. The theory result still somewhat overestimates the numerical result at the peak.

Figure 57 shows the comparison when the average shift $d_e = d + \langle\delta\rangle \approx 0.092$ m is used in the theory, for which we align this location in the scar component $u_p$ (since we have not inserted the shift or the Region 3 form), and the numerical histogram with the shift being determined for each eigenfunction represented from the shift theory discussed above $d + \delta$ (using the first value of $n$ giving a point to the right of the geometrical focus). This comparison thus depicts more consistent alignment between two quantities (since the numerical solutions contain the shifts). The theory result and the numerical result are somewhat closer at the peak. Note from the Appendix that the Region 3 contribution does not significantly change the theory result. The random plane wave projection discussed in the subsubsection below is plotted and the bow tie theory is also shown.

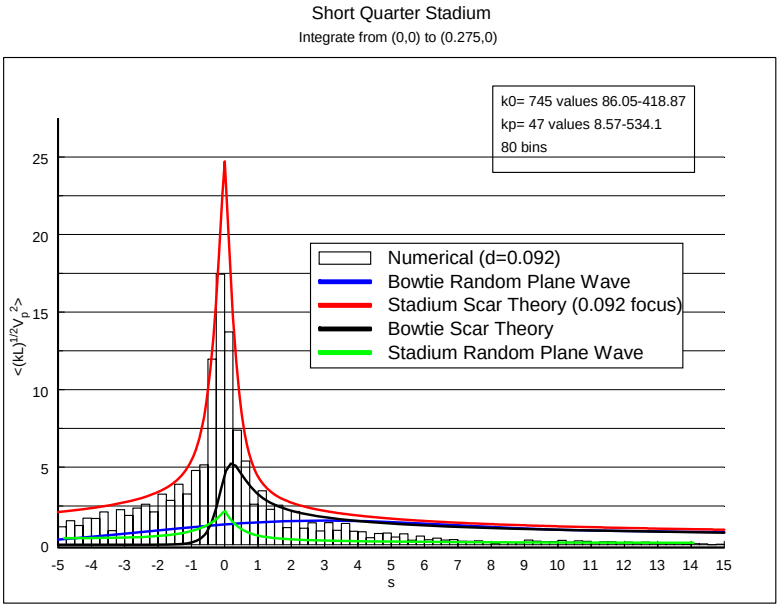


Figure 56. Comparison of scar projection and numerical histogram using average shift focal location of 0.092 m. The projection of the random plane wave is plotted. Also shown for reference is the bow tie scar theory.

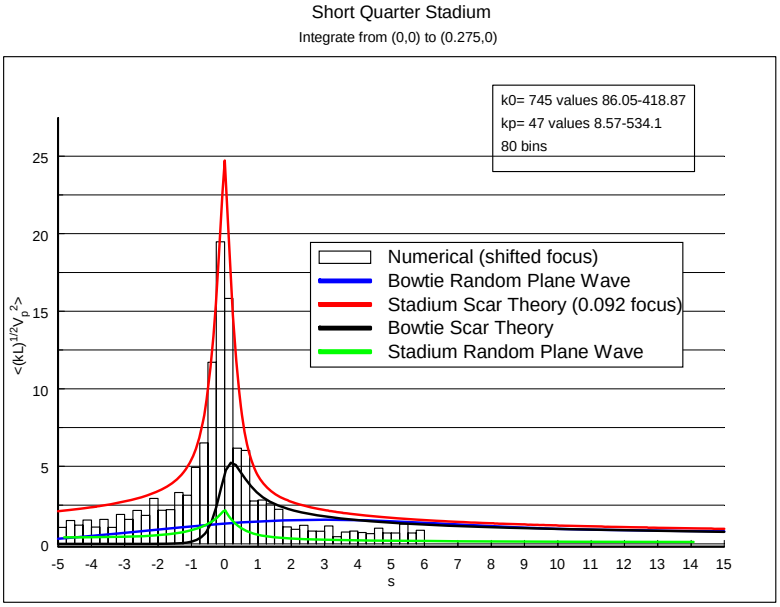


Figure 57. Comparison of scar projection and numerical histogram using average shift focal location of 0.092 m in the theory but the functional shift from the theory to define the projection operator in the numerical histogram. The projection of the random plane wave is plotted. Also shown for reference is the bow tie scar theory.

### 3.7.1 next components and orthogonality

The orthogonality using this elliptical projection operator is discussed in detail in the Appendix. The next modes using the projection

$$\exp\left(\pi\left|s'_p\right|/4\right)V_{p,p+m}=2\sqrt{d}e^{-\pi s'_p/4}\int_0^d u_{p+m}\left(x,0\right)\left(d^2-x^2\right)^{-1/4}\cos\left[k_px+p_1\left(x\right)\right]dx$$

$$+2\sqrt{d}e^{\pi s'_p/4}\int_d^\ell u_{p+m}\left(x,0\right)\left(x^2-d^2\right)^{-1/4}\cos\left[k_px-\pi/4+p_2\left(x\right)\right]dx$$

give

$$\exp\left(\pi\left|s'_p\right|/4\right)V_{p,p+m}\approx$$

$$\frac{2v\sqrt{2}d}{\left(2\gamma\right)^{1/4}\left|U'_+\left(-s'_{p+m},0\right)\right|\sqrt{A\ln\left(\frac{\ell+d}{\ell-d}\right)}}e^{-\pi s'_p/4}\int_0^1\left(1-x^2\right)^{-1/2}\cos\left[m\pi\ln\left(\frac{1+x}{1-x}\right)/\ln\left(\frac{\ell+d}{\ell-d}\right)\right]dx$$

$$+\frac{2v\sqrt{2}d}{\left(2\gamma\right)^{1/4}\left|U'_+\left(s'_{p+m},0\right)\right|\sqrt{A\ln\left(\frac{\ell+d}{\ell-d}\right)}}e^{\pi s'_p/4}\int_1^{\ell/d}\left(x^2-1\right)^{-1/2}\cos\left[m\pi\ln\left(\frac{x+1}{x-1}\right)/\ln\left(\frac{\ell+d}{\ell-d}\right)\right]dx$$

where

$$s'_{p+m}=2\left(k_{p+m}-k\right)\ell/\ln\left(\frac{\ell+d}{\ell-d}\right)$$

$$k_{p+m}\ell=\pi\left(p+m-1/4\right)$$

$$\frac{1}{2}\left(s'_{p+m}-s'_p\right)=\left(k_{p+m}-k_p\right)\ell/\ln\left(\frac{\ell+d}{\ell-d}\right)=m\pi/\ln\left(\frac{\ell+d}{\ell-d}\right)$$

In the first integral we let $\ln\left[\left(1+x\right)/\left(1-x\right)\right]=2y$ or $x=\tanh\left(y\right)$

$$\int_0^1\left(1-x^2\right)^{-1/2}\cos\left[m\pi\ln\left(\frac{1+x}{1-x}\right)/\ln\left(\frac{\ell+d}{\ell-d}\right)\right]dx=\int_0^\infty\cos\left[2m\pi y/\ln\left(\frac{\ell+d}{\ell-d}\right)\right]\frac{dy}{\cosh\left(y\right)}$$

$$=\frac{\pi}{2}/\cosh\left[m\pi^2/\ln\left(\frac{\ell+d}{\ell-d}\right)\right]$$

In the second integral we let $\ln\left(\left(x+1\right)/\left(x-1\right)\right)=2y$ or $x=\coth\left(y\right)$

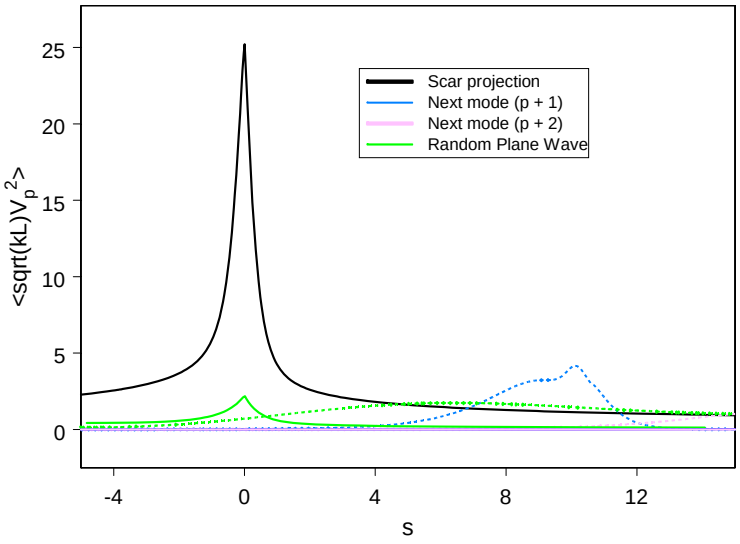


Figure 58. The black curve shows the scar projection using the geometrical focal point. The solid blue curve (which is almost zero) shows the projection for the $m = 1$ next component. The solid purple curve (again nearly zero) shows the projection for the $m = 2$ next component. The solid green curve is the random plane wave projection. The dotted blue and purple curves show the trigonometric projections of the $m = 1$ and $m = 2$ components.

$$\int_1^{\ell/d} \left(x^2-1\right)^{-1/2} \cos\left[m\pi \ln\left(\frac{x+1}{x-1}\right) / \ln\left(\frac{\ell+d}{\ell-d}\right)\right] dx = \int_{\frac{1}{2}\ln\left(\frac{\ell+d}{\ell-d}\right)}^{\infty} \cos\left[2m\pi y / \ln\left(\frac{\ell+d}{\ell-d}\right)\right] \frac{dy}{\sinh(y)}$$

$$= \frac{1}{2}\ln\left(\frac{\ell+d}{\ell-d}\right) \int_1^{\infty} \cos(m\pi y) \frac{dy}{\sinh\left[\frac{1}{2}y\ln\left(\frac{\ell+d}{\ell-d}\right)\right]}$$

$$= -\frac{1}{2}(-1)^m \ln\left(\frac{\ell+d}{\ell-d}\right) \int_0^{\infty} \cos(m\pi y) \frac{dy}{\sinh\left[\frac{1}{2}(y+1)\ln\left(\frac{\ell+d}{\ell-d}\right)\right]}$$

Figure 58 shows the $p$th elliptical projections for $(p+1)$th (blue solid curve near zero) and for the $(p+2)$ components (purple solid curve near zero). The preceding trigonometric projections are also shown, along with the $p$th elliptical scar projection. Notice that the new projections exhibit near othogonality.

### 3.7.2 random plane wave projection

Suppose we use the random plane waves and take the projection with

$$\exp(\pi|s'|/4) V_{pr} = 2e^{-\pi s'/4} \int_0^d \left(1 - x^2/d^2\right)^{-1/4} \cos\left[k_p x + p_1(x)\right] u_r(x,0)\, dx$$

$$+2e^{\pi s'/4}\int_d^\ell \left(x^2/d^2-1\right)^{-1/4}\cos\left[k_p x-\pi/4+p_2\left(x\right)\right]u_r\left(x,0\right)dx$$

The variance of this random variable is

$$\exp\left(\pi\left|s'\right|/2\right)\left\langle V_p^2\right\rangle_r=\frac{1}{2\pi A}\int_0^{2\pi}\left[F_+\left(\theta\right)+F_-\left(\theta\right)\right]^2 d\theta$$

$$F_+\left(\theta\right)+F_-\left(\theta\right)=2e^{-\pi s'/4}\int_0^d\left(1-x^2/d^2\right)^{-1/4}\cos\left[k_p x+p_1\left(x\right)\right]\cos\left(kx\cos\theta\right)dx$$

$$+2e^{\pi s'/4}\int_d^\ell\left(x^2/d^2-1\right)^{-1/4}\cos\left[k_p x-\pi/4+p_2\left(x\right)\right]\cos\left(kx\cos\theta\right)dx$$

$$=e^{-\pi s'/4}\int_0^d\left(1-x^2/d^2\right)^{-1/4}\left[\cos\left\{k_p x+p_1\left(x\right)+kx\cos\theta\right\}+\cos\left\{k_p x+p_1\left(x\right)-kx\cos\theta\right\}\right]dx$$

$$+e^{\pi s'/4}\int_d^\ell\left(x^2/d^2-1\right)^{-1/4}\left[\cos\left\{k_p x-\pi/4+p_2\left(x\right)+kx\cos\theta\right\}+\cos\left\{k_p x-\pi/4+p_2\left(x\right)-kx\cos\theta\right\}\right]dx$$

Now for large $k$ and $k_p$ we can take $k\to k_p$ and $\theta\to 0,\pi$ (and $\theta=\zeta/\sqrt{k\ell/2}$)

$$k_p-k\cos\theta\approx\left(k_p-k\right)+k\theta^2/2$$

$$k_p+k\cos\theta\approx\left(k_p-k\right)+k\left(\theta-\pi\right)^2/2$$

and

$$F_+\left(\theta\right)+F_-\left(\theta\right)\approx e^{-\pi s'/4}\int_0^d\left(1-x^2/d^2\right)^{-1/4}$$

$$\left[\cos\left\{\left(\left(k_p-k\right)+k\left(\theta-\pi\right)^2/2\right)x+p_1\left(x\right)\right\}+\cos\left\{\left(\left(k_p-k\right)+k\theta^2/2\right)x+p_1\left(x\right)\right\}\right]dx$$

$$+e^{\pi s'/4}\int_d^\ell\left(x^2/d^2-1\right)^{-1/4}$$

$$\left[\cos\left\{\left(\left(k_p-k\right)+k\left(\theta-\pi\right)^2/2\right)x-\pi/4+p_2\left(x\right)\right\}+\cos\left\{\left(\left(k_p-k\right)+k\theta^2/2\right)x-\pi/4+p_2\left(x\right)\right\}\right]dx$$

$$\exp\left(\pi\left|s'\right|/2\right)\left\langle V_p^2\right\rangle_r\approx\frac{1}{2\pi A}\int_0^{2\pi}\left[e^{-\pi s'/4}\int_0^d\left(1-x^2/d^2\right)^{-1/4}\cos\left\{\left(\left(k_p-k\right)+k\theta^2/2\right)x+p_1\left(x\right)\right\}dx\right.$$

$$+e^{\pi s'/4}\int_d^\ell \left(x^2/d^2-1\right)^{-1/4}\cos\left\{\left((k_p-k)+k\theta^2/2\right)x-\pi/4+p_2\left(x\right)\right\}dx\Bigg]^2 d\theta$$

$$+\frac{1}{2\pi A}\int_0^{2\pi}\Bigg[e^{-\pi s'/4}\int_0^d \left(1-x^2/d^2\right)^{-1/4}\cos\left\{\left((k_p-k)+k\left(\theta-\pi\right)^2/2\right)x+p_1\left(x\right)\right\}dx$$

$$+e^{\pi s'/4}\int_d^\ell \left(x^2/d^2-1\right)^{-1/4}\cos\left\{\left((k_p-k)+k\left(\theta-\pi\right)^2/2\right)x-\pi/4+p_2\left(x\right)\right\}dx\Bigg]^2 d\theta$$

$$\approx\frac{1}{\pi A\sqrt{k\ell/2}}\int_{-\infty}^{\infty}\Bigg[e^{-\pi s'/4}\int_0^d \left(1-x^2/d^2\right)^{-1/4}\cos\left\{\left((k_p-k)+\zeta^2/\ell\right)x+p_1\left(x\right)\right\}dx$$

$$+e^{\pi s'/4}\int_d^\ell \left(x^2/d^2-1\right)^{-1/4}\cos\left\{\left((k_p-k)+\zeta^2/\ell\right)x-\pi/4+p_2\left(x\right)\right\}dx\Bigg]^2 d\zeta$$

$$\approx\frac{2}{\pi A\sqrt{k\ell/2}}\int_0^{\infty}\Bigg[e^{-\pi s'/4}\int_0^d \left(1-x^2/d^2\right)^{-1/4}\cos\left\{\left(\lambda/4-\zeta^2\right)x/\ell-p_1\left(x\right)\right\}dx$$

$$+e^{\pi s'/4}\int_d^\ell \left(x^2/d^2-1\right)^{-1/4}\cos\left\{\left(\lambda/4-\zeta^2\right)x/\ell+\pi/4-p_2\left(x\right)\right\}dx\Bigg]^2 d\zeta$$

where

$$\lambda=2\left(k-k_p\right)L$$

$$s'\ln\left[\tanh\left(\zeta_0/2\right)\right]=s'\frac{1}{2}\ln\left(\frac{\ell-d}{\ell+d}\right)=\left(k-k_p\right)\ell=\lambda/4$$

or

$$\left\langle\sqrt{kL}V_p^2\right\rangle_r=L^2G\left(\lambda\right)/A$$

with

$$\exp\left(\pi\left|s'\right|/2\right)G\left(\lambda\right)=\frac{1}{\pi}\int_0^{\infty}\Bigg[e^{-\pi s'/4}\int_0^d \left(1-x^2/d^2\right)^{-1/4}\cos\left\{\left(\lambda/4-\zeta^2\right)x/\ell-p_1\left(x\right)\right\}dx/\ell$$

$$+e^{\pi s'/4}\int_d^\ell \left(x^2/d^2-1\right)^{-1/4}\cos\left\{\left(\lambda/4-\zeta^2\right)x/\ell+\pi/4-p_2\left(x\right)\right\}dx/\ell\Bigg]^2 d\zeta$$

Introducing the symmetries

$$G_s=4G$$

with

$$\left\langle \sqrt{kL}V_p^2 \right\rangle_r = L^2 G_s(\lambda)/A$$

and

$$\exp(\pi|s'|/2) G_s(\lambda) = \frac{4}{\pi}\int_0^\infty \left[ e^{-\pi s'/4} \int_0^d \left(1-x^2/d^2\right)^{-1/4} \cos\left\{\left(\lambda/4-\zeta^2\right)x/\ell - p_1(x)\right\} dx/\ell \right.$$

$$\left. + e^{\pi s'/4} \int_d^\ell \left(x^2/d^2-1\right)^{-1/4} \cos\left\{\left(\lambda/4-\zeta^2\right)x/\ell + \pi/4 - p_2(x)\right\} dx/\ell \right]^2 d\zeta$$

$$= \frac{4}{\pi}(d/\ell)^2 \int_0^\infty \left[ e^{-\pi s'/4} \int_0^1 \left(1-x^2\right)^{-1/4} \cos\left\{\left(\lambda/4-\zeta^2\right)x(d/\ell) - p_1(xd)\right\} dx \right.$$

$$\left. + e^{\pi s'/4} \int_1^{\ell/d} \left(x^2-1\right)^{-1/4} \cos\left\{\left(\lambda/4-\zeta^2\right)x(d/\ell) + \pi/4 - p_2(xd)\right\} dx \right]^2 d\zeta$$

$$p_1(xd) = \frac{1}{2}s' \left\{ \ln\left(\frac{1+x}{1-x}\right) - \ln\left(\frac{\ell+d}{\ell-d}\right)(xd/\ell) \right\}$$

$$p_2(xd) = \frac{1}{2}s' \left\{ \ln\left(\frac{x+1}{x-1}\right) - \ln\left(\frac{\ell+d}{\ell-d}\right)(xd/\ell) \right\}$$

To understand why the random plane wave projection is small for large $s$ we drop the phase and exponential factors in the projection with the random plane wave by setting $s=0$ (but we keep $\lambda \neq 0$). This gives the red curve in Figure 59.

### 3.8 Integral Of Square Along Scar

Consider the scar components of the eigenfunction

$$u \sim \sum_p u_p$$

Taking the integral along the orbit to be

$$P = \frac{1}{L}\int_{-\ell}^{\ell} u^2(x,0)\,dx \sim \sum_p \frac{1}{L}\int_{-\ell}^{\ell} u_p^2(x,0)\,dx$$

where we assumed approximate orthogonality. Thus a single $p$ component gives

$$P_p = \frac{1}{L}\int_{-\ell}^{\ell} u_p^2(x,0)\,dx \sim \frac{8v^2 d/\ell}{(2\gamma)^{1/2} A \ln\left(\frac{\ell+d}{\ell-d}\right)}$$

$$\left\{ \frac{1}{\left|U_+'(s,0)\right|^2} \int_0^d \left(d^2-x^2\right)^{-1/2} \cos^2\left[k_p x + p_1(x)\right] dx \right.$$

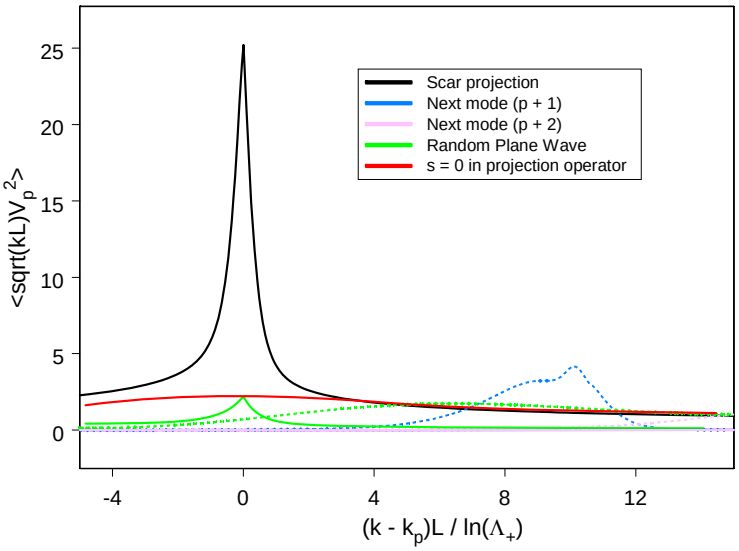


Figure 59. The phase and exponential factors have been dropped in the projection resulting in the red curve, which approaches the scar function. Note that the abscissa has the same values as $s$.

$$+\frac{1}{\left|U'_+(s',0)\right|^2}\int_d^\ell \left(x^2-d^2\right)^{-1/2}\cos^2\left[k_p x-\pi/4+p_2(x)\right]dx\Bigg\}$$

Averaging the cosines for high frequencies gives

$$P_p=\frac{1}{L}\int_{-\ell}^{\ell}u_p^2(x,0)\,dx\sim\frac{4v^2d/\ell}{(2\gamma)^{1/2}A\ln\left(\frac{\ell+d}{\ell-d}\right)}\left[\frac{\pi/2}{\left|U'_+(s,0)\right|^2}+\frac{\zeta_0}{\left|U'_+(s',0)\right|^2}\right]$$

Taking the mean value (and multiplying by $\sqrt{kL}$)

$$\left\langle\sqrt{kL}P_p\right\rangle\sim\frac{4\sqrt{d/\ell}}{A\ln\left(\frac{\ell+d}{\ell-d}\right)}\left[\frac{\pi/2}{\left|U'_+(s,0)\right|^2}+\frac{\zeta_0}{\left|U'_+(-s,0)\right|^2}\right]$$

$$\sim\frac{4\sqrt{d/\ell}}{A\left|U'_+(s,0)\,U'_+(s',0)\right|\ln\left(\frac{\ell+d}{\ell-d}\right)}\left(e^{\pi s/2}\pi/2+e^{\pi s'/2}\zeta_0\right)$$

$$\sim\frac{2\sqrt{2d/\ell}}{\pi A\ln\left(\frac{\ell+d}{\ell-d}\right)}\left|\Gamma(-is/2+1/4)\right|^2\left(e^{\pi s/2}\pi/2+e^{\pi s'/2}\zeta_0\right)$$

or

$$\left\langle\sqrt{kL}P_p\right\rangle\sim\frac{2}{A}(\ell/d)\frac{\exp(\pi|s|/2)}{e^{\pi s/2}\pi/2+e^{-\pi s/2}\zeta_0}G_1(s)$$

where we plot it against the abscissa with $p$ suppressed

$$\mu=(k-k_p)\,\ell/\pi=\lambda/(4\pi)=s\frac{1}{2\pi}\ln\left(\frac{\ell+d}{\ell-d}\right)=s\frac{1}{4\pi}\ln(\Lambda_+)\approx 0.099s$$

Figure 60 shows the result for the $p$th component along the horizontal orbit in the stadium cavity.

### 3.8.1 addition of random plane wave

Another approach to include other components in the eigenfunction is to add the random plane wave distribution (symmetrized on the even orbit). We again consider the approximation of the eigenfunction as

$$u\sim\sum_p u_p+u_r-\sum_p c'_{rp}u_p$$

where $u_p$ are the scar components (and might be a single term or a truncated sum) and $u_r$ is the random plane wave symmetrized field. We assume asymptotic orthogonality (see the Appendix) and remove the overlap of the scar components from the random plane wave

$$c'_{rp}\int_{-\ell}^{\ell}u_p^2dx\sim\int_{-\ell}^{\ell}u_r u_p dx$$

We expect the random plane wave term to capture high angle chaotic rays which do not exhibit foci along the orbit, whereas the scar components $u_p$ have foci along the orbit. Now we write the integral of the square along the orbit as

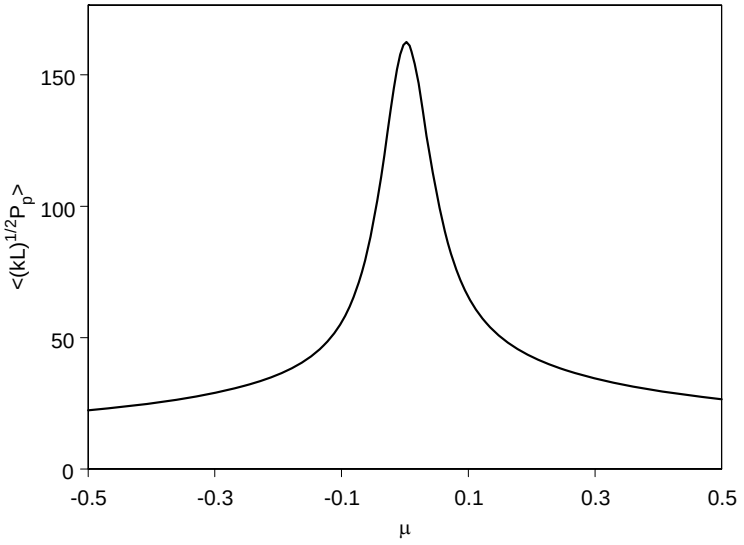


Figure 60. Integral of the square of the $p$th scar component along the horizontal orbit of the stadium cavity.

$$\int_{-\ell}^{\ell} u^2 dx \sim \sum_p \int_{-\ell}^{\ell} u_p^2 dx + \int_{-\ell}^{\ell} \left( u_r - \sum_p c'_{rp} u_p \right)^2 dx$$

or

$$2\ell \left( P - P_r \right) \sim \int_{-\ell}^{\ell} u^2 dx - \int_{-\ell}^{\ell} u_r^2 dx \approx \sum_p \left( 1 - c'^2_{rp} \right) \int_{-\ell}^{\ell} u_p^2 dx$$

$$\sim \sum_p \left[ 1 - \left( \int_{-\ell}^{\ell} u_r u_p dx / \int_{-\ell}^{\ell} u_p^2 dx \right)^2 \right] \int_{-\ell}^{\ell} u_p^2 dx$$

Taking the mean

$$\langle P \rangle - \langle P_r \rangle \approx \frac{1}{2\ell} \sum_p \left[ \int_{-\ell}^{\ell} \left\langle u_p^2 \right\rangle dx - \int_{-\ell}^{\ell} \left\langle c'^2_{rp} u_p^2 \right\rangle dx \right]$$

with

$$\left\langle c'^2_{rp} u_p^2 \right\rangle = \left\langle \left( u_p \int_{-\ell}^{\ell} u_r u_p dx / \int_{-\ell}^{\ell} u_p^2 dx \right)^2 \right\rangle$$

$$= \left\langle u_p^2 (x) \int_{-\ell}^{\ell} u_r (x'') u_p (x'') dx'' \int_{-\ell}^{\ell} u_r (x') u_p (x') dx' / \left( \int_{-\ell}^{\ell} u_p^2 (x) dx \right)^2 \right\rangle$$

$$= u_p^2 (x) \int_{-\ell}^{\ell} \int_{-\ell}^{\ell} \langle u_r (x') u_r (x'') \rangle u_p (x'') u_p (x') dx'' dx' / \left( \int_{-\ell}^{\ell} u_p^2 (x) dx \right)^2$$

$$= \left\langle u_p^2 (x) \right\rangle \int_{-\ell}^{\ell} \int_{-\ell}^{\ell} \langle u_r (x') u_r (x'') \rangle \langle u_p (x'') u_p (x') \rangle dx'' dx' / \left( \int_{-\ell}^{\ell} \left\langle u_p^2 (x) \right\rangle dx \right)^2$$

where the expression is homogenous in $u_p^2$ and thus the $v^2$ random variable cancels. Using the correlation with an image on the even orbit

$$\langle A u_r (x) u_r (x') \rangle = 4 J_0 \left( k \left( x - x' \right) \right)$$

we have

$$\langle P - P_r \rangle \approx \sum_p \left[ 1 - \frac{1}{L^2} \frac{4}{A} \int_{-\ell}^{\ell} \int_{-\ell}^{\ell} J_0 \left( k \left( x - x' \right) \right) \langle u_p (x) u_p (x') \rangle dx dx' / \left( \frac{1}{L} \int_{-\ell}^{\ell} \left\langle u_p^2 \right\rangle dx \right)^2 \right] \frac{1}{L} \int_{-\ell}^{\ell} \left\langle u_p^2 \right\rangle dx$$

Inserting the field on axis, in Region 1

$$u_p \sim \frac{2v}{(2\gamma)^{1/4}\left|U'_+(s,0)\right|\sqrt{A\ln\left(\frac{\ell+d}{\ell-d}\right)}}\sqrt{2d}\left(d^2-x^2\right)^{-1/4}\cos\left[k_p x+p_1(x)\right]\text{ , Region 1}$$

and in Region 2

$$u_p \sim \frac{2v}{(2\gamma)^{1/4}\left|U'_+(-s,0)\right|\sqrt{A\ln\left(\frac{\ell+d}{\ell-d}\right)}}\sqrt{2d}\left(x^2-d^2\right)^{-1/4}\cos\left[k_p x-\pi/4+p_2(x)\right]\text{ , Region 2}$$

where

$$s\ln\left(\frac{\ell+d}{\ell-d}\right)=2(k-k_p)\ell$$

$$p_1(x)=\frac{1}{2}s\left\{\ln\left(\frac{\ell+d}{\ell-d}\right)(x/\ell)-\ln\left(\frac{d+x}{d-x}\right)\right\}$$

$$p_2(x)=\frac{1}{2}s\left\{\ln\left(\frac{\ell+d}{\ell-d}\right)(x/\ell)-\ln\left(\frac{x+d}{x-d}\right)\right\}$$

gives

$$\frac{4}{A}\int_{-\ell}^{\ell}\int_{-\ell}^{\ell}J_0\left(k\left(x-x'\right)\right)\left\langle u_p(x)\,u_p\left(x'\right)\right\rangle dxdx'=\frac{64d}{A^2(2\gamma)^{1/2}\ln\left(\frac{\ell+d}{\ell-d}\right)}\left\{\right.$$

$$\frac{1}{\left|U'_+(-s,0)\right|^2}\int_d^{\ell}\left(x'^2-d^2\right)^{-1/4}\cos\left[k_p x'-\pi/4+p_2\left(x'\right)\right]$$

$$\int_d^{\ell}\left[J_0\left(k\left(x-x'\right)\right)+J_0\left(k\left(x+x'\right)\right)\right]\left(x^2-d^2\right)^{-1/4}\cos\left[k_p x-\pi/4+p_2(x)\right]dxdx'$$

$$+\frac{1}{\left|U'_+(-s,0)\right|\left|U'_+(s,0)\right|}\int_d^{\ell}\left(x'^2-d^2\right)^{-1/4}\cos\left[k_p x'-\pi/4+p_2\left(x'\right)\right]$$

$$\int_0^{d}\left[J_0\left(k\left(x-x'\right)\right)+J_0\left(k\left(x+x'\right)\right)\right]\left(d^2-x^2\right)^{-1/4}\cos\left[k_p x+p_1(x)\right]dxdx'$$

$$+\frac{1}{\left|U'_+(-s,0)\right|\left|U'_+(s,0)\right|}\int_0^{d}\left(d^2-x'^2\right)^{-1/4}\cos\left[k_p x'+p_1\left(x'\right)\right]$$

$$\int_d^{\ell}\left[J_0\left(k\left(x-x'\right)\right)+J_0\left(k\left(x+x'\right)\right)\right]\left(x^2-d^2\right)^{-1/4}\cos\left[k_p x-\pi/4+p_2(x)\right]dxdx'$$

$$+\frac{1}{\left|U'_+(s,0)\right|^2}\int_0^{d}\left(d^2-x'^2\right)^{-1/4}\cos\left[k_p x'+p_1\left(x'\right)\right]$$

$$\int_0^d \left[J_0\left(k\left(x-x'\right)\right)+J_0\left(k\left(x+x'\right)\right)\right]\left(d^2-x^2\right)^{-1/4}\cos\left[k_p x+p_1\left(x\right)\right]dxdx'\ \}$$

We want to find an approximate form which only involves the difference $k-k_p$. The first thing to do is to expand the Bessel functions for large argument

$$\frac{4}{A}\int_{-\ell}^{\ell}\int_{-\ell}^{\ell}J_0\left(k\left(x-x'\right)\right)\left\langle u_p\left(x\right)u_p\left(x'\right)\right\rangle dxdx' \sim \frac{32d\sqrt{2/\left(\pi k\right)}}{A^2\left(2\gamma\right)^{1/2}\ln\left(\frac{\ell+d}{\ell-d}\right)}\ \{$$

$$\frac{1}{\left|U_+'\left(-s,0\right)\right|^2}\int_d^{\ell}\left(x'^2-d^2\right)^{-1/4}\int_d^{\ell}\left(x^2-d^2\right)^{-1/4}\left[\frac{\cos\left(k\left|x'-x\right|-\pi/4\right)}{\sqrt{\left|x'-x\right|}}+\frac{\cos\left(k\left(x'+x\right)-\pi/4\right)}{\sqrt{x'+x}}\right]$$

$$\left[\cos\left(k_p\left(x-x'\right)+p_2\left(x\right)-p_2\left(x'\right)\right)+\sin\left(k_p\left(x+x'\right)+p_2\left(x\right)+p_2\left(x'\right)\right)\right]dxdx'$$

$$+\frac{2}{\left|U_+'\left(-s,0\right)\right|\left|U_+'\left(s,0\right)\right|}\int_d^{\ell}\left(x'^2-d^2\right)^{-1/4}\int_0^{d}\left(d^2-x^2\right)^{-1/4}\left[\frac{\cos\left(k\left(x'-x\right)-\pi/4\right)}{\sqrt{x'-x}}+\frac{\cos\left(k\left(x'+x\right)-\pi/4\right)}{\sqrt{x'+x}}\right]$$

$$\left[\cos\left(k_p\left(x-x'\right)+\pi/4+p_1\left(x\right)-p_2\left(x'\right)\right)+\cos\left(k_p\left(x+x'\right)-\pi/4+p_1\left(x\right)+p_2\left(x'\right)\right)\right]dxdx'$$

$$+\frac{1}{\left|U_+'\left(s,0\right)\right|^2}\int_0^{d}\left(d^2-x'^2\right)^{-1/4}\int_0^{d}\left(d^2-x^2\right)^{-1/4}\left[\frac{\cos\left(k\left|x'-x\right|-\pi/4\right)}{\sqrt{\left|x'-x\right|}}+\frac{\cos\left(k\left(x'+x\right)-\pi/4\right)}{\sqrt{x'+x}}\right]$$

$$\left[\cos\left(k_p\left(x-x'\right)+p_1\left(x\right)-p_1\left(x'\right)\right)+\cos\left(k_p\left(x+x'\right)+p_1\left(x\right)+p_1\left(x'\right)\right)\right]dxdx'\ \}$$

Now dropping terms without the difference wavenumber gives

$$\frac{1}{L^2}\frac{4}{A}\int_{-\ell}^{\ell}\int_{-\ell}^{\ell}J_0\left(k\left(x-x'\right)\right)\left\langle u_p\left(x\right)u_p\left(x'\right)\right\rangle dxdx' \sim \frac{4\sqrt{d/\pi}}{k\ell^2A^2\left|U_+'\left(-s,0\right)\right|\left|U_+'\left(s,0\right)\right|\ln\left(\frac{\ell+d}{\ell-d}\right)}\ \{$$

$$e^{\pi s'/2}\int_d^{\ell}\left(x'^2-d^2\right)^{-1/4}\int_d^{\ell}\left(x^2-d^2\right)^{-1/4}$$

$$\left[\frac{\cos\left(\left(k-k_p\right)\left|x'-x\right|-\pi/4+\left(p_2\left(x\right)-p_2\left(x'\right)\right)\mathrm{sgn}\left(x'-x\right)\right)}{\sqrt{\left|x'-x\right|}}\right.$$

$$\left.-\frac{\sin\left(\left(k-k_p\right)\left(x'+x\right)-\pi/4-p_2\left(x\right)-p_2\left(x'\right)\right)}{\sqrt{x'+x}}\right]dxdx'$$

$$+2\int_d^{\ell}\left(x'^2-d^2\right)^{-1/4}\int_0^{d}\left(d^2-x^2\right)^{-1/4}$$

$$\left[\frac{\cos\left(\left(k-k_p\right)\left(x'-x\right)+p_1\left(x\right)-p_2\left(x'\right)\right)}{\sqrt{x'-x}}+\frac{\cos\left(\left(k-k_p\right)\left(x'+x\right)-p_1\left(x\right)-p_2\left(x'\right)\right)}{\sqrt{x'+x}}\right]dxdx'$$

$$+e^{\pi s/2}\int_0^d\left(d^2-x'^2\right)^{-1/4}\int_0^d\left(d^2-x^2\right)^{-1/4}$$

$$\left[\frac{\cos\left(\left(k-k_p\right)\left|x'-x\right|-\pi/4+\left(p_1\left(x\right)-p_1\left(x'\right)\right)\operatorname{sgn}\left(x'-x\right)\right)}{\sqrt{\left|x'-x\right|}}\right.$$

$$\left.+\frac{\cos\left(\left(k-k_p\right)\left(x'+x\right)-\pi/4-p_1\left(x\right)-p_1\left(x'\right)\right)}{\sqrt{x'+x}}\right]dxdx'\ \}$$

$$=\frac{4\sqrt{\ell/d}}{A^2k\ell\ln\left(\frac{\ell+d}{\ell-d}\right)\left|U'_+\left(-s,0\right)\right|\left|U'_+\left(s,0\right)\right|}\exp\left(\pi\left|s'\right|/2\right)G_s\left(\lambda\right)$$

or

$$\sqrt{kL}\frac{1}{L}\int_{-\ell}^{\ell}\int_{-\ell}^{\ell}2J_0\left(k\left(x-x'\right)\right)u_p\left(x\right)u_p\left(x'\right)dxdx'/\left(\int_{-\ell}^{\ell}u_p^2\left(x,0\right)dx\right)\sim$$

$$=\frac{\left(\ell/d\right)\exp\left(\pi\left|s'\right|/2\right)}{\left(e^{\pi s/2}\pi/2+e^{\pi s'/2}\zeta_0\right)}G_s\left(\lambda\right)$$

The final identity can be verified numerically, where $G_s$ is the previous form of the random plane wave projection

$$\exp\left(\pi\left|s'\right|/2\right)G_s\left(\lambda\right)$$

$$=\frac{4}{\pi}\int_0^\infty\left[e^{-\pi s'/4}\int_0^d\left(1-x^2/d^2\right)^{-1/4}\cos\left\{\left(\lambda/4-\zeta^2\right)x/\ell-p_1\left(x\right)\right\}dx/\ell\right.$$

$$\left.+e^{\pi s'/4}\int_d^\ell\left(x^2/d^2-1\right)^{-1/4}\cos\left\{\left(\lambda/4-\zeta^2\right)x/\ell+\pi/4-p_2\left(x\right)\right\}dx/\ell\right]^2d\zeta$$

This is shown as the green and dashed red curves in Figure 61.

Note that the lack of a projection of the random plane wave representation on the $p$th scar, especially for large $|s|$, indicates that these two parts of the eigenfunction $u$ are largely orthogonal. In other words the contributions of the $p$th scar are separate in functional form from the random plane wave part. This is caused by wave interference associated with the $p_1$ and $p_2$ phase functions (and the exponential behavior between the two regions). We will not obtain acceleration of convergence from subtracting the random plane wave projections. We must therefore regard the $p$th contributions as a finite asymptotic series.

Thus we can write

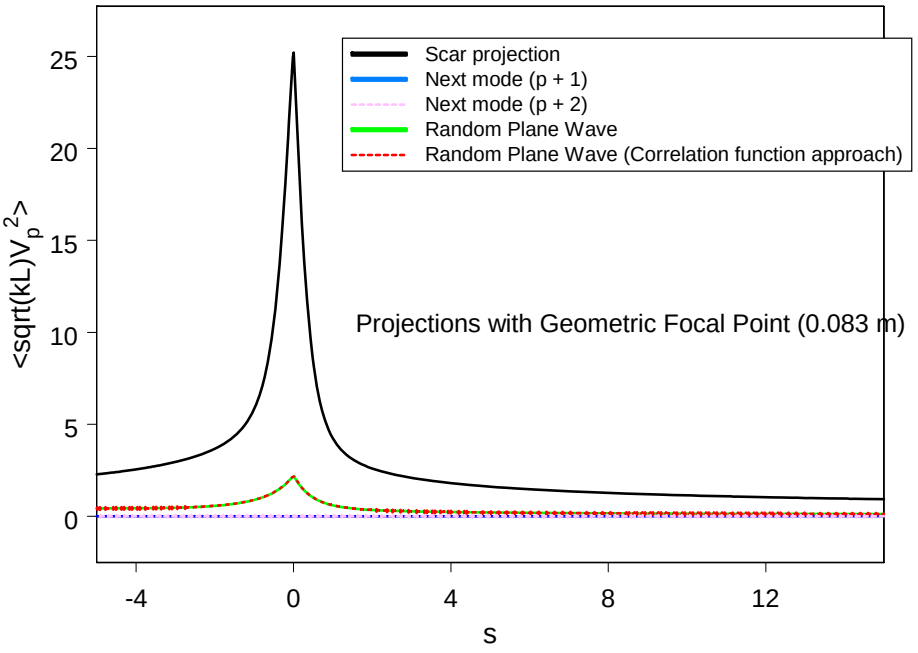


Figure 61. Comparison of random plane wave projections from original approach and from correlation function approach.

$$\left\langle \sqrt{kL}\left(P-P_r\right)\right\rangle \approx \sum_p \left[\left\langle \sqrt{kL}P_p\right\rangle - \left\langle \sqrt{kL}\right\rangle^2 \frac{1}{L^2}\frac{2}{A}\int_{-\ell}^{\ell}\int_{-\ell}^{\ell} J_0\left(k\left(x-x'\right)\right)\left\langle u_p\left(x\right)u_p\left(x'\right)\right\rangle dxdx' / \left\langle \sqrt{kL}P_p\right\rangle\right]$$

$$\approx \frac{2}{A}\sum_p \left[G_1\left(s_p\right)-G_s\left(\lambda_p\right)\right]\frac{\left(\ell/d\right)\exp\left(\pi\left|s_p\right|/2\right)}{\left(e^{\pi s_p/2}\pi/2+e^{-\pi s_p/2}\zeta_0\right)}$$

where again the subscript $p$ is added to $s$ and to $\lambda$ to denote that its definition is associated with the given term, and from the preceding subsubsection

$$\left\langle \sqrt{kL}P_p\right\rangle \sim \left(\frac{L/d}{A}\right)\frac{\exp\left(\pi\left|s\right|/2\right)}{e^{\pi s/2}\pi/2+e^{-\pi s/2}\zeta_0}G_1\left(s\right) \sim \frac{4\sqrt{d/\ell}}{A\left|U_+'\left(s,0\right)U_+'\left(s',0\right)\right|\ln\left(\frac{\ell+d}{\ell-d}\right)}\left(e^{\pi s/2}\pi/2+e^{\pi s'/2}\zeta_0\right)$$

To construct this average we note that the average without the scar modes using the random plane wave hypothesis gives

$$\left\langle P_r\right\rangle = 2/A$$

We take here the average of $\sqrt{k}$ for the eigenvalues by means of the Weyl asymptotic spacing $\Delta k^2 = k\Delta k \sim 16\pi/A$ to give $\Delta k/\Delta m \sim 16\pi/\left(kA\right)$ and thus over the 4 GHz to 16 GHz range we find

$$\left\langle \sqrt{k}\right\rangle = \int_{k_1}^{k_2}\sqrt{k}\frac{dm}{dk}dk / \int_{k_1}^{k_2}\frac{dm}{dk}dk = \int_{k_1}^{k_2}k^{3/2}dk / \int_{k_1}^{k_2}kdk = \frac{4}{5}\frac{k_2^{5/2}-k_1^{5/2}}{k_2^2-k_1^2} \approx 16.76\ \mathrm{m}^{-1/2}$$

We can write the random plane wave term, expected to describe the plateau level, as

$$\left\langle \sqrt{kL}P_r\right\rangle = \left\langle \sqrt{kL}\right\rangle \frac{2}{A} \approx 112.3\ \mathrm{m}^{-2}$$

### 3.8.2 comparison of histograms

Figure 62 shows the $p$th term of the sum for $\left\langle \sqrt{kL}\left(P-P_r\right)\right\rangle$. Notice that the effect of the scar is larger in the stadium than in the bow tie cavity result, which is also included (to put it on the same scale as the stadium result we multiply it by the ratio of bow tie to cavity areas). Figure 63 shows numerical histogram results for the difference of the integral of the field squared and the random plane wave representation along the horizontal orbit in the stadium cavity.

Figure 64 shows the integral of the field squared along the horizontal orbit in the stadium cavity. Notice that the "plateau" level 100 is near, but slightly smaller than, the random plane wave level derived in the preceding subsubsection. This fact accounts for the negative values in the preceding figure when the random plane wave level is removed. The reason for this slight discrepancy is not clear however the large frequency range covered and the required choice of an "average" $\sqrt{k}$ in the random plane wave result may be questioned (unlike in the bow tie cavity where the frequency range was limited). The theory also seems to overestimate the variation of the peak near $\mu = 0$, perhaps by as much as a factor of two (similar to the bow tie cavity).

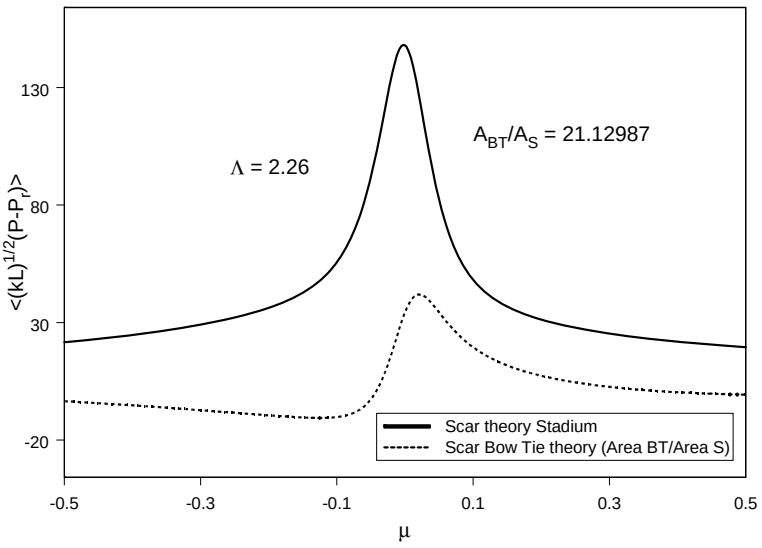


Figure 62. Integral of the square of the eigenfunction $p$th component minus the random plane wave projection for the stadium cavity. Also shown are the bow tie cavtiy results discussed previously scaled by the ratio of bow tie to stadium cavity areas (to put it on the same scale as the stadium results).

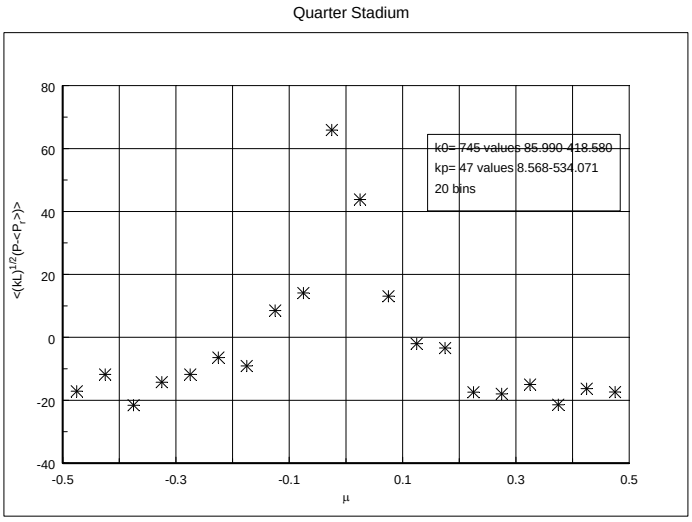


Figure 63. Numerical histogram results for the integral of the square of the field along the horizontal orbit minus the random plane wave integral in the stadium cavity.

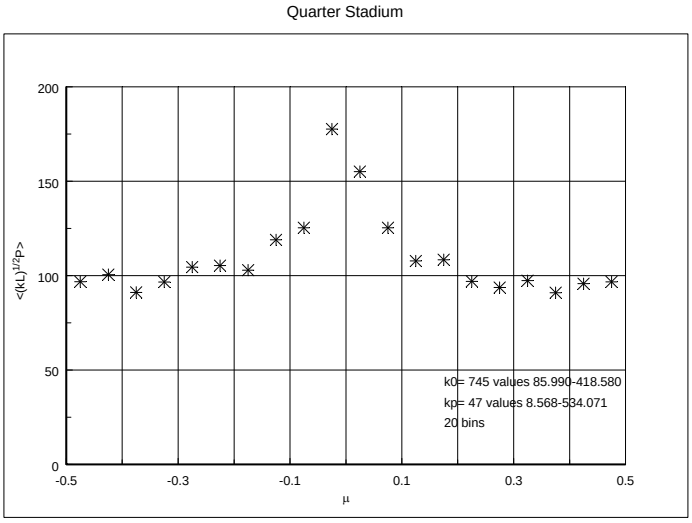


Figure 64. Numerical histogram results for the integral of the square of the field along the horizontal orbit in the stadium cavity.

## 3.9 Point Value Statistics

This section considers the point statistics at various locations in the stadium cavity, including near the focal point. We only consider the scar components and not the random plane wave part of the eigenfunction.

$$u \sim \sum_p u_p$$

where in Region 1

$$u_p \sim \frac{2v}{(2\gamma)^{1/4} \left|U_+'(-s',0)\right| \sqrt{A \ln\left(\frac{\ell+d}{\ell-d}\right)}} \sqrt{2d} \left(d^2-x^2\right)^{-1/4} \cos\left[k_p x + p_1(x)\right] \text{ , Region 1}$$

and in Region 2

$$u_p \sim \frac{2v}{(2\gamma)^{1/4} \left|U_+'(s',0)\right| \sqrt{A \ln\left(\frac{\ell+d}{\ell-d}\right)}} \sqrt{2d} \left(x^2-d^2\right)^{-1/4} \cos\left[k_p x - \pi/4 + p_2(x)\right] \text{ , Region 2}$$

with

$$s' \ln\left(\frac{\ell+d}{\ell-d}\right) = 2\left(k_p - k\right)\ell$$

$$s' = -s$$

$$p_1(x) = \frac{1}{2} s' \left\{ \ln\left(\frac{d+x}{d-x}\right) - \ln\left(\frac{\ell+d}{\ell-d}\right)(x/\ell) \right\}$$

$$p_2(x) = \frac{1}{2} s' \left\{ \ln\left(\frac{x+d}{x-d}\right) - \ln\left(\frac{\ell+d}{\ell-d}\right)(x/\ell) \right\}$$

$$d = \ell\sqrt{1-R/\ell}$$

$$k_p \ell = \pi\left(p - 1/4\right)$$

In Region 3 near the focus

$$u_p = (-1)^n (2\gamma)^{1/4} \frac{\left|U_+'(s',0)\right|}{\operatorname{Im}\left[U_+'(s',0)\right]} c \operatorname{Re}\left[U_+\left(s', \xi'\sqrt{2\gamma}\right) + e^{-i\Phi_0} U_+^*\left(s', \xi'\sqrt{2\gamma}\right)\right]$$

$$\operatorname{Re}\left[e^{-i\pi/4} U_+\left(-s', \zeta\sqrt{2\gamma}\right) + e^{i\pi/4} e^{i\Phi_0} U_+^*\left(-s', \zeta\sqrt{2\gamma}\right)\right]$$

$$\sim (-1)^n \frac{\sqrt{2}v}{\sqrt{A\ln\left(\frac{\ell+d}{\ell-d}\right)}} \frac{\left|U_+'(s',0)\right|^2}{\mathrm{Im}^2\left[U_+'(s',0)\right]} \mathrm{Re}\left[U_+\left(s',\xi'\sqrt{2\gamma}\right) - \frac{U_+'(s',0)}{U_+^{*\prime}(s',0)} U_+^*\left(s',\xi'\sqrt{2\gamma}\right)\right]$$

$$\mathrm{Re}\left[e^{-i\pi/4} U_+\left(-s',\zeta\sqrt{2\gamma}\right) - e^{-i\pi/4} \frac{U_+'(-s',0)}{U_+^{*\prime}(-s',0)} U_+^*\left(-s',\zeta\sqrt{2\gamma}\right)\right]$$

where

$$c = \frac{\sqrt{2}v\left|U_+'(s',0)\right|}{(2\gamma)^{1/4}\,\mathrm{Im}\left[U_+'(s',0)\right]\sqrt{A\ln\left(\frac{\ell+d}{\ell-d}\right)}}$$

On the $x$ axis this becomes

$$u_p(x,0) \sim (-1)^n \frac{\sqrt{2}v}{\sqrt{A\ln\left(\frac{\ell+d}{\ell-d}\right)}} \frac{1}{\mathrm{Im}\left[e^{-i\pi/4}U_+'(-s',0)\right]} \mathrm{Re}\left[U_+\left(s',\xi'\sqrt{2\gamma}\right) - \frac{U_+'(s',0)}{U_+^{*\prime}(s',0)} U_+^*\left(s',\xi'\sqrt{2\gamma}\right)\right]$$

$$\xi' \approx \sqrt{2\left(d_e - x\right)/d}$$

$$u_p(x,0) \sim (-1)^n \frac{\sqrt{2}v}{\sqrt{A\ln\left(\frac{\ell+d}{\ell-d}\right)}} \frac{1}{\mathrm{Im}\left[U_+'(s',0)\right]} \mathrm{Re}\left[e^{-i\pi/4}\left\{U_+\left(-s',\zeta\sqrt{2\gamma}\right) - \frac{U_+'(-s',0)}{U_+^{*\prime}(-s',0)} U_+^*\left(-s',\zeta\sqrt{2\gamma}\right)\right\}\right]$$

$$\zeta \approx \sqrt{2\left(x - d_e\right)/d}$$

where

$$d_e = d + \delta$$

and we have used

$$U_+'(-s',0) = e^{\pi s'/2 - i3\pi/4} U_+^{*\prime}(s',0)$$

or

$$\frac{\mathrm{Im}\left[U_+'(s',0)\right]}{\left|U_+'(s',0)\right|} = \frac{\mathrm{Im}\left[e^{-i\pi/4}U_+'(-s',0)\right]}{\left|U_+'(-s',0)\right|}$$

along with the Wronskian

$$U_+' U_+^* - U_+^{*\prime} U_+ = i$$

### 3.9.1 value at focus

Suppose we examine the value of the $p$th component of the field at the focus in Region 3

$$u_p\left(d_e,0\right)\sim\left(-1\right)^n\frac{\sqrt{2}v}{\left|U'_+\left(-s',0\right)U'_+\left(s',0\right)\right|\sqrt{A\ln\left(\frac{\ell+d}{\ell-d}\right)}}=\left(-1\right)^n v\frac{\left|\Gamma\left(is'/2+1/4\right)\Gamma\left(-is'/2+1/4\right)\right|}{\pi\sqrt{A\ln\left(\frac{\ell+d}{\ell-d}\right)}}$$

where we have used

$$U'_+\left(s',0\right)=e^{-\pi\left(s'+i3/2\right)/4}U'\left(-is',0\right)=-\frac{e^{-\pi\left(s'+i3/2\right)/4}\sqrt{\pi}}{2^{-is'/2-1/4}\Gamma\left(-is'/2+1/4\right)}$$

Thus we can write

$$\left\langle Au_p^2\left(d_e,0\right)\right\rangle\sim\frac{\left|\Gamma\left(is/2+1/4\right)\Gamma\left(-is/2+1/4\right)\right|^2}{\pi^2\ln\left(\frac{\ell+d}{\ell-d}\right)}$$

For large values of $s$

$$\left|\Gamma\left(is/2+1/4\right)\right|^2=\left|\Gamma\left(-is/2+1/4\right)\right|^2\sim e^{-\pi|s|/2}2\pi\sqrt{2/\left|s\right|}\ ,\ \ \left|s\right|>>1$$

The value at $s=0$ is

$$\left\langle Au_p^2\left(d_e,0\right)\right\rangle\sim\frac{2\Gamma^4\left(1/4\right)}{\pi^2\ln\left(\Lambda_+\right)}\approx 28.13$$

Notice that this result is independent of $k$ (as the bow tie extrapolation above was, although the rigorous coefficient is much larger here).

### 3.9.2 value for eigenvalue equal to scar frequency

Suppose we have $k=k_p$ and thus $s=0$. Then we can use the identity

$$U_+\left(0,\tau\right)=e^{-i\pi/4}\sqrt{\tau/\left(2\pi\right)}K_{1/4}\left(-i\tau^2/4\right)=e^{i3\pi/8}\frac{1}{2}\sqrt{\pi\tau/2}H_{1/4}^{(1)}\left(\tau^2/4\right)$$

to give

$$u_p\left(x,0\right)\sim\left(-1\right)^n\frac{\sqrt{2}v}{\sqrt{A\ln\left(\frac{\ell+d}{\ell-d}\right)}}\frac{1}{\sin\left(3\pi/8\right)\left[-U'\left(0,0\right)\right]}$$

$$\mathrm{Re}\left[\frac{1}{2}\sqrt{\pi\sqrt{k\left(d_e-x\right)}}e^{i3\pi/8}\left\{H_{1/4}^{(1)}\left(k\left(d_e-x\right)\right)-iH_{1/4}^{(2)}\left(\left(k\left(d_e-x\right)\right)\right)\right\}\right]$$

$$u_p\left(x,0\right)\sim\left(-1\right)^n\frac{\sqrt{2}v}{\sqrt{A\ln\left(\frac{\ell+d}{\ell-d}\right)}}\frac{1}{\sin\left(3\pi/8\right)\left[-U'\left(0,0\right)\right]}$$

$$\mathrm{Re}\left[\frac{1}{2}\sqrt{\pi\sqrt{k\left(x-d_e\right)}}e^{-i\pi/4}e^{i3\pi/8}\left\{H_{1/4}^{(1)}\left(k\left(x-d_e\right)\right)-iH_{1/4}^{(2)}\left(\left(k\left(x-d_e\right)\right)\right)\right\}\right]$$

or

$$u_p(x,0) \sim (-1)^n \frac{v\Gamma(1/4)}{\sqrt{A\ln\left(\frac{\ell+d}{\ell-d}\right)}} (k|d_e-x|/2)^{1/4} \left\{J_{1/4}(k|d_e-x|) - Y_{1/4}(k|d_e-x|)\right\}$$

where we have used

$$U'_+(0,0) = e^{-i3\pi/8} U'(0,0) = -e^{-i\pi 3/8} \frac{2^{1/4}\sqrt{\pi}}{\Gamma(1/4)}$$

Noting that

$$Y_{1/4}(z) = \frac{J_{1/4}(z)\cos(\pi/4) - J_{-1/4}(z)}{\sin(\pi/4)} = J_{1/4}(z) - \sqrt{2} J_{-1/4}(z)$$

this becomes

$$u_p(x,0) \sim (-1)^n \frac{v\Gamma(1/4)}{\sqrt{A\ln\left(\frac{\ell+d}{\ell-d}\right)}} (2k|d_e-x|)^{1/4} J_{-1/4}(k|d_e-x|)$$

and

$$\left\langle A u_p^2(x,0)\right\rangle \sim \frac{2\Gamma^2(1/4)}{\ln(\Lambda_+)} (2k_p|d_e-x|)^{1/2} J^2_{-1/4}(k_p|d_e-x|)$$

where

$$kd_e = k_p(d+\delta_0) = (n+1/8)\pi$$

If we take the limit $k_p|d_e-x| \to 0$ this becomes

$$\left\langle A u_p^2(x,0)\right\rangle \sim \frac{2\Gamma^4(1/4)}{\pi^2 \ln(\Lambda_+)}$$

the same as the preceding result. Figure 65 shows a plot of the function

$$\ln(\Lambda_+)\left\langle A u_p^2(x,0)\right\rangle / \left[2\Gamma^2(1/4)\right] \sim \sqrt{2z} J^2_{-1/4}(z)$$

Setting the derivative equal to zero gives $-2\sqrt{2z} J_{3/4}(z) J_{-1/4}(z) = 0$, which vanishes for $z = 0$. Figure shows this function.

### 3.9.3 value at fixed point

Because numerical simulations were done with fixed points along the orbit we calculate the solution at a fixed point $x_0$ near the focal point. The averages are thus

$$\left\langle A u_p^2(x_0,0)\right\rangle \sim \frac{2}{\ln\left(\frac{\ell+d}{\ell-d}\right)} \frac{1}{\mathrm{Im}^2\left[e^{-i\pi/4} U'_+(-s',0)\right]}$$

$$\mathrm{Re}^2\left[U_+\left(s',\xi'\sqrt{2\gamma}\right) - 2^{is'} \frac{\Gamma(is'/2+1/4)}{\Gamma(-is'/2+1/4)} e^{-i3\pi/4} U^*_+\left(s',\xi'\sqrt{2\gamma}\right)\right]$$

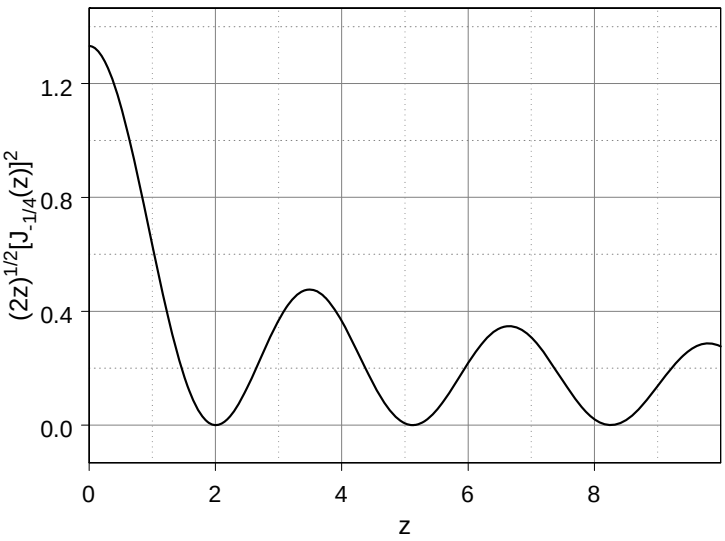


Figure 65. Plot of the scaled amplitude near the focal point for $k = k_p$.

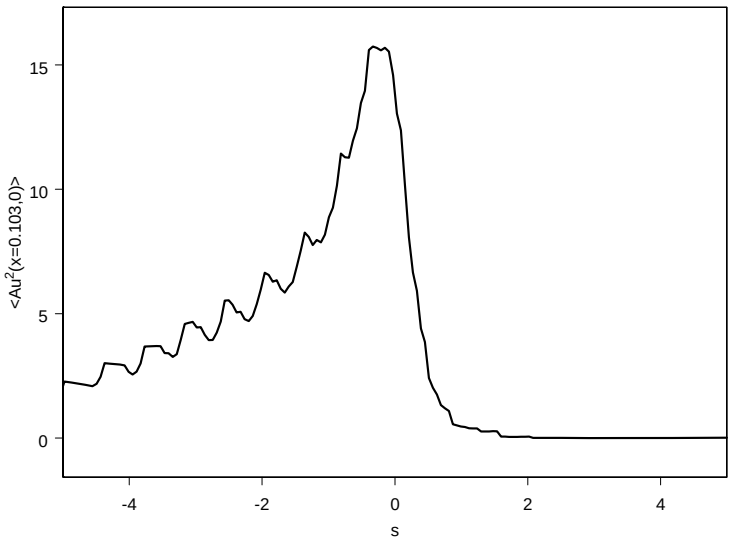


Figure 66. Scar component $p$ statistics as a function of $s$ at fixed location $x_0 = 0.103$ m along the horizontal orbit of the stadium. The focal point shifts according to the phase matching formulas, taking the first solution greater than or equal to $d$.

$$\xi' \approx \sqrt{2\left(d_e - x_0\right)/d}$$

$$\left\langle Au_p^2\left(x_0, 0\right)\right\rangle \sim \frac{2}{\ln\left(\frac{\ell+d}{\ell-d}\right)} \frac{1}{\mathrm{Im}^2\left[U_+'\left(s', 0\right)\right]}$$

$$\mathrm{Re}^2\left[e^{-i\pi/4}\left\{U_+\left(-s', \zeta\sqrt{2\gamma}\right) - 2^{-is'}\frac{\Gamma\left(-is'/2+1/4\right)}{\Gamma\left(is'/2+1/4\right)} e^{-i3\pi/4} U_+^*\left(-s', \zeta\sqrt{2\gamma}\right)\right\}\right]$$

$$\zeta \approx \sqrt{2\left(x_0 - d_e\right)/d}$$

where the shifted focal point $d_e$ is found from

$$kd_e = k\left(d+\delta\right) = -s'\ln\left(2\sqrt{\gamma}\right) + \arg\Gamma\left(1/4 + is'/2\right) + \left(n+1/8\right)\pi$$

or approximately

$$k_p d_e \approx \frac{1}{2} s' \ln\left(\frac{\ell+d}{\ell-d}\right)\left(d/\ell\right) - s'\ln\left(2\sqrt{k_p d}\right) + \arg\Gamma\left(1/4 + is'/2\right) + \left(n+1/8\right)\pi$$

and $n$ is taken to determine the first solution greater than or equal to $d$.

Figure 66 shows the resulting point value statistics at the location $x_0 = 0.103$ m along the horizontal orbit of the stadium cavity as a function of $s$. Notice that the shift has reduced the peak level from the preceding value of 28.13 (without focal shifts).

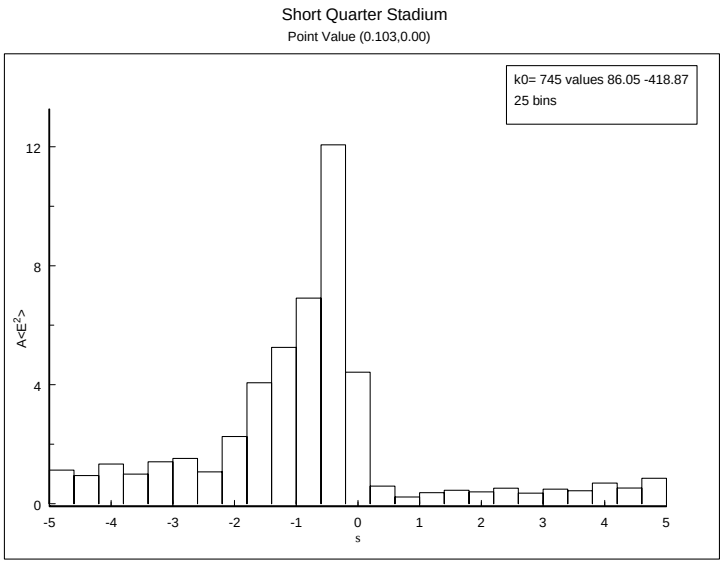


Figure 67. Numerical histogram of point value statistics along the horizontal orbit in the stadium cavity at location $x_0 = 0.103$ m.

Figure 67 shows the numerical histogram from the boundary element simulation of the stadium cavity. The location is again $x_0 = 0.103$ m along the horizontal orbit. Although the peak level is slightly less than the preceding prediction the behavior is very similar. The following subsubsection gives many histograms from the numerical simulations for locations about the stadium cavity.

### 3.9.4 histograms in stadium from numerical simulations

This section presents point statistics of $\langle Au^2(x,y)\rangle$ as a function of $s$ for various locations in the stadium cavity. The first set, consisting of Figures 68, 69, and 70, shows the behavior off the symmetry axes at $x = y$ for three values. These figures illustrate mean behavior near unity as expected.

The second set, consisting of Figures 71, 72, 73, 74 and 75, shows the behavior on the $y$ symmetry axis for five values of $y$ across the cavity. These figures illustrate mean behavior near two as expected.

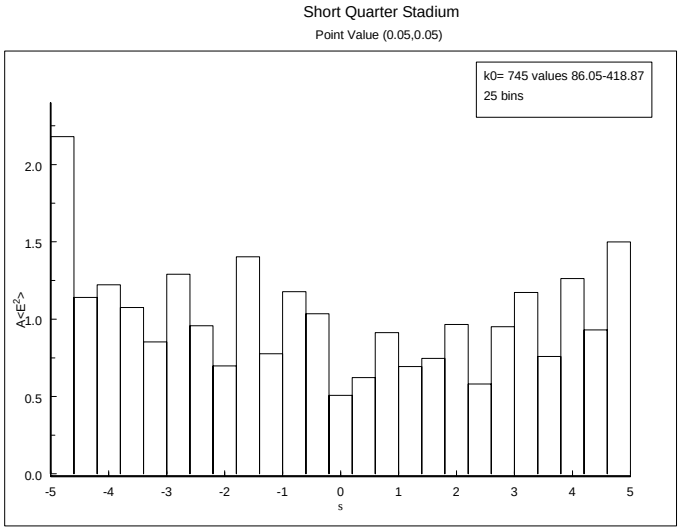


Figure 68. Histogram for point value of field for $x = y = 0.05$ m.

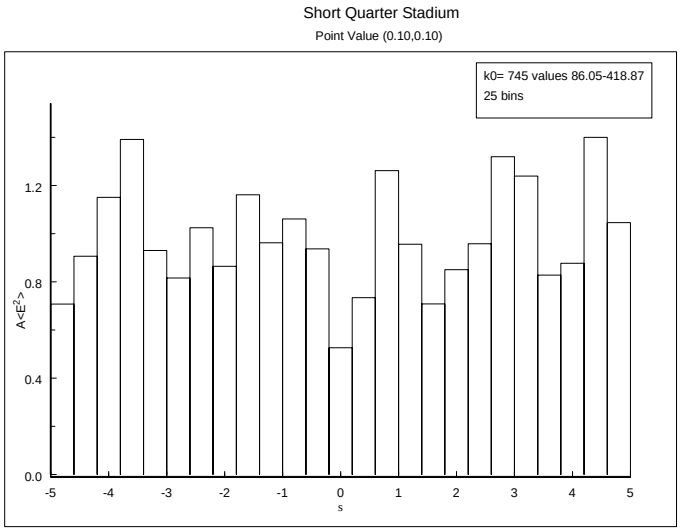


Figure 69. Histogram for point value of field for $x = y = 0.10$ m.

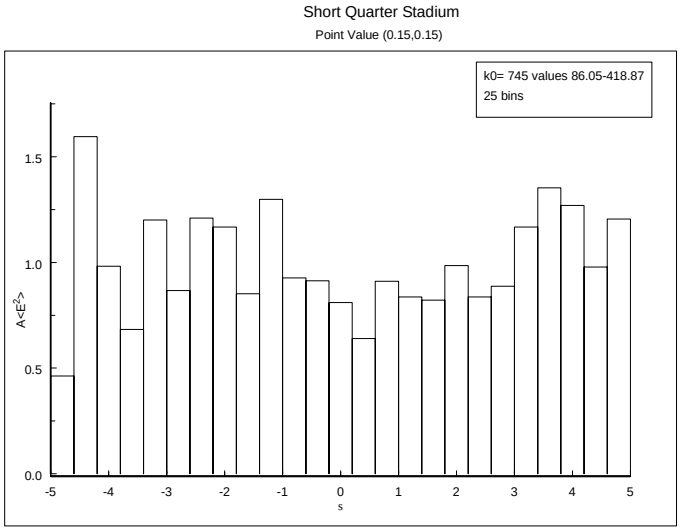


Figure 70. Histogram for point value of field for $x = y = 0.15$ m.

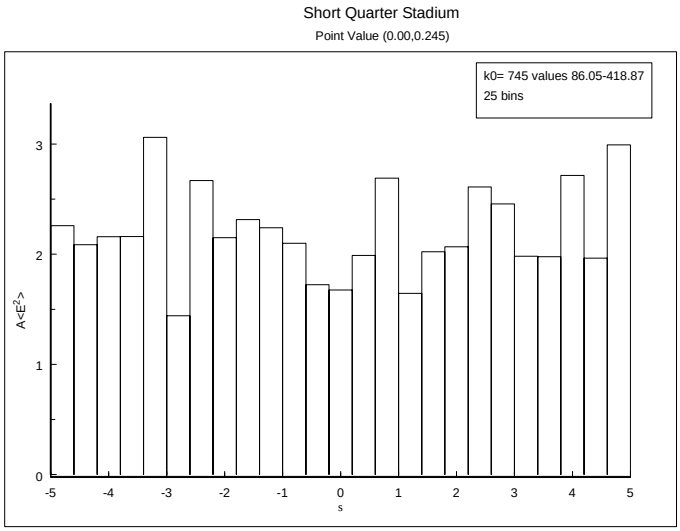


Figure 71. Histogram for point value at $x = 0$ and $y = 0.245$ m.

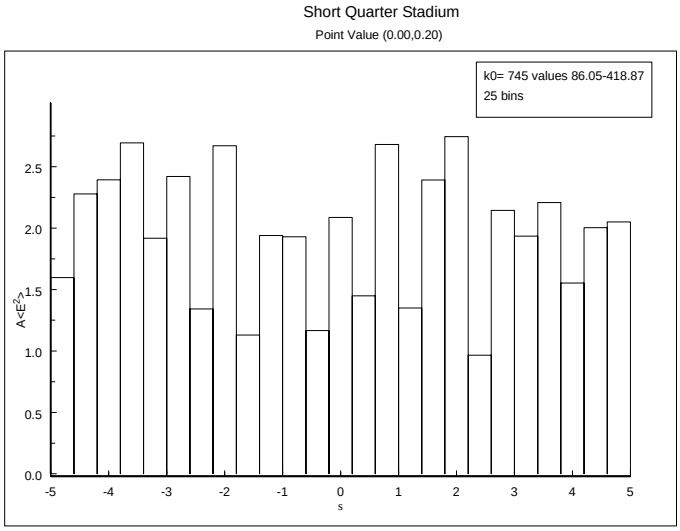


Figure 72. Histogram for point value at $x = 0$ and $y = 0.20$ m.

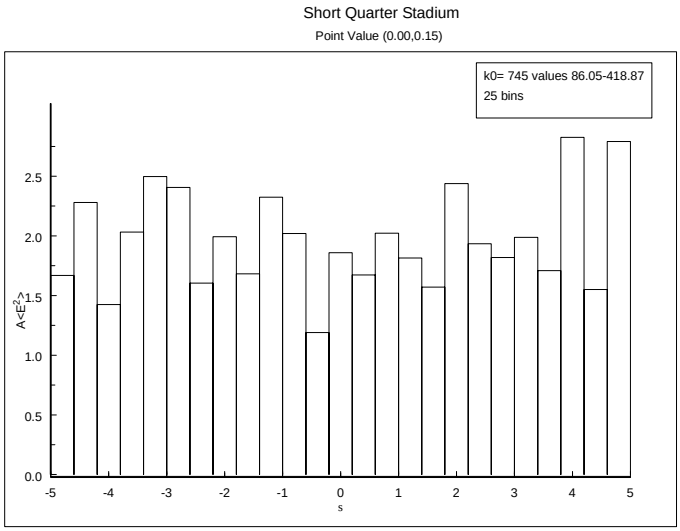


Figure 73. Histogram for point value at $x = 0$ and $y = 0.15$ m.

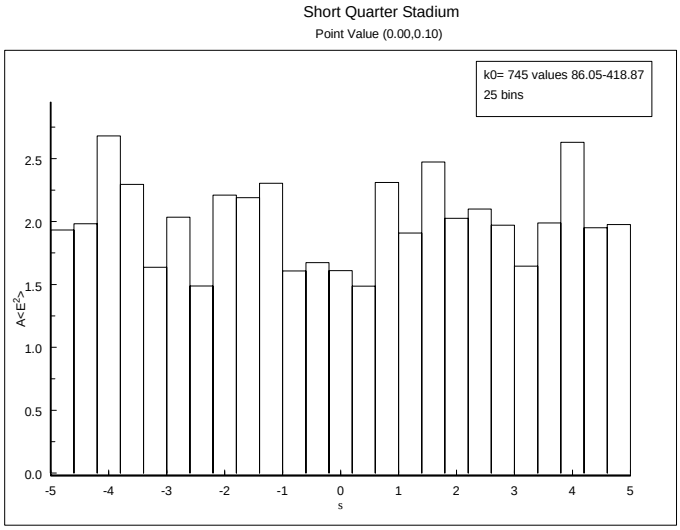


Figure 74. Histogram for point value at $x = 0$ and $y = 0.10$ m.

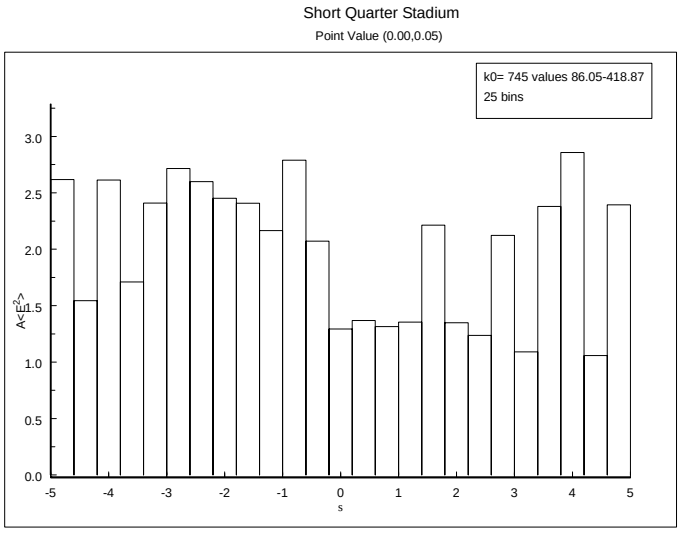


Figure 75. Histogram for point value at $x = 0$ and $y = 0.05$ m.

Figure 76 shows the behavior at the center of the cavity (on both symmetry axes $x$ and $y$). The mean behavior of four is expected however there is definitely more variation with $s$ on the horizontal scar orbit.

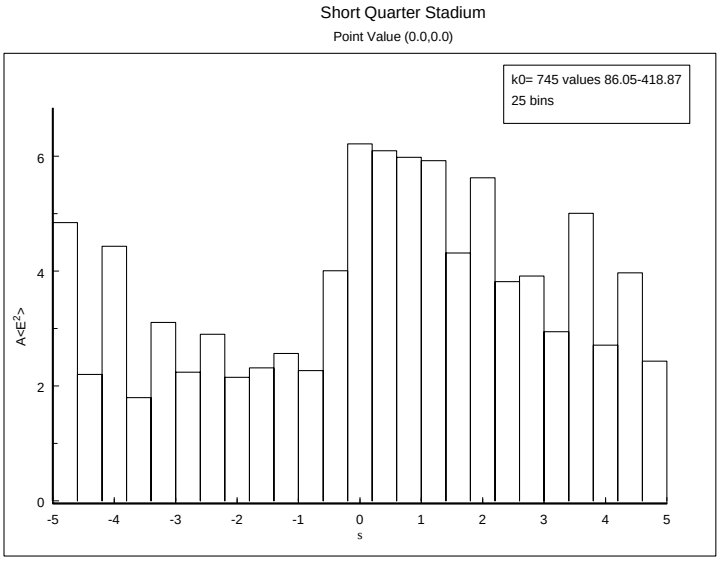


Figure 76. Histogram for point value at the center $x = y = 0$.

The next set, consisting of Figures 71 through 75 shows the behavior on the $x$ symmetry axis (the scarred bouncing ball orbit) for twenty four values of $x$ across the cavity. These figures illustrate focal point increases in level, which diminish in intensity near the wall and are largest near $s = 0$. Another interesting thing about the behavior is the existence of a discontinuous enhancement for positive and negative $s$. For example, up to 0.09 m the field is more enhanced for positive $s$. However this character then changes with negative $s$ more enhanced until 0.105 m is reached, at which point positive $s$ values are more enhanced again. It is interesting that the range of observation points between changes in behavior $O\,(0.015$ m) is in the range of the difference between focal point positions from the phase matching, discussed in section on focal point shift above (for the illustrated midrange value $p = 18$, noting that $8 \leq p \leq 36$ in these simulations).

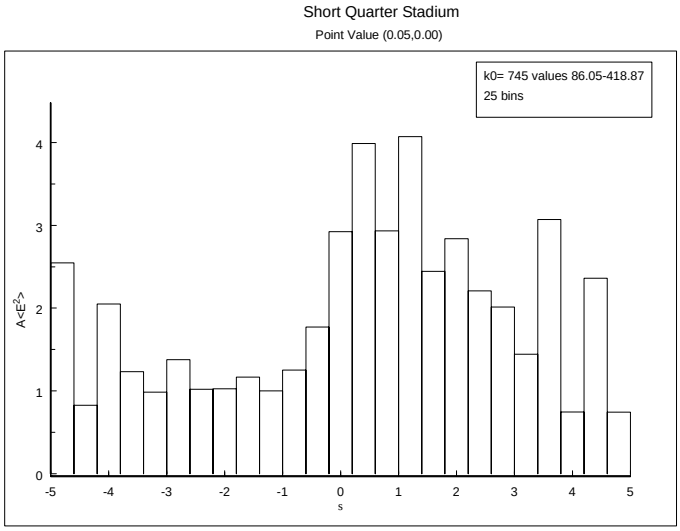


Figure 77. Histogram for point value on scar orbit at $x = 0.05$ m and $y = 0$.

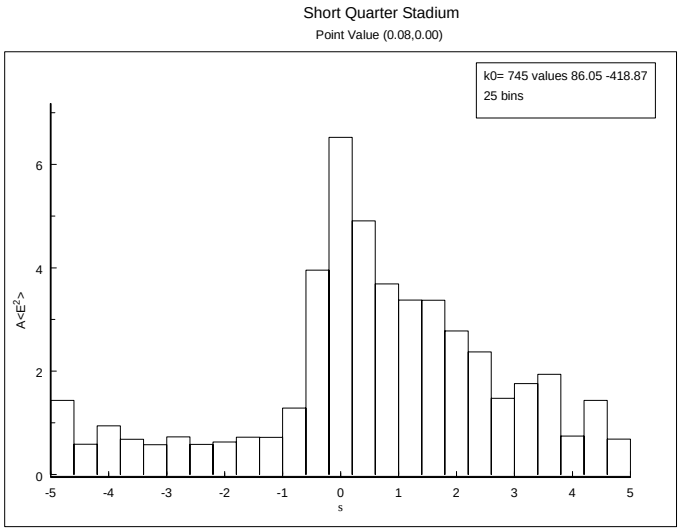


Figure 78. Histogram for point value on scar orbit at $x = 0.08$ m and $y = 0$.

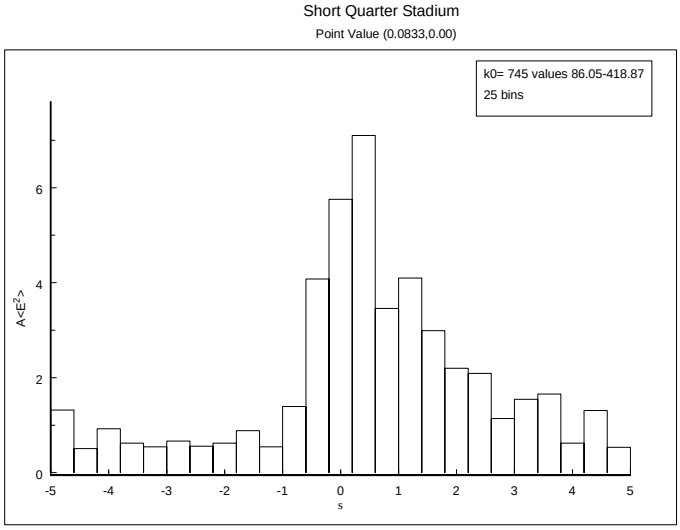


Figure 79. Histogram for point value on scar orbit at $x = 0.0833$ m (just to the right of the geometrical focal point) and $y = 0$.

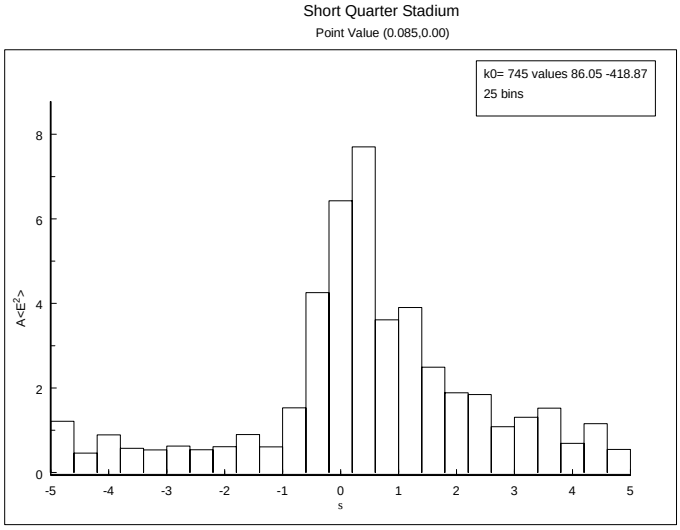


Figure 80. Histogram for point value on scar orbit at $x = 0.085$ m and $y = 0$.

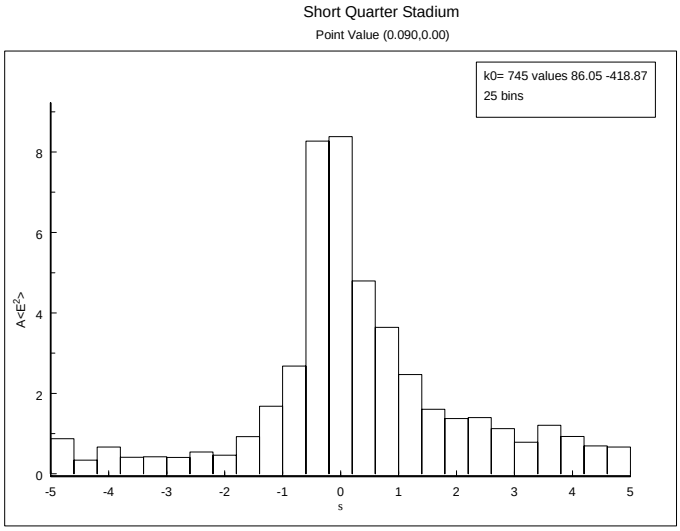


Figure 81. Histogram for point value on scar orbit at $x = 0.090$ m and $y = 0$.

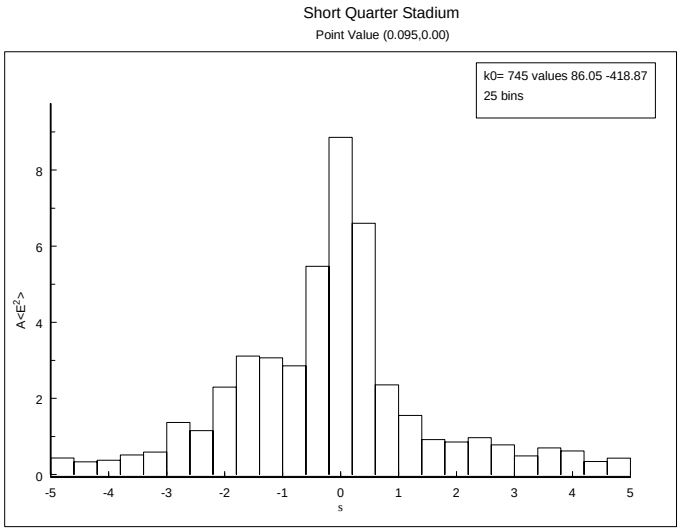


Figure 82. Histogram for point value on scar orbit at $x = 0.095$ m and $y = 0$.

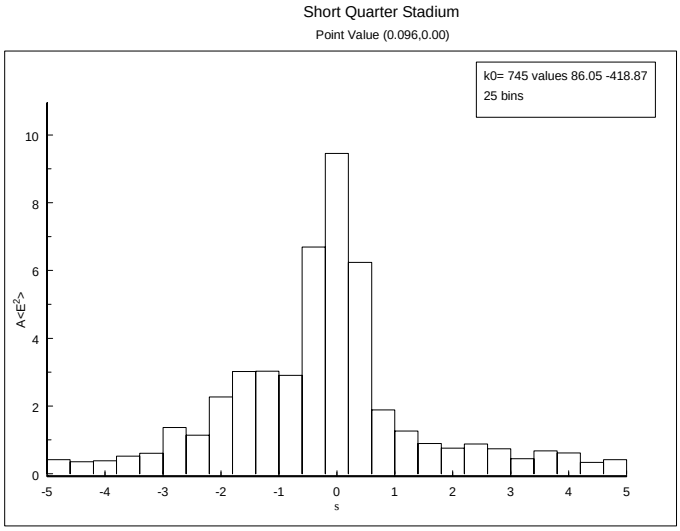


Figure 83. Histogram for point value on scar orbit at $x = 0.096$ m and $y = 0$.

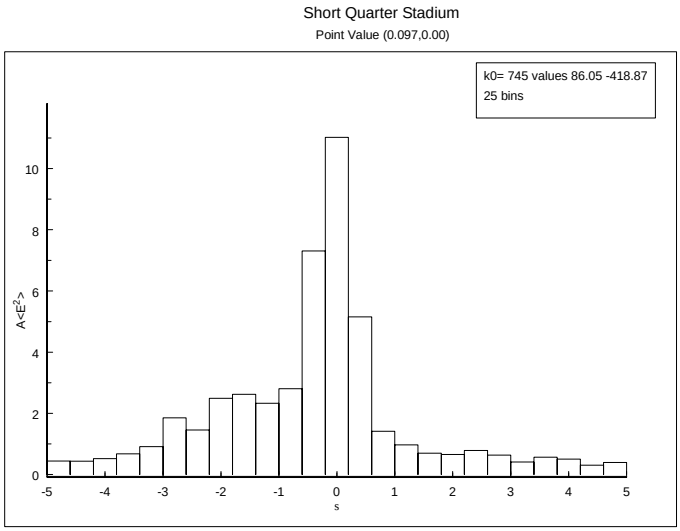


Figure 84. Histogram for point value on scar orbit at $x = 0.097$ m and $y = 0$.

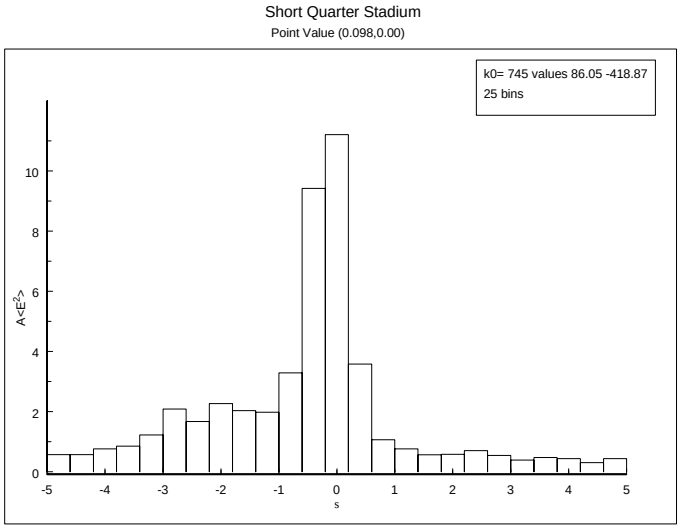


Figure 85. Histogram for point value on scar orbit at $x = 0.098$ m and $y = 0$.

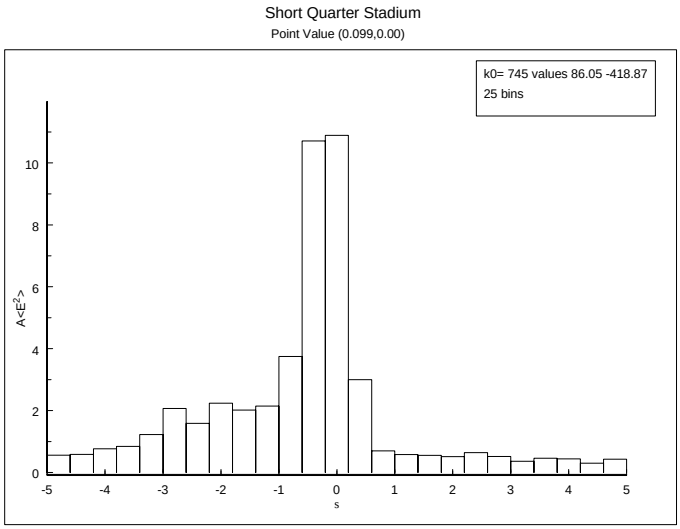


Figure 86. Histogram for point value on scar orbit at $x = 0.099$ m and $y = 0$.

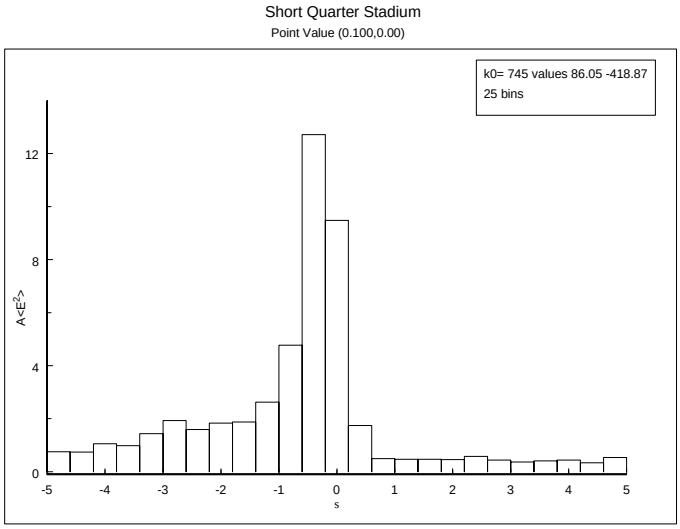


Figure 87. Histogram for point value on scar orbit at $x = 0.100$ m and $y = 0$.

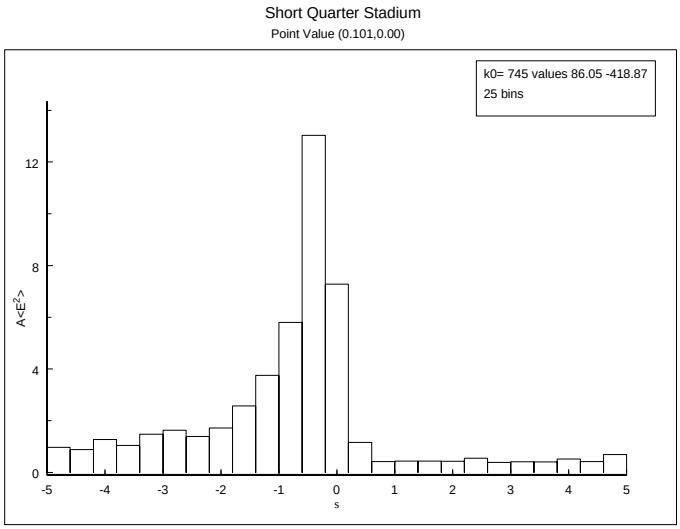


Figure 88. Histogram for point value on scar orbit at $x = 0.101$ m and $y = 0$.

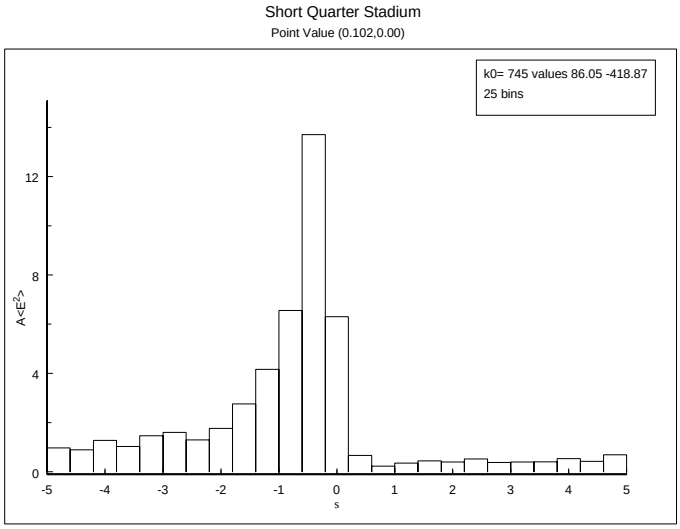


Figure 89. Histogram for point value on scar orbit at $x = 0.102$ m and $y = 0$.

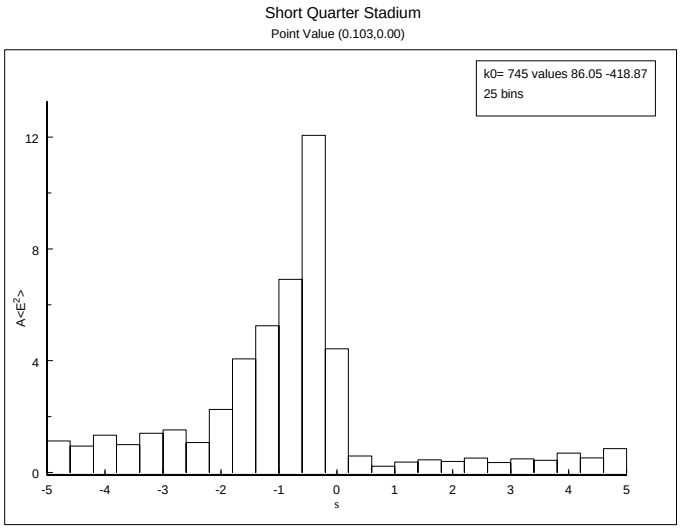


Figure 90. Histogram for point value on scar orbit at $x = 0.103$ m and $y = 0$.

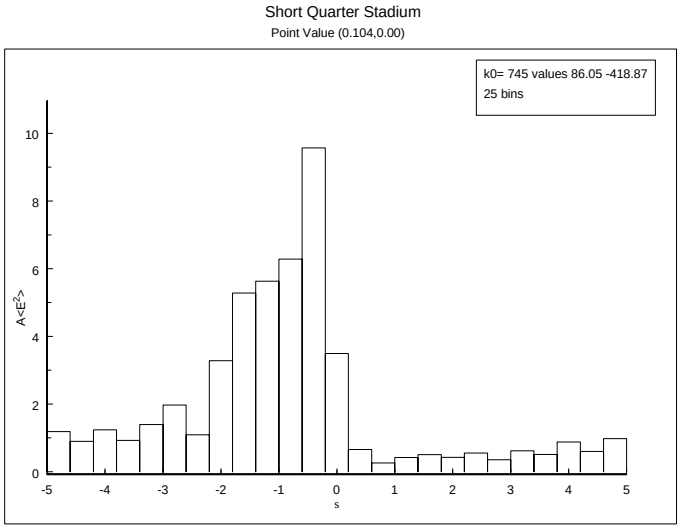


Figure 91. Histogram for point value on scar orbit at $x = 0.104$ m and $y = 0$.

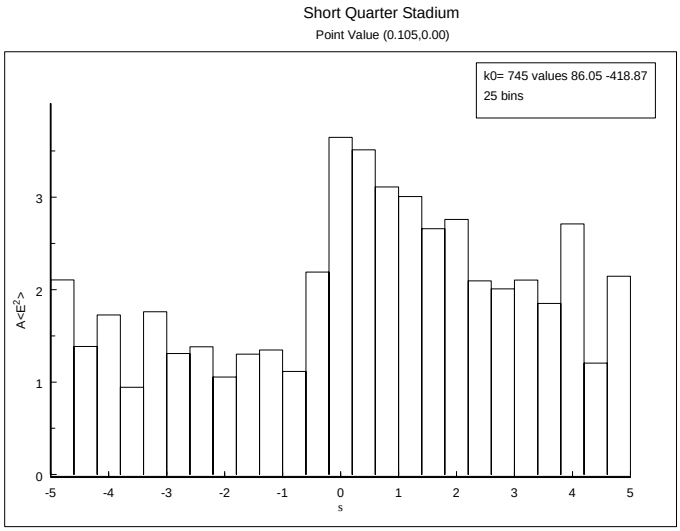


Figure 92. Histogram for point value on scar orbit at $x = 0.105$ m and $y = 0$.

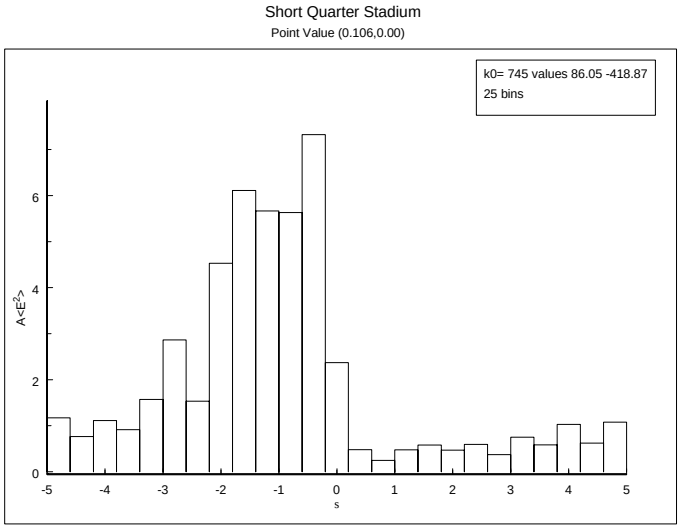


Figure 93. Histogram for point value on scar orbit at $x = 0.106$ m and $y = 0$.

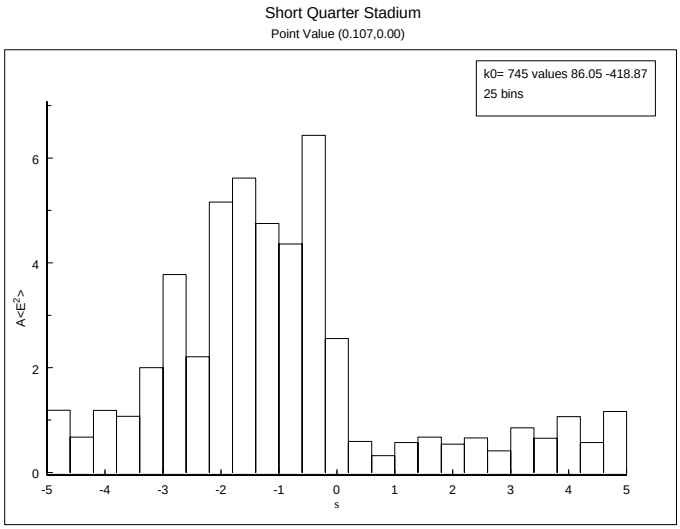


Figure 94. Histogram for point value on scar orbit at $x = 0.107$ m and $y = 0$.

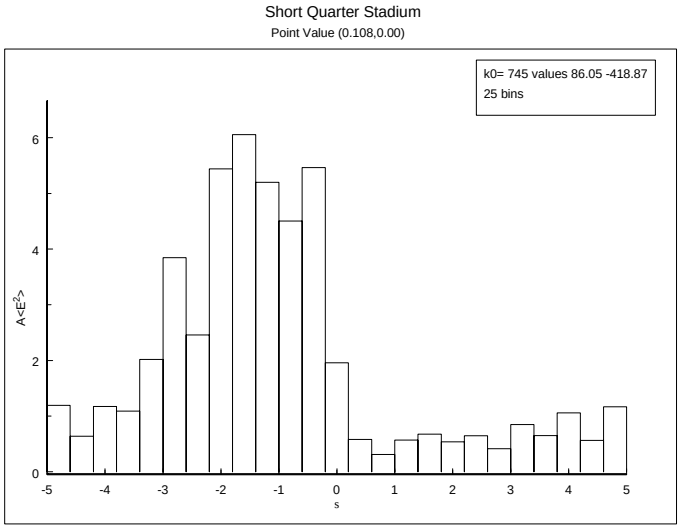


Figure 95. Histogram for point value on scar orbit at $x = 0.108$ m and $y = 0$.

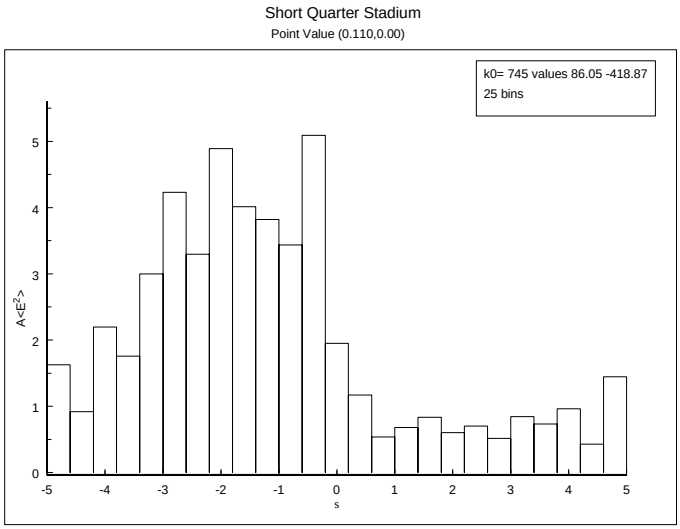


Figure 96. Histogram for point value on scar orbit at $x = 0.110$ m and $y = 0$.

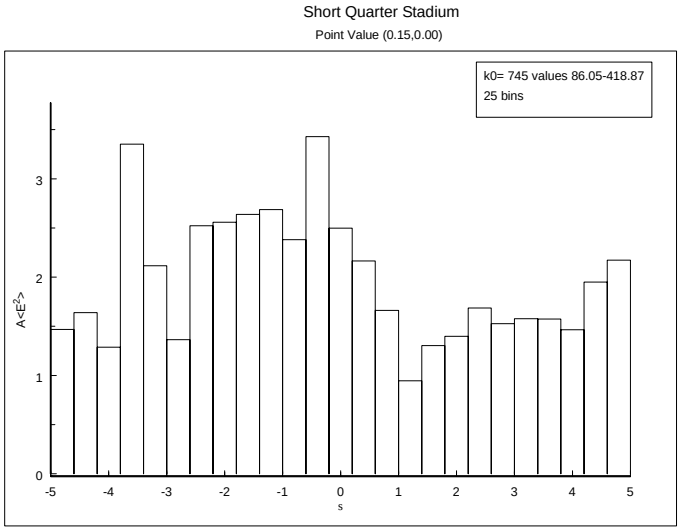


Figure 97. Histogram for point value on scar orbit at $x = 0.15$ m and $y = 0$.

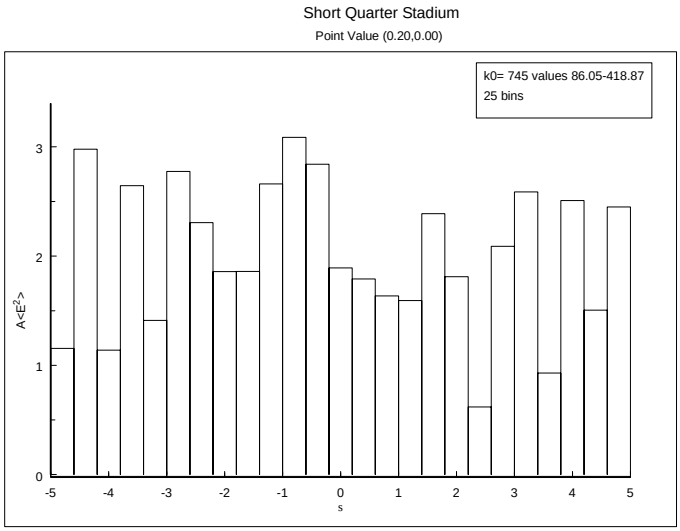


Figure 98. Histogram for point value on scar orbit at $x = 0.20$ m and $y = 0$.

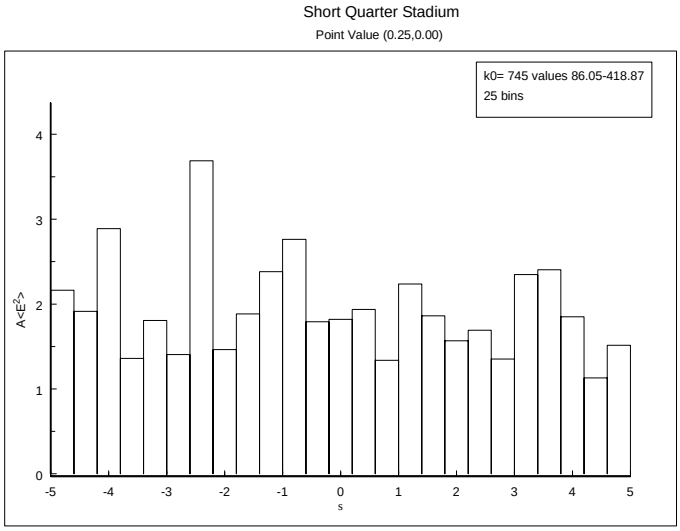


Figure 99. Histogram for point value on scar orbit at $x = 0.25$ m and $y = 0$.

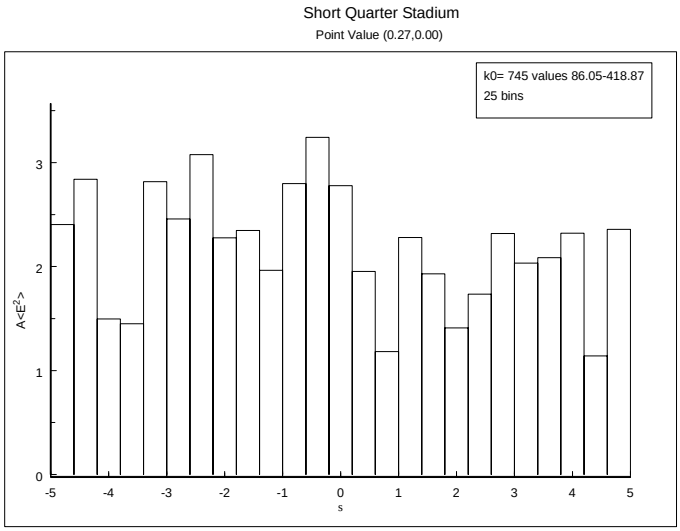


Figure 100. Histogram for point value on scar orbit at $x = 0.27$ m and $y = 0$.

# 4 CONCLUSIONS

Steady state fields in cavities, operating at high frequencies, exhibit chaotic behavior, where the modal fields can usually be described as a superposition of plane waves, generating Gaussian statistics for the field amplitude. However deviations resulting from periodic trajectories exist. Stable orbits (where perturbations of the ray remain in the vicinity of the periodic orbit) lead to concentrated cavity modes (the familiar laser cavity is an example) isolated from the remainder of the volume. Unstable orbits also lead to enhancements, which have been named scars. Recently a technique has been discussed for treating these time harmonic scars in two-dimensional cavities with nearly flat convex walls. This report carefully examines this method in two-dimensional geometries with both convex and concave walls.

The method is first summarized for the convex bow tie cavity. Then using ray techniques, which have been applied in the past to stable geometries, the method is generalized to elliptical paths along the periodic orbit. We focus on "bouncing-ball" modes in this report. This allows us to examine the accuracy of previous results and to see how the exact form of the stability exponents enter the theory. The random phase (from the outer regions of the cavity) boundary condition, which was introduced in this method, allows the ray construction to take into account the interaction with the remainder of the cavity in this unstable case. The normalization of the scarred eigenfunctions, introduced previously through circuit concepts, is put in the form of the electromagnetic energy theorem. Various quantities are examined in the bow tie cavity, including: projections of the field along the scarred orbit, integrals of the square of the field along the orbit, and values of the square of the field both on and off the orbit. Exhaustive boundary element simulations of the two-dimensional cavity are carried out to compare to the scar theory for both spatial distributions of the field along the orbit and statistical quantities. Scar deviations from the random plane wave background are most pronounced for the projections, considerably smaller for the integrals of the square, and smaller still for the point statistics. The larger the stability exponents along the orbit, the smaller these deviations become.

The case where the field is odd, both along and perpendicular to the orbit, is also addressed. The statistics of the scars for odd parity along the orbit are the same as the even case, but the spectra are interlaced. The statistics for scars which are odd with respect to the perpendicular of the orbit are different. The inclusion of the odd parity cases allows us to treat the asymmetric bow tie cavity (an example of which is discussed).

The canonical problem with concave walls can be taken as the stadium cavity. The stadium cavity contains interior foci, the treatment of which prompted the introduction of the elliptical analysis. We partitioned the horizontal orbit into three regions: between foci, outside the foci, and local to the foci. The ray analysis is applied to each region and asymptotic matching is done as the focus is approached. To accomplish this matching, a small shift needed to be introduced in the focal point location. Boundary element simulations were performed on many scarred modes and compared to the spatial distribution of the ray construction, including the focal region (with the focal shift applied). These comparisons confirm the form of these three region distributions. Normalization, using the electromagnetic energy theorem, in this case leads to an absolute value interpretation of the integration involved at the focus. The same statistical quantities were examined (projections, integrals of the square, and point values) and compared to results from the numerical simulations. Scar deviations from the chaotic background are larger in this geometry than in the bow tie geometry, even though we maintained the same stability exponents along the orbit. Both the projections and the point statistics near the foci show major deviations from the chaotic background.

# 5 REFERENCES

[1] K. S. H. Lee and F. C. Yang, "Trends and Bounds in RF Coupling to a Wire Inside a Slotted Cavity," IEEE Transactions on Electromagnetic Compatibility, Vol. 34, Aug. 1992, pp. 154-160.

[2] R. Holland and R. St. John, **Statistical Electromagnetics**, Philadelphia, PA: Taylor and Francis, 1999.

[3] D. A. Hill, "Linear Dipole Response in a Reverberation Chamber," IEEE Transactions on Electromagentic Compatibility, Vol. 41, Nov. 1999, pp. 365-368.

[4] L. K. Warne and K. S. H. Lee, "Some Remarks on Antenna Response in Reverberation Chamber," IEEE Transactions on Electromagnetic Compatibility, Vol. 13, No. 3, May 2001, pp. 239-240.

[5] M. C. Gutzwiller, **Chaos in Classical and Quantum Mechanics**, New York: Springer-Verlag, Inc., 1990, Ch. 15, p. 259.

[6] M. V. Berry, in **Chaotic Behavior of Deterministic Systems**, edited by G. Loose, R. H. G. Helleman and R. Storn, Amsterdam: North-Holland, 1983, pp. 171-271.

[7] S. W. McDonald and A. N. Kaufmann, "Wave Chaos in the Stadium: Statistical Properties of Short-Wave Solutions of the Helmholtz Equation," Phys. Rev. A, Vol. 37, No. 8, pp. 3067-3086, April 15, 1988.

[8] T. H. Lehman, "A Statistical Theory of Electromagnetic Fields in Complex Cavities," AFWL Interaction Note 494, May 1993.

[9] L. K. Warne, K. S. H. Lee, H. G. Hudson, W. A. Johnson, R. E. Jorgenson, "Statistical Properties of Linear Antenna Impedance in an Electrically Large Cavity," IEEE Transactions on Antennas and Propagation, Vol. 11, No. 5, May 2003, pp. 978-992.

[10] L. K. Warne, K. S. H. Lee, W. A. Johnson, and R. E. Jorgenson, "An Improved Statistical Model for Linear Antenna Input Impedance in an Electrically Large Cavity," Sandia National Laboratories Report, SAND2005-1505, March 2005.

[11] L. K. Warne, H. G. Hudson, R. E. Jorgenson, and W. A. Johnson, "Receiving Properties of Linear Antennas in High Frequency Cavities," Sandia National Laboratories Internal Report, October 7, 2002.

[12] X. Zheng, T. M. Antonsen, Jr., and E. Ott, "Statistics of Impedance and Scattering Matricies in Chaotic Microwave Cavities: Single Channel Case," Electromagnetics, Vol. 26, No. 1, Jan. 2006, pp. 3-35.

[13] X. Zheng, T. M. Antonsen, Jr., and E. Ott, "Statistics of Impedance and Scattering Matricies in Chaotic Microwave Cavities with Multiple Ports," Electromagnetics, Vol. 26, No. 1, Jan. 2006, pp. 37-55.

[14] H. J. Stockmann and J. Stein, "Quantum Chaos in Billiards Studied by Microwave Absorption," Physical Review Letters, Vol. 64, No. 19, May 1990, pp. 2215-2218.

[15] J. Stein, H. J. Stockmann, and U. Stoffregen, "Microwave Studies of Billiard Green Functions and Propagators," Physical Review Letters, Vol. 75, No. 1, July 1995, pp. 53-56.

[16] U. Dorr, H. J. Stockmann, M. Barth, and U. Kuhl, "Scarred and Chaotic Field Distributions in a Three-Dimensional Sinai-Microwave Resonator," Vol. 80, No. 5, Feb. 1998, pp. 1030-1033.

[17] S. Hemmady, X. Zheng, T. M. Antonsen, Jr., E. Ott, and S. M. Anlage, "Universal statistics of the scattering coefficient of chaotic microwave cavities," Physical Review E, Vol. 71, 2005, pp. 056215-1,9.

[18] L. A. Vaynshteyn, **Open Waveguides and Resonators**, Boulder, CO: Golem Press, 1969, Ch. 3.

[19] V. M. Babic and N. Y. Kirpicnikova, **The Boundary-Layer Method in Diffraction Problems**, Berlin: Springer-Verlag, 1979.

[20] V. M. Babic and V. S. Buldyrev, **Short-Wavelength Diffraction Theory**, Berlin: Springer-Verlag, 1991.

[21] E. J. Heller, "Bound-State Eigenfunctions of Classically Chaotic Hamiltonian Systems: Scars of Periodic Orbits," Phys. Rev. Lett., Vol. 53, No. 16, 1984, pp. 1515-1518.

[22] M. Brack and R. K. Bhaduri, **Semiclassical Physics**, Reading: Addion-Wesley Pub. Co., Inc., 1997,

pp. 39-42.

[23] L. E. Reichl, **The Transition to Chaos**, Berlin: Springer-Verlag, 1992, pp. 320, 368-376.

[24] L. Kaplan and E. J. Heller, "Linear and Nonlinear Theory of Eigenfunction Scars," Annals of Physics, Vol. 264, 1998, pp. 171-206.

[25] L. Kaplan, "Wave Function Intensity Statistics From Unstable Periodic Orbits," Physical Review Letters, Vol. 80, 1998, pp. 2582-2585.

[26] L. Kaplan, "Scars in quantum chaotic wavefunctions," Nonlinearity, Vol. 12, 1999, R1-R40.

[27] E. G. Vergini, "Semiclassical theory of short periodic orbits in quantum chaos," J. Phys. A: Math. Gen. 33, 2000, pp. 4709-4716.

[28] E. G. Vergini and G. G. Carlo, "Semiclassical construction of resonances with hyperbolic structure: the scar function," J. Phys. A: Math. Gen., 34, 2001, pp. 4525-4552.

[29] K. Damborsky and L. Kaplan, "Scar intensity statistics in the position representation," Physical Review E, Vol. 72, 2005, pp. 66204-1 to 66204-8.

[30] T. M. Antonsen, Jr., E. Ott, A. Chen, and R. N. Oerter, "Statistics of wave-function scars," Vol. 51, No. 1, Physical Review E, January 1995, pp. 111-121.

[31] M. Abramowitz and I. A. Stegun (editors), **Handbook of Mathematical Functions**, National Bureau of Standards, 1972.

[32] A. E. Siegman, **An Introduction to Lasers and Masers**, New York: McGraw-Hill, Inc., 1971, Section 8-1.

[33] C. H. Papas, **Theory of Electromagnetic Wave Propagation**, New York: McGraw-Hill Book Co., 1965, Ch. 1.

[34] G. L. James, **Geometrical Theory of Diffraction for Electromagnetic Waves**, New York: Peter Peregrinus LTD., 1980, p. 101.

[35] J. Kevorkian and J. D. Cole, **Perturbation methods in Applied Mathematics**, New York: Springer-Verlag, 1981, pp. 359-360.

[36] A. Erdelyi, **Asymptotic Expansions**, New York: Dover Pub., 1956, Chapter 2.

[37] I. S. Gradshteyn and I. M. Ryzhik, **Table of Integrals, Series, and Products**, Academic Press, New York, 1965, pp. 420, 730.

# Appendix A. APPENDICES FOR BOW TIE CAVITY

These are the appendices for the bow tie cavity.

## A.1 Bow Tie Cavity Area

The area of a bow tie cavity is now given. Referring to Figure A-1, the area of the red right triangle is

$$A_r = \frac{1}{2}\left(L_x/2 + R_x\right)\left(L_y/2 + R_y\right)$$

The vertex of the green triangle must now be located. Letting

$$c^2 = \left(L_x/2 + R_x\right)^2 + \left(L_y/2 + R_y\right)^2$$

and using the law of cosines

$$\frac{R_x^2 + R_y^2 - c^2}{2R_xR_y} = \cos\chi = \sin\left(\frac{\pi}{2} - \chi\right)$$

or

$$\frac{L_x^2/4 + R_xL_x + L_y^2/4 + R_yL_y}{2R_xR_y} = \sin\left(\chi - \frac{\pi}{2}\right)$$

Next the law of sines gives

$$\frac{\sin\alpha}{R_y} = \frac{\sin\beta}{R_x} = \frac{\sin\chi}{c}$$

The area of the green triangle is

$$A_g = \frac{1}{2}cR_x\sin\alpha = \frac{1}{2}cR_y\sin\beta = \frac{1}{2}R_xR_y\sin\chi$$

The area of the $R_y$ circle included in the red triangle is

$$A_y = \frac{1}{2}R_y^2\left[\arcsin\left(\frac{L_x/2 + R_x}{c}\right) - \beta\right]$$

The area of the $R_x$ circle included in the red triangle is

$$A_x = \frac{1}{2}R_x^2\left[\arcsin\left(\frac{L_y/2 + R_y}{c}\right) - \alpha\right]$$

One quarter area of the bow tie cavity is then

$$A/4 = A_r - A_g - A_x - A_y$$

As an example if we take $L_x = L_y = 2$, $R_x = 1.5$, and $R_y = 10$ then $A_r = 55/4$, $c = 11.28051$, $\sin\left(\chi - \pi/2\right) = 5/6$, $\sin\chi = 0.5527708$, $A_g = 4.145781$, $\alpha = 0.5121158$, $A_x = 0.9396044$, $\beta = 0.07356975$, $A_y = 7.495343$, $A = 4.677086$.

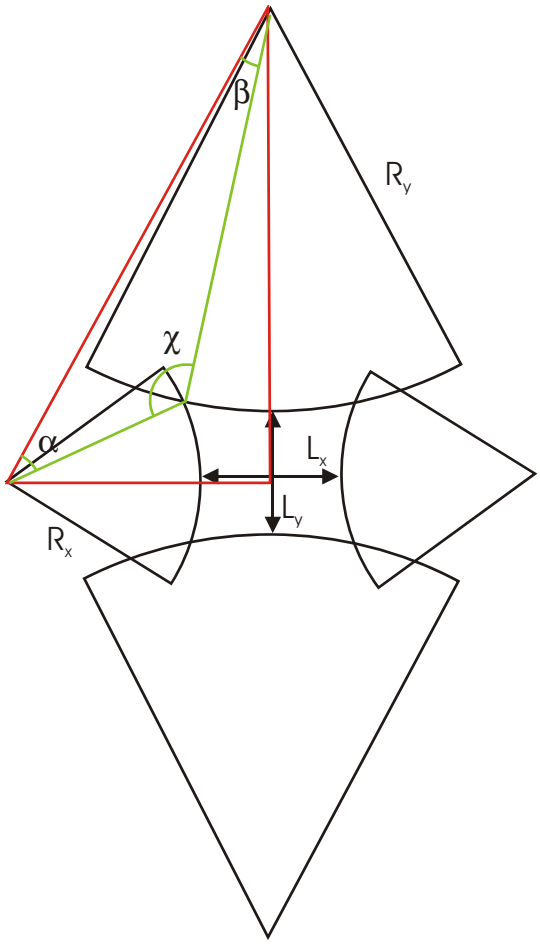


Figure A-1. Geometry of bow tie cavity and circular walls used in the calculation of the interior area.

## A.2 Peak Of Scar Curve

The scaled scar function is

$$G_1(\lambda_1,\Lambda)=\frac{2(\Lambda-1)^{-1/2}}{\left|U'_+(\lambda_1,0)\right|^2}=\frac{1}{\pi}(\Lambda-1)^{-1/2}\exp[\pi\lambda_1/2]\,2^{1/2}\left|\Gamma(1/4-i\lambda_1/2)\right|^2$$

Expanding near the peak [31]

$$\Gamma(1/4-i\lambda_1/2)\sim\Gamma(1/4)\left[1+\psi(1/4)(-i\lambda_1/2)+\frac{1}{2}\psi^2(1/4)(-i\lambda_1/2)^2+\frac{1}{2}\psi'(1/4)(-i\lambda_1/2)^2+\cdots\right]$$

and

$$\left|\Gamma(1/4-i\lambda_1/2)\right|^2\sim\Gamma^2(1/4)\left[1-\psi'(1/4)(\lambda_1/2)^2+\cdots\right]$$

where the digamma function [31] $\psi(z)$ has value

$$\psi(1/4)=-4.227454$$

and derivative

$$\psi'(1/4)=17.197329155$$

From the Taylor expansion

$$\exp\{\pi\lambda_1/2\}\sim1+\pi(\lambda_1/2)+\frac{\pi^2}{2}(\lambda_1/2)^2+\frac{\pi^3}{6}(\lambda_1/2)^3+\cdots$$

we find

$$G_1(\lambda_1,\Lambda)\sim G_1(0,\Lambda)\left[1+\chi_1+\left\{\frac{1}{2}-\frac{\psi'(1/4)}{\pi^2}\right\}\chi_1^2+\left\{\frac{1}{6}-\frac{\psi'(1/4)}{\pi^2}\right\}\chi_1^3\right]$$

where

$$\chi_1=\pi\lambda_1/2$$

The peak value is then the solution of the quadratic

$$\left\{\frac{3\psi'(1/4)}{\pi^2}-\frac{1}{2}\right\}\chi_1^2+\left\{\frac{2\psi'(1/4)}{\pi^2}-1\right\}\chi_1-1=0$$

or

$$\chi_{1pk}=\frac{2\sqrt{\left\{\psi'(1/4)+\pi^2\right\}^2-\frac{5}{4}\pi^4}-2\psi'(1/4)+\pi^2}{6\psi'(1/4)-\pi^2}\approx0.2669043$$

$$\lambda_{1pk}\approx0.16991658$$

$$\left|U'_+\left(\lambda_{1pk},0\right)\right|^{-2} \approx 3.39784$$

$$G_1\left(\lambda_{1pk},\Lambda\right) \approx 1.1484329 G_1\left(0,\Lambda\right)$$

$$\approx 6.795680\ \ \left(\Lambda-1\right)^{-1/2}$$

where

$$G_1\left(0,\Lambda\right) = \frac{1}{\pi}\left(\Lambda-1\right)^{-1/2} 2^{1/2}\Gamma^2\left(1/4\right)$$

$$\Gamma\left(1/4\right) \approx 3.6256099082$$

The peak of the projection is then

$$\left\langle \sqrt{kL} V_p^2 \right\rangle = L^2 G_1\left(\lambda_{1pk},\Lambda\right)/A \approx 5.1675842$$

## A.3 Calculation of Random Plane Wave Projection

We use the representation

$$G_s\left(\lambda_p\right) = \frac{4}{\sqrt{2\pi}}\int_0^1 \left(1-u\right)\cos\left(\lambda_p u/2 - \pi/4\right)\frac{du}{\sqrt{u}}$$

$$= 4\sqrt{\frac{2}{\pi}}\int_0^1 \left(1-u^2\right)\cos\left(\lambda_p u^2/2 - \pi/4\right) du$$

Integration by parts gives

$$\int_0^1 \sin\left(\lambda_p u^2/2 - \pi/4\right) du = \left. u\sin\left(\lambda_p u^2/2 - \pi/4\right)\right|_0^1 - \lambda_p\int_0^1 u^2\cos\left(\lambda_p u^2/2 - \pi/4\right) du$$

$$= \sin\left(\lambda_p/2 - \pi/4\right) - \lambda_p\int_0^1 u^2\cos\left(\lambda_p u^2/2 - \pi/4\right) du$$

Noting that

$$G_s\left(\lambda_p\right) = 4\sqrt{\frac{2}{\pi}}\int_0^1 \left(1-u^2\right)\cos\left(\left|\lambda_p\right| u^2/2 - \mathrm{sgn}\left(\lambda_p\right)\pi/4\right) du$$

thus gives

$$G_s\left(\lambda_p\right) = 4\sqrt{\frac{2}{\pi}}\int_0^1 \cos\left(\lambda_p u^2/2 - \pi/4\right) du - 4\sqrt{\frac{2}{\pi}}\int_0^1 u^2\cos\left(\lambda_p u^2/2 - \pi/4\right) du$$

$$= 4\sqrt{\frac{2}{\pi}}\int_0^1 \cos\left(\lambda_p u^2/2 - \pi/4\right) du - \frac{4}{\lambda_p}\sqrt{\frac{2}{\pi}}\left\{\sin\left(\lambda_p/2 - \pi/4\right) - \int_0^1 \sin\left(\lambda_p u^2/2 - \pi/4\right) du\right\}$$

$$= \frac{4}{\sqrt{\pi}} \left\{ \int_0^1 \cos\left(\lambda_p u^2/2\right) du + \int_0^1 \sin\left(\lambda_p u^2/2\right) du \right\}$$

$$-\frac{4}{\lambda_p \sqrt{\pi}} \left\{ \sin\left(\lambda_p/2\right) - \cos\left(\lambda_p/2\right) - \int_0^1 \sin\left(\lambda_p u^2/2\right) du + \int_0^1 \cos\left(\lambda_p u^2/2\right) du \right\}$$

$$= \frac{4}{\sqrt{\pi}} \left\{ \int_0^1 \cos\left(\left|\lambda_p\right| u^2/2\right) du + \operatorname{sgn}\left(\lambda_p\right) \int_0^1 \sin\left(\left|\lambda_p\right| u^2/2\right) du \right\}$$

$$-\frac{4}{\lambda_p \sqrt{\pi}} \left\{ \sin\left(\lambda_p/2\right) - \cos\left(\lambda_p/2\right) - \operatorname{sgn}\left(\lambda_p\right) \int_0^1 \sin\left(\left|\lambda_p\right| u^2/2\right) du + \int_0^1 \cos\left(\left|\lambda_p\right| u^2/2\right) du \right\}$$

$$= \frac{4}{\sqrt{\left|\lambda_p\right|}} \left\{ \left(1 - \frac{1}{\lambda_p}\right) \int_0^{\sqrt{\left|\lambda_p\right|/\pi}} \cos\left(\pi u^2/2\right) du + \operatorname{sgn}\left(\lambda_p\right) \left(1 + \frac{1}{\lambda_p}\right) \int_0^{\sqrt{\left|\lambda_p\right|/\pi}} \sin\left(\pi u^2/2\right) du \right\}$$

$$-\frac{4}{\lambda_p \sqrt{\pi}} \left\{ \sin\left(\lambda_p/2\right) - \cos\left(\lambda_p/2\right) \right\}$$

$$= \frac{4}{\sqrt{\left|\lambda_p\right|}} \left\{ \left(1 - \frac{1}{\lambda_p}\right) C\left(\sqrt{\left|\lambda_p\right|/\pi}\right) + \operatorname{sgn}\left(\lambda_p\right) \left(1 + \frac{1}{\lambda_p}\right) S\left(\sqrt{\left|\lambda_p\right|/\pi}\right) \right\} - \frac{4}{\lambda_p \sqrt{\pi}} \left\{ \sin\left(\lambda_p/2\right) - \cos\left(\lambda_p/2\right) \right\}$$

where the Fresnel integrals are [31]

$$C(z) = \int_0^z \cos\left(\pi t^2/2\right) dt = \frac{1}{2} - \int_z^\infty \cos\left(\pi t^2/2\right) dt = \frac{1}{2} - \frac{1}{2}\sqrt{\frac{2}{\pi}} \int_{\pi z^2/2}^\infty \cos(u) \frac{du}{\sqrt{u}}$$

$$S(z) = \int_0^z \sin\left(\pi t^2/2\right) dt = \frac{1}{2} - \int_z^\infty \sin\left(\pi t^2/2\right) dt = \frac{1}{2} - \frac{1}{2}\sqrt{\frac{2}{\pi}} \int_{\pi z^2/2}^\infty \sin(u) \frac{du}{\sqrt{u}}$$

Note that for small arguments we can approximate this as

$$G_s\left(\lambda_p\right) = \frac{4}{\sqrt{\pi}} \int_0^1 \left(1 - u^2\right) \left[\cos\left(\lambda_p u^2/2\right) + \sin\left(\lambda_p u^2/2\right)\right] du$$

$$\sim \frac{4}{\sqrt{\pi}} \int_0^1 \left(1 - u^2\right) \left[1 - \frac{1}{2}\left(\lambda_p u^2/2\right)^2 + \left(\lambda_p u^2/2\right) - \frac{1}{6}\left(\lambda_p u^2/2\right)^3\right] du$$

$$\sim \frac{4}{\sqrt{\pi}} \left[\left(1 - \frac{1}{3}\right) - \frac{1}{2}\left(\lambda_p/2\right)^2 \left(\frac{1}{5} - \frac{1}{7}\right) + \left(\lambda_p/2\right) \left(\frac{1}{3} - \frac{1}{5}\right) - \frac{1}{6}\left(\lambda_p/2\right)^3 \left(\frac{1}{7} - \frac{1}{9}\right)\right]$$

The asymptotic form for large $\lambda_p$ is facilitated by first substituting [31]

$$C(z) = \frac{1}{2} + f(z) \sin\left(\pi z^2/2\right) - g(z) \cos\left(\pi z^2/2\right)$$

$$S(z) = \frac{1}{2} - f(z)\cos\left(\pi z^2/2\right) - g(z)\sin\left(\pi z^2/2\right)$$

giving

$$G_s(\lambda_p) = \frac{4}{\sqrt{|\lambda_p|}}\left\{\left(1-\frac{1}{\lambda_p}\right)\left[f\left(\sqrt{|\lambda_p|/\pi}\right)\sin\left(|\lambda_p|/2\right) - g\left(\sqrt{|\lambda_p|/\pi}\right)\cos\left(|\lambda_p|/2\right)\right]\right.$$

$$\left.-\operatorname{sgn}(\lambda_p)\left(1+\frac{1}{\lambda_p}\right)\left[f\left(\sqrt{|\lambda_p|/\pi}\right)\cos\left(|\lambda_p|/2\right) + g\left(\sqrt{|\lambda_p|/\pi}\right)\sin\left(|\lambda_p|/2\right)\right]\right\}$$

$$+\frac{2}{\sqrt{|\lambda_p|}}\left\{\left(1-\frac{1}{\lambda_p}\right) + \operatorname{sgn}(\lambda_p)\left(1+\frac{1}{\lambda_p}\right)\right\} - \frac{4}{\lambda_p\sqrt{\pi}}\left\{\sin(\lambda_p/2) - \cos(\lambda_p/2)\right\}$$

Now we take for $z \to \infty$

$$f(z) = \frac{1}{\pi z} + O\left(z^{-5}\right)$$

$$g(z) \sim \frac{1}{\pi^2 z^3} + O\left(z^{-7}\right)$$

Thus

$$G_s(\lambda_p) \sim \frac{4/\sqrt{\pi}}{|\lambda_p|}\left\{\left(1-\frac{1}{\lambda_p}\right)\left[\sin\left(|\lambda_p|/2\right) - \frac{1}{|\lambda_p|}\cos\left(|\lambda_p|/2\right)\right]\right.$$

$$\left.-\operatorname{sgn}(\lambda_p)\left(1+\frac{1}{\lambda_p}\right)\left[\cos\left(|\lambda_p|/2\right) + \frac{1}{|\lambda_p|}\sin\left(|\lambda_p|/2\right)\right]\right\}$$

$$+\frac{2}{\sqrt{|\lambda_p|}}\left\{\left(1-\frac{1}{\lambda_p}\right) + \operatorname{sgn}(\lambda_p)\left(1+\frac{1}{\lambda_p}\right)\right\} - \frac{4}{\lambda_p\sqrt{\pi}}\left\{\sin(\lambda_p/2) - \cos(\lambda_p/2)\right\}$$

Suppose $\lambda_p > 0$

$$G_s(\lambda_p) \sim \frac{4}{\sqrt{\lambda_p}} - \frac{8/\sqrt{\pi}}{\lambda_p^2}\left\{\sin(\lambda_p/2) + \cos(\lambda_p/2)\right\}$$

Suppose $\lambda_p < 0$

$$G_s(\lambda_p) \sim \frac{4/\sqrt{\pi}}{|\lambda_p|}\left\{\left(1+\frac{1}{|\lambda_p|}\right)\left[\sin\left(|\lambda_p|/2\right) - \frac{1}{|\lambda_p|}\cos\left(|\lambda_p|/2\right)\right]\right.$$

$$\left.+\left(1-\frac{1}{|\lambda_p|}\right)\left[\cos\left(|\lambda_p|/2\right) + \frac{1}{|\lambda_p|}\sin\left(|\lambda_p|/2\right)\right]\right\}$$

$$+\frac{2}{\sqrt{|\lambda_p|}}\left\{\frac{2}{|\lambda_p|}\right\} - \frac{4}{|\lambda_p|\sqrt{\pi}}\left\{\sin\left(|\lambda_p|/2\right) + \cos\left(|\lambda_p|/2\right)\right\}$$

$$\sim \frac{4}{|\lambda_p|\sqrt{|\lambda_p|}} + \frac{8/\sqrt{\pi}}{|\lambda_p|^2}\left\{\sin\left(|\lambda_p|/2\right) - \cos\left(|\lambda_p|/2\right)\right\}$$

where

$$|\lambda_p|/2 = 2\,|k-k_p|\,\ell = 2\,|k\ell - \pi\,(p-1/2)|$$

### A.3.1 contributions to summation of p components

Here we list some results involved in the summation of the random plane wave projections. Note that the increments in $p$ result in oscillating signs in the preceding trigonometric functions and thus the summation of these terms is small. Therefore, dealing only with the leading terms, we can write

$$-\frac{2}{A}\sum_{p=P}^{\infty} G_s\left(\lambda_p\right) \sim -\frac{8}{A}\int_{k_P}^{\infty} \frac{dk_p}{|\lambda_p|^{3/2}}\frac{dp}{dk_p} \sim -\frac{8\ell}{A\pi}\int_{k_P}^{\infty}\frac{dk_p}{|\lambda_p|^{3/2}} = -\frac{2}{A\pi}\int_{-\lambda_P}^{\infty}\frac{d\lambda_p}{|\lambda_p|^{3/2}} = -\frac{2}{A}\frac{2/\pi}{\sqrt{|\lambda_P|}}$$

Note that

$$\int_0^{\infty} G_s\left(\lambda_p\right) dp = \frac{\ell}{\pi}\int_0^{\infty} G_s\left(\lambda_p\right) dk_p = \frac{1}{4\pi}\int_{-\infty}^{0} G_s\left(\lambda_p\right) d\lambda_p$$

$$\int_{-R}^{0} G_s\left(\lambda_p\right) d\lambda_p = 4\sqrt{\frac{2}{\pi}}\int_0^1 \left(1-u^2\right)\int_{-R}^{0}\cos\left(\lambda_p u^2/2 - \pi/4\right) d\lambda_p du$$

$$= 8\sqrt{\frac{2}{\pi}}\int_0^1 \left(1/u^2-1\right)\left[\sin\left(Ru^2/2+\pi/4\right) - \sin\left(\pi/4\right)\right] du$$

$$= \frac{8}{\sqrt{\pi}}\int_0^1 \left(1/u^2-1\right)\left[\left\{\cos\left(Ru^2/2\right)-1\right\} + \sin\left(Ru^2/2\right)\right] du$$

$$= -\frac{8}{\sqrt{\pi}}\left[\left\{\cos\left(R/2\right)-1\right\} + \sin\left(R/2\right)\right] + \frac{8}{\sqrt{\pi}}R\int_0^1\left[-\sin\left(Ru^2/2\right) + \cos\left(Ru^2/2\right)\right] du$$

$$-\frac{8}{\sqrt{\pi}}\int_0^1\left[\cos\left(Ru^2/2\right) - 1 + \sin\left(Ru^2/2\right)\right] du$$

$$= -\frac{8}{\sqrt{\pi}}\left[\left\{\cos\left(R/2\right)-2\right\} + \sin\left(R/2\right)\right] - \frac{8}{\sqrt{R}}\left(R+1\right)\int_0^{\sqrt{R/\pi}}\sin\left(\pi u^2/2\right) du + \frac{8}{\sqrt{R}}\left(R-1\right)\int_0^{\sqrt{R/\pi}}\cos\left(\pi u^2/2\right) du$$

$$= -\frac{8}{\sqrt{\pi}}\left[\left\{\cos\left(R/2\right)-2\right\} + \sin\left(R/2\right)\right] - \frac{8}{\sqrt{R}}\left(R+1\right)S\left(\sqrt{R/\pi}\right) + \frac{8}{\sqrt{R}}\left(R-1\right)C\left(\sqrt{R/\pi}\right)$$

$$\sim \frac{16}{\sqrt{\pi}} - \frac{8}{\sqrt{\pi}}\left[\cos\left(R/2\right) + \sin\left(R/2\right)\right]$$

$$\int_{-\infty}^{0} G_s\left(\lambda_p\right) d\lambda_p = \frac{16}{\sqrt{\pi}} \approx 9.027 \text{ (checked with integration)}$$

$$\int_{0}^{\infty} G_s\left(\lambda_p\right) dp = \frac{4}{\pi\sqrt{\pi}} \approx 0.718$$

$$\frac{2}{A}\int_{0}^{\infty} G_s\left(\lambda_p\right) dp = \frac{8}{\pi A\sqrt{\pi}} \approx 0.307$$

$$G_s\left(0\right) = \frac{8}{3\sqrt{\pi}} \approx 1.5045$$

$$\frac{2}{A}G_s\left(0\right) = \frac{16}{3A\sqrt{\pi}} \approx 0.64335$$

$$\frac{2}{A}G_1\left(\lambda_{1p}, \Lambda\right) \approx 2.6$$

Now it is better to only compute the remainder. Thus

$$\int_{-\infty}^{\Lambda_p} G_s\left(\lambda_p\right) d\lambda_p \sim 4\int_{-\infty}^{\Lambda_p} \frac{d\lambda_p}{\left|\lambda_p\right|^{3/2}} = 4\int_{-\Lambda_p}^{\infty} \frac{d\lambda_p}{\lambda_p^{3/2}} = 8/\sqrt{-\Lambda_p}$$

If we consider the case where $\lambda_p = 0$ we see that $\lambda_{p+1} = -4\pi$. We might take $\Lambda_p = -2\pi$ as an approximation to the summation. This then yields

$$\int_{-\infty}^{-\Lambda_p} G_s\left(\lambda_p\right) d\lambda_p \sim 8/\sqrt{2\pi}$$

and

$$\int_{P}^{\infty} G_s\left(\lambda_p\right) dp \sim \frac{1}{\pi\sqrt{\pi/2}} \approx 0.254$$

$$\frac{2}{A}\int_{P}^{\infty} G_s\left(\lambda_p\right) dp \sim \frac{2}{\pi A\sqrt{\pi/2}} \approx 0.1086$$

Actually the summation is

$$\sum_{p=1}^{\infty} G_s\left(\lambda_p\right) \sim \sum_{p=1}^{\infty} \frac{4}{\left(4\pi p\right)^{3/2}} = \frac{1}{2\pi^{3/2}}\sum_{p=1}^{\infty} \frac{1}{p^{3/2}} = \frac{\zeta\left(3/2\right)}{2\pi^{3/2}} \approx \frac{1}{2\pi^{3/2}}\left[\sum_{p=1}^{P} \frac{1}{p^{3/2}} + \int_{P+1/2}^{\infty} \frac{dp}{p^{3/2}}\right]$$

$$\approx \frac{1}{2\pi^{3/2}}\left[\sum_{p=1}^{P} \frac{1}{p^{3/2}} + 2/\sqrt{P+1/2}\right] \approx \frac{2.6124}{2\pi^{3/2}} \approx 0.2346$$

$$\frac{2}{A}\sum_{p=1}^{\infty} \frac{4}{\left(4\pi p\right)^{3/2}} = \frac{\zeta\left(3/2\right)}{A\pi^{3/2}} \approx 0.1003$$

At the lower end of the summation how many terms of $G_s\left(\lambda_p\right)$ are required?

$$\frac{2}{A}\sum_{p=-P}^{-1} G_s\left(\lambda_p\right) \sim \frac{2}{A}\sum_{p=1}^{P}\frac{4}{\sqrt{4\pi p}} = \frac{4}{A\sqrt{\pi}}\sum_{p=1}^{P}\frac{1}{\sqrt{p}}$$

The coefficient is 0.4825. Thus with $P = 3$ this sum is 1.102. With 2 as the starting value we need $P = 5$ to get 1.0768.

## A.4 Ray Reflection and Stability

In two dimensions let us take a ray to be directed by the two dimensional velocity vector

$$\underline{v} = v_x\underline{e}_x + v_y\underline{e}_y = \begin{pmatrix} v_x \\ v_y \end{pmatrix}$$

The position along the ray is taken as

$$\underline{s} = s_x\underline{e}_x + s_y\underline{e}_y = \begin{pmatrix} s_x \\ s_y \end{pmatrix}$$

The inward normal from a boundary is taken as

$$\underline{n} = n_x\underline{e}_x + n_y\underline{e}_y = \begin{pmatrix} n_x \\ n_y \end{pmatrix}$$

A reflection from a boundary takes the form

$$\underline{v}_r = \underline{v}_i - 2\left(\underline{n}\cdot\underline{v}_i\right)\underline{n}$$

This can be written as the dyadic operation

$$\underline{v}_r = \left(\underline{u} - 2\underline{nn}\right)\cdot\underline{v}_i$$

where $\underline{u} = \underline{e}_x\underline{e}_x + \underline{e}_y\underline{e}_y$ is the unit dyadic. The position between the $n$th and $(n+1)$th reflections is

$$\underline{s} = \underline{s}_n + \underline{v}_n t$$

where $t$ is the time.

Suppose we have a periodic trajectory around the cavity. Then we can say

$$\underline{s} = \underline{s} + \sum_{n=1}^{N}\underline{\Delta s}_n = \underline{s} + \sum_{n=1}^{N}\underline{v}_n\Delta t_n$$

where $\underline{s}$ is any point on the trajectory and where $\underline{\Delta s}_n$ are the straight sides of the orbit. Thus we have

$$\sum_{n=1}^{N}\underline{\Delta s}_n = \sum_{n=1}^{N}\underline{v}_n\Delta t_n = 0$$

Now let us consider an orbit, say along the $y$ axis, between $0 < y < L$ and near $x = 0$. Let us choose the origin at the reflection point of the closed orbit on one boundary $y = 0$ near the origin of the $x$ axis. Points on the orbit at the lower reflection point (with convex mirror) are taken as

$$y = \sqrt{a^2 - x^2} - a = a\left(\cos\theta - 1\right)\ ,\ x = a\sin\theta$$

Then we have normal direction to the mirror

$$\underline{n} = \sin\theta \underline{e}_x + \cos\theta \underline{e}_y = (x/a)\,\underline{e}_x + \sqrt{1 - (x/a)^2}\underline{e}_y$$

Consider near the axis a reflection between walls that are actually parabolic in profile rather than circular (but with the proper radius of curvature $R = a$)

$$y = -x^2/\left(2R\right)$$

$$\underline{n} = (x/R)\,\underline{e}_x + \left\{1 - \frac{1}{2}\left(x/R\right)^2\right\}\underline{e}_y$$

which are the approximation of the preceding equations for small $x$. The side length is

$$\underline{\Delta s}_n = L\underline{e}_y$$

Let us start near the middle of the orbit and take a small perturbation from the center of the orbit $\delta$

$$\underline{s}_0 = \delta\underline{e}_x + \underline{e}_y L/2$$

with velocity $(v = 1)$

$$\underline{v}_0 = \varepsilon\underline{e}_x - \sqrt{1 - \varepsilon^2}\underline{e}_y \sim \varepsilon\underline{e}_x - \left(1 - \varepsilon^2/2\right)\underline{e}_y$$

The position of impact on the bottom mirror is found from the simultaneous solution of

$$\underline{s}_1 = \underline{s}_0 + \underline{v}_0 t = \delta\underline{e}_x + \underline{e}_y L/2 + \left\{\varepsilon\underline{e}_x - \left(1 - \varepsilon^2/2\right)\underline{e}_y\right\}\left(t_0 + \tau\right)$$

$$\sim \delta\underline{e}_x + \left(L/2 + \tau\right)\varepsilon\underline{e}_x + \left(\varepsilon^2 L/4 - \tau\right)\underline{e}_y$$

where $t_0 = \left(L/2\right)/v = L/2$ and $\tau$ is small

$$x = \delta + \varepsilon\left(L/2 + \tau\right)$$

$$y = \varepsilon^2 L/4 - \tau$$

(eliminating the parameter $\tau$)

$$x = \delta + \varepsilon\left(L/2 + \varepsilon^2 L/4 - y\right) \sim \delta + \varepsilon\left(L/2 - y\right)$$

and the mirror position

$$y = -x^2/\left(2R\right)$$

or as expected

$$x \sim \delta + \varepsilon L/2$$

and

$$y = -\left(\delta + \varepsilon L/2\right)^2 / \left(2R\right)$$

$$\tau = \varepsilon^2 L/4 + \left(\delta + \varepsilon L/2\right)^2 / \left(2R\right)$$

Hitting the bottom mirror we have

$$\underline{n} = \left(\left(\delta + \varepsilon L/2\right)/R\right)\underline{e}_x + \left\{1 - \frac{1}{2}\left(\left(\delta + \varepsilon L/2\right)/R\right)^2\right\}\underline{e}_y$$

and

$$\underline{v}_1 = \left(\underline{u} - 2\underline{nn}\right)\cdot \underline{v}_0 \sim \varepsilon \underline{e}_x - \left(1 - \varepsilon^2/2\right)\underline{e}_y$$

$$-2\left[\left(\left(\delta + \varepsilon L/2\right)/R\right)\underline{e}_x + \left\{1 - \frac{1}{2}\left(\left(\delta + \varepsilon L/2\right)/R\right)^2\right\}\underline{e}_y\right]\left[\left(\varepsilon\delta + \varepsilon^2 L/2\right)/R - \left\{1 - \varepsilon^2/2 - \frac{1}{2}\left(\left(\delta + \varepsilon L/2\right)/R\right)^2\right\}\right]$$

$$\sim \varepsilon \underline{e}_x - \left(1 - \varepsilon^2/2\right)\underline{e}_y$$

$$+2\left[\left(\left(\delta + \varepsilon L/2\right)/R\right)\underline{e}_x + \left\{1 - \frac{1}{2}\left(\left(\delta + \varepsilon L/2\right)/R\right)^2\right\}\underline{e}_y\right]\left[1 - \varepsilon^2/2 - \frac{1}{2}\left(\left(\delta + \varepsilon L/2\right)/R\right)^2 - \left(\varepsilon\delta + \varepsilon^2 L/2\right)/R\right]$$

$$\sim \left[\varepsilon + 2\left(\delta + \varepsilon L/2\right)/R\right]\underline{e}_x + \left[1 - \varepsilon^2/2 - 2\left(\left(\delta + \varepsilon L/2\right)/R\right)^2 - 2\varepsilon\left(\delta + \varepsilon L/2\right)/R\right]$$

and thus

$$v_{1x} \sim \varepsilon + 2\left(\delta + \varepsilon L/2\right)/R$$

$$v_{1y} \sim 1 - \varepsilon^2/2 - 2\left(\left(\delta + \varepsilon L/2\right)/R\right)^2 - 2\varepsilon\left(\delta + \varepsilon L/2\right)/R$$

Thus back up at the middle at time $t_1 - t_0 - \tau \sim L/2 + \tau_1 = L/2 + \tau_1$

$$s_{1x} \sim \delta + \varepsilon L/2 + v_{1x}\left(L/2 + \tau_1\right) \sim \delta + \varepsilon L/2 + \left\{\varepsilon + 2\left(\delta + \varepsilon L/2\right)/R\right\}\left(L/2 + \tau_1\right)$$

$$s_{1y} \sim -\left(\delta + \varepsilon L/2\right)^2 / \left(2R\right) + v_{1y}\left(L/2 + \tau_1\right)$$

$$\sim L/2 - \left(\delta + \varepsilon L/2\right)^2 / \left(2R\right) + \left\{\tau_1 - \varepsilon^2/2 - 2\left(\left(\delta + \varepsilon L/2\right)/R\right)^2 - 2\varepsilon\left(\delta + \varepsilon L/2\right)/R\right\} L/2$$

Let us determine $\tau_1$ to make $s_{1y} = L/2$, the center

$$\left(\delta+\varepsilon L/2\right)^2/\left(2R\right)+\left\{\varepsilon^2/2+2\left(\left(\delta+\varepsilon L/2\right)/R\right)^2+2\varepsilon\left(\delta+\varepsilon L/2\right)/R\right\}L/2=\tau_1 L/2$$

Thus $\tau_1$ is a quadratic quantity. Then we find

$$v_{1x}\sim\varepsilon+2\left(\delta+\varepsilon L/2\right)/R$$

$$s_{1x}\sim\delta+\varepsilon L/2+v_{1x}L/2$$

or

$$v_{1x}\sim\left(2/R\right)s_{0x}+\left(1+L/R\right)v_{0x}$$

$$s_{1x}\sim\left(1+L/R\right)s_{0x}+L\left(1+L/\left(2R\right)\right)v_{0x}$$

In matrix form we can write the transformation over half the orbit as

$$A_{n+1}=CA_n$$

where the row vector of displacement and velocity is

$$A_n=\begin{pmatrix}v_{nx}\\s_{nx}\end{pmatrix}$$

and where the transformation matrix is

$$C=\begin{pmatrix}1+L/R & 2/R\\ L\left(1+L/\left(2R\right)\right) & 1+L/R\end{pmatrix}$$

Then over the full orbit we have a transformation matrix

$$C^2=\begin{pmatrix}1+L/R & 2/R\\ L\left(1+L/\left(2R\right)\right) & 1+L/R\end{pmatrix}\begin{pmatrix}1+L/R & 2/R\\ L\left(1+L/\left(2R\right)\right) & 1+L/R\end{pmatrix}$$

$$=\begin{pmatrix}2\left(1+L/R\right)^2-1 & 2\left(1+L/R\right)\left(2/R\right)\\ 2\left(1+L/R\right)\left\{\left(1+L/R\right)^2-1\right\}\left(R/2\right) & 2\left(1+L/R\right)^2-1\end{pmatrix}$$

The eigenvalues are found from

$$\det\left(C-\lambda I\right)=\left(1+L/R-\lambda\right)^2-\left(L/R\right)\left(2+L/R\right)=0$$

$$\lambda^2-\lambda 2\left(1+L/R\right)+1=0$$

or

$$\lambda_{\pm}=1+L/R\pm\sqrt{\left(1+L/R\right)^2-1}$$

The eigenvalues of $C^2$ are then the stability exponents

$$\Lambda_{\pm} = \lambda_{\pm}^2 = \left[2\left(L/R\right)\left(2 + L/R\right) + 1 \pm 2\left(1 + L/R\right)\sqrt{\left(L/R\right)\left(2 + L/R\right)}\right]$$

Note that

$$1 = \lambda_+ \lambda_- = \Lambda_+ \Lambda_-$$

## A.5 Higher Order Bow Tie Cavity

Starting from the exact form of the Helmholtz equation with the substitution

$$u = W\left(\xi, \zeta\right) e^{i\gamma \sin \xi} + W\left(-\xi, \zeta\right) e^{-i\gamma \sin \xi}$$

gives

$$\frac{\partial^2 W}{\partial \xi^2} + \frac{\partial^2 W}{\partial \zeta^2} + 2i\gamma \cos \xi \frac{\partial W}{\partial \xi} + \left(\gamma^2 \sinh^2 \zeta - i\gamma \sin \xi\right) W = 0$$

and using $\sinh^2 \zeta \approx \zeta^2 + \zeta^4/3$, we have

$$\frac{\partial^2 W}{\partial \xi^2} + \frac{\partial^2 W}{\partial \zeta^2} + 2i\gamma \cos \xi \frac{\partial W}{\partial \xi} + \left(\gamma^2 \zeta^2 + \gamma^2 \zeta^4/3 - i\gamma \sin \xi\right) W \approx 0$$

Transforming to the variable

$$\tau = \sqrt{2\gamma}\zeta$$

gives

$$\frac{\partial^2 W}{\partial \xi^2} + 2\gamma \frac{\partial^2 W}{\partial \tau^2} + 2i\gamma \cos \xi \frac{\partial W}{\partial \xi} + \left(\frac{1}{2}\gamma \tau^2 + \frac{1}{4}\tau^4/3 - i\gamma \sin \xi\right) W \approx 0$$

Letting

$$W = \frac{1}{\sqrt{\cos \xi}} \Psi$$

gives

$$\frac{\partial^2 \Psi}{\partial \tau^2} + i \cos \xi \frac{\partial \Psi}{\partial \xi} + \frac{1}{4}\tau^2 \Psi \approx -\frac{1}{2\gamma}\left[\frac{\partial^2 \Psi}{\partial \xi^2} + \tan \xi \frac{\partial \Psi}{\partial \xi} + \frac{1}{2}\left(1 + \frac{3}{2}\tan^2 \xi\right)\Psi + \frac{1}{12}\tau^4 \Psi\right]$$

Now taking the expansion in the large parameter $\gamma$

$$\Psi = \sum_{n=0}^{\infty} \left(2\gamma\right)^{-n} \Psi_n$$

gives

$$\frac{\partial^2 \Psi_0}{\partial \tau^2} + i \cos \xi \frac{\partial \Psi_0}{\partial \xi} + \frac{1}{4}\tau^2 \Psi_0 \approx 0$$

and

$$\frac{\partial^2\Psi_1}{\partial\tau^2}+i\cos\xi\frac{\partial\Psi_1}{\partial\xi}+\frac{1}{4}\tau^2\Psi_1\approx-\left[\frac{\partial^2\Psi_0}{\partial\xi^2}+\tan\xi\frac{\partial\Psi_0}{\partial\xi}+\frac{1}{2}\left(1+\frac{3}{2}\tan^2\xi\right)\Psi_0+\frac{1}{12}\tau^4\Psi_0\right]$$

Next taking

$$\frac{\partial\sigma}{\partial\xi}=\sec\xi$$

or

$$\sigma=\int_0^\xi\frac{d\xi}{\cos\xi}=\operatorname{arcsinh}\left(\tan\xi\right)$$

yields

$$\frac{\partial^2\Psi_0}{\partial\tau^2}+i\frac{\partial\Psi_0}{\partial\sigma}+\frac{1}{4}\tau^2\Psi_0\approx0$$

With

$$\sinh\sigma=\tan\xi$$

$$\cosh\sigma=\sec\xi$$

we also find

$$\frac{\partial^2\Psi_1}{\partial\tau^2}+i\frac{\partial\Psi_1}{\partial\sigma}+\frac{1}{4}\tau^2\Psi_1\approx-\left[\cosh^2\sigma\frac{\partial^2\Psi_0}{\partial\sigma^2}+2\sinh\sigma\cosh\sigma\frac{\partial\Psi_0}{\partial\sigma}+\frac{1}{2}\left(1+\frac{3}{2}\sinh^2\sigma\right)\Psi_0+\frac{1}{12}\tau^4\Psi_0\right]$$

Letting

$$\Psi_0\left(\sigma,\tau\right)=e^{-is\sigma}\psi_0\left(s,\tau\right)$$

gives

$$\frac{\partial^2\psi_0}{\partial\tau^2}+\left(\frac{\tau^2}{4}+s\right)\psi_0=0$$

Then

$$\frac{\partial^2\Psi_1}{\partial\tau^2}+i\frac{\partial\Psi_1}{\partial\sigma}+\frac{1}{4}\tau^2\Psi_1\approx$$

$$-\left[-\frac{1}{4}s^2\psi_0\left(e^{2\sigma}+2+e^{-2\sigma}\right)-is\frac{1}{2}\psi_0\left(e^{2\sigma}-e^{-2\sigma}\right)+\left(\frac{1}{8}+\frac{3}{16}e^{2\sigma}+\frac{3}{16}e^{-2\sigma}\right)\psi_0+\frac{1}{12}\tau^4\psi_0\right]e^{-is\sigma}$$

Thus we take

$$\Psi_1=\psi_{1,0}e^{-is\sigma}+\psi_{1,1}e^{-is\sigma}+\psi_{1,2}e^{(2-is)\sigma}+\psi_{1,-2}e^{-(2+is)\sigma}$$

$$= \psi_1 e^{-is\sigma} + \psi_{1,2} e^{(2-is)\sigma} + \psi_{1,-2} e^{-(2+is)\sigma}$$

where

$$\frac{\partial^2 \psi_{1,0}}{\partial \tau^2} + \left(\frac{\tau^2}{4} + s\right) \psi_{1,0} = -\frac{1}{2}\left(-s^2 + \frac{1}{4}\right) \psi_0(s,\tau)$$

$$\frac{\partial^2 \psi_{1,1}}{\partial \tau^2} + \left(\frac{\tau^2}{4} + s\right) \psi_{1,1} = -\frac{1}{12}\tau^4 \psi_0(s,\tau)$$

$$\frac{\partial^2 \psi_{1,2}}{\partial \tau^2} + \left(\frac{\tau^2}{4} + i2 + s\right) \psi_{1,2} = -\frac{1}{2}\left(-\frac{1}{2}s^2 - is + \frac{3}{8}\right) \psi_0(s,\tau)$$

$$\frac{\partial^2 \psi_{1,-2}}{\partial \tau^2} + \left(\frac{\tau^2}{4} - i2 + s\right) \psi_{1,-2} = -\frac{1}{2}\left(-\frac{1}{2}s^2 + is + \frac{3}{8}\right) \psi_0(s,\tau)$$

These are forms of the equation of the parabolic cylinder functions. Notice that if we set

$$\psi_{1,\pm 2} = \pm\frac{i}{4}\left(-\frac{1}{2}s^2 \mp is + \frac{3}{8}\right) \psi_0(s,\tau) = \left[\frac{s}{4} \pm \frac{i}{4}\left(-\frac{1}{2}s^2 + \frac{3}{8}\right)\right] \psi_0(s,\tau)$$

$$\psi^*_{1,+2} = \psi_{1,-2}$$

$$\frac{d\psi_{1,\pm 2}}{d\tau}(0) = 0$$

$$\psi_{1,2} e^{(2-is)\sigma} + \psi_{1,-2} e^{-(2+is)\sigma} = \left[\psi_{1,2} e^{2\sigma} + \psi_{1,-2} e^{-2\sigma}\right] e^{-is\sigma} = \left[\psi_{1,2} e^{2\sigma} + \psi^*_{1,2} e^{-2\sigma}\right] e^{-is\sigma}$$

$$= 2\left[\mathrm{Re}\left(\psi_{1,2}\right)\cosh(2\sigma) + i\,\mathrm{Im}\left(\psi_{1,2}\right)\sinh(2\sigma)\right] e^{-is\sigma}$$

The solution that is outgoing in $\tau$ is [30]

$$U_+(s,\tau) = e^{-\pi(s+i/2)/4} U\left(-is, \tau e^{-i\pi/4}\right)$$

$$\psi_0(s,\tau) = c_0\,\mathrm{Re}\left[U_+(s,\tau) + e^{i\Phi_0} U^*_+(s,\tau)\right]$$

$$= \frac{1}{2} c_0 \left[\left(1 + e^{-i\Phi_0}\right) U_+(s,\tau) + \left(1 + e^{i\Phi_0}\right) U^*_+(s,\tau)\right]$$

Thus since we must solve these equations for right hand sides which consist of the function plus its conjugate we can write

$$\psi_{1,2} = \psi^{(1)}_{1,2} + \psi^{(2)}_{1,2}$$

$$\frac{\partial^2 \psi_{1,2}^{(1)}}{\partial \tau^2} + \left(\frac{\tau^2}{4} + i2 + s\right)\psi_{1,2}^{(1)} = -\frac{1}{2}\left(-\frac{1}{2}s^2 - is + \frac{3}{8}\right)cU_+$$

$$\frac{\partial^2 \psi_{1,2}^{(2)}}{\partial \tau^2} + \left(\frac{\tau^2}{4} + i2 + s\right)\psi_{1,2}^{(2)} = -\frac{1}{2}\left(-\frac{1}{2}s^2 - is + \frac{3}{8}\right)c^*U_+^*$$

$$\psi_{1,-2} = \psi_{1,-2}^{(1)} + \psi_{1,-2}^{(2)}$$

$$\frac{\partial^2 \psi_{1,-2}^{(1)}}{\partial \tau^2} + \left(\frac{\tau^2}{4} - i2 + s\right)\psi_{1,-2}^{(1)} = -\frac{1}{2}\left(-\frac{1}{2}s^2 + is + \frac{3}{8}\right)cU_+$$

$$\frac{\partial^2 \psi_{1,-2}^{(2)}}{\partial \tau^2} + \left(\frac{\tau^2}{4} - i2 + s\right)\psi_{1,-2}^{(2)} = -\frac{1}{2}\left(-\frac{1}{2}s^2 + is + \frac{3}{8}\right)c^*U_+^*$$

We thus see by comparison that

$$\psi_{1,2}^{(1)} = \psi_{1,-2}^{(2)*}$$

$$\psi_{1,2}^{(2)} = \psi_{1,-2}^{(1)*}$$

Therefore

$$\psi_{1,2}e^{(2-is)\sigma} + \psi_{1,-2}e^{-(2+is)\sigma} = \left(\psi_{1,2}^{(1)} + \psi_{1,2}^{(2)}\right)e^{(2-is)\sigma} + \left(\psi_{1,2}^{(2)*} + \psi_{1,2}^{(1)*}\right)e^{-(2+is)\sigma} = \psi_{1,2}e^{(2-is)\sigma} + \psi_{1,2}^*e^{-(2+is)\sigma}$$

and

$$\left(\psi_{1,2}e^{(2-is)\sigma} + \psi_{1,-2}e^{-(2+is)\sigma}\right)e^{i\gamma\sin\xi} + \left(\psi_{1,2}e^{-(2-is)\sigma} + \psi_{1,-2}e^{(2+is)\sigma}\right)e^{-i\gamma\sin\xi}$$

$$= \left(\psi_{1,2}e^{2\sigma} + \psi_{1,2}^*e^{-2\sigma}\right)e^{i\gamma\sin\xi - is\sigma} + \left(\psi_{1,2}e^{-2\sigma} + \psi_{1,2}^*e^{2\sigma}\right)e^{-i\gamma\sin\xi + is\sigma}$$

$$= \mathrm{Re}\left\{\psi_{1,2}\right\}\left(e^{2\sigma} + e^{-2\sigma}\right)\left(e^{i\gamma\sin\xi - is\sigma} + e^{-i\gamma\sin\xi + is\sigma}\right) + i\,\mathrm{Im}\left\{\psi_{1,2}\right\}\left(e^{2\sigma} - e^{-2\sigma}\right)\left(e^{i\gamma\sin\xi - is\sigma} - e^{-i\gamma\sin\xi + is\sigma}\right)$$

$$= 4\,\mathrm{Re}\left\{\psi_{1,2}\right\}\cosh(2\sigma)\cos(\gamma\sin\xi - s\sigma) - 4\,\mathrm{Im}\left\{\psi_{1,2}\right\}\sinh(2\sigma)\sin(\gamma\sin\xi - s\sigma)$$

$$= s\psi_0(s,\tau)\cosh(2\sigma)\cos(\gamma\sin\xi - s\sigma) + \frac{1}{2}\left(s^2 - \frac{3}{4}\right)\psi_0(s,\tau)\sinh(2\sigma)\sin(\gamma\sin\xi - s\sigma)$$

Note that these obey the evenness condition. There are also homogeneous solutions to these equations, but these in general do not satisfy the evenness condition at the same value of $s$.

Note that

$$\left[\frac{\partial^2}{\partial\tau^2}+\left(\frac{\tau^2}{4}+s\right)\right]\frac{\partial U_+}{\partial s}=-U_+$$

can be used to easily solve for that part of $\psi_1$ except the $\tau^4$ term on the right hand side

$$\frac{\partial^2\psi_{1,0}}{\partial\tau^2}+\left(\frac{\tau^2}{4}+s\right)\psi_{1,0}=-\frac{1}{2}\left(-s^2+\frac{1}{4}\right)\psi_0\left(s,\tau\right)$$

$$\psi_{1,0}=\frac{1}{2}\left(-s^2+\frac{1}{4}\right)\frac{\partial}{\partial s}\psi_0\left(s,\tau\right)$$

or we can also take (because $\psi_0$ satisfies the homogeneous operator)

$$\psi_{1,0}=\frac{1}{2}\frac{\partial}{\partial s}\left(-s^2+\frac{1}{4}\right)\psi_0\left(s,\tau\right)$$

The method of variation of parameters can be used to solve the remaining equation for the $\tau^4$ term

$$\frac{\partial^2\psi_{1,1}}{\partial\tau^2}+\left(\frac{\tau^2}{4}+s\right)\psi_{1,1}=-\frac{1}{12}\tau^4\psi_0$$

But we can also guess the form

$$\left[\frac{\partial^2}{\partial\tau^2}+\left(\frac{\tau^2}{4}+s\right)\right]\psi_0=0$$

$$\frac{d}{d\tau}\left[\frac{\partial^2}{\partial\tau^2}+\left(\frac{\tau^2}{4}+s\right)\right]\psi_0=\left[\frac{\partial^2}{\partial\tau^2}+\left(\frac{\tau^2}{4}+s\right)\right]\frac{d\psi_0}{d\tau}+\frac{1}{2}\tau\psi_0=0$$

$$\frac{d^2}{d\tau^2}\left[\frac{\partial^2}{\partial\tau^2}+\left(\frac{\tau^2}{4}+s\right)\right]\psi_0=\left[\frac{\partial^2}{\partial\tau^2}+\left(\frac{\tau^2}{4}+s\right)\right]\frac{d^2\psi_0}{d\tau^2}+\tau\frac{d\psi_0}{d\tau}+\frac{1}{2}\psi_0=0$$

$$\psi_{1,1}=\tau^n\frac{d\psi_0}{d\tau}$$

$$\frac{\partial^2\psi_{1,1}}{\partial\tau^2}+\left(\frac{\tau^2}{4}+s\right)\psi_{1,1}=\left[\frac{\partial^2}{\partial\tau^2}+\left(\frac{\tau^2}{4}+s\right)\right]\left(\tau^n\frac{d\psi_0}{d\tau}\right)=-\tau^{n+1}\frac{1}{2}\psi_0+\left(n\left(n-1\right)\tau^{n-2}\frac{d\psi_0}{d\tau}+2n\tau^{n-1}\frac{d^2\psi_0}{d\tau^2}\right)$$

If we take $n=3$

$$\psi_{1,1}=\tau^3\frac{d\psi_0}{d\tau}+A\tau\frac{d\psi_0}{d\tau}+B\tau^2\psi_0+C\frac{\partial\psi_0}{\partial s}$$

$$\frac{\partial^2\psi_{1,1}}{\partial\tau^2}+\left(\frac{\tau^2}{4}+s\right)\psi_{1,1}=6\tau\frac{d\psi_0}{d\tau}-\tau^2\left(2\tau^2+6s\right)\psi_0-A\left(\tau^2+2s\right)\psi_0+B\left(2\psi_0+4\tau\frac{d\psi_0}{d\tau}\right)-C\psi_0$$

Setting $A=-6s$, $B=-3/2$, and $C=12s^2-3$

$$24\psi_{1,1} = \tau\left(\tau^2 - 6s\right)\frac{d\psi_0}{d\tau} - \frac{3}{2}\tau^2\psi_0 + 3\left(4s^2 - 1\right)\frac{\partial\psi_0}{\partial s}$$

$$\frac{\partial^2\psi_{1,1}}{\partial\tau^2} + \left(\frac{\tau^2}{4} + s\right)\psi_{1,1} = -\frac{1}{12}\tau^4\psi_0$$

Note that

$$\psi_1 = \psi_{1,0} + \psi_{1,1} = \frac{\tau}{4}\left(\frac{\tau^2}{6} - s\right)\frac{d\psi_0}{d\tau} - \frac{1}{16}\tau^2\psi_0$$

Because

$$\frac{d\psi_1}{d\tau}(0) = -\frac{s}{4}\frac{d\psi_0}{d\tau}(0) = 0$$

we see that this correction already satisfies the evenness condition. Indeed all the preceding terms satisfy the evenness condition.

### A.5.1 boundary conditions

Now let us examine the boundary conditions for this higher order solution. First it must vanish at the wall. We assemble the solution as

$$u = W(\xi,\zeta)\,e^{i\gamma\sin\xi} + W(-\xi,\zeta)\,e^{-i\gamma\sin\xi}$$

$$= \frac{1}{\sqrt{\cos\xi}}\left[\Psi(\xi,\zeta)\,e^{i\gamma\sin\xi} + \Psi(-\xi,\zeta)\,e^{-i\gamma\sin\xi}\right]$$

$$\sim \frac{1}{\sqrt{\cos\xi}}\left[\Psi_0(\xi,\zeta)\,e^{i\gamma\sin\xi} + \Psi_0(-\xi,\zeta)\,e^{-i\gamma\sin\xi}\right] + \frac{1}{2\gamma}\frac{1}{\sqrt{\cos\xi}}\left[\Psi_1(\xi,\zeta)\,e^{i\gamma\sin\xi} + \Psi_1(-\xi,\zeta)\,e^{-i\gamma\sin\xi}\right]$$

$$\sim \frac{2}{\sqrt{\cos\xi}}\cos(\gamma\sin\xi - s\sigma)\left[\psi_0(s,\tau) + \frac{1}{2\gamma}\psi_1(s,\tau)\right]$$

$$+\frac{1}{2\gamma}\frac{1}{\sqrt{\cos\xi}}\left[\left\{\psi_{1,2}e^{2\sigma} + \psi_{1,-2}e^{-2\sigma}\right\}e^{i\gamma\sin\xi - is\sigma} + \left\{\psi_{1,2}e^{-2\sigma} + \psi_{1,-2}e^{2\sigma}\right\}e^{-i\gamma\sin\xi + is\sigma}\right]$$

$$\sim \frac{2}{\sqrt{\cos\xi}}\cos(\gamma\sin\xi - s\sigma)\left[\psi_0(s,\tau) + \frac{1}{2\gamma}\psi_1(s,\tau)\right]$$

$$+\frac{1}{2\gamma}\frac{1}{\sqrt{\cos\xi}}\left[\left(\psi_{1,2}e^{2\sigma} + \psi_{1,2}^*e^{-2\sigma}\right)e^{i\gamma\sin\xi - is\sigma} + \left(\psi_{1,2}e^{-2\sigma} + \psi_{1,2}^*e^{2\sigma}\right)e^{-i\gamma\sin\xi + is\sigma}\right]$$

$$\sim \frac{2}{\sqrt{\cos\xi}}\cos(\gamma\sin\xi - s\sigma)\left[\psi_0(s,\tau) + \frac{1}{2\gamma}\psi_1(s,\tau)\right]$$

$$+\frac{1}{2\gamma}\frac{1}{\sqrt{\cos\xi}}\left[4\,\mathrm{Re}\left\{\psi_{1,2}\left(s,\tau\right)\right\}\cosh\left(2\sigma\right)\cos\left(\gamma\sin\xi-s\sigma\right)-4\,\mathrm{Im}\left\{\psi_{1,2}\left(s,\tau\right)\right\}\sinh\left(2\sigma\right)\sin\left(\gamma\sin\xi-s\sigma\right)\right]$$

$$\sim\frac{2}{\sqrt{\cos\xi}}\cos\left(\gamma\sin\xi-s\sigma\right)\left[\psi_0\left(s,\tau\right)+\frac{1}{2\gamma}\left\{\frac{\tau}{4}\left(\frac{\tau^2}{6}-s\right)\frac{d\psi_0}{d\tau}-\frac{1}{16}\tau^2\psi_0\right\}\right]$$

$$+\frac{1}{2\gamma}\frac{1}{\sqrt{\cos\xi}}\left[s\psi_0\left(s,\tau\right)\cosh\left(2\sigma\right)\cos\left(\gamma\sin\xi-s\sigma\right)+\frac{1}{2}\left(s^2-\frac{3}{4}\right)\psi_0\left(s,\tau\right)\sinh\left(2\sigma\right)\sin\left(\gamma\sin\xi-s\sigma\right)\right]$$

The second term $\sin\left(\gamma\sin\xi-s\sigma\right)$ does not obey the wall boundary condition at the same frequency as the cosine part. Now we assume there is a small shift in the value of $k_p$ and $k$, still maintaining the value of $s$ to satisfy the zero normal derivative (evenness) condition at $\tau=0$. This redefinition of $k_p$ allows the $\cos\left(\gamma\sin\xi_0-s\sigma_0\right)$ factor in the zero order solution to be slightly different than zero at the wall, so that it can be made to cancel the term involving $\sin\left(\gamma\sin\xi_0-s\sigma_0\right)$ at the wall. This also means that the first order correction leads to a first order correction in the eigenvalue $k$ to maintain the same value of $s$. The new value of $k$ is found by setting

$$\gamma\cot\left(\gamma\sin\xi_0-s\sigma_0\right)\sim\frac{1}{4}\left(s^2-\frac{3}{4}\right)\sinh\left(\sigma_0\right)\cosh\left(\sigma_0\right)$$

with

$$\sin\xi_0=\tanh\sigma_0$$

$$\sigma_0=\frac{1}{2}\ln\left(\frac{d+\ell}{d-\ell}\right)=\mathrm{Arcsinh}\left(\sqrt{\ell/R}\right)$$

It will be a small perturbation $k\rightarrow k\left[1+O\left(1/\gamma^2\right)\right]$. Note that the definition of the reflection phase $\Phi_0$ must be consistent with the $p$th component of the eigenfunction, now with both zero and first order (etc.) variations included; the construction of $u$ in this section is really $u_p$.

## A.6 Asymptotic Orthogonality In The Bow Tie

Let us consider the orthogonality properties along the scarred orbit if we take the line integral along the orbit

$$\int_C u_p\frac{\partial u_{p'}}{\partial n}d\ell=\int_0^{\xi_0}u_p\frac{1}{h_\zeta}\frac{\partial u_{p'}}{\partial\zeta}h_\xi d\xi=\int_0^{\xi_0}u_p\frac{\partial u_{p'}}{\partial\zeta}d\xi$$

where the metric coefficients in this elliptic cylinder system are

$$h_\zeta=h_\xi=d\sqrt{\sinh^2\zeta+\cos^2\xi}$$

This form is important in the normalization condition where integrals of the form

$$\int_{-\ell}^{\ell}u\frac{\partial^2 u}{\partial\omega\partial n}d\ell$$

arise. We might also have defined the projection operator in this manner

$$\int_{-\ell}^{\ell} u \frac{\partial^2 u_{p'}}{\partial \omega \partial n} d\ell$$

and thus also required

$$\int_{-\ell}^{\ell} \left( u_r - \sum_p c'_{pr} u_p \right) \frac{\partial^2 u_{p'}}{\partial \omega \partial n} d\ell = 0$$

Thus we investigate the orthogonality of the integral

$$\int_0^{\xi_0} u_p \frac{\partial u_{p'}}{\partial \zeta} d\xi =$$

$$\psi\left(s_p, \zeta\sqrt{2kd}\right) \frac{\partial \psi}{\partial \zeta}\left(s_{p'}, \zeta\sqrt{2kd}\right) \int_0^{\xi_0} \cos\left[kd\sin\xi - s_p \mathrm{Arcsinh}\left(\tan\xi\right)\right] \cos\left[kd\sin\xi - s_{p'}\mathrm{Arcsinh}\left(\tan\xi\right)\right] d\xi / \cos\xi$$

$$= \psi\left(s_p, \zeta\sqrt{2kd}\right) \frac{\partial \psi}{\partial \zeta}\left(s_{p'}, \zeta\sqrt{2kd}\right) \int_0^{\mathrm{Arcsinh}(\tan\xi_0)} \cos\left(kd\tanh u - s_p u\right) \cos\left(kd\tanh u - s_{p'} u\right) du$$

$$= \frac{1}{2}\psi\left(s_p, \zeta\sqrt{2kd}\right) \frac{\partial \psi}{\partial \zeta}\left(s_{p'}, \zeta\sqrt{2kd}\right) \int_0^{\mathrm{Arcsinh}\left(\sqrt{\ell/R}\right)} \cos\left[\left(s_p - s_{p'}\right) u\right] du$$

$$+\frac{1}{2}\psi\left(s_p, \zeta\sqrt{2kd}\right) \frac{\partial \psi}{\partial \zeta}\left(s_{p'}, \zeta\sqrt{2kd}\right) \int_0^{\mathrm{Arcsinh}\left(\sqrt{\ell/R}\right)} \cos\left[2kd\tanh u - \left(s_p + s_{p'}\right) u\right] du$$

where

$$u = \mathrm{Arcsinh}\left(\tan\xi\right)$$

$$\tan\xi = \sinh u$$

$$\sec^2\xi = \cosh^2 u$$

$$\cos\xi = \mathrm{sech}\left(u\right)$$

$$\frac{du}{d\xi} = \frac{d}{d\xi}\mathrm{Arcsinh}\left(\tan\xi\right) = \frac{1}{\sqrt{1+\tan^2\xi}}\sec^2\xi = \sec\xi$$

$$\frac{d}{d\xi}\sin\xi = \cos\xi$$

and

$$kd\sin\xi_0 - s_p \text{arcsinh}\left(\tan\xi_0\right) = k\ell - s_p \text{Arcsinh}\left(\sqrt{\ell/R}\right) = \left(p - 1/2\right)\pi = k_p\ell\,,\; p = 1, 2, 3, ...$$

$$\text{arcsinh}\left(\tan\xi_0\right) = \frac{1}{2}\ln\left(\frac{d+\ell}{d-\ell}\right) = \text{Arcsinh}\left(\sqrt{\ell/R}\right) = \ln\left(\sqrt{\ell/R} + \sqrt{1+\ell/R}\right)$$

$$kd\sin\xi_0 = k\ell$$

Noting that

$$\left(s_p - s_{p'}\right)\text{Arcsinh}\left(\sqrt{\ell/R}\right) = \left(p' - p\right)\pi$$

the first integral can be written as

$$\int_0^{\text{Arcsinh}\left(\sqrt{\ell/R}\right)} \cos\left[\left(s_p - s_{p'}\right)u\right]du = \frac{1}{\pi}\text{Arcsinh}\left(\sqrt{\ell/R}\right)\int_0^{\pi}\cos\left[\left(p' - p\right)v\right]dv$$

$$= \delta_{pp'}\,\text{Arcsinh}\left(\sqrt{\ell/R}\right)$$

Noting that

$$\left(s_p + s_{p'}\right)\text{Arcsinh}\left(\sqrt{\ell/R}\right) = 2k\ell - \left(p + p' - 1\right)\pi$$

the second integral can be written as

$$\int_0^{\text{Arcsinh}\left(\sqrt{\ell/R}\right)} \cos\left[2kd\tanh u - \left(s_p + s_{p'}\right)u\right]du$$

$$= \text{Arcsinh}\left(\sqrt{\ell/R}\right)\int_0^1 \cos\left[2kd\tanh\left\{u\text{Arcsinh}\left(\sqrt{\ell/R}\right)\right\} - u2k\ell + \left(p + p' - 1\right)\pi u\right]du$$

Now because of the large values of $kd$ at high frequencies we expect this to be well approximated by the method of stationary phase. Setting the derivative of the cosine argument to zero

$$2kd\text{sech}^2\left\{u\text{Arcsinh}\left(\sqrt{\ell/R}\right)\right\}\text{Arcsinh}\left(\sqrt{\ell/R}\right) - 2k\ell + \left(p + p' - 1\right)\pi = 0$$

$$= 2kd\text{sech}^2\left\{u\text{Arcsinh}\left(\sqrt{\ell/R}\right)\right\}\text{Arcsinh}\left(\sqrt{\ell/R}\right) - 2k\ell + \left(k_p + k_{p'}\right)\ell = 0$$

Taking $k_p$, $k_{p'}$ and $k$ to all be near one another, we see that this equation becomes

$$2kd\text{sech}^2\left\{u\text{Arcsinh}\left(\sqrt{\ell/R}\right)\right\}\text{Arcsinh}\left(\sqrt{\ell/R}\right) \approx 0$$

Because $\text{sech}(z)$ is monotonically decreasing we can write

$$\frac{2kd}{1+\ell/R}\ln\left(\sqrt{\ell/R} + \sqrt{1+\ell/R}\right) < 2kd\text{sech}^2\left\{u\text{Arcsinh}\left(\sqrt{\ell/R}\right)\right\}\text{Arcsinh}\left(\sqrt{\ell/R}\right)$$

$$< 2kd \ln\left(\sqrt{\ell/R} + \sqrt{1+\ell/R}\right)$$

Thus because $kd$ and $k\ell$ are presumed to be large, we do not expect a stationary point to be in $1 > u > 0$. Thus the asymptotic evaluation of this second integral arises from the end points of the interval. However because the argument ranges from 0 to $(p+p'-1)\,\pi$, an integration by parts evaluation [36] leads to a contribution only at the second term, or

$$\int_0^1 \cos\left[2kd\tanh\left\{u\text{Arcsinh}\left(\sqrt{\ell/R}\right)\right\} - u2k\ell + (p+p'-1)\,\pi u\right] du = O\left(\gamma^{-2}\right)$$

Alternatively if we consider the line integral along the orbit

$$\int_C u_p u_{p'} d\ell = \int_0^{\xi_0} u_p u_{p'} h_\xi d\xi = d\int_0^{\xi_0} u_p u_{p'} \sqrt{\sinh^2\zeta + \cos^2\xi} d\xi \sim d\int_0^{\xi_0} u_p u_{p'} \cos\xi d\xi$$

where the final form is near the axis. This form arises in the integral of the square of the eigenfunction

$$\int_{-\ell}^{\ell} u^2 d\ell$$

as well as in the projection operator

$$\int_{-\ell}^{\ell} u\ u_{p'} d\ell$$

and in

$$\int_{-\ell}^{\ell} \left(u_r - \sum_p c'_{pr} u_p\right) u_{p'} d\ell = 0$$

This form amounts to keeping the metric coefficient in the integral so that

$$d\int_0^{\xi_0} u_p u_{p'} \cos\xi d\xi =$$

$$d\psi\left(s_p, \zeta\sqrt{2kd}\right)\psi\left(s_{p'}, \zeta\sqrt{2kd}\right)\int_0^{\xi_0} \cos\left[kd\sin\xi - s_p\text{Arcsinh}\left(\tan\xi\right)\right]\cos\left[kd\sin\xi - s_{p'}\text{Arcsinh}\left(\tan\xi\right)\right] d\xi$$

$$= d\psi\left(s_p, \zeta\sqrt{2kd}\right)\psi\left(s_{p'}, \zeta\sqrt{2kd}\right)\int_0^{\text{Arcsinh}\left(\sqrt{\ell/R}\right)} \cos\left(kd\tanh u - s_p u\right)\cos\left(kd\tanh u - s_{p'} u\right)\text{sech}\left(u\right) du$$

$$= \frac{d}{2}\psi\left(s_p, \zeta\sqrt{2kd}\right)\psi\left(s_{p'}, \zeta\sqrt{2kd}\right)\int_0^{\text{Arcsinh}\left(\sqrt{\ell/R}\right)} \cos\left\{\left(s_p - s_{p'}\right)u\right\}\text{sech}\left(u\right) du$$

$$+\frac{d}{2}\psi\left(s_p, \zeta\sqrt{2kd}\right)\psi\left(s_{p'}, \zeta\sqrt{2kd}\right)\int_0^{\text{Arcsinh}\left(\sqrt{\ell/R}\right)} \cos\left(2kd\tanh u - s_p u - s_{p'} u\right)\text{sech}\left(u\right) du$$

Because, for large radius the upper limit is less than unity, the hyperbolic function $\cosh u$ does not vary much from unity. Thus orthogonality almost holds again to second order.

## A.7 Comparison of Source and Boundary Forms Of Energy Theorem And Normalization

The normalization of the function, or the choice of $c$, is now considered. We wish to compare a source free form of the energy theorem with the source form discussed previously.

### A.7.1 source free form of energy theorem

The energy theorem can be written as [33]

$$\nabla \cdot \left( \frac{\partial \underline{E}}{\partial \omega} \times \underline{H}^* + \underline{E}^* \times \frac{\partial \underline{H}}{\partial \omega} \right) = i \left[ \frac{\partial (\omega \mu)}{\partial \omega} \underline{H} \cdot \underline{H}^* + \frac{\partial (\omega \varepsilon)}{\partial \omega} \underline{E} \cdot \underline{E}^* \right] - \frac{\partial \underline{E}}{\partial \omega} \cdot \underline{J}^* - \underline{E}^* \cdot \frac{\partial \underline{J}}{\partial \omega}$$

Taking the cavity region to be source free and simple and applying the energy theorem to the upper half of the symmetric cavity we obtain

$$\oint_S \left( \frac{\partial \underline{E}}{\partial \omega} \times \underline{H}^* + \underline{E}^* \times \frac{\partial \underline{H}}{\partial \omega} \right) \cdot \underline{n} dS = \int_{S_{scar}} \left( \frac{\partial \underline{E}}{\partial \omega} \times \underline{H}^* + \underline{E}^* \times \frac{\partial \underline{H}}{\partial \omega} \right) \cdot \underline{n} dS = i \int_V \left( \mu \underline{H} \cdot \underline{H}^* + \varepsilon \underline{E} \cdot \underline{E}^* \right) dV$$

where $S_{scar}$ is the surface of the scarred orbit and $\underline{n}$ in the divergence theorem points out of the upper region. Noting from $i\omega\mu\underline{H} = \nabla \times \underline{E}$ that $\mu \underline{H} \cdot \underline{H}^* = (\nabla \times \underline{E}) \cdot (\nabla \times \underline{E}^*) \varepsilon / k^2$. In two dimensions, taking $\underline{E} = u \underline{e}_z$, we find that $\nabla \times \underline{E} = \nabla \times (u \underline{e}_z) = \nabla u \times \underline{e}_z$, $\underline{e}_z \times (\nabla u \times \underline{e}_z) = \nabla u$, $\varepsilon \underline{E} \cdot \underline{E}^* = \varepsilon |u|^2$, $\mu \underline{H} \cdot \underline{H}^* = |\nabla u|^2 \varepsilon / k^2$ so that

$$\int_{S_{scar}} \left[ \frac{\partial u}{\partial \omega} \left( \frac{1}{\omega} \nabla u^* \right) - u^* \frac{\partial}{\partial \omega} \left( \frac{1}{\omega} \nabla u \right) \right] \cdot \underline{n} dS = \frac{1}{\omega^2} \int_V \left( k^2 |u|^2 + |\nabla u|^2 \right) dV$$

Now using

$$|\nabla u|^2 = \nabla u \cdot \nabla u^* = \nabla \cdot (u^* \nabla u) - u^* \nabla^2 u = \nabla \cdot (u^* \nabla u) + k^2 |u|^2$$

and the divergence theorem gives

$$\int_{S_{scar}} \left[ \frac{\partial u}{\partial \omega} \left( \frac{1}{\omega} \nabla u^* \right) - u^* \frac{\partial}{\partial \omega} \left( \frac{1}{\omega} \nabla u \right) \right] \cdot \underline{n} dS = 2 \frac{k^2}{\omega^2} \int_V |u|^2 dV + \frac{1}{\omega^2} \oint_S (u^* \nabla u) \cdot \underline{n} dS$$

or

$$\int_{S_{scar}} \left[ \frac{\partial u}{\partial \omega} \nabla u^* - u^* \frac{\partial}{\partial \omega} \nabla u \right] \cdot \underline{n} dS = \int_{S_{scar}} \left[ \frac{\partial u}{\partial \omega} \frac{\partial u^*}{\partial n} - u^* \frac{\partial^2 u}{\partial \omega \partial n} \right] dS = 2 \frac{k^2}{\omega} \int_V |u|^2 dV$$

Specializing the integral to an area and applying this just above the scarred orbit, taking the wavefunction to be normalized to unity over the entire symmetrical cavity

$$\int_A |u|^2 dA = 1/2$$

gives

$$\int_{C_{scar}} \left[ \frac{\partial u}{\partial \omega} \frac{\partial u^*}{\partial n} - u^* \frac{\partial^2 u}{\partial \omega \partial n} \right] d\ell = \frac{k^2}{\omega}$$

Now if $u$ is constructed as a real function

$$\frac{k^2}{\omega} = -\int_{C_{scar}} u^2 \frac{\partial}{\partial \omega} \left( \frac{\partial u}{\partial n} / u \right) d\ell = -\int_{C_{scar}} u \frac{\partial^2 u}{\partial \omega \partial n} d\ell$$

To obtain the final form, we are assuming that the normal derivative, without the frequency derivative applied, vanishes on the symmetry axis at the eigenvalue.

### A.7.2 source free symmetric bow tie trigonometric series

The source free energy theorem along the horizontal orbit thus gives

$$\int_{-\ell}^{\ell} u \frac{\partial^2 u}{\partial \omega \partial y} dx = \omega \mu_0 \varepsilon_0$$

If we substitute the Fourier series expansion for the eigenfunction $u$

$$u(x,0) = \sum_p u_p(x,0)$$

and invoke orthogonality, we find

$$\sum_p \int_{-\ell}^{\ell} u_p(x,0) \frac{\partial^2 u_p}{\partial \omega \partial y}(x,0)\, dx = \omega \mu_0 \varepsilon_0$$

### A.7.3 source form with entire eigenfunction current

Alternatively if we use the energy theorem with the current source over the entire cavity

$$\int_A \left( \frac{\partial u}{\partial \omega} J_z^* + u^* \frac{\partial J_z}{\partial \omega} \right) dS = i2\varepsilon_0 \int_A |u|^2 \, dS$$

Now in this symmetric case, if we take the current source to be

$$J_z = \frac{i2}{\omega \mu_0} \frac{\partial u}{\partial y} \delta(y) \ , \ y = 0$$

and the integral over the entire area of the cavity to be unity, we find

$$\int_{-\ell}^{\ell} u(x,0) \frac{\partial^2 u}{\partial \omega \partial y}(x,0)\, dx = \omega \mu_0 \varepsilon_0$$

the same as the preceding result. This seems to confirm that the source should include the entire eigenfunction expansion.

### A.7.4 source form with single component

Next we instead take the source to be a single Fourier component

$$J_z = \frac{i2}{\omega\mu_0}\frac{\partial u_p}{\partial y}\delta(y)\,S_0\,,\; y=0$$

where the strength $S_0$ will be discussed in a moment. Inserting this gives

$$\int_{-\ell}^{\ell} u(x,0)\,\frac{\partial^2 u_p}{\partial\omega\partial y}(x,0)\,dx = \omega\mu_0\varepsilon_0$$

Inserting the Fourier expansion and using orthogonality gives

$$S_0\int_{-\ell}^{\ell} u_p(x,0)\,\frac{\partial^2 u_p}{\partial\omega\partial y}(x,0)\,dx = \omega\mu_0\varepsilon_0$$

Now comparing this with the preceding results

$$\int_{-\ell}^{\ell} u_p(x,0)\,S_0\frac{\partial^2 u_p}{\partial\omega\partial y}(x,0)\,dx = \sum_p\int_{-\ell}^{\ell} u_p(x,0)\,\frac{\partial^2 u_p}{\partial\omega\partial y}(x,0)\,dx$$

This seems to imply that the normalization of the eigenfunction is connected with source strength $S_0$ in the energy theorem.

### A.7.5 comments on source current strength

The frequency derivatives in the energy theorem, in preceding sections of the report, were estimated by using the Weyl asymptotic eigenvalue spacing for $\Delta k^2$ and a phase shift of the $p$th component alone of $\Delta\Phi_0 \sim 2\pi$. This average ratio was then multiplied by the square of a Gaussian random variable (with unit variance). If more than one $p$ component is simultaneously present, it is not clear how to define the phase shift from eigenfunction to eigenfunction. Yet, evidently this approach applied separately to each term (with $S_0$ lumped into the frequency derivative and providing the full phase shift), seems to yield the correct normalization term by term.

Perhaps a physical view of the justification can be conjectured. Suppose we place in the cavity above the scarred orbit a filter which is transparent to fields with $\cos(k_p x)$ variation (or the elliptical $p$th variation), but a perfect reflector for all other $p$ variations. We might expect that this filter, being passive and lossless, and only filtering out other $p$ components in the vicinity of the orbit (which at high frequencies is a small fraction of the area), will not disturb the general behavior of the eigenmode, and not enter into the energy theorem. If this is so, then the scar region is simplified to involve only one $p$ component at a time, and the application of the method in such a fashion, seems reasonable.

# Appendix B. APPENDICES FOR STADIUM CAVITY

These are the appendices for the stadium cavity.

## B.1 Higher Order Stadium

Suppose now we consider the higher order case. The approach used in the bow tie cavity above is sketched here for the stadium case.

### B.1.1 region one

From the bow tie we have for Region 1

$$u \sim C_1 \frac{2}{\sqrt{\cos\xi}} \cos\left(\gamma \sin\xi - s\sigma\right) \left[\psi_0\left(s,\tau\right) + \frac{1}{2\gamma}\left\{\frac{\tau}{4}\left(\frac{\tau^2}{6} - s\right)\frac{d}{d\tau}\psi_0\left(s,\tau\right) - \frac{1}{16}\tau^2\psi_0\left(s,\tau\right)\right\}\right]$$

$$+C_1 \frac{1}{2\gamma}\frac{1}{\sqrt{\cos\xi}}\left[s\psi_0\left(s,\tau\right)\cosh\left(2\sigma\right)\cos\left(\gamma\sin\xi - s\sigma\right) + \frac{1}{2}\left(s^2 - \frac{3}{4}\right)\psi_0\left(s,\tau\right)\sinh\left(2\sigma\right)\sin\left(\gamma\sin\xi - s\sigma\right)\right]$$

$$\psi\left(s,\tau\right) = c\,\mathrm{Re}\left[e^{-i\pi/4}U_+\left(s,\tau\right) + e^{i\pi/4}e^{i\Phi_0}U_+^*\left(s,\tau\right)\right]$$

$$\sigma = \int_0^\xi \frac{d\xi}{\cos\xi} = \mathrm{arcsinh}\left(\tan\xi\right)$$

$$\tau = \sqrt{2\gamma}\zeta$$

Next let us examine the behavior as the focal region is approached $\xi' = \pi/2 - \xi \to 0$

$$\sin\xi = \cos\xi' \sim 1 - \xi'^2/2 + \xi'^4/24$$

$$\cos\xi = \sin\xi' \sim \xi'\left(1 - \xi'^2/6\right)$$

$$\sigma = \mathrm{arcsinh}\left(\cot\xi'\right) = \ln\left(\cot\xi' + \csc\xi'\right) \sim \ln\left(2/\xi'\right) - \xi'^2/12$$

$$\cos\left(\gamma\sin\xi - s\sigma\right) \sim \cos\left\{\gamma\left(1 - \xi'^2/2 + \xi'^4/24\right) + s\ln\left(\xi'/2\right) + s\xi'^2/12\right\}$$

$$\sim \cos\left\{\gamma\left(1 - \xi'^2/2\right) + s\ln\left(\xi'/2\right)\right\} - \frac{\xi'^2}{12}\left(\gamma\xi'^2/2 + s\right)\sin\left\{\gamma\left(1 - \xi'^2/2\right) + s\ln\left(\xi'/2\right)\right\}$$

$$\cosh\left(2\sigma\right) \sim \frac{1}{2}e^{2\sigma} \sim 2/\xi'^2 \sim \sinh\left(2\sigma\right)$$

$$u \sim C_1 \frac{2}{\sqrt{\xi'}} \left(1 + \xi'^2/12\right)$$

$$\left[\cos\left\{\gamma\left(1 - \xi'^2/2\right) + s\ln\left(\xi'/2\right)\right\} - \frac{\xi'^2}{12}\left(\gamma\xi'^2/2 + s\right)\sin\left\{\gamma\left(1 - \xi'^2/2\right) + s\ln\left(\xi'/2\right)\right\}\right]$$

$$\left[\psi_0(s,\tau) + \frac{1}{2\gamma}\left\{\frac{\tau}{4}\left(\frac{\tau^2}{6} - s\right)\frac{d}{d\tau}\psi_0(s,\tau) - \frac{1}{16}\tau^2\psi_0(s,\tau)\right\}\right]$$

$$+C_1 \frac{1}{2\gamma}\frac{1}{\sqrt{\xi'}}\frac{2}{\xi'^2}$$

$$\left[s\psi_0(s,\tau)\cos\left\{\gamma\left(1 - \xi'^2/2\right) + s\ln\left(\xi'/2\right)\right\} + \frac{1}{2}\left(s^2 - \frac{3}{4}\right)\psi_0(s,\tau)\sin\left\{\gamma\left(1 - \xi'^2/2\right) + s\ln\left(\xi'/2\right)\right\}\right]$$

If we take $\tau' = \sqrt{2\gamma}\xi'$ and $s' = -s$

$$u \sim C_1 \frac{2\left(2\gamma\right)^{1/4}}{\sqrt{\tau'}}\left(1 + \frac{\tau'^2}{24\gamma}\right)$$

$$\left[\cos\left\{\gamma - \frac{\tau'^2}{4} - \frac{1}{2}s'\ln\left(\frac{\tau'^2}{8\gamma}\right)\right\} - \frac{\tau'^2}{24\gamma}\left(\tau'^2/4 - s'\right)\sin\left\{\gamma - \frac{\tau'^2}{4} - \frac{1}{2}s'\ln\left(\frac{\tau'^2}{8\gamma}\right)\right\}\right]$$

$$\left[\psi_0(s,\tau) + \frac{1}{2\gamma}\left\{\frac{\tau}{4}\left(\frac{\tau^2}{6} - s\right)\frac{d}{d\tau}\psi_0(s,\tau) - \frac{1}{16}\tau^2\psi_0(s,\tau)\right\}\right]$$

$$+C_1 \frac{\left(2\gamma\right)^{1/4}}{\sqrt{\tau'}}\frac{2}{\tau'^2}$$

$$\left[-s'\psi_0(s,\tau)\cos\left\{\gamma - \frac{\tau'^2}{4} - \frac{1}{2}s'\ln\left(\frac{\tau'^2}{8\gamma}\right)\right\} + \frac{1}{2}\left(s'^2 - \frac{3}{4}\right)\psi_0(s,\tau)\sin\left\{\gamma - \frac{\tau'^2}{4} - \frac{1}{2}s'\ln\left(\frac{\tau'^2}{8\gamma}\right)\right\}\right]$$

### B.1.2 region two

Second let us look at Region 2 where the substitution

$$u = e^{-i\pi/4}C_2\left[W(\xi,\zeta)\,e^{i\gamma\cosh\zeta} + W(\xi,\zeta - i\pi)\,e^{-i\gamma\cosh\zeta}\right] \;\;,\;\; |\xi| > \xi_0$$

$$\psi(s',\tau') = c\,\mathrm{Re}\left[U_+(s',\tau') + e^{-i\Phi_0}U_+^*(s',\tau')\right]$$

gives

$$\frac{\partial^2 W}{\partial\xi^2} + \frac{\partial^2 W}{\partial\zeta^2} + 2i\gamma\sinh\zeta\frac{\partial W}{\partial\zeta} + \left(i\gamma\cosh\zeta + \gamma^2\cos^2\xi\right)W = 0$$

Now taking $\xi' = \pm\pi/2 - \xi$

$$\frac{\partial^2 W}{\partial \xi'^2}+\frac{\partial^2 W}{\partial \zeta^2}+2i\gamma\sinh\zeta\frac{\partial W}{\partial \zeta}+\left(i\gamma\cosh\zeta+\gamma^2\sin^2\xi'\right)W=0$$

Expanding to two terms in $\xi'$

$$\frac{\partial^2 W}{\partial \xi'^2}+\frac{\partial^2 W}{\partial \zeta^2}+2i\gamma\sinh\zeta\frac{\partial W}{\partial \zeta}+\left(i\gamma\cosh\zeta+\gamma^2\xi'^2-\gamma^2\xi'^4/3\right)W=0$$

Now letting

$$W=\frac{1}{\sqrt{\sinh\zeta}}\Psi$$

gives

$$\frac{1}{\sqrt{\sinh\zeta}}\frac{\partial^2\Psi}{\partial\xi'^2}+\left(\frac{1}{\sqrt{\sinh\zeta}}\frac{\partial^2\Psi}{\partial\zeta^2}-\frac{1}{\sqrt{\sinh\zeta}}\coth\zeta\frac{\partial\Psi}{\partial\zeta}\right)+\left(\frac{3}{4}\frac{1}{\sqrt{\sinh\zeta}}\coth^2\zeta\Psi-\frac{1}{2}\frac{1}{\sqrt{\sinh\zeta}}\Psi\right)$$

$$+2i\gamma\sinh\zeta\frac{1}{\sqrt{\sinh\zeta}}\frac{\partial\Psi}{\partial\zeta}-i\gamma\cosh\zeta\frac{1}{\sqrt{\sinh\zeta}}\Psi+\left(i\gamma\cosh\zeta+\gamma^2\xi'^2-\gamma^2\xi'^4/3\right)\frac{1}{\sqrt{\sinh\zeta}}\Psi=0$$

$$\frac{\partial^2\Psi}{\partial\xi'^2}+\frac{\partial^2\Psi}{\partial\zeta^2}+\left(2i\gamma\sinh\zeta-\coth\zeta\right)\frac{\partial\Psi}{\partial\zeta}+\left(\gamma^2\xi'^2+\frac{3}{4}\coth^2\zeta-\frac{1}{2}-\gamma^2\xi'^4/3\right)\Psi=0$$

$$\tau'=\sqrt{2\gamma}\xi'$$

$$\frac{\partial^2\Psi}{\partial\tau'^2}+i\sinh\zeta\frac{\partial\Psi}{\partial\zeta}+\frac{\tau'^2}{4}\Psi=\frac{1}{2\gamma}\left[\coth\zeta\frac{\partial\Psi}{\partial\zeta}-\left(\frac{3}{4}\coth^2\zeta-\frac{1}{2}-\tau'^4/12\right)\Psi-\frac{\partial^2\Psi}{\partial\zeta^2}\right]$$

$$\sigma'=\int_\infty^\zeta\frac{d\zeta}{\sinh\zeta}=\ln\left[\tanh\left(\zeta/2\right)\right]$$

$$\cosh\zeta=-\coth\sigma'$$

$$1/\sinh\zeta=\sinh\sigma'$$

$$\frac{\partial^2\Psi}{\partial\tau'^2}+i\frac{\partial\Psi}{\partial\sigma'}+\frac{\tau'^2}{4}\Psi=\frac{1}{2\gamma}\left[-2\sinh\sigma'\cosh\sigma'\frac{\partial\Psi}{\partial\sigma'}-\left(\frac{3}{4}\cosh^2\sigma'-\frac{1}{2}-\tau'^4/12\right)\Psi-\sinh^2\sigma'\frac{\partial^2\Psi}{\partial\sigma'^2}\right]$$

Substituting the expansion

$$\Psi=\sum_{n=0}^{\infty}\left(2\gamma\right)^{-n}\Psi_n$$

gives

$$\frac{\partial^2}{\partial\tau'^2}\Psi_0 + i\frac{\partial\Psi_0}{\partial\sigma'} + \frac{1}{4}\tau'^2\Psi_0 \approx 0$$

and

$$\frac{\partial^2\Psi_1}{\partial\tau'^2} + i\frac{\partial\Psi_1}{\partial\sigma'} + \frac{\tau'^2}{4}\Psi_1 = \left[-2\sinh\sigma'\cosh\sigma'\frac{\partial\Psi_0}{\partial\sigma'} - \left(\frac{3}{4}\cosh^2\sigma' - \frac{1}{2} - \tau'^4/12\right)\Psi_0 - \sinh^2\sigma'\frac{\partial^2\Psi_0}{\partial\sigma'^2}\right]$$

Taking

$$\Psi_0 = e^{-is'\sigma'}\psi_0$$

$$\frac{\partial^2}{\partial\tau'^2}\psi_0 + \left(\frac{1}{4}\tau'^2 + s'\right)\psi_0 = 0$$

and

$$\frac{\partial^2\Psi_1}{\partial\tau'^2} + i\frac{\partial\Psi_1}{\partial\sigma'} + \frac{\tau'^2}{4}\Psi_1 = \left[is'2\sinh\sigma'\cosh\sigma' - \left(\frac{3}{4}\cosh^2\sigma' - \frac{1}{2} - \tau'^4/12\right) + s'^2\sinh^2\sigma'\right]e^{-is'\sigma'}\psi_0$$

$$= \left[\frac{is'}{2}\left(e^{2\sigma'} - e^{-2\sigma'}\right) - \frac{3}{16}\left(e^{2\sigma'} + 2 + e^{-2\sigma'}\right) + \frac{1}{2} + \tau'^4/12 + \frac{s'^2}{4}\left(e^{2\sigma'} - 2 + e^{-2\sigma'}\right)\right]e^{-is'\sigma'}\psi_0$$

Letting

$$\Psi_1 = \psi_1 e^{-is'\sigma} + \psi_{1,2}e^{\left(2-is'\right)\sigma'} + \psi_{1,-2}e^{-\left(2+is'\right)\sigma'}$$

$$\left(\frac{\partial^2}{\partial\tau'^2} + \frac{1}{4}\tau'^2 + s'\right)\psi_1 = \frac{1}{2}\left(\frac{1}{4} - s'^2 + \frac{1}{6}\tau'^4\right)\psi_0$$

$$\left(\frac{\partial^2}{\partial\tau'^2} \pm i2 + \frac{1}{4}\tau'^2 + s'\right)\psi_{1,\pm2} = \frac{1}{2}\left(\pm is' - \frac{3}{8} + \frac{s'^2}{2}\right)\psi_0$$

From the bow tie work we see that the only difference is that the $\psi_1$ terms have reversed sign. Thus

$$\psi_1 = -\frac{\tau'}{4}\left(\frac{\tau'^2}{6} - s'\right)\frac{d\psi_0}{d\tau'} + \frac{1}{16}\tau'^2\psi_0$$

$$\psi_{1,\pm2} = \pm\frac{i}{4}\left(-\frac{1}{2}s'^2 \mp is' + \frac{3}{8}\right)\psi_0\left(s',\tau'\right) = \left[\frac{s'}{4} \pm \frac{i}{4}\left(-\frac{1}{2}s'^2 + \frac{3}{8}\right)\right]\psi_0\left(s',\tau'\right)$$

and

$$\Psi \sim \left[1 + \frac{1}{8\gamma}\left\{-\tau'\left(\frac{\tau'^2}{6} - s'\right)\frac{d}{d\tau'} + \frac{1}{4}\tau'^2\right\}\right]\psi_0\left(s',\tau'\right)e^{-is'\sigma'}$$

$$+\frac{1}{4\gamma}\left[-\frac{i}{2}\left(s'^2-\frac{3}{4}\right)\sinh\left(2\sigma'\right)+s'\cosh\left(2\sigma'\right)\right]e^{-is'\sigma'}\psi_0\left(s',\tau'\right)$$

$$W=\frac{1}{\sqrt{\sinh\zeta}}\Psi$$

$$u=e^{-i\pi/4}C_2\left[W\left(\xi,\zeta\right)e^{i\gamma\cosh\zeta}+W\left(\xi,\zeta-i\pi\right)e^{-i\gamma\cosh\zeta}\right]$$

$$=e^{-i\pi/4}C_2\frac{1}{\sqrt{\sinh\zeta}}\left[\Psi\left(\xi,\zeta\right)e^{i\gamma\cosh\zeta}+i\Psi\left(\xi,\zeta-i\pi\right)e^{-i\gamma\cosh\zeta}\right]$$

and

$$u\sim C_2\frac{2}{\sqrt{\sinh\zeta}}$$

$$\left[\psi_0\left(s',\tau'\right)+\frac{1}{8\gamma}\left\{-\tau'\left(\frac{\tau'^2}{6}-s'\right)\frac{d}{d\tau'}\psi_0\left(s',\tau'\right)+\frac{1}{4}\tau'^2\psi_0\left(s',\tau'\right)\right\}\right]\cos\left(\gamma\cosh\zeta-s'\sigma'-\pi/4\right)$$

$$+C_2\frac{2}{\sqrt{\sinh\zeta}}\frac{1}{4\gamma}$$

$$\left[\frac{1}{2}\left(s'^2-\frac{3}{4}\right)\sinh\left(2\sigma'\right)\sin\left(\gamma\cosh\zeta-s'\sigma'-\pi/4\right)+s'\cosh\left(2\sigma'\right)\cos\left(\gamma\cosh\zeta-s'\sigma'-\pi/4\right)\right]\psi_0\left(s',\tau'\right)$$

where we have used

$$\sigma'=\int_\infty^{\zeta-i\pi}\frac{d\zeta}{\sinh\zeta}=-\int_\infty^{\zeta}\frac{d\zeta}{\sinh\zeta}$$

$$\sigma'_0=\ln\left[\tanh\left(\zeta_0/2\right)\right]$$

$$\sqrt{\sinh\left(\zeta-i\pi\right)}\rightarrow-i\sqrt{\sinh\zeta}$$

Now let us examine the limit as the focal region is approached $\zeta\rightarrow0$

$$\sinh\zeta\sim\zeta\left(1+\zeta^2/6\right)$$

$$\cosh\zeta\sim1+\zeta^2/2+\zeta^4/24$$

$$\sigma'=\ln\left[\tanh\left(\zeta/2\right)\right]\sim-\ln\left(2/\zeta\right)-\zeta^2/12$$

$$\cosh(2\sigma') \sim \frac{1}{2}e^{-2\sigma'} \sim 2/\zeta^2 \sim -\sinh(2\sigma')$$

$$\cos\left(\gamma\cosh\zeta - s'\zeta' - \pi/4\right) \sim \cos\left\{\gamma\left(1+\zeta^2/2+\zeta^4/24\right) - s'\ln(\zeta/2) - \pi/4 + s\zeta^2/12\right\}$$

$$\sim \cos\left\{\gamma\left(1+\zeta^2/2\right) - s'\ln(\zeta/2) - \pi/4\right\} - \frac{\zeta^2}{12}\left(\gamma\zeta^2/2+s\right)\sin\left\{\gamma\left(1+\zeta^2/2\right) - s'\ln(\zeta/2) - \pi/4\right\}$$

$$u \sim C_2\frac{2}{\sqrt{\zeta}}\left(1-\zeta^2/6\right)\left[\psi_0(s',\tau') + \frac{1}{8\gamma}\left\{-\tau'\left(\frac{\tau'^2}{6}-s'\right)\frac{d}{d\tau'}\psi_0(s',\tau') + \frac{1}{4}\tau'^2\psi_0(s',\tau')\right\}\right]$$

$$\left[\cos\left\{\gamma\left(1+\zeta^2/2\right) - s'\ln(\zeta/2) - \pi/4\right\} - \frac{\zeta^2}{12}\left(\gamma\zeta^2/2+s\right)\sin\left\{\gamma\left(1+\zeta^2/2\right) - s'\ln(\zeta/2) - \pi/4\right\}\right]$$

$$+C_2\frac{2}{\sqrt{\zeta}}\frac{1}{4\gamma}\frac{2}{\zeta^2}$$

$$\left[-\frac{1}{2}\left(s'^2-\frac{3}{4}\right)\sin\left\{\gamma\left(1+\zeta^2/2\right) - s'\ln(\zeta/2) - \pi/4\right\} + s'\cos\left\{\gamma\left(1+\zeta^2/2\right) - s'\ln(\zeta/2) - \pi/4\right\}\right]\psi_0(s',\tau')$$

Now if we set $\tau = \sqrt{2\gamma}\zeta$ and $s = -s'$

$$u \sim (-1)^n C_2\frac{2(2\gamma)^{1/4}}{\sqrt{\tau}}\left(1-\frac{\tau^2}{12\gamma}\right)\left[\psi_0(s',\tau') + \frac{1}{8\gamma}\left\{-\tau'\left(\frac{\tau'^2}{6}-s'\right)\frac{d}{d\tau'}\psi_0(s',\tau') + \frac{1}{4}\tau'^2\psi_0(s',\tau')\right\}\right]$$

$$\left[\cos\left\{\gamma+\tau^2/4+\frac{1}{2}s\ln\left(\frac{\tau^2}{8\gamma}\right)-\pi/4\right\} - \frac{\tau^2}{24\gamma}\left(\tau^2/4+s\right)\sin\left\{\gamma+\tau^2/4+\frac{1}{2}s\ln\left(\frac{\tau^2}{8\gamma}\right)-\pi/4\right\}\right]$$

$$+(-1)^n C_2\frac{2(2\gamma)^{1/4}}{\sqrt{\tau}}\frac{1}{\tau^2}$$

$$\left[-\frac{1}{2}\left(s^2-\frac{3}{4}\right)\sin\left\{\gamma+\tau^2/4+\frac{1}{2}s\ln\left(\frac{\tau^2}{8\gamma}\right)-\pi/4\right\} - s\cos\left\{\gamma+\tau^2/4+\frac{1}{2}s\ln\left(\frac{\tau^2}{8\gamma}\right)-\pi/4\right\}\right]\psi_0(s',\tau')$$

### B.1.3 region three

Near the focus $\xi = \pi/2$ and $\zeta = 0$ we might try approximating the Helmholtz equation

$$\frac{\partial^2 u}{\partial\xi^2} + \frac{\partial^2 u}{\partial\zeta^2} + \gamma^2\left(\cosh^2\zeta - \sin^2\xi\right)u = 0$$

or

$$\frac{\partial^2 u}{\partial \xi^2} + \frac{\partial^2 u}{\partial \zeta^2} + \gamma^2 \left( \sinh^2 \zeta + \cos^2 \xi \right) u = 0$$

as $\xi' = \pi/2 - \xi$ (we are assuming that $\zeta^4 << 1$ and that $\xi'^4 << 1$)

$$\frac{\partial^2 u}{\partial \xi^2} + \frac{\partial^2 u}{\partial \zeta^2} + \gamma^2 \left( \sinh^2 \zeta + \sin^2 \xi' \right) u = 0$$

or

$$\frac{\partial^2 u}{\partial \xi'^2} + \frac{\partial^2 u}{\partial \zeta^2} + \gamma^2 \left( \zeta^2 + \zeta^4/3 + \xi'^2 - \xi'^4/3 \right) u = 0$$

Separating variables

$$u = X\left(\xi'\right) Z\left(\zeta\right)$$

$$\left( \frac{1}{X} \frac{\partial^2 X}{\partial \xi'^2} + \gamma^2 \xi'^2 - \gamma^2 \xi'^4/3 \right) + \left( \frac{1}{Z} \frac{\partial^2 Z}{\partial \zeta^2} + \gamma^2 \zeta^2 + \gamma^2 \zeta^4/3 \right) = 0$$

Taking the separation constant to be $2\gamma g$ we find

$$\frac{\partial^2 X}{\partial \xi'^2} + \left( -2\gamma g + \gamma^2 \xi'^2 - \gamma^2 \xi'^4/3 \right) X = 0$$

$$\frac{\partial^2 Z}{\partial \zeta^2} + \left( 2\gamma g + \gamma^2 \zeta^2 + \gamma^2 \zeta^4/3 \right) Z = 0$$

Thus we find parabolic cylinder equations in both directions. Letting

$$\xi' \sqrt{2\gamma} = \tau'$$

in the first and

$$\zeta \sqrt{2\gamma} = \tau$$

in the second, gives

$$\frac{\partial^2 X}{\partial \tau'^2} + \left( -g + \frac{1}{4} \tau'^2 \right) X = \frac{1}{2\gamma} \frac{\tau'^4}{12} X$$

$$\frac{\partial^2 Z}{\partial \tau^2} + \left( g + \frac{1}{4} \tau^2 \right) Z = -\frac{1}{2\gamma} \frac{\tau^4}{12} Z$$

Substituting the expansions

$$X = \sum_{n=0}^{\infty} \left(2\gamma\right)^{-n} X_n$$

$$Z = \sum_{n=0}^{\infty} (2\gamma)^{-n} Z_n$$

the resulting leading equations can be solved easily. The leading solutions are

$$u = \frac{C_0}{c} XZ = C_0 c \,\mathrm{Re}\left[U_+(-g,\tau') + B'U_+^*(-g,\tau')\right] \mathrm{Re}\left[U_+(g,\tau) + BU_+^*(g,\tau)\right]$$

$$= C_0 c \,\mathrm{Re}\left[U_+\left(-g,\xi'\sqrt{2\gamma}\right) + B'U_+^*\left(-g,\xi'\sqrt{2\gamma}\right)\right]$$

$$\mathrm{Re}\left[e^{-i\pi/4}U_+\left(g,\zeta\sqrt{2\gamma}\right) + e^{i\pi/4}BU_+^*\left(g,\zeta\sqrt{2\gamma}\right)\right]$$

For purposes of matching we take $g = s = -s'$ and $B = e^{i\Phi_0}$ and $B' = e^{i\Phi_0'} = e^{-i\Phi_0}$

$$u = \frac{C_0}{c} c \,\mathrm{Re}\left[U_+\left(s',\xi'\sqrt{2\gamma}\right) + e^{-i\Phi_0}U_+^*\left(s',\xi'\sqrt{2\gamma}\right)\right]$$

$$c \,\mathrm{Re}\left[e^{-i\pi/4}U_+\left(-s',\zeta\sqrt{2\gamma}\right) + e^{i\pi/4}e^{i\Phi_0}U_+^*\left(-s',\zeta\sqrt{2\gamma}\right)\right]$$

Now we need to obtain the first order solutions.

$$\frac{\partial^2 X_1}{\partial \tau'^2} + \left(s' + \frac{1}{4}\tau'^2\right) X_1 = \frac{\tau'^4}{12} X_0$$

$$X_0 = c \,\mathrm{Re}\left[U_+(s',\tau') + e^{-i\Phi_0}U_+^*(s',\tau')\right]$$

$$\frac{\partial^2 Z_1}{\partial \tau^2} + \left(s + \frac{1}{4}\tau^2\right) Z_1 = -\frac{\tau^4}{12} Z_0$$

$$Z_0 = c \,\mathrm{Re}\left[e^{-i\pi/4}U_+(-s',\tau) + e^{i\pi/4}e^{i\Phi_0}U_+^*(-s',\tau)\right]$$

From the bow tie

$$24\psi_{1,1} = \tau\left(\tau^2 - 6s\right)\frac{d\psi_0}{d\tau} - \frac{3}{2}\tau^2\psi_0 + 3\left(4s^2 - 1\right)\frac{\partial \psi_0}{\partial s}$$

$$\frac{\partial^2 \psi_{1,1}}{\partial \tau^2} + \left(\frac{\tau^2}{4} + s\right)\psi_{1,1} = -\frac{1}{12}\tau^4\psi_0$$

$$\psi_0 = c \,\mathrm{Re}\left[U_+(s,\tau) + e^{i\Phi_0}U_+^*(s,\tau)\right]$$

we see that

$$-24X_1 = \tau'\left(\tau'^2 - 6s'\right)\frac{dX_0}{d\tau'} - \frac{3}{2}\tau'^2 X_0 + 3\left(4s'^2 - 1\right)\frac{\partial X_0}{\partial s'}$$

$$24Z_1 = \tau\left(\tau^2 - 6s\right)\frac{dZ_0}{d\tau} - \frac{3}{2}\tau^2 Z_0 + 3\left(4s^2 - 1\right)\frac{\partial Z_0}{\partial s}$$

However it may be convenient to introduce a first order constant to the separation constants

$$g = s - \frac{1}{2\gamma}\frac{1}{8}\left(4s^2 - 1\right) = -s' - \frac{1}{2\gamma}\frac{1}{8}\left(4s'^2 - 1\right)$$

yielding

$$\frac{\partial^2 Z_1}{\partial \tau^2} + \left(s + \frac{1}{4}\tau^2\right) Z_1 = -\frac{\tau^4}{12} Z_0 + \frac{1}{8}\left(4s^2 - 1\right) Z_0$$

$$\frac{\partial^2 X_1}{\partial \tau'^2} + \left(s' + \frac{1}{4}\tau'^2\right) X_1 = \frac{\tau'^4}{12} X_0 - \frac{1}{8}\left(4s'^2 - 1\right) X_0$$

From the bow tie we had

$$\frac{\partial^2 \psi_1}{\partial \tau^2} + \left(\frac{\tau^2}{4} + s\right)\psi_1 = -\frac{1}{2}\left(-s^2 + \frac{1}{4}\right)\psi_0(s,\tau) - \frac{1}{12}\tau^4\psi_0$$

and thus

$$-24X_1 = \tau'\left(\tau'^2 - 6s'\right)\frac{dX_0}{d\tau'} - \frac{3}{2}\tau'^2 X_0$$

$$24Z_1 = \tau\left(\tau^2 - 6s\right)\frac{dZ_0}{d\tau} - \frac{3}{2}\tau^2 Z_0$$

Now the first order solutions obey the symmetry conditions on the scar orbit. The solution is then

$$u \sim X_0 Z_0 + \frac{1}{2\gamma}\left(X_0 Z_1 + X_1 Z_0\right)$$

$$\sim \frac{C_0}{c} X_0 Z_0 + \frac{C_0}{c}\frac{1}{48\gamma}\left[X_0\left\{\tau\left(\tau^2 - 6s\right)\frac{dZ_0}{d\tau} - \frac{3}{2}\tau^2 Z_0\right\} - Z_0\left\{\tau'\left(\tau'^2 - 6s'\right)\frac{dX_0}{d\tau'} - \frac{3}{2}\tau'^2 X_0\right\}\right]$$

$$\sim C_0 c\,\mathrm{Re}\left[U_+(s',\tau') + e^{-i\Phi_0}U_+^*(s',\tau')\right]\mathrm{Re}\left[e^{-i\pi/4}U_+(s,\tau) + e^{i\pi/4}e^{i\Phi_0}U_+^*(s,\tau)\right]$$

$$+\frac{1}{48\gamma}C_0 c\,\mathrm{Re}\left[U_+(s',\tau') + e^{-i\Phi_0}U_+^*(s',\tau')\right]\left\{\tau\left(\tau^2 - 6s\right)\frac{d}{d\tau} - \frac{3}{2}\tau^2\right\}\mathrm{Re}\left[e^{-i\pi/4}U_+(s,\tau) + e^{i\pi/4}e^{i\Phi_0}U_+^*(s,\tau)\right]$$

$$-\frac{1}{48\gamma}C_0 c\,\mathrm{Re}\left[e^{-i\pi/4}U_+(s,\tau) + e^{i\pi/4}e^{i\Phi_0}U_+^*(s,\tau)\right]\left\{\tau'\left(\tau'^2 - 6s'\right)\frac{d}{d\tau'} - \frac{3}{2}\tau'^2\right\}$$

$$\mathrm{Re}\left[U_+(s',\tau') + e^{-i\Phi_0}U_+^*(s',\tau')\right]$$

or

$$u \sim \frac{C_0}{c}\psi_0\left(s',\tau'\right)\psi_0\left(s,\tau\right)$$

$$+\frac{1}{48\gamma}\frac{C_0}{c}\psi_0\left(s',\tau'\right)\left\{\tau\left(\tau^2-6s\right)\frac{d}{d\tau}-\frac{3}{2}\tau^2\right\}\psi_0\left(s,\tau\right)$$

$$-\frac{1}{48\gamma}\frac{C_0}{c}\psi_0\left(s,\tau\right)\left\{\tau'\left(\tau'^2-6s'\right)\frac{d}{d\tau'}-\frac{3}{2}\tau'^2\right\}\psi_0\left(s',\tau'\right)$$

In order to approach the other two regions we use the expansions

$$U_+\left(s,\tau\right)=e^{-\pi(s+i/2)/4}U\left(-is,\tau e^{-i\pi/4}\right)$$

$$U_+\left(s,\tau\right)\sim e^{i\tau^2/4-(1/2-is)\ln\tau}=e^{i\tau^2/4}\tau^{is-1/2}\ ,\ \tau\rightarrow+\infty$$

$$U_+\left(s,\tau\right)=e^{-i\pi/4-i\phi_2/2}E\left(-s,\tau\right)/\sqrt{2}$$

$$\phi_2=\arg\Gamma\left(1/2-is\right)$$

$$U_+\left(s,\tau\right)\sim e^{i\tau^2/4}\tau^{is-1/2}\sum_{n=0}^{\infty}\left(-i\right)^n\frac{\Gamma\left(2n+1/2-is\right)}{\Gamma\left(1/2-is\right)}\frac{1}{2^n n!\tau^{2n}}$$

$$\sim e^{i\tau^2/4}\tau^{is-1/2}\left\{1-i\left(1-i2s\right)\left(3-i2s\right)/\left(8\tau^2\right)\right\}$$

$$\psi_0\left(s,\tau\right)\sim 2c\cos\left(\Phi_0/2\right)\tau^{-1/2}\cos\left[\tau^2/4+s\ln\left(\tau\right)-\Phi_0/2-\pi/4\right]+2c\cos\left(\Phi_0/2\right)\tau^{-5/2}$$

$$\left[-s\cos\left\{\tau^2/4+s\ln\left(\tau\right)-\Phi_0/2-\pi/4\right\}+\frac{1}{2}\left(\frac{3}{4}-s^2\right)\sin\left\{\tau^2/4+s\ln\left(\tau\right)-\Phi_0/2-\pi/4\right\}\right]$$

$$\psi_0\left(s',\tau'\right)\sim 2c\cos\left(\Phi_0/2\right)\tau'^{-1/2}\cos\left[\tau'^2/4+s'\ln\left(\tau'\right)+\Phi_0/2\right]$$

$$+2c\cos\left(\Phi_0/2\right)\tau'^{-5/2}\left[-s'\cos\left\{\tau'^2/4+s'\ln\left(\tau'\right)+\Phi_0/2\right\}+\frac{1}{2}\left(\frac{3}{4}-s'^2\right)\sin\left\{\tau'^2/4+s'\ln\left(\tau'\right)+\Phi_0/2\right\}\right]$$

### B.1.4 matching

If we move the Region 3 solution into Region 1, then $\tau' >> 1$

$$u\sim C_0\cos\left(\Phi_0/2\right)\tau'^{-1/2}$$

$$\left[\left(1-s'/\tau'^2\right)\cos\left\{\tau'^2/4+s'\ln\left(\tau'\right)+\Phi_0/2\right\}+\frac{1}{2\tau'^2}\left(\frac{3}{4}-s'^2\right)\sin\left\{\tau'^2/4+s'\ln\left(\tau'\right)+\Phi_0/2\right\}\right]\psi_0\left(s,\tau\right)$$

$$+\frac{1}{2\gamma}\frac{C_0}{c}\psi_0\left(s',\tau'\right)\left\{\frac{\tau}{4}\left(\frac{\tau^2}{6}-s\right)\frac{d}{d\tau}-\frac{1}{16}\tau^2\right\}\psi_0\left(s,\tau\right)$$

$$-\frac{1}{2\gamma}\frac{C_0}{c}\psi_0\left(s,\tau\right)\left\{\frac{\tau'}{4}\left(\frac{\tau'^2}{6}-s'\right)\frac{d}{d\tau'}-\frac{1}{16}\tau'^2\right\}\psi_0\left(s',\tau'\right)$$

If we move the Region 3 solution into Region 2, we take $\tau >> 1$

$$u\sim\frac{C_0}{c}\psi_0\left(s',\tau'\right)\psi_0\left(s,\tau\right)$$

$$+\frac{1}{48\gamma}\frac{C_0}{c}\psi_0\left(s',\tau'\right)\left\{\tau\left(\tau^2-6s\right)\frac{d}{d\tau}-\frac{3}{2}\tau^2\right\}\psi_0\left(s,\tau\right)$$

$$-\frac{1}{48\gamma}\frac{C_0}{c}\psi_0\left(s,\tau\right)\left\{\tau'\left(\tau'^2-6s'\right)\frac{d}{d\tau'}-\frac{3}{2}\tau'^2\right\}\psi_0\left(s',\tau'\right)$$

The focal shift $\delta$ is introduced in Region 3 by means of the replacement

$$\tau'\rightarrow\widehat{\tau}'=\sqrt{4k\delta+\tau'^2}\sim\tau'\left(1+\frac{2k\delta}{\tau'^2}\right)$$

when moving into Region 1 and

$$\tau\rightarrow\widehat{\tau}=\sqrt{\tau^2-4k\delta}\sim\tau\left(1-\frac{2k\delta}{\tau'^2}\right)$$

when moving into Region 2.

There are a number of questions here about how we order the terms. For example, are $\tau'^2$ terms in the outer region small? Are $1/\tau'^2$ terms in the inner region small? Are terms that are $1/\left(\gamma\tau'^2\right)$ in the outer region small? Should we have expansions of the coefficient amplitudes

$$C_0\sim C_0^{(0)}+\frac{1}{2\gamma}C_0^{(1)}+\cdots$$

$$C_1\sim C_1^{(0)}+\frac{1}{2\gamma}C_1^{(1)}+\cdots$$

Is it possible that the $1/\gamma$ expansions are all associated with the first order solutions to the equations and all we needed was to keep the $1/\tau'^2$ terms from the parabolic cylinder expansions? In other words could these different order terms be a clue that there is one expansion for the zero order and another for the first order solutions? Should we also take the expansion

$$\delta\sim\delta_0+\delta_1+\cdots$$

where we regard successive terms as small $\delta_1 << \delta_0$? Then since $k\delta_0 = O\left(1\right)$ we have that $k\delta_1 << 1$. These questions are out of scope in this report and we simply leave the higher order construction to future work.

## B.2 Asymptotic Orthogonality In The Stadium

The orthogonality of the scarred components are examined in this section. We first look at the simplified trigonometric approximation to the functions (which in the bow tie cavity, being Fourier components, were strictly orthogonal) and then at the scar functions from the elliptical analysis.

### B.2.1 trigonometric approximation

Suppose we first examine the trigonometric approximate forms for the scar functions, which exhibit the proper phase shift through the focal point in the stadium cavity. For the even case we take

$$u_p^T = c\cos\left(k_p x\right) \ , \ d < |x|$$

$$= c\cos\left(k_p\left|x\right| - \pi/4\right) \ , \ d < |x| < \ell$$

where

$$k_p \ell = \pi\left(p - 1/4\right)$$

Consider the inner product

$$\int_{-\ell}^{\ell} u_p^T\left(x,0\right) u_{p'}^T\left(x,0\right) dx = 2c^2 \int_0^d \cos\left(k_p x\right)\cos\left(k_{p'} x\right) dx$$

$$+2c^2 \int_d^{\ell} \cos\left(k_p x - \pi/4\right)\cos\left(k_{p'} x - \pi/4\right) dx$$

$$= c^2 \int_0^d \left[\cos\left(k_p - k_{p'}\right) x + \cos\left(k_p + k_{p'}\right) x\right] dx$$

$$+c^2 \int_d^{\ell} \left[\cos\left(k_p - k_{p'}\right) x + \sin\left(k_p + k_{p'}\right) x\right] dx$$

$$= c^2\left[\frac{\sin\left(k_p + k_{p'}\right) d}{k_p + k_{p'}} + \frac{\sin\left(k_p - k_{p'}\right)\ell}{k_p - k_{p'}} - \frac{\cos\left(k_p + k_{p'}\right)\ell}{k_p + k_{p'}} + \frac{\cos\left(k_p + k_{p'}\right) d}{k_p + k_{p'}}\right]$$

$$= c^2\left[\frac{\sin\left\{\pi\left(p + p' - 1/2\right) d/\ell\right\}}{\pi\left(p + p' - 1/2\right)/\ell} + \frac{\sin\left\{\pi\left(p - p'\right)\right\}}{\pi\left(p - p'\right)/\ell} - \frac{\cos\left\{\pi\left(p + p' - 1/2\right)\right\}}{\pi\left(p + p' - 1/2\right)/\ell} + \frac{\cos\left\{\pi\left(p + p' - 1/2\right) d/\ell\right\}}{\pi\left(p + p' - 1/2\right)/\ell}\right]$$

$$= c^2\ell\left[\sqrt{2}\frac{\cos\left\{\pi\left(p + p' - 1/2\right) d/\ell - \pi/4\right\}}{\pi\left(p + p' - 1/2\right)} + \delta_{pp'}\right]$$

where the Kronecker delta $\delta_{pp'}$ is unity for $p = p'$ and vanishes otherwise. Thus orthogonality holds asymptotically in the high frequency limit $\left(k_p + k_{p'}\right)\ell = \pi\left(p + p' - 1/2\right) \to \infty$ to order $O\left[1/\left\{\left(k_p + k_{p'}\right)\ell\right\}\right]$.

Suppose we enforced strict orthogonality by requiring

$$\cos\left\{\pi\left(p+p'-1/2\right)d/\ell-\pi/4\right\}=0$$

or

$$\pi\left(p+p'-1/2\right)d/\ell-\pi/4=\pi\left(n-1/2\right)$$

or

$$d/\ell=\frac{n-1/4}{p+p'-1/2}$$

A focal shift, discussed in the main body of the report, was required to enforce the continuity at $x=d+\delta_0$ for $s=0$. It is instructive to examine the effect of this shift on the orthogonality. Noting that the shift for $s=0$ is defined by

$$k_p\left(d+\delta_{0p}\right)=\left(n+1/8\right)\pi$$

$$\cos\left(k_p x\right)=\cos\left(k_p x-\pi/4\right)\ ,\ x=d+\delta_{0p}$$

we consider the inner product for, say $p\geq p'$,

$$\int_{-\ell}^{\ell}u_p^T\left(x,0\right)u_{p'}^T\left(x,0\right)dx=2c^2\int_0^{d+\delta_{0p'}}\cos\left(k_p x\right)\cos\left(k_{p'}x\right)dx$$

$$+2c^2\int_{d+\delta_{0p'}}^{d+\delta_{0p}}\cos\left(k_p x\right)\cos\left(k_{p'}x-\pi/4\right)dx+2c^2\int_{d+\delta_p}^{\ell}\cos\left(k_p x-\pi/4\right)\cos\left(k_{p'}x-\pi/4\right)dx$$

$$=c^2\int_0^{d+\delta_{0p'}}\left[\cos\left(k_p-k_{p'}\right)x+\cos\left(k_p+k_{p'}\right)x\right]dx$$

$$+c^2\int_{d+\delta_{0p'}}^{d+\delta_{0p}}\left[\cos\left(\left(k_p-k_{p'}\right)x+\pi/4\right)+\cos\left(\left(k_p+k_{p'}\right)x-\pi/4\right)\right]dx$$

$$+c^2\int_{d+\delta_{0p}}^{\ell}\left[\cos\left(k_p-k_{p'}\right)x+\cos\left(\left(k_p+k_{p'}\right)x-\pi/2\right)\right]dx$$

$$=c^2\left[\frac{\sin\left\{\left(k_p-k_{p'}\right)\left(d+\delta_{0p'}\right)\right\}}{k_p-k_{p'}}+\frac{\sin\left\{\left(k_p+k_{p'}\right)\left(d+\delta_{0p'}\right)\right\}}{k_p+k_{p'}}\right]$$

$$+c^2\left[\frac{\sin\left\{\left(k_p-k_{p'}\right)\left(d+\delta_{0p}\right)+\pi/4\right\}}{k_p-k_{p'}}-\frac{\sin\left\{\left(k_p-k_{p'}\right)\left(d+\delta_{0p'}\right)+\pi/4\right\}}{k_p-k_{p'}}\right.$$

$$\left.+\frac{\sin\left\{\left(k_p+k_{p'}\right)\left(d+\delta_{0p}\right)-\pi/4\right\}}{k_p+k_{p'}}-\frac{\sin\left\{\left(k_p+k_{p'}\right)\left(d+\delta_{0p'}\right)-\pi/4\right\}}{k_p+k_{p'}}\right]$$

$$+c^2\left[\frac{\sin\left(k_p-k_{p'}\right)\ell}{k_p-k_{p'}}-\frac{\sin\left\{\left(k_p-k_{p'}\right)\left(d+\delta_{0p}\right)\right\}}{k_p-k_{p'}}\right.$$

$$\left.+\frac{\sin\left\{\left(k_p+k_{p'}\right)\ell-\pi/2\right\}}{k_p+k_{p'}}-\frac{\sin\left\{\left(k_p+k_{p'}\right)\left(d+\delta_{0p}\right)-\pi/2\right\}}{k_p+k_{p'}}\right]$$

$$=\frac{c^2}{k_p-k_{p'}}\left[\sin\left(p-p'\right)\pi+\sin\left\{k_p\left(\delta_{0p'}-\delta_{0p}\right)\right\}-\sin\left\{k_{p'}\left(\delta_{0p'}-\delta_{0p}\right)\right\}\right.$$

$$\left.+\sin\left\{k_{p'}\left(\delta_{0p'}-\delta_{0p}\right)+\pi/4\right\}-\sin\left\{k_p\left(\delta_{0p'}-\delta_{0p}\right)+\pi/4\right\}\right]$$

$$+\frac{c^2}{k_p+k_{p'}}\left[\sin\left\{\left(p+p'-1\right)\pi\right\}+\sin\left\{k_{p'}\left(\delta_{0p'}-\delta_{0p}\right)+\pi/4\right\}-\sin\left\{k_{p'}\left(\delta_{0p'}-\delta_{0p}\right)\right\}\right.$$

$$\left.-\sin\left\{k_p\left(\delta_{0p'}-\delta_{0p}\right)\right\}+\sin\left\{\pi/4+k_p\left(\delta_{0p'}-\delta_{0p}\right)\right\}\right]$$

$$=c^2\ell\frac{\sin\left(p-p'\right)\pi}{\left(p-p'\right)\pi}+\frac{c^2}{k_p-k_{p'}}\left[2\sin\left\{\frac{1}{2}\left(k_p-k_{p'}\right)\left(\delta_{0p'}-\delta_{0p}\right)\right\}\cos\left\{\frac{1}{2}\left(k_p+k_{p'}\right)\left(\delta_{0p'}-\delta_{0p}\right)\right\}\right.$$

$$\left.-2\sin\left\{\frac{1}{2}\left(k_p-k_{p'}\right)\left(\delta_{0p'}-\delta_{0p}\right)\right\}\cos\left\{\frac{1}{2}\left(k_p+k_{p'}\right)\left(\delta_{0p'}-\delta_{0p}\right)+\frac{\pi}{4}\right\}\right]$$

$$+\frac{c^2}{k_p+k_{p'}}\left[2\sin\left\{\frac{1}{2}\left(k_p+k_{p'}\right)\left(\delta_{0p'}-\delta_{0p}\right)+\frac{\pi}{4}\right\}\cos\left\{\frac{1}{2}\left(k_p-k_{p'}\right)\left(\delta_{0p'}-\delta_{0p}\right)\right\}\right.$$

$$\left.-2\sin\left\{\frac{1}{2}\left(k_p+k_{p'}\right)\left(\delta_{0p'}-\delta_{0p}\right)\right\}\cos\left\{\frac{1}{2}\left(k_p-k_{p'}\right)\left(\delta_{0p'}-\delta_{0p}\right)\right\}\right]$$

where

$$k_p\ell=\left(p-1/4\right)\pi$$

$$k_{p'}\ell=\left(p'-1/4\right)\pi$$

$$k_p\left(d+\delta_{0p}\right)=\left(n+1/8\right)\pi$$

$$k_{p'}\left(d+\delta_{0p'}\right)=\left(n+1/8\right)\pi$$

$$k_p\left(d+\delta_{0p'}\right)=\left(n+1/8\right)\pi-k_p\left(\delta_{0p}-\delta_{0p'}\right)$$

$$k_{p'}\left(d+\delta_{0p}\right)=\left(n+1/8\right)\pi-k_{p'}\left(\delta_{0p'}-\delta_{0p}\right)$$

$$\left(k_p-k_{p'}\right)\left(d+\delta_{0p}\right)=k_{p'}\left(\delta_{0p'}-\delta_{0p}\right)$$

$$\left(k_p-k_{p'}\right)\left(d+\delta_{0p'}\right)=k_p\left(\delta_{0p'}-\delta_{0p}\right)$$

$$\left(k_p+k_{p'}\right)\left(d+\delta_{0p}\right)=2n\pi+\pi/4-k_{p'}\left(\delta_{0p'}-\delta_{0p}\right)$$

$$\left(k_p+k_{p'}\right)\left(d+\delta_{0p'}\right)=2n\pi+\pi/4+k_p\left(\delta_{0p'}-\delta_{0p}\right)$$

$$\delta_{0p'}-\delta_{0p}=\frac{\left(p-p'\right)\left(n+1/8\right)}{\left(p-1/4\right)\left(p'-1/4\right)}=O\left(\frac{k_p-k_{p'}}{k_p}d\right)$$

Now because we expect

$$\frac{1}{2}\left(k_p-k_{p'}\right)\left(\delta_{0p'}-\delta_{0p}\right)=O\left[\frac{\left(k_p-k_{p'}\right)^2d^2}{k_pd}\right]<<1$$

we can expand the sinusoids to find

$$\int_{-\ell}^{\ell}u_p^T\left(x,0\right)u_{p'}^T\left(x,0\right)dx\sim c^2\ell\frac{\sin\left(p-p'\right)\pi}{\left(p-p'\right)\pi}$$

$$+c^2\left(\delta_{0p'}-\delta_{0p}\right)\left[\cos\left\{\frac{1}{2}\left(k_p+k_{p'}\right)\left(\delta_{0p'}-\delta_{0p}\right)\right\}-\cos\left\{\frac{1}{2}\left(k_p+k_{p'}\right)\left(\delta_{0p'}-\delta_{0p}\right)+\frac{\pi}{4}\right\}\right]$$

$$+\frac{2c^2}{k_p+k_{p'}}\left[\sin\left\{\frac{1}{2}\left(k_p+k_{p'}\right)\left(\delta_{0p'}-\delta_{0p}\right)+\frac{\pi}{4}\right\}-\sin\left\{\frac{1}{2}\left(k_p+k_{p'}\right)\left(\delta_{0p'}-\delta_{0p}\right)\right\}\right]$$

$$\sim c^2\ell\frac{\sin\left(p-p'\right)\pi}{\left(p-p'\right)\pi}+2c^2\left(\delta_{0p'}-\delta_{0p}\right)\sin\left(\frac{\pi}{8}\right)\sin\left\{\frac{1}{2}\left(k_p+k_{p'}\right)\left(\delta_{0p'}-\delta_{0p}\right)+\frac{\pi}{8}\right\}$$

$$+\frac{4c^2}{k_p+k_{p'}}\sin\left(\frac{\pi}{8}\right)\cos\left\{\frac{1}{2}\left(k_p+k_{p'}\right)\left(\delta_{0p'}-\delta_{0p}\right)+\frac{\pi}{8}\right\}$$

$$=c^2\ell\left[\delta_{pp'}+O\left\{\frac{\left(k_p-k_{p'}\right)d}{k_p\ell}\right\}+O\left\{\frac{1}{\left(k_p+k_{p'}\right)\ell}\right\}\right]$$

Thus orthogonality approximately holds.

### B.2.2 scar functions from elliptical analysis

Suppose we test the orthogonality with the Region 1 and 2 functions. The field on axis, in Region 1

$$u_p(x,0) \sim \frac{2v}{(2\gamma)^{1/4}\left|U_+'(s,0)\right|\sqrt{A\ln\left(\frac{\ell+d}{\ell-d}\right)}}\sqrt{2d}\left(d^2-x^2\right)^{-1/4}\cos\left[k_p x + p_1(x)\right] \text{ , Region 1}$$

$$\sim c_3\frac{e^{\pi s/4}}{\exp\left(\pi|s|/4\right)}\left(1-x^2/d^2\right)^{-1/4}\cos\left[k_p x + p_1(x)\right]$$

and in Region 2

$$u_p(x,0) \sim \frac{2v}{(2\gamma)^{1/4}\left|U_+'(-s,0)\right|\sqrt{A\ln\left(\frac{\ell+d}{\ell-d}\right)}}\sqrt{2d}\left(x^2-d^2\right)^{-1/4}\cos\left[k_p x - \pi/4 + p_2(x)\right] \text{ , Region 2}$$

$$\sim c_3\frac{e^{-\pi s/4}}{\exp\left(\pi|s|/4\right)}\left(x^2/d^2-1\right)^{-1/4}\cos\left[k_p x - \pi/4 + p_2(x)\right]$$

$$s\ln\left(\frac{\ell+d}{\ell-d}\right) = 2(k-k_p)\ell$$

$$\frac{\left|U_+'(-s,0)\right|}{\left|U_+'(s,0)\right|} = e^{\pi s/2}$$

$$d = \ell\sqrt{1-R/\ell}$$

$$k_p\ell = \pi(p-1/4)$$

$$p_1(x) = \frac{1}{2}s\left\{\ln\left(\frac{\ell+d}{\ell-d}\right)(x/\ell) - \ln\left(\frac{d+x}{d-x}\right)\right\}$$

$$p_2(x) = \frac{1}{2}s\left\{\ln\left(\frac{\ell+d}{\ell-d}\right)(x/\ell) - \ln\left(\frac{x+d}{x-d}\right)\right\}$$

We are interested in

$$I_{pp'} = 2\int_0^d u_p(x,0)\,u_{p'}(x,0)\,dx + 2\int_d^\ell u_p(x,0)\,u_{p'}(x,0)\,dx$$

$$= 2c_3^2\frac{e^{\pi\left(s_p+s_{p'}\right)/4}}{e^{\pi\left(|s_p|+|s_{p'}|\right)/4}}\int_0^d\left(1-x^2/d^2\right)^{-1/2}\cos\left[k_p x + p_1^{(p)}(x)\right]\cos\left[k_{p'}x + p_1^{(p')}(x)\right]dx$$

$$+2c_3^2\frac{e^{-\pi\left(s_p+s_{p'}\right)/4}}{e^{\pi\left(|s_p|+|s_{p'}|\right)/4}}\int_d^\ell\left(x^2/d^2-1\right)^{-1/2}\cos\left[k_p x - \pi/4 + p_2^{(p)}(x)\right]\cos\left[k_{p'}x - \pi/4 + p_2^{(p')}(x)\right]dx$$

First look at $p = p'$

$$I_{pp} = 2\int_0^d u_p^2(x,0)\,dx + 2\int_d^\ell u_p^2(x,0)\,dx$$

$$= 2c_3^2\frac{e^{\pi s_p/2}}{e^{\pi|s_p|/2}}\int_0^d \left(1-x^2/d^2\right)^{-1/2}\cos^2\left[k_p x + p_1(x)\right]dx$$

$$+2c_3^2\frac{e^{-\pi s_p/2}}{e^{\pi|s_p|/2}}\int_d^\ell \left(x^2/d^2-1\right)^{-1/2}\cos^2\left[k_p x - \pi/4 + p_2(x)\right]dx$$

If we average over the rapidly varying cosines

$$I_{pp} \approx c_3^2 d\frac{e^{\pi s_p/2}}{e^{\pi|s_p|/2}}\int_0^1 \left(1-x^2\right)^{-1/2}dx + c_3^2 d\frac{e^{-\pi s_p/2}}{e^{\pi|s_p|/2}}\int_1^{\ell/d}\left(x^2-1\right)^{-1/2}dx$$

$$\approx c_3^2 d\frac{e^{\pi s_p/2}}{e^{\pi|s_p|/2}}\pi/2 + c_3^2 d\frac{e^{-\pi s_p/2}}{e^{\pi|s_p|/2}}\mathrm{Arccosh}\left(\ell/d\right)$$

Next look at $p' \neq p$ but $p' - p << p$

$$I_{p,p'} = 2\int_0^d u_p(x,0)\,u_{p'}(x,0)\,dx + 2\int_d^\ell u_p(x,0)\,u_{p'}(x,0)\,dx$$

$$= 2c_3^2\frac{e^{\pi\left(s_p+s_{p'}\right)/4}}{e^{\pi\left(|s_p|+|s_{p'}|\right)/4}}\int_0^d \left(1-x^2/d^2\right)^{-1/2}\cos\left[k_p x + p_1^{(p)}(x)\right]\cos\left[k_{p'} x + p_1^{(p')}(x)\right]dx$$

$$+2c_3^2\frac{e^{-\pi\left(s_p+s_{p'}\right)/4}}{e^{\pi\left(|s_p|+|s_{p'}|\right)/4}}\int_d^\ell \left(x^2/d^2-1\right)^{-1/2}\cos\left[k_p x - \pi/4 + p_2^{(p)}(x)\right]\cos\left[k_{p'} x - \pi/4 + p_2^{(p')}(x)\right]dx$$

$$= c_3^2\frac{e^{\pi\left(s_p+s_{p'}\right)/4}}{e^{\pi\left(|s_p|+|s_{p'}|\right)/4}}\int_0^d \left(1-x^2/d^2\right)^{-1/2}$$

$$\left\{\cos\left[\left(k_{p'}-k_p\right)x + p_1^{(p')}(x) - p_1^{(p)}(x)\right] + \cos\left[\left(k_{p'}+k_p\right)x + p_1^{(p')}(x) + p_1^{(p)}(x)\right]\right\}dx$$

$$+c_3^2\frac{e^{-\pi\left(s_p+s_{p'}\right)/4}}{e^{\pi\left(|s_p|+|s_{p'}|\right)/4}}\int_d^\ell \left(x^2/d^2-1\right)^{-1/2}$$

$$\left\{\cos\left[\left(k_{p'}-k_p\right)x + p_2^{(p')}(x) - p_2^{(p)}(x)\right] + \sin\left[\left(k_{p'}+k_p\right)x + p_2^{(p')}(x) + p_2^{(p)}(x)\right]\right\}dx$$

The second terms in the integrands are rapidly varying and generate contributions that are $O\left[\left(k_{p'}+k_p\right)^{-1/2}\ell^{-1/2}\right]$ [36]. Because these are in reality nonsingular and continuous, if Region 3 is included, we expect them to be even smaller. These contributions were also neglected when $p = p'$ due to the application of the averaging to the trigonometric functions in the integrand. Noting that

$$(k_{p'}-k_p)\,\ell=(p'-p)\,\pi=\frac{1}{2}\,(s_p-s_{p'})\ln\left(\frac{\ell+d}{\ell-d}\right)$$

$$p_1^{(p')}(x)-p_1^{(p)}(x)=\frac{1}{2}\,(s_{p'}-s_p)\left\{\ln\left(\frac{\ell+d}{\ell-d}\right)(x/\ell)-\ln\left(\frac{d+x}{d-x}\right)\right\}$$

$$p_2^{(p')}(x)-p_2^{(p)}(x)=\frac{1}{2}\,(s_{p'}-s_p)\left\{\ln\left(\frac{\ell+d}{\ell-d}\right)(x/\ell)-\ln\left(\frac{x+d}{x-d}\right)\right\}$$

we can write

$$I_{pp'}\sim c_3^2 d\frac{e^{\pi\left(s_p+s_{p'}\right)/4}}{e^{\pi\left(|s_p|+|s_{p'}|\right)/4}}\int_0^1\left(1-x^2\right)^{-1/2}\cos\left[(p'-p)\,\pi\ln\left(\frac{1+x}{1-x}\right)/\ln\left(\frac{\ell+d}{\ell-d}\right)\right]dx$$

$$+c_3^2\frac{e^{-\pi\left(s_p+s_{p'}\right)/4}}{e^{\pi\left(|s_p|+|s_{p'}|\right)/4}}\int_1^{\ell/d}\left(x^2-1\right)^{-1/2}\cos\left[(p'-p)\,\pi\ln\left(\frac{x+1}{x-1}\right)/\ln\left(\frac{\ell+d}{\ell-d}\right)\right]dx$$

In the first integral we let $\ln\left[(1+x)/(1-x)\right]=2y$ or $x=\tanh(y)$

$$\int_0^1\left(1-x^2\right)^{-1/2}\cos\left[(p'-p)\,\pi\ln\left(\frac{1+x}{1-x}\right)/\ln\left(\frac{\ell+d}{\ell-d}\right)\right]dx$$

$$=\int_0^\infty\cos\left[2\pi\,(p'-p)\,y/\ln\left(\frac{\ell+d}{\ell-d}\right)\right]\frac{dy}{\cosh(y)}$$

$$=\frac{\pi}{2}/\cosh\left[(p'-p)\,\pi^2/\ln\left(\frac{\ell+d}{\ell-d}\right)\right]$$

For the parameters here this equals $\pi/2\approx 1.570796$ , $|p-p'|=0$ and $4\times10^{-7}$ , $|p-p'|=\dot{1}$ (it is smaller still for $|p-p'|\geq 2$); it can thus be neglected unless $p=p'$. In the second integral we let $\ln\left((x+1)/(x-1)\right)=2y$ or $x=\coth(y)$

$$\int_1^{\ell/d}\left(x^2-1\right)^{-1/2}\cos\left[(p'-p)\,\pi\ln\left(\frac{x+1}{x-1}\right)/\ln\left(\frac{\ell+d}{\ell-d}\right)\right]dx$$

$$=\int_{\frac{1}{2}\ln\left(\frac{\ell+d}{\ell-d}\right)}^\infty\cos\left[2\pi\,(p'-p)\,y/\ln\left(\frac{\ell+d}{\ell-d}\right)\right]\frac{dy}{\sinh(y)}$$

$$=\frac{1}{2}\ln\left(\frac{\ell+d}{\ell-d}\right)\int_1^\infty\cos\left(\pi\,(p'-p)\,y\right)\frac{dy}{\sinh\left[\frac{1}{2}y\ln\left(\frac{\ell+d}{\ell-d}\right)\right]}$$

$$=-\frac{1}{2}\,(-1)^{p'-p}\ln\left(\frac{\ell+d}{\ell-d}\right)\int_0^\infty\cos\left(\pi\,(p'-p)\,y\right)\frac{dy}{\sinh\left[\frac{1}{2}\,(y+1)\ln\left(\frac{\ell+d}{\ell-d}\right)\right]}$$

For the parameters here this equals $\mathrm{Arccosh}(\ell/d)\approx 1.8685511$ , $|p'-p|=0$; $-0.075259327$ , $|p'-p|=1$; $0.0229565$ , $|p'-p|=2$; $-0.010795965$ , $|p'-p|=3$. It is thus quite small unless $p=p'$.

### B.2.3 orthogonality with normal derivative

We are also interested in examination of the integration involving the normal derivative of the scar functions along the orbit

$$I^n_{pp'} = 2\int_0^d \frac{\partial}{\partial\omega}\frac{1}{\omega}\frac{\partial u_p}{\partial y}(x,0)\,u_{p'}(x,0)\,dx + 2\int_d^\ell \frac{\partial}{\partial\omega}\frac{1}{\omega}\frac{\partial u_p}{\partial y}(x,0)\,u_{p'}(x,0)\,dx$$

This arises in the normalization condition. To avoid a pole singularity at the focus we must also use the solution in Region 3. In fact we could define a correction to the orthogonality resulting from Region 3 as

$$I^n_{pp'} = 2\int_0^{d-\Delta} \frac{\partial}{\partial\omega}\frac{1}{\omega}\frac{\partial u^1_p}{\partial y}(x,0)\,u^1_{p'}(x,0)\,dx + 2\int_{d+\Delta}^\ell \frac{\partial}{\partial\omega}\frac{1}{\omega}\frac{\partial u^2_p}{\partial y}(x,0)\,u^2_{p'}(x,0)\,dx + N^3_{pp'}$$

where

$$N^3_{pp'} = 2\int_{\sqrt{2\Delta_0/d}}^{\sqrt{2\Delta/d}} \left[u_{p'}\frac{\partial}{\partial\omega}\frac{1}{\omega}\left(\frac{\partial u_p}{\partial\zeta}\right) - u^1_{p'}\frac{\partial}{\partial\omega}\frac{1}{\omega}\left(\frac{\partial u^1_p}{\partial\zeta}\right)\right]d\xi'$$

$$+2\int_{\sqrt{2\Delta_0/d}}^{\sqrt{2\Delta/d}} \left[u_{p'}\frac{\partial}{\partial\omega}\frac{1}{\omega}\left(\frac{\partial u_p}{\partial\xi'}\right) - u^2_{p'}\frac{\partial}{\partial\omega}\frac{1}{\omega}\left(\frac{\partial u^2_p}{\partial\xi'}\right)\right]d\zeta$$

where $\Delta_0 << \Delta$ is introduced to avoid singularities at the focal point. The idea is to let $\Delta_0$ shrink toward 0 and allow $\Delta$ to grow to allow cancellation between the Region 3 and Region 1 and 2 solutions, but still approximate the functions near the focal point. Approximating near the focal point for small $\xi'$ and small $\zeta$ in Region 1

$$\frac{\partial}{\partial\omega}\frac{1}{\omega}\left(\frac{\partial u^1_p}{\partial\zeta}\right) \sim 2c\frac{1}{\omega}\sqrt{2\gamma}\frac{\partial\Phi_0}{\partial\omega}\,\mathrm{Im}\left[e^{-i\pi/4}U'_+(s,0)\right]\frac{1}{\sqrt{\xi'}}\cos\left\{\gamma\left(1-\xi'^2/2\right)-s\sigma\right\}$$

$$u^1_p \sim 2\frac{1}{\sqrt{\xi'}}c\frac{\mathrm{Im}\left[e^{-i\pi/4}U'_+(s,0)\right]}{\left|U'_+(s,0)\right|^2}\cos\left\{\gamma\left(1-\xi'^2/2\right)-s\sigma\right\}$$

and in Region 2

$$\frac{\partial}{\partial\omega}\frac{1}{\omega}\left(\frac{\partial u^2_p}{\partial\xi'}\right) = -\sqrt{2\gamma}\frac{2}{\sqrt{\zeta}}c\frac{1}{\omega}\frac{\partial\Phi_0}{\partial\omega}\,\mathrm{Im}\left[U'_+(-s,0)\right]\cos\left\{\gamma\left(1+\zeta^2/2\right)+s\sigma'-\pi/4\right\}$$

$$u^2_p \sim \frac{2}{\sqrt{\zeta}}c\frac{\mathrm{Im}\left[U'_+(-s,0)\right]}{\left|U'_+(-s,0)\right|^2}\cos\left\{\gamma\left(1+\zeta^2/2\right)+s\sigma'-\pi/4\right\}$$

In Region 3 we have to introduce the focal shift $\delta$. To the left of the focus at $d+\delta$

$$\frac{\partial}{\partial\omega}\frac{1}{\omega}\left(\frac{\partial u_p}{\partial\zeta}\right) = \frac{1}{2}(-1)^n(2\gamma)^{3/4}\sec(\Phi_0/2)$$

$$c\,\mathrm{Re}\left[U_+\left(-s,\widetilde{\xi}'\sqrt{2\gamma}\right)+e^{-i\Phi_0}U^*_+\left(-s,\widetilde{\xi}'\sqrt{2\gamma}\right)\right]\frac{1}{\omega}\frac{\partial\Phi_0}{\partial\omega}\,\mathrm{Re}\left[ie^{i\pi/4}e^{i\Phi_0}U^{*\prime}_+(s,0)\right]$$

$$= \frac{1}{2}(-1)^n (2\gamma)^{3/4} \left|U_+'(s,0)\right| c\,\mathrm{Re}\left[U_+\left(-s,\widehat{\xi}'\sqrt{2\gamma}\right) - \frac{U_+'(-s,0)}{U_+^{*\prime}(-s,0)} U_+^*\left(-s,\widehat{\xi}'\sqrt{2\gamma}\right)\right] \frac{1}{\omega}\frac{\partial \Phi_0}{\partial \omega}$$

$$u_p = (-1)^n (2\gamma)^{1/4} \sec(\Phi_0/2)$$

$$c\,\mathrm{Re}\left[U_+\left(-s,\widehat{\xi}'\sqrt{2\gamma}\right) + e^{-i\Phi_0} U_+^*\left(-s,\widehat{\xi}'\sqrt{2\gamma}\right)\right] \mathrm{Re}\left[e^{-i\pi/4} U_+(s,0) + e^{i\pi/4} e^{i\Phi_0} U_+^*(s,0)\right]$$

$$= (-1)^n (2\gamma)^{1/4} c\,\mathrm{Re}\left[U_+\left(-s,\widehat{\xi}'\sqrt{2\gamma}\right) - \frac{U_+'(-s,0)}{U_+^{*\prime}(-s,0)} U_+^*\left(-s,\widehat{\xi}'\sqrt{2\gamma}\right)\right] / \left|U_+'(s,0)\right|$$

$$\widehat{\xi}' \approx \sqrt{2(d+\delta-x)/d}$$

where

$$x = d\cos\xi'$$

$$x = \delta + d\cos\widehat{\xi}'$$

$$\widehat{\xi}' = \sqrt{2\delta/d + \xi'^2}$$

$$\mathrm{Re}\left[e^{-i\pi/4} U_+(s,0) + e^{i\pi/4} e^{i\Phi_0} U_+^*(s,0)\right] = \mathrm{Im}\left[e^{-i\pi/4} U_+'(s,0)\right] / \left|U_+'(s,0)\right|^2$$

$$e^{i\Phi_0} = i\frac{U_+'(s,0)}{U_+^{*\prime}(s,0)}$$

To the right of the focus

$$\frac{\partial}{\partial\omega}\frac{1}{\omega}\left(\frac{\partial u_p}{\partial\zeta}\right) = \frac{1}{2}(-1)^n (2\gamma)^{3/4} \sec(\Phi_0/2)$$

$$c\frac{1}{\omega}\frac{\partial\Phi_0}{\partial\omega}\,\mathrm{Re}\left[-ie^{-i\Phi_0} U_+^{*\prime}(-s,0)\right] \mathrm{Re}\left[e^{-i\pi/4} U_+\left(s,\widehat{\zeta}\sqrt{2\gamma}\right) + e^{i\pi/4} e^{i\Phi_0} U_+^*\left(s,\widehat{\zeta}\sqrt{2\gamma}\right)\right]$$

$$= -\frac{1}{2}(-1)^n (2\gamma)^{3/4} \left|U_+'(-s,0)\right| c\frac{1}{\omega}\frac{\partial\Phi_0}{\partial\omega}\,\mathrm{Re}\left[e^{-i\pi/4} U_+\left(s,\widehat{\zeta}\sqrt{2\gamma}\right) + e^{i\pi/4} i\frac{U_+'(s,0)}{U_+^{*\prime}(s,0)} U_+^*\left(s,\widehat{\zeta}\sqrt{2\gamma}\right)\right]$$

$$u_p = (-1)^n (2\gamma)^{1/4} \sec(\Phi_0/2)$$

$$c\,\mathrm{Re}\left[U_+(-s,0) + e^{-i\Phi_0} U_+^*(-s,0)\right] \mathrm{Re}\left[e^{-i\pi/4} U_+\left(s,\widehat{\zeta}\sqrt{2\gamma}\right) + e^{i\pi/4} e^{i\Phi_0} U_+^*\left(s,\widehat{\zeta}\sqrt{2\gamma}\right)\right]$$

$$= (-1)^n (2\gamma)^{1/4} c \operatorname{Re}\left[e^{-i\pi/4} U_+\left(s, \widehat{\zeta}\sqrt{2\gamma}\right) + e^{i\pi/4} i \frac{U'_+(s,0)}{U^{*\prime}_+(s,0)} U^*_+\left(s, \widehat{\zeta}\sqrt{2\gamma}\right)\right] / \left|U'_+(-s,0)\right|$$

$$\widehat{\zeta} \approx \sqrt{2(x-d-\delta)/d}$$

where

$$x = d\cosh\zeta$$

$$x = \delta + d\cosh\widehat{\zeta}$$

$$\sqrt{\zeta^2 - 2\delta/d} = \widehat{\zeta}$$

$$x = \delta + d\cos\widehat{\xi}'$$

$$\widehat{\xi}' = \sqrt{2\delta/d - \zeta^2}$$

$$\operatorname{Re}\left[U_+(-s,0) + e^{-i\Phi_0} U^*_+(-s,0)\right] = \operatorname{Im}\left[U'_+(-s,0)\right] / \left|U'_+(-s,0)\right|^2$$

$$e^{-i\Phi_0} = -\frac{U'_+(-s,0)}{U^{*\prime}_+(-s,0)}$$

$$\sec(\Phi_0/2) = \frac{\left|U'_+(-s,0)\right|}{\operatorname{Im}\left[U'_+(-s,0)\right]} = \frac{\left|U'_+(s,0)\right|}{\operatorname{Im}\left[e^{-i\pi/4} U'_+(s,0)\right]}$$

This procedure is quite complicated, but can be carried out. We have not written out the fact that $u_{p'}$ may require a shifted focal point location from the normal derivative with order $p$. Instead, we make the following qualitative argument. Since the scar functions and their normal derivatives are continuous and nonsingular when Region 3 is included, we expect that for $p = p'$ there will be phase coherence along the orbit and a large integrated value for $I^n_{pp}$. When $p \neq p'$ we expect phase incoherence along the orbit and a smaller value for $I^n_{pp'}$. In this latter case the local region within, say half a wavelength of the focal point, will contribute to the integral, however this is only a limited contribution compared to the integral along the entire orbit length when $p = p'$. Furthermore, when $p \neq p'$ these shifted focal points will not align between the function and derivative, which should decrease the contribution near this point relative to the $p = p'$ term.

## B.3 Normalization in Stadium Cavity And Focal Point Contribution

In this section we bring in the focal region into the calculation involved in the energy theorem

$$i2\varepsilon_0 \int_A |u|^2 \, dS = \frac{i}{\mu_0} \int_C \left[-\frac{\partial u}{\partial \omega}\frac{1}{\omega}\left(\frac{\partial u^+_p}{\partial n} - \frac{\partial u^-_p}{\partial n}\right)^* + u^* \frac{\partial}{\partial \omega}\frac{1}{\omega}\left(\frac{\partial u^+_p}{\partial n} - \frac{\partial u^-_p}{\partial n}\right)\right] d\ell$$

for the normalization of the scar component. This leads to the condition along the orbit

$$2\mu_0\varepsilon_0\int_A |u|^2\,dS = \int_{-\ell}^{\ell}\left[u_p\frac{1}{\omega}\frac{\partial}{\partial\omega}\left(\frac{\partial u_p^+}{\partial n}-\frac{\partial u_p^-}{\partial n}\right)\right]d\ell$$

or setting the area integral to unity and specializing to the elliptic cylinder system

$$\varepsilon_0\mu_0 = \int_0^{\pi/2}\left[-\frac{\partial u_p}{\partial\omega}\frac{1}{\omega}\left(\frac{\partial u_p^+}{\partial\zeta}-\frac{\partial u_p^-}{\partial\zeta}\right)+u_p\frac{\partial}{\partial\omega}\frac{1}{\omega}\left(\frac{\partial u_p^+}{\partial\zeta}-\frac{\partial u_p^-}{\partial\zeta}\right)\right]d\xi$$

$$+\int_0^{\zeta_0}\left[-\frac{\partial u_p}{\partial\omega}\frac{1}{\omega}\left(\frac{\partial u_p^+}{\partial\xi'}-\frac{\partial u_p^-}{\partial\xi'}\right)+u_p\frac{\partial}{\partial\omega}\frac{1}{\omega}\left(\frac{\partial u_p^+}{\partial\xi'}-\frac{\partial u_p^-}{\partial\xi'}\right)\right]d\zeta$$

**B.3.1 transition to region three**

The principal value in the main body of the report requires some further justification. Suppose we first transition from Region 1 to Region 3 and back to Region 2 by adding a correction $N_3(s)$ to the energy theorem result from the main body of the report

$$\varepsilon_0\mu_0 = 16c^2\sqrt{2\gamma}\mu_0\varepsilon_0\frac{\partial\Phi_0}{\partial k^2}\frac{\mathrm{Im}^2\left[e^{-i\pi/4}U_+'(s,0)\right]}{\left|U_+'(s,0)\right|^2}\int_{\sqrt{2\Delta/d}}^{\pi/2}\cos^2\left(\gamma\cos\xi'-s\sigma\right)\frac{d\xi'}{\sin\xi'}$$

$$-16c^2\sqrt{2\gamma}\mu_0\varepsilon_0\frac{\partial\Phi_0}{\partial k^2}\frac{\mathrm{Im}^2\left[U_+'(-s,0)\right]}{\left|U_+'(-s,0)\right|^2}\int_{\sqrt{2\Delta/d}}^{\zeta_0}\cos^2\left(\gamma\cosh\zeta+s\sigma'-\pi/4\right)\frac{d\zeta}{\sinh\zeta}$$

$$+N_3(s)$$

where

$$N_3(s) = \int_0^{\sqrt{2\Delta/d}}u_p\frac{\partial}{\partial\omega}\frac{1}{\omega}\left(\frac{\partial u_p^+}{\partial\zeta}-\frac{\partial u_p^-}{\partial\zeta}\right)d\xi'$$

$$+\int_0^{\sqrt{2\Delta/d}}u_p\frac{\partial}{\partial\omega}\frac{1}{\omega}\left(\frac{\partial u_p^+}{\partial\xi'}-\frac{\partial u_p^-}{\partial\xi'}\right)d\zeta$$

and

$$\frac{\mathrm{Im}^2\left[U_+'(-s,0)\right]}{\left|U_+'(-s,0)\right|^2} = \frac{\mathrm{Im}^2\left[e^{-i\pi/4}U_+'(s,0)\right]}{\left|U_+'(s,0)\right|^2}$$

The question is how we can simplify these expressions, including the Region 3 term, for high frequency? First from a trigonometric identity

$$\varepsilon_0\mu_0 = 8c^2\sqrt{2\gamma}\mu_0\varepsilon_0\frac{\partial\Phi_0}{\partial k^2}\frac{\mathrm{Im}^2\left[e^{-i\pi/4}U_+'(s,0)\right]}{\left|U_+'(s,0)\right|^2}\int_{\sqrt{2\Delta/d}}^{\pi/2}\left[1+\cos\left(2\gamma\cos\xi'-2s\sigma\right)\right]\frac{d\xi'}{\sin\xi'}$$

$$-8c^2\sqrt{2\gamma}\mu_0\varepsilon_0\frac{\partial\Phi_0}{\partial k^2}\frac{\mathrm{Im}^2\left[U_+'\left(-s,0\right)\right]}{\left|U_+'\left(-s,0\right)\right|^2}\int_{\sqrt{2\Delta/d}}^{\zeta_0}\left[1+\cos\left(2\gamma\cosh\zeta+2s\sigma'-\pi/2\right)\right]\frac{d\zeta}{\sinh\zeta}$$

$$+N_3\left(s\right)$$

The leading terms lead to the principal value result we had previously because $2\Delta/d << 1$

$$\varepsilon_0\mu_0=4c^2\sqrt{2\gamma}\mu_0\varepsilon_0\frac{\partial\Phi_0}{\partial k^2}\frac{\mathrm{Im}^2\left[e^{-i\pi/4}U_+'\left(s,0\right)\right]}{\left|U_+'\left(s,0\right)\right|^2}\ln\left(\frac{\ell+d}{\ell-d}\right)$$

$$+8c^2\sqrt{2\gamma}\mu_0\varepsilon_0\frac{\partial\Phi_0}{\partial k^2}\frac{\mathrm{Im}^2\left[e^{-i\pi/4}U_+'\left(s,0\right)\right]}{\left|U_+'\left(s,0\right)\right|^2}\int_{\sqrt{2\Delta/d}}^{\pi/2}\cos\left(2\gamma\cos\xi'-2s\sigma\right)\frac{d\xi'}{\sin\xi'}$$

$$-8c^2\sqrt{2\gamma}\mu_0\varepsilon_0\frac{\partial\Phi_0}{\partial k^2}\frac{\mathrm{Im}^2\left[U_+'\left(-s,0\right)\right]}{\left|U_+'\left(-s,0\right)\right|^2}\int_{\sqrt{2\Delta/d}}^{\zeta_0}\sin\left(2\gamma\cosh\zeta+2s\sigma'\right)\frac{d\zeta}{\sinh\zeta}$$

$$+N_3\left(s\right)$$

Expansion of the coordinate transformations near the focal point

$$x=d\cosh\zeta\cos\xi'\sim d\left(1+\zeta^2/2\right)\left(1-\xi'^2/2\right)\sim d\left(1+\zeta^2/2-\xi'^2/2\right)$$

$$y=d\sinh\zeta\sin\xi'\sim d\zeta\xi'\left(1+\zeta^2/6\right)\left(1-\xi'^2/6\right)\sim d\zeta\xi'\left(1+\zeta^2/6-\xi'^2/6\right)$$

leads to

$$\widehat{\xi}'\approx\sqrt{2\left(d+\delta-x\right)/d}$$

$$x=d\cos\xi'$$

$$x=\delta+d\cos\widehat{\xi}'$$

$$\widehat{\xi}'=\sqrt{2\delta/d+\xi'^2}$$

and

$$\widehat{\zeta}\approx\sqrt{2\left(x-d-\delta\right)/d}$$

$$x=d\cosh\zeta$$

$$x=\delta+d\cosh\widehat{\zeta}$$

$$\sqrt{\zeta^2 - 2\delta/d} = \widehat{\zeta}$$

$$x = \delta + d\cos\widehat{\xi}'$$

$$\widehat{\xi}' = \sqrt{2\delta/d - \zeta^2}$$

where the $\widehat{\xi}', \widehat{\zeta}$ coordinates are shifted relative to the $\xi', \zeta$ coordinates by the focal shift $\delta$.

### B.3.2 Cartesian justification of principal value

Because of complications in the calculation associated with the focal point shift, it is much simpler to perform the calculation in Cartesian coordinates. In Region 1

$$u_p = 2\frac{\mathrm{Im}\left[e^{-i\pi/4}U'_+(s,0)\right]}{\left|U'_+(s,0)\right|^2} c\left(1 - x^2/d^2\right)^{-1/4} \cos\left[kx + \frac{1}{2}s\ln\left(\frac{d-x}{d+x}\right)\right],\ \xi' = \pi/2 - \xi$$

$$\sim 2^{3/4}\frac{\mathrm{Im}\left[e^{-i\pi/4}U'_+(s,0)\right]}{\left|U'_+(s,0)\right|^2} c\left(1 - x/d\right)^{-1/4} \cos\left[kx + \frac{1}{2}s\ln\left(\frac{d-x}{2d}\right)\right]$$

$$\frac{\partial}{\partial\omega}\frac{1}{\omega}\left(\frac{\partial u_p^+}{\partial n} - \frac{\partial u_p^-}{\partial n}\right)$$

$$= 4\,\mathrm{Im}\left[e^{-i\pi/4}U'_+(s,0)\right] c\left(1 - x^2/d^2\right)^{-3/4} \frac{1}{\omega}\frac{\partial\Phi_0}{\partial\omega}\frac{1}{d}\sqrt{2\gamma}\cos\left[kx + \frac{1}{2}s\ln\left(\frac{d-x}{d+x}\right)\right]$$

$$\sim 2^{5/4}\,\mathrm{Im}\left[e^{-i\pi/4}U'_+(s,0)\right] c\left(1 - x/d\right)^{-3/4} \frac{1}{\omega}\frac{\partial\Phi_0}{\partial\omega}\frac{1}{d}\sqrt{2\gamma}\cos\left[kx + \frac{1}{2}s\ln\left(\frac{d-x}{2d}\right)\right]$$

In Region 2

$$u_p = 2\frac{\mathrm{Im}\left[U'_+(-s,0)\right]}{\left|U'_+(-s,0)\right|^2} c\left(x^2/d^2 - 1\right)^{-1/4} \cos\left[kx + \frac{1}{2}s\ln\left(\frac{x-d}{x+d}\right) - \pi/4\right]$$

$$\sim 2^{3/4}\frac{\mathrm{Im}\left[U'_+(-s,0)\right]}{\left|U'_+(-s,0)\right|^2} c\left(x/d - 1\right)^{-1/4} \cos\left[kx + \frac{1}{2}s\ln\left(\frac{x-d}{2d}\right) - \pi/4\right]$$

$$\frac{\partial}{\partial\omega}\frac{1}{\omega}\left(\frac{\partial u_p^+}{\partial n} - \frac{\partial u_p^-}{\partial n}\right)$$

$$= -4\,\mathrm{Im}\left[U'_+(-s,0)\right] c\left(x^2/d^2 - 1\right)^{-3/4} \frac{1}{d}\sqrt{2\gamma}\frac{1}{\omega}\frac{\partial\Phi_0}{\partial\omega}\cos\left[kx + \frac{1}{2}s\ln\left(\frac{x-d}{x+d}\right) - \pi/4\right]$$

$$\sim -2^{5/4}\,\mathrm{Im}\left[U'_+(-s,0)\right] c\left(x/d - 1\right)^{-3/4} \frac{1}{d}\sqrt{2\gamma}\frac{1}{\omega}\frac{\partial\Phi_0}{\partial\omega}\cos\left[kx + \frac{1}{2}s\ln\left(\frac{x-d}{2d}\right) - \pi/4\right]$$

In Region 3 to the left of the focus at $d+\delta$

$$\frac{\partial}{\partial\omega}\frac{1}{\omega}\left(\frac{\partial u_p^+}{\partial n}-\frac{\partial u_p^-}{\partial n}\right)$$

$$=(-1)^n 2(2\gamma)^{3/4}\left|U_+'(s,0)\right|\frac{c}{d\widehat{\xi}'}\operatorname{Re}\left[U_+\left(-s,\widehat{\xi}'\sqrt{2\gamma}\right)-\frac{U_+'(-s,0)}{U_+^{*\prime}(-s,0)}U_+^*\left(-s,\widehat{\xi}'\sqrt{2\gamma}\right)\right]\frac{1}{\omega}\frac{\partial\Phi_0}{\partial\omega}$$

$$u_p=(-1)^n(2\gamma)^{1/4}c\operatorname{Re}\left[U_+\left(-s,\widehat{\xi}'\sqrt{2\gamma}\right)-\frac{U_+'(-s,0)}{U_+^{*\prime}(-s,0)}U_+^*\left(-s,\widehat{\xi}'\sqrt{2\gamma}\right)\right]/\left|U_+'(s,0)\right|$$

$$\widehat{\xi}'\approx\sqrt{2(d+\delta-x)/d}$$

To the right of the focus at $d+\delta$

$$\frac{\partial}{\partial\omega}\frac{1}{\omega}\left(\frac{\partial u_p^+}{\partial n}-\frac{\partial u_p^-}{\partial n}\right)$$

$$=-(-1)^n 2(2\gamma)^{3/4}\frac{1}{d\widehat{\zeta}}\left|U_+'(-s,0)\right|c\frac{1}{\omega}\frac{\partial\Phi_0}{\partial\omega}\operatorname{Re}\left[e^{-i\pi/4}U_+\left(s,\widehat{\zeta}\sqrt{2\gamma}\right)+e^{i\pi/4}i\frac{U_+'(s,0)}{U_+^{*\prime}(s,0)}U_+^*\left(s,\widehat{\zeta}\sqrt{2\gamma}\right)\right]$$

$$u_p=(-1)^n(2\gamma)^{1/4}c\operatorname{Re}\left[e^{-i\pi/4}U_+\left(s,\widehat{\zeta}\sqrt{2\gamma}\right)+e^{i\pi/4}i\frac{U_+'(s,0)}{U_+^{*\prime}(s,0)}U_+^*\left(s,\widehat{\zeta}\sqrt{2\gamma}\right)\right]/\left|U_+'(-s,0)\right|$$

$$\widehat{\zeta}\approx\sqrt{2(x-d-\delta)/d}$$

The normalization integral is

$$\varepsilon_0\mu_0=\frac{1}{2}\int_C\left[-\frac{\partial u_p}{\partial\omega}\frac{1}{\omega}\left(\frac{\partial u_p^+}{\partial n}-\frac{\partial u_p^-}{\partial n}\right)+u_p\frac{\partial}{\partial\omega}\frac{1}{\omega}\left(\frac{\partial u_p^+}{\partial n}-\frac{\partial u_p^-}{\partial n}\right)\right]d\ell$$

Let us assume that the problem is totally even from left to right so that

$$\varepsilon_0\mu_0=\int_{C_+}u_p\frac{\partial}{\partial\omega}\frac{1}{\omega}\left(\frac{\partial u_p^+}{\partial n}-\frac{\partial u_p^-}{\partial n}\right)d\ell$$

where $C_+$ is the contour for positive $x$ values. Thus we write this in terms of the Region 1 and 2 solutions plus a correction from Region 3

$$\varepsilon_0\mu_0=\int_0^d u_p\frac{\partial}{\partial\omega}\frac{1}{\omega}\left(\frac{\partial u_p^+}{\partial n}-\frac{\partial u_p^-}{\partial n}\right)d\ell+\int_d^\ell u_p\frac{\partial}{\partial\omega}\frac{1}{\omega}\left(\frac{\partial u_p^+}{\partial n}-\frac{\partial u_p^-}{\partial n}\right)d\ell$$

$$=\int_0^d u_p^1\frac{\partial}{\partial\omega}\frac{1}{\omega}\left(\frac{\partial u_p^{1+}}{\partial n}-\frac{\partial u_p^{1-}}{\partial n}\right)d\ell+\int_d^\ell u_p^2\frac{\partial}{\partial\omega}\frac{1}{\omega}\left(\frac{\partial u_p^{2+}}{\partial n}-\frac{\partial u_p^{2-}}{\partial n}\right)d\ell$$

$$+N_3(s)$$

where the Region 3 correction is

$$N_3(s) = \int_0^d \left[ u_p \frac{\partial}{\partial \omega} \frac{1}{\omega} \left( \frac{\partial u_p^+}{\partial n} - \frac{\partial u_p^-}{\partial n} \right) - u_p^1 \frac{\partial}{\partial \omega} \frac{1}{\omega} \left( \frac{\partial u_p^{1+}}{\partial n} - \frac{\partial u_p^{1-}}{\partial n} \right) \right] d\ell$$

$$+ \int_d^{d+\delta} \left[ u_p \frac{\partial}{\partial \omega} \frac{1}{\omega} \left( \frac{\partial u_p^+}{\partial n} - \frac{\partial u_p^-}{\partial n} \right) - u_p^2 \frac{\partial}{\partial \omega} \frac{1}{\omega} \left( \frac{\partial u_p^{2+}}{\partial n} - \frac{\partial u_p^{2-}}{\partial n} \right) \right] d\ell$$

$$+ \int_{d+\delta}^{\ell} \left[ u_p \frac{\partial}{\partial \omega} \frac{1}{\omega} \left( \frac{\partial u_p^+}{\partial n} - \frac{\partial u_p^-}{\partial n} \right) - u_p^2 \frac{\partial}{\partial \omega} \frac{1}{\omega} \left( \frac{\partial u_p^{2+}}{\partial n} - \frac{\partial u_p^{2-}}{\partial n} \right) \right] d\ell$$

Note that there may be a cancellation problem as $x \to d$ with the subtracted terms not matching (we only know that the averaged forms match) and thus not forming a principal value integral. This might require displacement to $d \pm \Delta_0$, where $\Delta_0 \to 0$. More will be said about this problem for the case $s = 0$ below.

### B.3.3 region three correction for s equal to zero

Inserting the solutions in this limit

$$u^1 \sim 2^{3/4} c \frac{\cos(\pi/8)}{-U'(0,0)} (1 - x/d)^{-1/4} \cos(k_p x) \text{ , Region 1}$$

$$\frac{\partial}{\partial \omega} \frac{1}{\omega} \left( \frac{\partial u_p^{1+}}{\partial n} - \frac{\partial u_p^{1-}}{\partial n} \right) \sim 2^{5/4} \cos(\pi/8) \left[ -U'(0,0) \right] c (1 - x/d)^{-3/4} \frac{1}{\omega} \frac{\partial \Phi_0}{\partial \omega} \frac{1}{d} \sqrt{2\gamma} \cos(k_p x)$$

$$u^2 \sim 2^{3/4} c \frac{\cos(\pi/8)}{-U'(0,0)} (x/d - 1)^{-1/4} \cos(k_p x - \pi/4) \text{ , Region 2}$$

$$\frac{\partial}{\partial \omega} \frac{1}{\omega} \left( \frac{\partial u_p^{2+}}{\partial n} - \frac{\partial u_p^{2-}}{\partial n} \right) \sim -2^{5/4} \cos(\pi/8) \left[ -U'(0,0) \right] c (x/d - 1)^{-3/4} \frac{1}{d} \sqrt{2\gamma} \frac{1}{\omega} \frac{\partial \Phi_0}{\partial \omega} \cos(k_p x - \pi/4)$$

and

$$u^1 \frac{\partial}{\partial \omega} \frac{1}{\omega} \left( \frac{\partial u_p^{1+}}{\partial n} - \frac{\partial u_p^{1-}}{\partial n} \right) \sim 4c^2 \cos^2(\pi/8) \frac{1}{\omega} \frac{\partial \Phi_0}{\partial \omega} \frac{1}{d} \sqrt{2\gamma} (1 - x/d)^{-1} \cos^2(k_p x)$$

$$u^2 \frac{\partial}{\partial \omega} \frac{1}{\omega} \left( \frac{\partial u_p^{2+}}{\partial n} - \frac{\partial u_p^{2-}}{\partial n} \right) \sim -4c^2 \cos^2(\pi/8) \frac{1}{\omega} \frac{\partial \Phi_0}{\partial \omega} \frac{1}{d} \sqrt{2\gamma} (x/d - 1)^{-1} \cos^2(k_p x - \pi/4)$$

$$\sim 4c^2 \cos^2(\pi/8) \frac{1}{\omega} \frac{\partial \Phi_0}{\partial \omega} \frac{1}{d} \sqrt{2\gamma} (1 - x/d)^{-1} \cos^2(k_p x - \pi/4)$$

where we have used

$$U'_+(0,0) = e^{-i3\pi/8}U'(0,0) = -e^{-i\pi 3/8}\frac{2^{1/4}\sqrt{\pi}}{\Gamma(1/4)}$$

We note that for $s = 0$

$$k_p(d+\delta_0) = (n+1/8)\pi$$

for which

$$\cos(k_p(d+\delta_0)) = \cos(k_p(d+\delta_0) - \pi/4)$$

Thus if we displace the singularity $(1-x/d)^{-1}$ to $(1-x/(d+\delta))^{-1}$ in the above outer region solutions, then the resulting expression is continuous and converges in a principal value sense. Alternatively we can average the rapidly varying cosines and subtract the result

$$2c^2\cos^2(\pi/8)\frac{1}{\omega}\frac{\partial\Phi_0}{\partial\omega}\frac{1}{d}\sqrt{2\gamma}(1-x/d)^{-1}$$

from either side. This averaged result gives a principal value with the singularity at $x = d$. This was the approach used in the main body of the report. Thus any correction should be defined in the same way by subtracting the averaged outer region quantity.

In Region 3 to the left of the focus at $d+\delta$

$$\frac{\partial}{\partial\omega}\frac{1}{\omega}\left(\frac{\partial u_p^+}{\partial n} - \frac{\partial u_p^-}{\partial n}\right)$$

$$= (-1)^n(2\gamma)\left[-U'(0,0)\right]\sqrt{\pi/2}\frac{c}{\sqrt{\widehat{\xi}'}\,d}\,\mathrm{Re}\left[e^{i3\pi/8}\left\{H_{1/4}^{(1)}\left(\gamma\widehat{\xi}'^2/2\right) - iH_{1/4}^{(2)}\left(\gamma\widehat{\xi}'^2/2\right)\right\}\right]\frac{1}{\omega}\frac{\partial\Phi_0}{\partial\omega}$$

$$= (-1)^n(2\gamma)\left[-U'(0,0)\right]\sqrt{\pi}\frac{c}{\sqrt{\widehat{\xi}'}\,d}\cos(\pi/8)\left[J_{1/4}\left(\gamma\widehat{\xi}'^2/2\right) - Y_{1/4}\left(\gamma\widehat{\xi}'^2/2\right)\right]\frac{1}{\omega}\frac{\partial\Phi_0}{\partial\omega}$$

$$= (-1)^n 2(2\gamma)\left[-U'(0,0)\right]\sqrt{\pi/2}\frac{c}{\sqrt{\widehat{\xi}'}\,d}\cos(\pi/8)J_{-1/4}\left(\gamma\widehat{\xi}'^2/2\right)\frac{1}{\omega}\frac{\partial\Phi_0}{\partial\omega}$$

$$u_p = (-1)^n(2\gamma)^{1/2}\sqrt{\widehat{\xi}'}\sqrt{\pi/2}\frac{1}{2}c\,\mathrm{Re}\left[e^{i3\pi/8}\left\{H_{1/4}^{(1)}\left(\gamma\widehat{\xi}'^2/2\right) - iH_{1/4}^{(2)}\left(\gamma\widehat{\xi}'^2/2\right)\right\}\right]/\left[-U'(0,0)\right]$$

$$= (-1)^n(2\gamma)^{1/2}\sqrt{\widehat{\xi}'}\sqrt{\pi}\frac{1}{2}c\cos(\pi/8)\left[J_{1/4}\left(\gamma\widehat{\xi}'^2/2\right) - Y_{1/4}\left(\gamma\widehat{\xi}'^2/2\right)\right]/\left[-U'(0,0)\right]$$

$$= (-1)^n(2\gamma)^{1/2}\sqrt{\widehat{\xi}'}\sqrt{\pi/2}c\cos(\pi/8)J_{-1/4}\left(\gamma\widehat{\xi}'^2/2\right)/\left[-U'(0,0)\right]$$

$$\widehat{\xi}' \approx \sqrt{2(d+\delta_0-x)/d}$$

and the right of the focus at $d+\delta$

$$\frac{\partial}{\partial\omega}\frac{1}{\omega}\left(\frac{\partial u_p^+}{\partial n}-\frac{\partial u_p^-}{\partial n}\right)$$

$$=-\left(-1\right)^n\left(2\gamma\right)\sqrt{\pi/2}\frac{1}{\sqrt{\widehat{\zeta}}d}\left[-U'\left(0,0\right)\right]c\frac{1}{\omega}\frac{\partial\Phi_0}{\partial\omega}\operatorname{Re}\left[e^{i\pi/8}\left\{H_{1/4}^{(1)}\left(\gamma\widehat{\zeta}^2/2\right)-iH_{1/4}^{(2)}\left(\gamma\widehat{\zeta}^2/2\right)\right\}\right]$$

$$=-\left(-1\right)^n\left(2\gamma\right)\sqrt{\pi}\frac{1}{\sqrt{\widehat{\zeta}}d}\left[-U'\left(0,0\right)\right]c\cos\left(\pi/8\right)\frac{1}{\omega}\frac{\partial\Phi_0}{\partial\omega}\left[J_{1/4}\left(\gamma\widehat{\zeta}^2/2\right)-Y_{1/4}\left(\gamma\widehat{\zeta}^2/2\right)\right]$$

$$=-\left(-1\right)^n 2\left(2\gamma\right)\sqrt{\pi/2}\frac{1}{\sqrt{\widehat{\zeta}}d}\left[-U'\left(0,0\right)\right]c\cos\left(\pi/8\right)\frac{1}{\omega}\frac{\partial\Phi_0}{\partial\omega}J_{-1/4}\left(\gamma\widehat{\zeta}^2/2\right)$$

$$u_p=\left(-1\right)^n\left(2\gamma\right)^{1/2}\sqrt{\widehat{\zeta}}\sqrt{\pi/2}\frac{1}{2}c\operatorname{Re}\left[e^{i\pi/8}\left\{H_{1/4}^{(1)}\left(\gamma\widehat{\zeta}^2/2\right)-iH_{1/4}^{(2)}\left(\gamma\widehat{\zeta}^2/2\right)\right\}\right]/\left[-U'\left(0,0\right)\right]$$

$$=\left(-1\right)^n\left(2\gamma\right)^{1/2}\sqrt{\widehat{\zeta}}\sqrt{\pi}\frac{1}{2}c\cos\left(\pi/8\right)\left[J_{1/4}\left(\gamma\widehat{\zeta}^2/2\right)-Y_{1/4}\left(\gamma\widehat{\zeta}^2/2\right)\right]/\left[-U'\left(0,0\right)\right]$$

$$=\left(-1\right)^n\left(2\gamma\right)^{1/2}\sqrt{\widehat{\zeta}}\sqrt{\pi/2}c\cos\left(\pi/8\right)J_{-1/4}\left(\gamma\widehat{\zeta}^2/2\right)/\left[-U'\left(0,0\right)\right]$$

$$\widehat{\zeta}\approx\sqrt{2\left(x-d-\delta_0\right)/d}$$

and thus

$$u_p\frac{\partial}{\partial\omega}\frac{1}{\omega}\left(\frac{\partial u_p^+}{\partial n}-\frac{\partial u_p^-}{\partial n}\right)=2\pi\gamma\sqrt{2\gamma}\frac{c^2}{d}\frac{1}{\omega}\frac{\partial\Phi_0}{\partial\omega}\cos^2\left(\pi/8\right)J_{-1/4}^2\left(\gamma\widehat{\xi}'^2/2\right)$$

$$=2\pi\gamma\sqrt{2\gamma}\frac{c^2}{d}\frac{1}{\omega}\frac{\partial\Phi_0}{\partial\omega}\cos^2\left(\pi/8\right)J_{-1/4}^2\left(k_p\left(d+\delta-x\right)\right)$$

$$\widehat{\xi}'\approx\sqrt{2\left(d+\delta_0-x\right)/d}$$

$$u_p\frac{\partial}{\partial\omega}\frac{1}{\omega}\left(\frac{\partial u_p^+}{\partial n}-\frac{\partial u_p^-}{\partial n}\right)=-2\pi\gamma\sqrt{2\gamma}\frac{c^2}{d}\frac{1}{\omega}\frac{\partial\Phi_0}{\partial\omega}\cos^2\left(\pi/8\right)J_{-1/4}^2\left(\gamma\widehat{\zeta}^2/2\right)$$

$$=-2\pi\gamma\sqrt{2\gamma}\frac{c^2}{d}\frac{1}{\omega}\frac{\partial\Phi_0}{\partial\omega}\cos^2\left(\pi/8\right)J_{-1/4}^2\left(k_p\left(x-d-\delta\right)\right)$$

$$\widehat{\zeta}\approx\sqrt{2\left(x-d-\delta_0\right)/d}$$

where we have used

$$U_+(0,\tau) = e^{i3\pi/8}\sqrt{\frac{\pi\tau}{2}}\frac{1}{2}H^{(1)}_{1/4}\left(\tau^2/4\right)$$

$$Y_{1/4}(z) = J_{1/4}(z) - \sqrt{2}J_{-1/4}(z)$$

We note that these can be written as

$$u_p\frac{\partial}{\partial\omega}\frac{1}{\omega}\left(\frac{\partial u_p^+}{\partial n} - \frac{\partial u_p^-}{\partial n}\right)$$

$$= -\mathrm{sgn}(x-d-\delta_0)\,2\pi\gamma\sqrt{2\gamma}\frac{c^2}{d}\frac{1}{\omega}\frac{\partial\Phi_0}{\partial\omega}\cos^2(\pi/8)\,J^2_{-1/4}(k_p|x-d-\delta_0|)$$

Using the asymptotic form of the Bessel function for large argument

$$u_p\frac{\partial}{\partial\omega}\frac{1}{\omega}\left(\frac{\partial u_p^+}{\partial n} - \frac{\partial u_p^-}{\partial n}\right)$$

$$\sim -\mathrm{sgn}(x-d-\delta_0)\sqrt{2\gamma}4c^2\frac{1}{\omega}\frac{\partial\Phi_0}{\partial\omega}\cos^2(\pi/8)\frac{1}{|x-d-\delta_0|}\cos^2(k_p|x-d-\delta_0|-\pi/8)$$

$$\sim 4c^2\sqrt{2\gamma}\frac{1}{\omega}\frac{\partial\Phi_0}{\partial\omega}\cos^2(\pi/8)\frac{1}{d+\delta_0-x}\cos^2(k_p|x-d-\delta_0|-\pi/8)$$

Noting that

$$\cos^2(k_p|x-d-\delta_0|-\pi/8) = \cos^2(k_px-n\pi) = \cos^2(k_px)\ ,\ x < d+\delta_0$$

$$\cos^2(k_p|x-d-\delta_0|-\pi/8) = \cos^2(k_px-n\pi-\pi/4) = \cos^2(k_px-\pi/4)\ ,\ x > d+\delta_0$$

shows that the Region 3 solution equals the outer terms for large arguments (this is also true if we average these quantities in the integration, which allows us to use the limit as the focal point is approached). Thus the difference can be integrated to infinity and the correction can be defined by

$$N_3(0) = \int_{-\infty}^{d}\left[u_p\frac{\partial}{\partial\omega}\frac{1}{\omega}\left(\frac{\partial u_p^+}{\partial n} - \frac{\partial u_p^-}{\partial n}\right) - u_p^1\frac{\partial}{\partial\omega}\frac{1}{\omega}\left(\frac{\partial u_p^{1+}}{\partial n} - \frac{\partial u_p^{1-}}{\partial n}\right)\right]d\ell$$

$$+\int_{d}^{d+\delta}\left[u_p\frac{\partial}{\partial\omega}\frac{1}{\omega}\left(\frac{\partial u_p^+}{\partial n} - \frac{\partial u_p^-}{\partial n}\right) - u_p^2\frac{\partial}{\partial\omega}\frac{1}{\omega}\left(\frac{\partial u_p^{2+}}{\partial n} - \frac{\partial u_p^{2-}}{\partial n}\right)\right]d\ell$$

$$+\int_{d+\delta}^{\infty}\left[u_p\frac{\partial}{\partial\omega}\frac{1}{\omega}\left(\frac{\partial u_p^+}{\partial n} - \frac{\partial u_p^-}{\partial n}\right) - u_p^2\frac{\partial}{\partial\omega}\frac{1}{\omega}\left(\frac{\partial u_p^{2+}}{\partial n} - \frac{\partial u_p^{2-}}{\partial n}\right)\right]d\ell$$

We find it convenient to write the correction as the limit $R\to\infty$ of

$$N_3(0) = \int_{-R+d}^{R+d}u_p\frac{\partial}{\partial\omega}\frac{1}{\omega}\left(\frac{\partial u_p^+}{\partial n} - \frac{\partial u_p^-}{\partial n}\right)dx - \int_{d}^{R+d}u_p^2\frac{\partial}{\partial\omega}\frac{1}{\omega}\left(\frac{\partial u_p^{2+}}{\partial n} - \frac{\partial u_p^{2-}}{\partial n}\right)dx$$

$$-\int_{-R+d}^{d} u_p^1 \frac{\partial}{\partial\omega}\frac{1}{\omega}\left(\frac{\partial u_p^{1+}}{\partial n}-\frac{\partial u_p^{1-}}{\partial n}\right)dx$$

Using the averaged outer quantities

$$N_3(0) = -2\pi\gamma\sqrt{2\gamma}\frac{c^2}{d}\frac{1}{\omega}\frac{\partial\Phi_0}{\partial\omega}\cos^2(\pi/8)\int_{-R+d}^{R+d}\operatorname{sgn}(x-d-\delta_0)\,J_{-1/4}^2(k_p|x-d-\delta_0|)\,dx$$

$$-2c^2\cos^2(\pi/8)\frac{1}{\omega}\frac{\partial\Phi_0}{\partial\omega}\sqrt{2\gamma}\int_{-R+d}^{R+d}(d-x)^{-1}\,dx$$

or

$$N_3(0) = -2\pi\gamma\sqrt{2\gamma}\frac{c^2}{d}\frac{1}{\omega}\frac{\partial\Phi_0}{\partial\omega}\cos^2(\pi/8)\int_{-R}^{R}\operatorname{sgn}(x)\,J_{-1/4}^2(k_p|x|)\,dx$$

$$+2\pi\gamma\sqrt{2\gamma}\frac{c^2}{d}\frac{1}{\omega}\frac{\partial\Phi_0}{\partial\omega}\cos^2(\pi/8)\left(\int_{R+d}^{R+d+\delta_0}-\int_{-R+d+\delta_0}^{-R+d}\right)J_{-1/4}^2(k_p|x-d-\delta_0|)\,dx$$

$$+2c^2\cos^2(\pi/8)\frac{1}{\omega}\frac{\partial\Phi_0}{\partial\omega}\sqrt{2\gamma}\int_{-R}^{R}\frac{dx}{x}$$

or

$$N_3(0) =$$

$$2\pi\gamma\sqrt{2\gamma}\frac{c^2}{d}\frac{1}{\omega}\frac{\partial\Phi_0}{\partial\omega}\cos^2(\pi/8)\left(\int_{R-\delta_0}^{R}+\int_{R}^{R+\delta_0}\right)J_{-1/4}^2(k_p|x|)\,dx$$

$$\approx 2\pi\gamma\sqrt{2\gamma}\frac{c^2}{d}\frac{1}{\omega}\frac{\partial\Phi_0}{\partial\omega}\cos^2(\pi/8)\,2\delta_0 J_{-1/4}^2(k_p|R|)\to 0$$

Thus we have shown that, at least for the peak $s=0$, the principle value interpretation is correct.

## B.4 Focal Point Correction To Projection Operator

Let us consider a focal point correction to the projection operator. Note that the focal point shift must be used otherwise there will be a phase discontinuity at infinity. We define the correction as the difference between Region 3 (no superscript) and the outer Region 1 and Region 2 representations (with superscripts)

$$\exp(\pi|s'|/4)\,\Delta V_p \sim 2\sqrt{d}e^{-\pi s'/4}\int_{d-\varepsilon}^{d}\left[u(x,0)-u^1(x,0)\right]\left(d^2-x^2\right)^{-1/4}\cos\left[k_p x+p_1(x)\right]dx$$

$$+2\sqrt{d}e^{\pi s'/4}\int_{d}^{d+\varepsilon}\left[u(x,0)-u^2(x,0)\right]\left(x^2-d^2\right)^{-1/4}\cos\left[k_p x-\pi/4+p_2(x)\right]dx$$

$$\sim 2\sqrt{d}e^{-\pi s'/4}\int_{d-\varepsilon}^{d}\left[u\left(x,0\right)-u^{1}\left(x,0\right)\right]\left(d^{2}-x^{2}\right)^{-1/4}\cos\left[kx-s'\frac{1}{2}\ln\left(\frac{d-x}{d+x}\right)\right]dx$$

$$+2\sqrt{d}e^{\pi s'/4}\int_{d}^{d+\varepsilon}\left[u\left(x,0\right)-u^{2}\left(x,0\right)\right]\left(x^{2}-d^{2}\right)^{-1/4}\cos\left[kx-s'\frac{1}{2}\ln\left(\frac{x-d}{x+d}\right)-\pi/4\right]dx$$

$$\sim 2\left(d/2\right)^{1/4}e^{-\pi s'/4}\int_{d-\varepsilon}^{d}\left[u\left(x,0\right)-u^{1}\left(x,0\right)\right]\left(d-x\right)^{-1/4}\cos\left[kx-s'\frac{1}{2}\ln\left(\frac{d-x}{2d}\right)\right]dx$$

$$+2\left(d/2\right)^{1/4}e^{\pi s'/4}\int_{d}^{d+\varepsilon}\left[u\left(x,0\right)-u^{2}\left(x,0\right)\right]\left(x-d\right)^{-1/4}\cos\left[kx-s'\frac{1}{2}\ln\left(\frac{x-d}{2d}\right)-\pi/4\right]dx$$

$$\sim 2\left(d/2\right)^{1/4}e^{-\pi s'/4}\int_{-\infty}^{d}\left[u\left(x,0\right)-u^{1}\left(x,0\right)\right]\left(d-x\right)^{-1/4}\cos\left[kx-s'\frac{1}{2}\ln\left(\frac{d-x}{2d}\right)\right]dx$$

$$+2\left(d/2\right)^{1/4}e^{\pi s'/4}\int_{d}^{\infty}\left[u\left(x,0\right)-u^{2}\left(x,0\right)\right]\left(x-d\right)^{-1/4}\cos\left[kx-s'\frac{1}{2}\ln\left(\frac{x-d}{2d}\right)-\pi/4\right]dx$$

The $p$th component of the field on axis in Region 1 is (the second expressions are approximated near the focal point $d$)

$$u^{1}\sim c_{2}e^{-\pi s'/2}\sqrt{2d}\left(d^{2}-x^{2}\right)^{-1/4}\cos\left[kx-s'\frac{1}{2}\ln\left(\frac{d-x}{d+x}\right)\right],\text{ Region 1}$$

$$\approx c_{2}e^{-\pi s'/2}\left(2d\right)^{1/4}\left(d-x\right)^{-1/4}\cos\left[kx-s'\frac{1}{2}\ln\left(\frac{d-x}{2d}\right)\right]$$

and in Region 2 is

$$u^{2}\sim c_{2}\sqrt{2d}\left(x^{2}-d^{2}\right)^{-1/4}\cos\left[kx-s'\frac{1}{2}\ln\left(\frac{x-d}{x+d}\right)-\pi/4\right],\text{ Region 2}$$

$$\approx c_{2}\left(2d\right)^{1/4}\left(x-d\right)^{-1/4}\cos\left[kx-s'\frac{1}{2}\ln\left(\frac{x-d}{2d}\right)-\pi/4\right]$$

where

$$c_{2}=\frac{2v}{\left(2\gamma\right)^{1/4}\left|U'_{+}\left(-s',0\right)\right|\sqrt{A\ln\left(\frac{\ell+d}{\ell-d}\right)}}e^{\pi s'/2}$$

$$\frac{\left|U'_{+}\left(s',0\right)\right|}{\left|U'_{+}\left(-s',0\right)\right|}=e^{-\pi s'/2}$$

$$s'\ln\left(\frac{\ell+d}{\ell-d}\right)=2\left(k_{p}-k\right)\ell$$

$$d = \ell\sqrt{1 - R/\ell}$$

$$k_p \ell = \pi\left(p - 1/4\right)$$

The Region 3 solution on axis is

$$u\left(x,0\right) = -\left(-1\right)^n \left(\gamma/2\right)^{1/4} \frac{\left|\Gamma\left(is'/2+1/4\right)\right|}{\mathrm{Im}\left\{2^{is'/2}e^{-i3\pi/8}\Gamma\left(is'/2+1/4\right)\right\}}$$

$$c_2 \,\mathrm{Re}\left[e^{-i\pi/4}U_+\left(-s',\zeta\sqrt{2\gamma}\right) - e^{-i\pi/4}\frac{U_+'\left(-s',0\right)}{U_+'^*\left(-s',0\right)}U_+^*\left(-s',\zeta\sqrt{2\gamma}\right)\right]$$

$$= -\left(-1\right)^n \left(\gamma/2\right)^{1/4} \frac{\left|\Gamma\left(is'/2+1/4\right)\right|}{\mathrm{Im}\left\{2^{is'/2}e^{-i3\pi/8}\Gamma\left(is'/2+1/4\right)\right\}}$$

$$c_2 \,\mathrm{Re}\left[e^{-i\pi/4}U_+\left(-s',\zeta\sqrt{2\gamma}\right) + 2^{-is'}\frac{\Gamma\left(-is'/2+1/4\right)}{\Gamma\left(is'/2+1/4\right)}U_+^*\left(-s',\zeta\sqrt{2\gamma}\right)\right]$$

$$\zeta \approx \sqrt{2\left(x-d-\delta\right)/d}$$

$$u\left(x,0\right) = -\left(-1\right)^n \left(\gamma/2\right)^{1/4} \frac{\left|\Gamma\left(is'/2+1/4\right)\right|}{\mathrm{Im}\left\{2^{is'/2}e^{-i3\pi/8}\Gamma\left(is'/2+1/4\right)\right\}}$$

$$c_2 e^{-\pi s'/2} \,\mathrm{Re}\left[U_+\left(s',\xi'\sqrt{2\gamma}\right) - \frac{U_+'\left(s',0\right)}{U_+'^*\left(s',0\right)}U_+^*\left(s',\xi'\sqrt{2\gamma}\right)\right]$$

$$= -\left(-1\right)^n \left(\gamma/2\right)^{1/4} \frac{\left|\Gamma\left(is'/2+1/4\right)\right|}{\mathrm{Im}\left\{2^{is'/2}e^{-i3\pi/8}\Gamma\left(is'/2+1/4\right)\right\}}$$

$$c_2 e^{-\pi s'/2} \,\mathrm{Re}\left[U_+\left(s',\xi'\sqrt{2\gamma}\right) + 2^{is'}e^{i\pi/4}\frac{\Gamma\left(is'/2+1/4\right)}{\Gamma\left(-is'/2+1/4\right)}U_+^*\left(s',\xi'\sqrt{2\gamma}\right)\right]$$

$$\xi' \approx \sqrt{2\left(d+\delta-x\right)/d}$$

If we take the limit as we move away from Region 3

$$U_+\left(s,\tau\right) \sim e^{i\tau^2/4-\left(1/2-is\right)\ln\tau} = e^{i\tau^2/4}\tau^{is-1/2}\ ,\ \tau \to +\infty$$

$$U_+'\left(s',0\right) = e^{-\pi\left(s'+i3/2\right)/4}U'\left(-is',0\right) = -\frac{e^{-\pi\left(s'+i3/2\right)/4}\sqrt{\pi}}{2^{-is'/2-1/4}\Gamma\left(-is'/2+1/4\right)}$$

$$e^{i\Phi_0} = i\frac{U_+'\left(-s',0\right)}{U_+'^*\left(-s',0\right)} = i\frac{\left[U_+'\left(-s',0\right)\right]^2}{\left|U_+'\left(-s',0\right)\right|^2}$$

$$\cos\left(\Phi_0/2\right)=\frac{\operatorname{Im}\left[U_+'\left(s',0\right)\right]}{\left|U_+'\left(s',0\right)\right|}=-\frac{\operatorname{Im}\left\{2^{is'/2}e^{-i3\pi/8}\Gamma\left(is'/2+1/4\right)\right\}}{\left|\Gamma\left(is'/2+1/4\right)\right|}$$

and

$$u\left(x,0\right)=-\left(-1\right)^n\left(\gamma/2\right)^{1/4}\frac{\left|\Gamma\left(is'/2+1/4\right)\right|}{\operatorname{Im}\left\{2^{is'/2}e^{-i3\pi/8}\Gamma\left(is'/2+1/4\right)\right\}}$$

$$c_2\operatorname{Re}\left[e^{-i\pi/4}U_+\left(-s',\zeta\sqrt{2\gamma}\right)+e^{i\pi/4}e^{i\Phi_0}U_+^*\left(-s',\zeta\sqrt{2\gamma}\right)\right]$$

$$\sim-\left(-1\right)^n\left(\gamma/2\right)^{1/4}\frac{\left|\Gamma\left(is'/2+1/4\right)\right|}{\operatorname{Im}\left\{2^{is'/2}e^{-i3\pi/8}\Gamma\left(is'/2+1/4\right)\right\}}$$

$$c_2\frac{1}{\sqrt{\zeta\sqrt{2\gamma}}}\left[\cos\left\{\zeta^2\gamma/2-s'\ln\left(\zeta\sqrt{2\gamma}\right)-\pi/4\right\}+\cos\left\{\zeta^2\gamma/2-s'\ln\left(\zeta\sqrt{2\gamma}\right)-\pi/4-\Phi_0\right\}\right]$$

$$\sim-\left(-1\right)^n\frac{\left|\Gamma\left(is'/2+1/4\right)\right|}{\operatorname{Im}\left\{2^{is'/2}e^{-i3\pi/8}\Gamma\left(is'/2+1/4\right)\right\}}c_2\sqrt{\frac{2}{\zeta}}\cos\left(\Phi_0/2\right)\cos\left\{\zeta^2\gamma/2-s'\ln\left(\zeta\sqrt{2\gamma}\right)-\pi/4-\Phi_0/2\right\}$$

$$\sim\left(-1\right)^n c_2\sqrt{\frac{2}{\zeta}}\cos\left\{\zeta^2\gamma/2-s'\ln\left(\zeta\sqrt{2\gamma}\right)-\pi/4-\Phi_0/2\right\}$$

$$\sim\left(-1\right)^n c_2\left(\frac{2d}{x-d-\delta}\right)^{1/4}\cos\left\{k\left(x-d-\delta\right)-s'\ln\left(2\sqrt{k\left(x-d-\delta\right)}\right)-\pi/4-\Phi_0/2\right\}$$

$$u\left(x,0\right)=-\left(-1\right)^n\left(\gamma/2\right)^{1/4}\frac{\left|\Gamma\left(is'/2+1/4\right)\right|}{\operatorname{Im}\left\{2^{is'/2}e^{-i3\pi/8}\Gamma\left(is'/2+1/4\right)\right\}}$$

$$c_2e^{-\pi s'/2}\operatorname{Re}\left[U_+\left(s',\xi'\sqrt{2\gamma}\right)+e^{-i\Phi_0}U_+^*\left(s',\xi'\sqrt{2\gamma}\right)\right]$$

$$\sim-\left(-1\right)^n\left(\gamma/2\right)^{1/4}\frac{\left|\Gamma\left(is'/2+1/4\right)\right|}{\operatorname{Im}\left\{2^{is'/2}e^{-i3\pi/8}\Gamma\left(is'/2+1/4\right)\right\}}\frac{1}{\sqrt{\xi'\sqrt{2\gamma}}}$$

$$c_2e^{-\pi s'/2}\left[\cos\left\{\xi'^2\gamma/2+s'\ln\left(\xi'\sqrt{2\gamma}\right)\right\}+\cos\left\{\xi'^2\gamma/2+s'\ln\left(\xi'\sqrt{2\gamma}\right)+\Phi_0\right\}\right]$$

$$\sim-\left(-1\right)^n\frac{\left|\Gamma\left(is'/2+1/4\right)\right|}{\operatorname{Im}\left\{2^{is'/2}e^{-i3\pi/8}\Gamma\left(is'/2+1/4\right)\right\}}c_2e^{-\pi s'/2}\sqrt{\frac{2}{\xi'}}\cos\left(\Phi_0/2\right)\cos\left\{\xi'^2\gamma/2+s'\ln\left(\xi'\sqrt{2\gamma}\right)+\Phi_0/2\right\}$$

$$\sim\left(-1\right)^n c_2e^{-\pi s'/2}\sqrt{\frac{2}{\xi'}}\cos\left\{\xi'^2\gamma/2+s'\ln\left(\xi'\sqrt{2\gamma}\right)+\Phi_0/2\right\}$$

$$\sim (-1)^n c_2 e^{-\pi s'/2} \left(\frac{2d}{d+\delta-x}\right)^{1/4} \cos\left\{k\left(d+\delta-x\right) + s' \ln\left(2\sqrt{k\left(d+\delta-x\right)}\right) + \Phi_0/2\right\}$$

Thus we have

$$u_1 \approx c_2 e^{-\pi s'/2} \left(2d\right)^{1/4} \left(d-x\right)^{-1/4} \cos\left[kx - s'\frac{1}{2}\ln\left(\frac{d-x}{2d}\right)\right]$$

$$u \sim (-1)^n c_2 e^{-\pi s'/2} \left(\frac{2d}{d-x}\right)^{1/4} \cos\left\{k\left(d+\delta-x\right) + \frac{1}{2}s' \ln\left(4k\left(d-x\right)\right) + \Phi_0/2\right\}$$

$$u_2 \approx c_2 \left(2d\right)^{1/4} \left(x-d\right)^{-1/4} \cos\left[kx - s'\frac{1}{2}\ln\left(\frac{x-d}{2d}\right) - \pi/4\right]$$

$$u \sim (-1)^n c_2 \left(\frac{2d}{x-d}\right)^{1/4} \cos\left\{k\left(x-d-\delta\right) - \frac{1}{2}s' \ln\left(4k\left(x-d\right)\right) - \pi/4 - \Phi_0/2\right\}$$

These pairs match if the phases match

$$kx - s'\frac{1}{2}\ln\left(\frac{d-x}{2d}\right) - n\pi = -k\left(d+\delta-x\right) - \frac{1}{2}s' \ln\left(4k\left(d-x\right)\right) - \Phi_0/2$$

and

$$kx - s'\frac{1}{2}\ln\left(\frac{x-d}{2d}\right) - \pi/4 - n\pi = k\left(x-d-\delta\right) - \frac{1}{2}s' \ln\left(4k\left(x-d\right)\right) - \pi/4 - \Phi_0/2$$

which are equivalent to

$$\frac{1}{2}s' \ln\left(8kd\right) = -k\left(d+\delta\right) - \Phi_0/2 + n\pi$$

Now we want to evaluate the correction

$$\exp\left(\pi\left|s'\right|/4\right)\Delta V_p \sim 2\left(d/2\right)^{1/4} e^{-\pi s'/4} \int_{-\infty}^{d} \left[u\left(x,0\right) - u^1\left(x,0\right)\right] \left(d-x\right)^{-1/4} \cos\left[kx - s'\frac{1}{2}\ln\left(\frac{d-x}{2d}\right)\right] dx$$

$$+2\left(d/2\right)^{1/4} e^{-\pi s'/4} \int_{d}^{d+\delta} \left[u\left(x,0\right) - u^2\left(x,0\right)\right] \left(x-d\right)^{-1/4} \cos\left[kx - s'\frac{1}{2}\ln\left(\frac{x-d}{2d}\right) - \pi/4\right] dx$$

$$+2\left(d/2\right)^{1/4} e^{\pi s'/4} \int_{d+\delta}^{\infty} \left[u\left(x,0\right) - u^2\left(x,0\right)\right] \left(x-d\right)^{-1/4} \cos\left[kx - s'\frac{1}{2}\ln\left(\frac{x-d}{2d}\right) - \pi/4\right] dx$$

$$u^1 \approx c_2 e^{-\pi s'/2} \left(2d\right)^{1/4} \left(d-x\right)^{-1/4} \cos\left[kx - s'\frac{1}{2}\ln\left(\frac{d-x}{2d}\right)\right]$$

$$u^2 \approx c_2 \left(2d\right)^{1/4} \left(x-d\right)^{-1/4} \cos\left[kx - s'\frac{1}{2}\ln\left(\frac{x-d}{2d}\right) - \pi/4\right]$$

$$u\left(x,0\right) = -\left(-1\right)^n \left(\gamma/2\right)^{1/4} \frac{\left|\Gamma\left(is'/2+1/4\right)\right|}{\mathrm{Im}\left\{2^{is'/2}e^{-i3\pi/8}\Gamma\left(is'/2+1/4\right)\right\}}$$

$$c_2 \,\mathrm{Re}\left[e^{-i\pi/4}U_+\left(-s',\sqrt{4k\left(x-d-\delta\right)}\right) + 2^{-is'}\frac{\Gamma\left(-is'/2+1/4\right)}{\Gamma\left(is'/2+1/4\right)}U_+^*\left(-s',\sqrt{4k\left(x-d-\delta\right)}\right)\right]$$

$$u\left(x,0\right) = -\left(-1\right)^n \left(\gamma/2\right)^{1/4} \frac{\left|\Gamma\left(is'/2+1/4\right)\right|}{\mathrm{Im}\left\{2^{is'/2}e^{-i3\pi/8}\Gamma\left(is'/2+1/4\right)\right\}}$$

$$c_2 e^{-\pi s'/2}\,\mathrm{Re}\left[U_+\left(s',\sqrt{4k\left(d+\delta-x\right)}\right) + 2^{is'}e^{i\pi/4}\frac{\Gamma\left(is'/2+1/4\right)}{\Gamma\left(-is'/2+1/4\right)}U_+^*\left(s',\sqrt{4k\left(d+\delta-x\right)}\right)\right]$$

### B.4.1 correction for s equal to zero

Suppose we direct attention on the important $s'=0$ ($\Phi_0 = -\pi/4$, $k = k_p = \left(p-1/4\right)\pi/\ell$) limit (the peak region)

$$u^1 \sim \Gamma\left(1/4\right)\sqrt{2/\pi}c\cos\left(\pi/8\right)\left(1-x/d\right)^{-1/4}\cos\left(k_p x\right)\text{ , Region 1}$$

$$u^2 \sim \Gamma\left(1/4\right)\sqrt{2/\pi}c\cos\left(\pi/8\right)\left(x/d-1\right)^{-1/4}\cos\left(k_p x-\pi/4\right)\text{ , Region 2}$$

where we have used

$$U_+'\left(0,0\right) = e^{-i3\pi/8}U'\left(0,0\right) = -e^{-i\pi 3/8}\frac{2^{1/4}\sqrt{\pi}}{\Gamma\left(1/4\right)}$$

and

$$c = \frac{\sqrt{2}v}{\left(2\gamma\right)^{1/4}\cos\left(\pi/8\right)\sqrt{A\ln\left(\frac{\ell+d}{\ell-d}\right)}} = \frac{c_2 2^{-1/4}\sqrt{\pi}}{\cos\left(\pi/8\right)\Gamma\left(1/4\right)}$$

We note that for $s=0$

$$k_p\left(d+\delta_0\right) = \left(n+1/8\right)\pi$$

for which

$$\cos\left(k_p\left(d+\delta_0\right)\right) = \cos\left(k_p\left(d+\delta_0\right)-\pi/4\right)$$

In Region 3

$$u_p = \left(-1\right)^n\Gamma\left(1/4\right)\gamma^{1/2}c\cos\left(\pi/8\right)\left|\left(x-d-\delta_0\right)/d\right|^{1/4}J_{-1/4}\left(k_p\left|x-d-\delta_0\right|\right)$$

where we have used

$$U_+(0,\tau) = e^{i3\pi/8}\sqrt{\frac{\pi\tau}{2}}\frac{1}{2}H_{1/4}^{(1)}\left(\tau^2/4\right)$$

$$Y_{1/4}(z) = J_{1/4}(z) - \sqrt{2}J_{-1/4}(z)$$

The asymptotic form is

$$u_p \sim (-1)^n \Gamma(1/4)\, c\cos(\pi/8)\sqrt{2/\pi}\frac{\cos\left(k_p\left|x-d-\delta_0\right|-\pi/8\right)}{\left|\left(x-d-\delta_0\right)/d\right|^{1/4}}$$

Noting that

$$\cos\left(k_p\left|x-d-\delta_0\right|-\pi/8\right) = \cos\left(k_p x - n\pi\right) = (-1)^n\cos\left(k_p x\right)\ ,\ x < d+\delta_0$$

$$\cos\left(k_p\left|x-d-\delta_0\right|-\pi/8\right) = \cos\left(k_p x - n\pi - \pi/4\right) = (-1)^n\cos\left(k_p x - \pi/4\right)\ ,\ x > d+\delta_0$$

shows that the Region 3 solution equals the outer terms for large arguments (this is also true if we average these quantities in the integration).

$$\Delta V_p \sim 2\left(d/2\right)^{1/4}\int_{-\infty}^{d}\left[u(x,0)-u^1(x,0)\right](d-x)^{-1/4}\cos\left(k_p x\right)dx$$

$$+2\left(d/2\right)^{1/4}\int_{d}^{d+\delta_0}\left[u(x,0)-u^2(x,0)\right](x-d)^{-1/4}\cos\left(k_p x-\pi/4\right)dx$$

$$+2\left(d/2\right)^{1/4}\int_{d+\delta_0}^{\infty}\left[u(x,0)-u^2(x,0)\right](x-d)^{-1/4}\cos\left(k_p x-\pi/4\right)dx$$

or

$$\Delta V_p \sim 2^{3/4}d^{1/2}c\cos(\pi/8)\,\Gamma(1/4)\,\{$$

$$\int_{-\infty}^{d}\left[(-1)^n k_p^{1/2}\left|x-d-\delta_0\right|^{1/4}J_{-1/4}\left(k_p\left|x-d-\delta_0\right|\right)-\sqrt{2/\pi}\left(d-x\right)^{-1/4}\cos\left(k_p x\right)\right]$$

$$\left(d-x\right)^{-1/4}\cos\left(k_p x\right)dx$$

$$+\int_{d}^{d+\delta_0}\left[(-1)^n k_p^{1/2}\left|x-d-\delta_0\right|^{1/4}J_{-1/4}\left(k_p\left|x-d-\delta_0\right|\right)-\sqrt{2/\pi}\left(x-d\right)^{-1/4}\cos\left(k_p x-\pi/4\right)\right]$$

$$\left(x-d\right)^{-1/4}\cos\left(k_p x-\pi/4\right)dx$$

$$+\int_{d+\delta_0}^{\infty}\left[(-1)^n k_p^{1/2}\left|x-d-\delta_0\right|^{1/4} J_{-1/4}\left(k_p\left|x-d-\delta_0\right|\right)-\sqrt{2/\pi}\,(x-d)^{-1/4}\cos\left(k_p x-\pi/4\right)\right]$$

$$(x-d)^{-1/4}\cos\left(k_p x-\pi/4\right)dx$$

$$\}$$

or

$$\Delta V_p \sim 2^{3/4}\left(d/k_p\right)^{1/2} c\cos\left(\pi/8\right)\Gamma\left(1/4\right)\{$$

$$\int_{-\infty}^{k_p d}\left[(-1)^n\left|x-k_p\left(d+\delta_0\right)\right|^{1/4} J_{-1/4}\left(\left|x-k_p\left(d+\delta_0\right)\right|\right)-\sqrt{2/\pi}\,(k_p d-x)^{-1/4}\cos\left(x\right)\right]$$

$$(k_p d-x)^{-1/4}\cos\left(x\right)dx$$

$$+\int_{k_p d}^{k_p(d+\delta_0)}\left[(-1)^n\left|x-k_p\left(d+\delta_0\right)\right|^{1/4} J_{-1/4}\left(\left|x-k_p\left(d+\delta_0\right)\right|\right)-\sqrt{2/\pi}\,(x-k_p d)^{-1/4}\cos\left(x-\pi/4\right)\right]$$

$$(x-k_p d)^{-1/4}\cos\left(x-\pi/4\right)dx$$

$$+\int_{k_p(d+\delta_0)}^{\infty}\left[(-1)^n\left|x-k_p\left(d+\delta_0\right)\right|^{1/4} J_{-1/4}\left(\left|x-k_p\left(d+\delta_0\right)\right|\right)-\sqrt{2/\pi}\,(x-k_p d)^{-1/4}\cos\left(x-\pi/4\right)\right]$$

$$(x-k_p d)^{-1/4}\cos\left(x-\pi/4\right)dx$$

$$\}$$

or

$$\Delta V_p \sim 2^{3/4}\left(d/k_p\right)^{1/2} c\cos\left(\pi/8\right)\Gamma\left(1/4\right)\{$$

$$\int_{-\infty}^{k_p d}\left[(-1)^n\left|x-(n+1/8)\,\pi\right|^{1/4} J_{-1/4}\left(\left|x-(n+1/8)\,\pi\right|\right)-\sqrt{2/\pi}\,(k_p d-x)^{-1/4}\cos\left(x\right)\right]$$

$$(k_p d-x)^{-1/4}\cos\left(x\right)dx$$

$$+\int_{k_p d}^{(n+1/8)\pi}\left[(-1)^n\left|x-(n+1/8)\,\pi\right|^{1/4} J_{-1/4}\left(\left|x-(n+1/8)\,\pi\right|\right)-\sqrt{2/\pi}\,(x-k_p d)^{-1/4}\cos\left(x-\pi/4\right)\right]$$

$$(x-k_pd)^{-1/4}\cos(x-\pi/4)\,dx$$

$$+\int_{(n+1/8)\pi}^{\infty}\left[(-1)^n\left|x-(n+1/8)\,\pi\right|^{1/4}J_{-1/4}\left(\left|x-(n+1/8)\,\pi\right|\right)-\sqrt{2/\pi}\,(x-k_pd)^{-1/4}\cos(x-\pi/4)\right]$$

$$(x-k_pd)^{-1/4}\cos(x-\pi/4)\,dx$$

$$\}$$

Thus

$$\Delta V_p\sim 2^{3/4}\left(d/k_p\right)^{1/2}c\cos(\pi/8)\,\Gamma(1/4)\,\{$$

$$\int_{k_p\delta_0}^{\infty}\left[x^{1/4}J_{-1/4}(x)-\sqrt{2/\pi}\,(x-k_p\delta_0)^{-1/4}\cos(x-\pi/8)\right](x-k_p\delta_0)^{-1/4}\cos(x-\pi/8)\,dx$$

$$+\int_0^{k_p\delta_0}\left[x^{1/4}J_{-1/4}(x)-\sqrt{2/\pi}\left|x-k_p\delta_0\right|^{-1/4}\cos(x+\pi/8)\right]$$

$$\left|x-k_p\delta_0\right|^{-1/4}\cos(x+\pi/8)\,dx$$

$$+\int_0^{\infty}\left[x^{1/4}J_{-1/4}(x)-\sqrt{2/\pi}\,(x+k_p\delta_0)^{-1/4}\cos(x-\pi/8)\right]$$

$$(x+k_p\delta_0)^{-1/4}\cos(x-\pi/8)\,dx$$

$$\}$$

where

$$k_p\delta_0=k_p\left(d+\delta_0\right)-k_pd=(n+1/8)\,\pi-(p-1/4)\,\pi d/\ell$$

### B.4.2 subtraction of averaged values

If we redefine the subtraction as the average of the square of the cosine we obtain

$$\Delta V_p\sim 2^{3/4}\left(d/k_p\right)^{1/2}c\cos(\pi/8)\,\Gamma(1/4)\,\{$$

$$\int_{k_p\delta_0}^{\infty}\left[x^{1/4}J_{-1/4}(x)\cos(x-\pi/8)-\frac{1}{2}\sqrt{2/\pi}\,(x-k_p\delta_0)^{-1/4}\right](x-k_p\delta_0)^{-1/4}\,dx$$

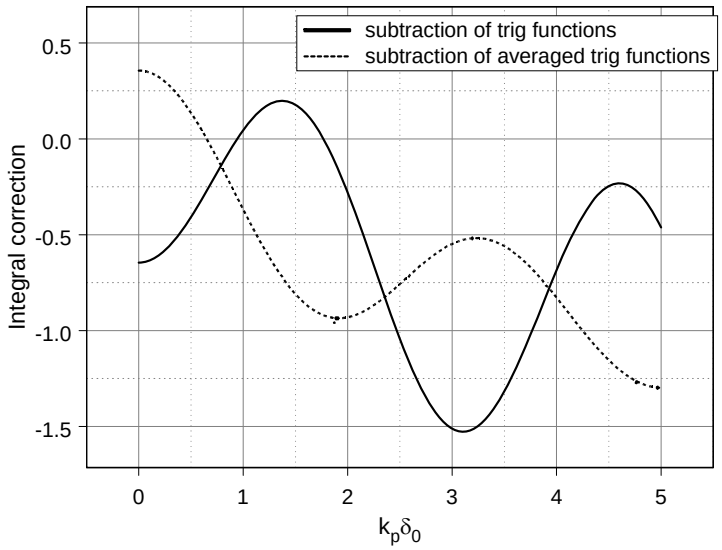


Figure B-1. Integral values of correction from Region 3. The solid curve has the trigonometric functions subtracted and the dashed curve has the averaged values subtracted.

$$+\int_0^{k_p\delta_0}\left[x^{1/4}J_{-1/4}(x)\cos(x+\pi/8)-\frac{1}{2}\sqrt{2/\pi}\,|x-k_p\delta_0|^{-1/4}\right]|x-k_p\delta_0|^{-1/4}\,dx$$

$$+\int_0^{\infty}\left[x^{1/4}J_{-1/4}(x)\cos(x-\pi/8)-\frac{1}{2}\sqrt{2/\pi}\,(x+k_p\delta_0)^{-1/4}\right](x+k_p\delta_0)^{-1/4}\,dx$$

$$\}$$

This is a more consistent correction with the value of $V_p$ in the main body of the report (since we averaged the cosines to obtain the value of the projection). Figure B-1 shows the sum of the integrals in braces of the preceding expressions (solid curve has trigonometric functions subtracted and dashed curve has averaged values subtracted).

The value of the dashed curve near $\pi/2$ (the average of the shift in the main body of the report $k_p\langle\delta_0\rangle = \pi/2$) is $-0.85$. Therefore

$$\Delta V_p \sim (-0.85)\frac{2vd}{(k_pd)^{3/4}\sqrt{A\ln\left(\frac{\ell+d}{\ell-d}\right)}}\Gamma(1/4)$$

Noting from the main body of the report that

$$V_p \sim \frac{2}{\sqrt{\pi}}\frac{vd}{(k_pd)^{1/4}\sqrt{A\ln\left(\frac{\ell+d}{\ell-d}\right)}}\left(\frac{\pi}{2}+\zeta_0\right)\Gamma(1/4)$$

we find

$$V_p + \Delta V_p \sim \frac{vd}{(k_p d)^{1/4} \sqrt{A \ln\left(\frac{\ell+d}{\ell-d}\right)}} \left[\frac{2}{\sqrt{\pi}}\left(\frac{\pi}{2} + \zeta_0\right) - \frac{1.7}{\sqrt{k_p d}}\right] \Gamma(1/4)$$

and

$$\left\langle \sqrt{kL}\left(V_p + \Delta V_p\right)^2 \right\rangle \approx \frac{d^2}{(d/L)^{1/2} A \ln\left(\frac{\ell+d}{\ell-d}\right)} \left[\frac{2}{\sqrt{\pi}}\left(\frac{\pi}{2} + \zeta_0\right) - \frac{1.7}{\sqrt{k_p d}}\right]^2 \Gamma^2(1/4)$$

This correction reduces the peak value from $\left\langle \sqrt{kL} V_p^2 \right\rangle \approx 25.5$ to approximately (using $p = 20$ as an average in the correction term)

$$\left\langle \sqrt{kL}\left(V_p + \Delta V_p\right)^2 \right\rangle \approx 20.5$$

much closer to the peak value of the histogram in Figure 55.

### B.4.3 shifted projection operator

Suppose that the projection operator is defined by taking the limit between the two regions as $d \to d + \delta_0$ for each eigenfunction. Then we can write the correction as

$$\Delta V_p \sim 2^{3/4} d^{1/2} c \cos(\pi/8) \Gamma(1/4) \{$$

$$\int_{-\infty}^{d+\delta_0} \left[(-1)^n k_p^{1/2} |x - d - \delta_0|^{1/4} J_{-1/4}(k_p |x - d - \delta_0|) - \sqrt{2/\pi}(d + \delta_0 - x)^{-1/4} \cos(k_p x)\right]$$

$$(d + \delta_0 - x)^{-1/4} \cos(k_p x)\, dx$$

$$+ \int_{d+\delta_0}^{\infty} \left[(-1)^n k_p^{1/2} |x - d - \delta_0|^{1/4} J_{-1/4}(k_p |x - d - \delta_0|) - \sqrt{2/\pi}(x - d - \delta_0)^{-1/4} \cos(k_p x - \pi/4)\right]$$

$$(x - d - \delta_0)^{-1/4} \cos(k_p x - \pi/4)\, dx$$

$$\}$$

$$\Delta V_p \sim 2^{3/4} \gamma^{1/2} c \cos(\pi/8) \Gamma(1/4) \{$$

$$\int_0^{\infty} \left[(-1)^n J_{-1/4}(k_p x) - \sqrt{2/(\pi k_p x)} \cos(k_p (x - d - \delta_0))\right] \cos(k_p (x - d - \delta_0))\, dx$$

$$+\int_0^\infty \left[(-1)^n J_{-1/4}(k_p x) - \sqrt{2/(\pi k_p x)}\cos(k_p(x+d+\delta_0)-\pi/4)\right]\cos(k_p(x+d+\delta_0)-\pi/4)\,dx$$

$$\}$$

Using

$$k_p(d+\delta_0) = (n+1/8)\pi$$

gives

$$\Delta V_p \sim 2^{7/4}\gamma^{1/2} c\cos(\pi/8)\Gamma(1/4)\{$$

$$\int_0^\infty \left[J_{-1/4}(k_p x) - \sqrt{2/(\pi k_p x)}\cos(k_p x-\pi/8)\right]\cos(k_p x-\pi/8)\,dx$$

$$\}$$

or

$$\Delta V_p \sim 2^{7/4}(d/k_p)^{1/2} c\cos(\pi/8)\Gamma(1/4)\{$$

$$\int_0^\infty \left[J_{-1/4}(z) - \sqrt{2/(\pi z)}\cos(z-\pi/8)\right]\cos(z-\pi/8)\,dz$$

$$\}$$

Now using the identities [31]

$$\int_0^\infty J_{-1/4}(z)\cos(bz)\,dz = \frac{\cos\left(\frac{1}{4}\arcsin b\right)}{\sqrt{1-b^2}}$$

$$\int_0^\infty J_{-1/4}(z)\sin(bz)\,dz = -\frac{\sin\left(\frac{1}{4}\arcsin b\right)}{\sqrt{1-b^2}}$$

gives

$$\int_0^\infty J_{-1/4}(z)\cos(bz-\pi/8)\,dz = \frac{\cos\left(\frac{1}{4}\arcsin b+\pi/8\right)}{\sqrt{1-b^2}}$$

In addition [37] using

$$\int_0^\infty \cos(bz)\frac{dz}{\sqrt{z}} = \int_0^\infty \sin(bz)\frac{dz}{\sqrt{z}} = \sqrt{\frac{\pi}{2b}}$$

gives

$$\frac{2}{\sqrt{\pi}}\int_0^\infty z^{-1/2}\cos\left(z-\pi/8\right)\cos\left(bz-\pi/8\right)dz=\frac{1}{\sqrt{\pi}}\int_0^\infty z^{-1/2}\left[\cos\left(1-b\right)z+\cos\left(\left(1+b\right)z-\pi/4\right)\right]dz$$

$$=\frac{1}{\sqrt{\pi}}\int_0^\infty z^{-1/2}\cos\left(1-b\right)zdz+\frac{1}{\sqrt{2\pi}}\int_0^\infty z^{-1/2}\cos\left(1+b\right)zdz+\frac{1}{\sqrt{2\pi}}\int_0^\infty z^{-1/2}\sin\left(1+b\right)zdz$$

$$=\frac{1}{\sqrt{2\left(1-b\right)}}+\frac{1}{\sqrt{1+b}}$$

Thus we can write

$$\int_0^\infty\left[J_{-1/4}\left(z\right)-\sqrt{2/\left(\pi z\right)}\cos\left(z-\pi/8\right)\right]\cos\left(bz-\pi/8\right)dz$$

$$=\frac{1}{\sqrt{1-b^2}}\cos\left(\pi/8+\frac{1}{4}\arcsin b\right)-\frac{1}{2\sqrt{1-b}}-\frac{1}{\sqrt{2\left(1+b\right)}}$$

$$=\frac{1}{\sqrt{1-b^2}}\cos\left[\pi/8+\frac{1}{4}\arcsin\left(1-1+b\right)\right]-\frac{1}{2\sqrt{1-b}}-\frac{1}{\sqrt{2\left(1+b\right)}}$$

$$\sim\frac{1}{\sqrt{1-b^2}}\cos\left[\pi/4-\frac{1}{4}\sqrt{2\left(1-b\right)}\right]-\frac{1}{2\sqrt{1-b}}-\frac{1}{\sqrt{2\left(1+b\right)}}$$

$$\sim\frac{1}{\sqrt{2\left(1-b^2\right)}}\left\{\cos\left[\frac{1}{4}\sqrt{2\left(1-b\right)}\right]+\sin\left[\frac{1}{4}\sqrt{2\left(1-b\right)}\right]\right\}-\frac{1}{2\sqrt{1-b}}-\frac{1}{\sqrt{2\left(1+b\right)}}$$

$$\sim\frac{1}{\sqrt{2\left(1-b\right)}}\left(\frac{1}{\sqrt{1+b}}-\frac{1}{\sqrt{2}}\right)+\left(\frac{1}{4}-\frac{1}{\sqrt{2}}\right)\frac{1}{\sqrt{1+b}}$$

$$\sim\frac{1}{\sqrt{2\left(1-b\right)}}\left[\frac{1}{\sqrt{2-\left(1-b\right)}}-\frac{1}{\sqrt{2}}\right]+\left(\frac{1}{4}-\frac{1}{\sqrt{2}}\right)\frac{1}{\sqrt{2}}$$

$$\sim-\frac{1}{2}\left(1-\frac{1}{2\sqrt{2}}\right)$$

Therefore

$$\Delta V_p\sim-2^{1/4}\left(2d/k_p\right)^{1/2}c\cos\left(\pi/8\right)\Gamma\left(1/4\right)\left(1-\frac{1}{2\sqrt{2}}\right)$$

$$=-\frac{1}{2}c_2\sqrt{\pi d/k_p}\left(2\sqrt{2}-1\right)$$

### B.4.4 subtraction of averaged values from shifted projection

Because we averaged the square of the cosine to obtain the projection operator value in the main body of the report, to be consistent we should calculate the correction as

$$\Delta V_p \sim 2^{7/4} \left(d/k_p\right)^{1/2} c \cos\left(\pi/8\right) \Gamma\left(1/4\right) \{$$

$$\int_0^\infty \left[ J_{-1/4}\left(z\right) \cos\left(z-\pi/8\right) - 1/\sqrt{2\pi z} \right] dz \; \}$$

or

$$\Delta V_p \sim 2^{7/4} \left(d/k_p\right)^{1/2} c \cos\left(\pi/8\right) \Gamma\left(1/4\right) \{$$

$$\int_0^\infty \left[ J_{-1/4}\left(z\right) - \sqrt{2/\left(\pi z\right)} \cos\left(z-\pi/8\right) \right] \cos\left(z-\pi/8\right) dz$$

$$+ \int_0^\infty \left[ \sqrt{2/\left(\pi z\right)} \cos^2\left(z-\pi/8\right) - 1/\sqrt{2\pi z} \right] dz \; \}$$

or

$$\Delta V_p \sim 2^{7/4} \left(d/k_p\right)^{1/2} c \cos\left(\pi/8\right) \Gamma\left(1/4\right) \{$$

$$-\frac{1}{2}\left(1 - \frac{1}{2\sqrt{2}}\right)$$

$$+\frac{1}{\sqrt{2\pi}} \int_0^\infty \cos\left(2z-\pi/4\right) \frac{dz}{\sqrt{z}} \; \}$$

or

$$\Delta V_p \sim 2^{3/4} \left(d/k_p\right)^{1/2} c \cos\left(\pi/8\right) \Gamma\left(1/4\right) \{$$

$$-\left(1 - \frac{1}{2\sqrt{2}}\right)$$

$$+1 \; \}$$

Notice that $-1 + 1/\left(2\sqrt{2}\right) \approx -0.646$ and $1/\left(2\sqrt{2}\right) \approx 0.354$ are the $k_p \delta_0 \to 0$ limit of the solid and dashed curves on B-1. Therefore

$$\Delta V_p \sim 2^{-1/4} \left(d/k_p\right)^{1/2} \Gamma\left(1/4\right) \frac{v}{\left(2\gamma\right)^{1/4} \sqrt{A \ln\left(\frac{\ell+d}{\ell-d}\right)}}$$

$$\Delta V_p \sim \frac{vd}{\left(k_p d\right)^{3/4} \sqrt{A \ln\left(\frac{\ell+d}{\ell-d}\right)}} \frac{\Gamma\left(1/4\right)}{\sqrt{2}}$$

Noting from the main body of the report that

$$V_p \sim \frac{2}{\sqrt{\pi}} \frac{vd}{(k_p d)^{1/4} \sqrt{A \ln\left(\frac{\ell+d}{\ell-d}\right)}} \left(\frac{\pi}{2} + \zeta_0\right) \Gamma(1/4)$$

we find

$$V_p + \Delta V_p \sim \frac{vd}{(k_p d)^{1/4} \sqrt{A \ln\left(\frac{\ell+d}{\ell-d}\right)}} \left[\frac{2}{\sqrt{\pi}} \left(\frac{\pi}{2} + \zeta_0\right) + \frac{1}{\sqrt{2kd}}\right] \Gamma(1/4)$$

and

$$\left\langle \sqrt{kL} \left(V_p + \Delta V_p\right)^2 \right\rangle \approx \frac{d^2}{(d/L)^{1/2} A \ln\left(\frac{\ell+d}{\ell-d}\right)} \left[\frac{2}{\sqrt{\pi}} \left(\frac{\pi}{2} + \zeta_0\right) + \frac{1}{\sqrt{2kd}}\right]^2 \Gamma^2(1/4)$$

$$\zeta_0 = \text{Arccosh}\left(\ell/d\right) = \ln\left(\ell/d + \sqrt{\ell^2/d^2 - 1}\right)$$

$$A = \pi R^2 + 2R\left(L - 2R\right) = 4R^2 \left(\pi/4 + \frac{d^2}{\ell R}\right)$$

### B.4.5 including higher order terms in the oscillatory functions of the projection operator

We could ask what happens if we include higher order terms in the oscillatory integrals of the projections operator for Regions 1 and 2 and then use the original correction above (with the asymptotic forms for the Region 1 and 2 solutions as the focal point is approached rather than the averaged forms). Taking the projection operator for the outer two regions with $s = 0$, and using

$$\left|U'_+(0,0)\right|^{-1} = \frac{1}{2^{1/4}\sqrt{\pi}} \Gamma(1/4)$$

gives

$$V_p = 2 \frac{2vd}{(kd)^{1/4} \sqrt{\pi A \ln\left(\frac{\ell+d}{\ell-d}\right)}} \Gamma(1/4)$$

$$\left[\int_0^d \left(d^2 - x^2\right)^{-1/2} \cos^2\left(k_p x\right) dx + \int_d^\ell \left(x^2 - d^2\right)^{-1/2} \cos^2\left(k_p x - \pi/4\right) dx\right]$$

or using a trigonometric identity

$$V_p = \frac{2vd}{(kd)^{1/4} \sqrt{\pi A \ln\left(\frac{\ell+d}{\ell-d}\right)}} \Gamma(1/4)$$

$$\left[\int_0^d \left(d^2 - x^2\right)^{-1/2} dx + \int_d^\ell \left(x^2 - d^2\right)^{-1/2} dx\right.$$

$$+\int_0^d \left(d^2-x^2\right)^{-1/2}\cos\left(2k_px\right)dx+\int_d^\ell \left(x^2-d^2\right)^{-1/2}\sin\left(2k_px\right)dx\Bigg]$$

$$=\frac{2vd}{\left(kd\right)^{1/4}\sqrt{\pi A\ln\left(\frac{\ell+d}{\ell-d}\right)}}\Gamma\left(1/4\right)$$

$$\left[\int_0^1 \left(1-z^2\right)^{-1/2}dz+\int_1^{\ell/d}\left(z^2-1\right)^{-1/2}du\right.$$

$$\left.+\int_0^{kd}\left(k^2d^2-z^2\right)^{-1/2}\cos\left(2z\right)dz+\int_{kd}^{k\ell}\left(z^2-k^2d^2\right)^{-1/2}\sin\left(2z\right)dz\right]$$

Noting that for the focus shifted in the projection, with $s=0$ and $k=k_p$, we have

$$kd=\left(n+1/8\right)\pi$$

$$k_p\ell=\left(p-1/4\right)\pi$$

and

$$V_p=\frac{2vd}{\left(kd\right)^{1/4}\sqrt{\pi A\ln\left(\frac{\ell+d}{\ell-d}\right)}}\Gamma\left(1/4\right)$$

$$\left[\frac{\pi}{2}+\zeta_0+\int_0^{(n+1/8)\pi}\left\{\left(n+1/8\right)^2\pi^2-z^2\right\}^{-1/2}\cos\left(2z\right)dz+\int_{(n+1/8)\pi}^{(p-1/4)\pi}\left\{z^2-\left(n+1/8\right)^2\pi^2\right\}^{-1/2}\sin\left(2z\right)dz\right]$$

$$=\frac{2vd}{\left(kd\right)^{1/4}\sqrt{\pi A\ln\left(\frac{\ell+d}{\ell-d}\right)}}\left(-1\right)^n\Gamma\left(1/4\right)\left[\frac{\pi}{2}+\zeta_0\right.$$

$$+\int_0^{(n+1/8)\pi} z^{-1/2}\left\{\left(n+1/8\right)2\pi-z\right\}^{-1/2}\cos\left\{2\left(\left(n+1/8\right)\pi-z\right)\right\}dz$$

$$\left.+\int_0^{(p-1/4)\pi-(n+1/8)\pi} z^{-1/2}\left\{z+\left(n+1/8\right)2\pi\right\}^{-1/2}\sin\left\{2\left(\left(n+1/8\right)\pi+z\right)\right\}dz\right]$$

$$=\frac{2vd^2}{\left(kd\right)^{1/4}\sqrt{\pi dA\ln\left(\frac{\ell+d}{\ell-d}\right)}}\Gamma\left(1/4\right)$$

$$\left[\frac{\pi}{2}+\zeta_0+\frac{1}{\sqrt{2\left(n+1/8\right)\pi}}\int_0^{(n+1/8)\pi}\left\{1-\frac{z}{\left(n+1/8\right)2\pi}\right\}^{-1/2}\cos\left(\pi/4-z\right)z^{-1/2}dz\right.$$

$$+\frac{1}{\sqrt{2\left(n+1/8\right)\pi}}\int_0^{(p-n-3/8)\pi}\left\{1+\frac{z}{\left(n+1/8\right)2\pi}\right\}^{-1/2}\cos\left(v-\pi/4\right)z^{-1/2}dz\Bigg]$$

For large upper limits the dominant contributions are near zero. Note also that the phases of the trigonometric functions are such that the leading contributions at the other limits vanish (and thus the corrections for the other limits are quite small at high frequencies). Thus we can write this as

$$V_p\sim\frac{2vd}{\left(kd\right)^{1/4}\sqrt{\pi A\ln\left(\frac{\ell+d}{\ell-d}\right)}}\Gamma\left(1/4\right)\left[\frac{\pi}{2}+\zeta_0+\frac{\sqrt{2}}{\sqrt{\left(n+1/8\right)\pi}}\int_0^{\infty}\cos\left(\pi/4-z\right)z^{-1/2}dz\right]$$

$$\sim\frac{2vd}{\left(kd\right)^{1/4}\sqrt{\pi A\ln\left(\frac{\ell+d}{\ell-d}\right)}}\Gamma\left(1/4\right)\left[\frac{\pi}{2}+\zeta_0+\frac{1}{\sqrt{n+1/8}}\right]$$

$$\sim\frac{2vd}{\left(kd\right)^{1/4}\sqrt{\pi A\ln\left(\frac{\ell+d}{\ell-d}\right)}}\Gamma\left(1/4\right)\left[\frac{\pi}{2}+\zeta_0+\frac{1}{\sqrt{kd/\pi}}\right]$$

Thus if we include the oscillatory functions in the definition of $V_p$ we also include this additive term. When added onto the correction of the previous sections this extra term eliminates the negative 2 in the correction and returns us to the same value as obtained previously by redefining the correction in terms of the average values. Thus we obtain a small positive correction.

## B.5 Random Plane Wave Representations And Treatment Of Integral Near Focal Point

This section gives integrations near the focal point needed in the evaluation of the random plane wave projections.

### B.5.1 random plane wave projection

The random plane wave projection in the main body of the report involves the function

$$\exp\left(\pi\left|s'\right|/2\right)G_s\left(\lambda\right)=\frac{4}{\pi}\int_0^{\infty}\Bigg[e^{-\pi s'/4}\int_0^{d}\left(1-x^2/d^2\right)^{-1/4}\cos\left\{\left(\lambda/4-\zeta^2\right)x/\ell-p_1\left(x\right)\right\}dx/\ell$$

$$+e^{\pi s'/4}\int_d^{\ell}\left(x^2/d^2-1\right)^{-1/4}\cos\left\{\left(\lambda/4-\zeta^2\right)x/\ell+\pi/4-p_2\left(x\right)\right\}dx/\ell\Bigg]^2d\zeta$$

$$=\frac{1}{\pi}\left(d/\ell\right)^2\int_0^{\infty}\Bigg[e^{-\pi s'/4}\int_0^{1}\left(1-x^2\right)^{-1/4}\cos\left\{\left(\lambda/4-\zeta^2\right)x\left(d/\ell\right)-p_1\left(xd\right)\right\}dx$$

$$+e^{\pi s'/4}\int_1^{\ell/d}\left(x^2-1\right)^{-1/4}\cos\left\{\left(\lambda/4-\zeta^2\right)x\left(d/\ell\right)+\pi/4-p_2\left(xd\right)\right\}dx\Bigg]^2d\zeta$$

$$p_1(xd) = \frac{1}{2}s'\left\{\ln\left(\frac{1+x}{1-x}\right) - \ln\left(\frac{\ell+d}{\ell-d}\right)(xd/\ell)\right\}$$

$$p_2(xd) = \frac{1}{2}s'\left\{\ln\left(\frac{x+1}{x-1}\right) - \ln\left(\frac{\ell+d}{\ell-d}\right)(xd/\ell)\right\}$$

Now for evaluation we need to include contributions near the focus at $x/d = 1$. Thus we write

$$\int_{1-\varepsilon}^{1} \left(1-x^2\right)^{-1/4} \cos\left\{\left(\lambda/4-\zeta^2\right)x\,(d/\ell) - p_1(xd)\right\}dx$$

$$\sim 2^{-5/4}\int_{1-\varepsilon}^{1}(1-x)^{-1/4}\left[\exp\left\{i\left(\lambda/4-\zeta^2\right)(d/\ell) - i\frac{1}{2}s'\left\{\ln(2)-\ln(1-x)-\ln\left(\frac{\ell+d}{\ell-d}\right)(d/\ell)\right\}\right\}\right.$$

$$\left.+\exp\left\{-i\left(\lambda/4-\zeta^2\right)(d/\ell) + i\frac{1}{2}s'\left\{\ln(2)-\ln(1-x)-\ln\left(\frac{\ell+d}{\ell-d}\right)(d/\ell)\right\}\right\}\right]dx$$

$$\sim 2^{-5/4}\int_{0}^{\varepsilon}\left[\exp\left\{i\left(\lambda/4-\zeta^2\right)(d/\ell) - i\frac{1}{2}s'\left\{\ln(2)-\ln\left(\frac{\ell+d}{\ell-d}\right)(d/\ell)\right\}\right\}x^{is'/2-1/4}\right.$$

$$\left.+\exp\left\{-i\left(\lambda/4-\zeta^2\right)(d/\ell) + i\frac{1}{2}s'\left\{\ln(2)-\ln\left(\frac{\ell+d}{\ell-d}\right)(d/\ell)\right\}\right\}x^{-is'/2-1/4}\right]dx$$

$$\sim 2^{-5/4}\left[\exp\left\{i\left(\lambda/4-\zeta^2\right)(d/\ell) - i\frac{1}{2}s'\left\{\ln(2)-\ln\left(\frac{\ell+d}{\ell-d}\right)(d/\ell)\right\}\right\}\varepsilon^{is'/2+3/4}\right.$$

$$\left.+\exp\left\{-i\left(\lambda/4-\zeta^2\right)(d/\ell) + i\frac{1}{2}s'\left\{\ln(2)-\ln\left(\frac{\ell+d}{\ell-d}\right)(d/\ell)\right\}\right\}\varepsilon^{-is'/2+3/4}\right]$$

$$\sim 2^{-1/4}\varepsilon^{3/4}\cos\left\{\left(\lambda/4-\zeta^2\right)(d/\ell) - \frac{1}{2}s'\left\{\ln(2/\varepsilon)-\ln\left(\frac{\ell+d}{\ell-d}\right)(d/\ell)\right\}\right\}$$

and

$$\int_{1}^{1+\varepsilon}\left(x^2-1\right)^{-1/4}\cos\left\{\left(\lambda/4-\zeta^2\right)x\,(d/\ell)+\pi/4-p_2(xd)\right\}dx$$

$$\sim 2^{-5/4}\int_{1}^{1+\varepsilon}(x-1)^{-1/4}\left[\exp\left\{i\left(\lambda/4-\zeta^2\right)(d/\ell)+i\pi/4 - i\frac{1}{2}s'\left\{\ln(2)-\ln(x-1)-\ln\left(\frac{\ell+d}{\ell-d}\right)(d/\ell)\right\}\right\}\right.dx$$

$$\left.\exp\left\{-i\left(\lambda/4-\zeta^2\right)(d/\ell)-i\pi/4 + i\frac{1}{2}s'\left\{\ln(2)-\ln(x-1)-\ln\left(\frac{\ell+d}{\ell-d}\right)(d/\ell)\right\}\right\}\right]dx$$

$$\sim 2^{-5/4}\int_{0}^{\varepsilon}\left[\exp\left\{i\left(\lambda/4-\zeta^2\right)(d/\ell)+i\pi/4 - i\frac{1}{2}s'\left\{\ln(2)-\ln\left(\frac{\ell+d}{\ell-d}\right)(d/\ell)\right\}\right\}x^{is'/2-1/4}\,dx\right.$$

$$\exp\left\{-i\left(\lambda/4-\zeta^2\right)(d/\ell)-i\pi/4+i\frac{1}{2}s'\left\{\ln(2)-\ln\left(\frac{\ell+d}{\ell-d}\right)(d/\ell)\right\}\right\}x^{-is'/2-1/4}\Big]\,dx$$

$$\sim 2^{-1/4}\varepsilon^{3/4}\cos\left\{\left(\lambda/4-\zeta^2\right)(d/\ell)+\pi/4-\frac{1}{2}s'\left\{\ln(2/\varepsilon)-\ln\left(\frac{\ell+d}{\ell-d}\right)(d/\ell)\right\}\right\}$$

Thus

$$e^{-\pi s'/4}\int_{1-\varepsilon}^{1}\left(1-x^2\right)^{-1/4}\cos\left\{\left(\lambda/4-\zeta^2\right)x\,(d/\ell)-p_1\,(xd)\right\}dx$$

$$+e^{\pi s'/4}\int_{1}^{1+\varepsilon}\left(x^2-1\right)^{-1/4}\cos\left\{\left(\lambda/4-\zeta^2\right)x\,(d/\ell)-p_2\,(xd)\right\}dx$$

$$\sim 2^{-1/4}\varepsilon^{3/4}\left[e^{-\pi s'/4}\cos\left\{\left(\lambda/4-\zeta^2\right)(d/\ell)-\frac{1}{2}s'\left\{\ln(2/\varepsilon)-\ln\left(\frac{\ell+d}{\ell-d}\right)(d/\ell)\right\}\right\}\right.$$

$$\left.+e^{\pi s'/4}\cos\left\{\left(\lambda/4-\zeta^2\right)(d/\ell)+\pi/4-\frac{1}{2}s'\left\{\ln(2/\varepsilon)-\ln\left(\frac{\ell+d}{\ell-d}\right)(d/\ell)\right\}\right\}\right]$$

### B.5.2 another approach to stadium integral of the square

Another representation for the random plane wave projection arose from consideration of the approximate representation

$$u\approx\sum_p u_p+u_r-\sum_p c'_{rp}u_p$$

This led to

$$\langle P-P_r\rangle\approx\sum_p\left[\frac{1}{L}\int_{-\ell}^{\ell}\left\langle u_p^2\right\rangle dx-\frac{1}{L^2}\frac{4}{A}\int_{-\ell}^{\ell}\int_{-\ell}^{\ell}J_0\left(k\left(x-x'\right)\right)\left\langle u_p\left(x\right)u_p\left(x'\right)\right\rangle dxdx'/\left(\frac{1}{L}\int_{-\ell}^{\ell}\left\langle u_p^2\right\rangle dx\right)\right]$$

Identification of the second term in the summand with the random plane wave projections gave

$$\frac{1}{L^2}\frac{4}{A}\int_{-\ell}^{\ell}\int_{-\ell}^{\ell}J_0\left(k\left(x-x'\right)\right)\left\langle u_p\left(x\right)u_p\left(x'\right)\right\rangle dxdx'=\frac{4\sqrt{\ell/d}}{A^2k\ell\ln\left(\frac{\ell+d}{\ell-d}\right)\left|U'_+\left(-s,0\right)\right|\left|U'_+\left(s,0\right)\right|}G_s\left(\lambda\right)\exp\left(\pi\left|s\right|/2\right)$$

where

$$\exp\left(\pi\left|s\right|/2\right)G_s\left(\lambda\right)\sim\frac{1}{\sqrt{\pi}}\left(d/\ell\right)^{3/2}\{$$

$$e^{-\pi s/2}\int_1^{\ell/d}\left(x'^2-1\right)^{-1/4}\int_1^{\ell/d}\left(x^2-1\right)^{-1/4}$$

$$\left[\frac{\cos\left(\lambda\left|x'-x\right|\frac{d}{4\ell}-\pi/4-\left(p_2\left(x'd\right)-p_2\left(xd\right)\right)\mathrm{sgn}\left(x'-x\right)\right)}{\sqrt{\left|x'-x\right|}}\right.$$

$$\left.-\frac{\sin\left(\lambda\left(x'+x\right)\frac{d}{4\ell}-\pi/4-p_2\left(x'd\right)-p_2\left(xd\right)\right)}{\sqrt{x'+x}}\right]dxdx'$$

$$+2\int_1^{\ell/d}\left(x'^2-1\right)^{-1/4}\int_0^1\left(1-x^2\right)^{-1/4}$$

$$\left[\frac{\cos\left(\lambda\left(x'-x\right)\frac{d}{4\ell}-\left(p_2\left(x'd\right)-p_1\left(xd\right)\right)\right)}{\sqrt{x'-x}}+\frac{\cos\left(\lambda\left(x'+x\right)\frac{d}{4\ell}-p_2\left(x'd\right)-p_1\left(xd\right)\right)}{\sqrt{x'+x}}\right]dxdx'$$

$$+e^{\pi s/2}\int_0^1\left(1-x'^2\right)^{-1/4}\int_0^1\left(1-x^2\right)^{-1/4}$$

$$\left[\frac{\cos\left(\lambda\left|x'-x\right|\frac{d}{4\ell}-\pi/4-\left(p_1\left(x'd\right)-p_1\left(xd\right)\right)\mathrm{sgn}\left(x'-x\right)\right)}{\sqrt{\left|x'-x\right|}}\right.$$

$$\left.+\frac{\cos\left(\lambda\left(x'+x\right)\frac{d}{4\ell}-\pi/4-p_1\left(x'd\right)-p_1\left(xd\right)\right)}{\sqrt{x'+x}}\right]dxdx'\ \}$$

and

$$\lambda=4\left(k-k_p\right)\ell$$

$$p_2\left(xd\right)-p_2\left(x'd\right)=-\frac{1}{2}s'\left\{\ln\left(\frac{\ell+d}{\ell-d}\right)\left(\left(x-x'\right)d/\ell\right)-\ln\left(\frac{x+1}{x-1}\right)+\ln\left(\frac{x'+1}{x'-1}\right)\right\}$$

$$p_2\left(xd\right)+p_2\left(x'd\right)=-\frac{1}{2}s'\left\{\ln\left(\frac{\ell+d}{\ell-d}\right)\left(\left(x+x'\right)d/\ell\right)-\ln\left(\frac{x+1}{x-1}\right)-\ln\left(\frac{x'+1}{x'-1}\right)\right\}$$

$$p_1\left(xd\right)-p_2\left(x'd\right)=-\frac{1}{2}s'\left\{\ln\left(\frac{\ell+d}{\ell-d}\right)\left(\left(x-x'\right)d/\ell\right)-\ln\left(\frac{1+x}{1-x}\right)+\ln\left(\frac{x'+1}{x'-1}\right)\right\}$$

$$p_1\left(xd\right)+p_2\left(x'd\right)=-\frac{1}{2}s'\left\{\ln\left(\frac{\ell+d}{\ell-d}\right)\left(\left(x+x'\right)d/\ell\right)-\ln\left(\frac{1+x}{1-x}\right)-\ln\left(\frac{x'+1}{x'-1}\right)\right\}$$

$$p_1\left(xd\right)-p_1\left(x'd\right)=-\frac{1}{2}s'\left\{\ln\left(\frac{\ell+d}{\ell-d}\right)\left(\left(x-x'\right)d/\ell\right)-\ln\left(\frac{1+x}{1-x}\right)+\ln\left(\frac{1+x'}{1-x'}\right)\right\}$$

$$p_1\left(xd\right)+p_1\left(x'd\right)=-\frac{1}{2}s'\left\{\ln\left(\frac{\ell+d}{\ell-d}\right)\left(\left(x+x'\right)d/\ell\right)-\ln\left(\frac{1+x}{1-x}\right)-\ln\left(\frac{1+x'}{1-x'}\right)\right\}$$

To treat the region about unity we write (we assume that $\varepsilon << |1-x'|$)

$$\int_1^{1+\varepsilon} \left(x^2-1\right)^{-1/4} \frac{\cos\left\{\lambda\left|x'-x\right|\frac{d}{4\ell}-\pi/4-\left(p_2\left(x'd\right)-p_2\left(xd\right)\right)\operatorname{sgn}\left(x'-x\right)\right\}}{\sqrt{\left|x'-x\right|}}dx$$

$$= \int_1^{1+\varepsilon} \left(x^2-1\right)^{-1/4}$$

$$\frac{\cos\left(\lambda\left|x'-x\right|\frac{d}{4\ell}-\pi/4+\frac{1}{2}s'\left(\ln\left(\frac{\ell+d}{\ell-d}\right)\left(x'-x\right)d/\ell-\ln\left(\frac{x'+1}{x'-1}\right)+\ln\left(\frac{x+1}{x-1}\right)\right)\operatorname{sgn}\left(x'-x\right)\right)}{\sqrt{\left|x'-x\right|}}dx$$

$$\sim \frac{1}{2^{1/4}\sqrt{\left|x'-1\right|}} \int_1^{1+\varepsilon} \left(x-1\right)^{-1/4}$$

$$\cos\left(\lambda\left|x'-1\right|\frac{d}{4\ell}-\pi/4+\frac{1}{2}s'\left(\ln\left(\frac{\ell+d}{\ell-d}\right)\left(x'-1\right)d/\ell-\ln\left(\frac{x'+1}{x'-1}\right)+\ln 2-\ln\left(x-1\right)\right)\operatorname{sgn}\left(x'-1\right)\right)dx$$

$$\sim \frac{1}{2^{1/4}\sqrt{\left|x'-1\right|}} \int_1^{1+\varepsilon} \left(x-1\right)^{-1/4}$$

$$\cos\left(\lambda\left(x'-1\right)\frac{d}{4\ell}-\operatorname{sgn}\left(x'-1\right)\pi/4+\frac{1}{2}s'\left(\ln\left(\frac{\ell+d}{\ell-d}\right)\left(x'-1\right)d/\ell-\ln\left(\frac{x'+1}{x'-1}\right)+\ln 2-\ln\left(x-1\right)\right)\right)dx$$

$$\sim \frac{1}{2^{5/4}\sqrt{\left|x'-1\right|}}$$

$$\exp\left\{i\left(\lambda\left(x'-1\right)\frac{d}{4\ell}-\operatorname{sgn}\left(x'-1\right)\pi/4+\frac{1}{2}s'\left(\ln\left(\frac{\ell+d}{\ell-d}\right)\left(x'-1\right)d/\ell-\ln\left(\frac{x'+1}{x'-1}\right)+\ln 2\right)\right)\right\}$$

$$\int_0^{\varepsilon} v^{-1/4-is'/2}dv + \frac{1}{2^{5/4}\sqrt{\left|x'-1\right|}}$$

$$\exp\left\{-i\left(\lambda\left(x'-1\right)\frac{d}{4\ell}-\operatorname{sgn}\left(x'-1\right)\pi/4+\frac{1}{2}s'\left(\ln\left(\frac{\ell+d}{\ell-d}\right)\left(x'-1\right)d/\ell-\ln\left(\frac{x'+1}{x'-1}\right)+\ln 2\right)\right)\right\}$$

$$\int_0^{\varepsilon} v^{-1/4+is'/2}dv \sim \frac{1}{2^{5/4}\sqrt{\left|x'-1\right|}} \exp\left\{i\right.$$

$$\left(\lambda\left(x'-1\right)\frac{d}{4\ell}-\operatorname{sgn}\left(x'-1\right)\pi/4+\frac{1}{2}s'\left(\ln\left(\frac{\ell+d}{\ell-d}\right)\left(x'-1\right)d/\ell-\ln\left(\frac{x'+1}{x'-1}\right)+\ln 2\right)\right)\Bigg\}\frac{\varepsilon^{3/4-is'/2}}{3/4-is'/2}$$

$$+\frac{1}{2^{5/4}\sqrt{\left|x'-1\right|}} \exp\left\{-i\right.$$

$$\left(\lambda\left(x'-1\right)\frac{d}{4\ell}-\operatorname{sgn}\left(x'-1\right)\pi/4+\frac{1}{2}s'\left(\ln\left(\frac{\ell+d}{\ell-d}\right)\left(x'-1\right)d/\ell-\ln\left(\frac{x'+1}{x'-1}\right)+\ln 2\right)\right)\Bigg\}\frac{\varepsilon^{3/4+is'/2}}{3/4+is'/2}$$

$$\sim\frac{\varepsilon^{3/4}}{2^{5/4}\sqrt{\left|x'-1\right|}}\exp\{i$$

$$\left(\lambda\left(x'-1\right)\frac{d}{4\ell}-\operatorname{sgn}\left(x'-1\right)\pi/4+\frac{1}{2}s'\left(\ln\left(\frac{\ell+d}{\ell-d}\right)\left(x'-1\right)d/\ell-\ln\left(\frac{x'+1}{x'-1}\right)+\ln\left(2/\varepsilon\right)\right)\right)\Bigg\}\frac{1}{3/4-is'/2}$$

$$+\frac{\varepsilon^{3/4}}{2^{5/4}\sqrt{\left|x'-1\right|}}\exp\{-i$$

$$\left(\lambda\left(x'-1\right)\frac{d}{4\ell}-\operatorname{sgn}\left(x'-1\right)\pi/4+\frac{1}{2}s'\left(\ln\left(\frac{\ell+d}{\ell-d}\right)\left(x'-1\right)d/\ell-\ln\left(\frac{x'+1}{x'-1}\right)+\ln\left(2/\varepsilon\right)\right)\right)\Bigg\}\frac{1}{3/4+is'/2}$$

$$\sim\frac{3\varepsilon^{3/4}}{2^{1/4}\left(9/4+s'^2\right)\sqrt{\left|x'-1\right|}}$$

$$\cos\left\{\lambda\left(x'-1\right)\frac{d}{4\ell}-\operatorname{sgn}\left(x'-1\right)\pi/4+\frac{1}{2}s'\left(\ln\left(\frac{\ell+d}{\ell-d}\right)\left(x'-1\right)d/\ell-\ln\left(\frac{x'+1}{x'-1}\right)+\ln\left(2/\varepsilon\right)\right)\right\}$$

$$-\frac{2s'\varepsilon^{3/4}}{2^{1/4}\left(9/4+s'^2\right)\sqrt{\left|x'-1\right|}}$$

$$\sin\left\{\lambda\left(x'-1\right)\frac{d}{4\ell}-\operatorname{sgn}\left(x'-1\right)\pi/4+\frac{1}{2}s'\left(\ln\left(\frac{\ell+d}{\ell-d}\right)\left(x'-1\right)d/\ell-\ln\left(\frac{x'+1}{x'-1}\right)+\ln\left(2/\varepsilon\right)\right)\right\}$$

and

$$\int_{1-\varepsilon}^{1}\left(1-x^2\right)^{-1/4}\frac{\cos\left(\lambda\left|x'-x\right|\frac{d}{4\ell}-\pi/4-\left(p_1\left(x'd\right)-p_1\left(xd\right)\right)\operatorname{sgn}\left(x'-x\right)\right)}{\sqrt{\left|x'-x\right|}}dx$$

$$=\int_{1-\varepsilon}^{1}\left(1-x^2\right)^{-1/4}$$

$$\frac{\cos\left\{\lambda\left|x'-x\right|\frac{d}{4\ell}-\pi/4+\frac{1}{2}s'\left(\ln\left(\frac{\ell+d}{\ell-d}\right)\left(x'-x\right)d/\ell-\ln\left(\frac{1+x'}{1-x'}\right)+\ln\left(\frac{1+x}{1-x}\right)\right)\operatorname{sgn}\left(x'-x\right)\right\}}{\sqrt{\left|x'-x\right|}}dx$$

$$\sim\frac{1}{2^{1/4}\sqrt{\left|x'-1\right|}}\int_{1-\varepsilon}^{1}\left(1-x\right)^{-1/4}$$

$$\cos\left\{\lambda\left|x'-1\right|\frac{d}{4\ell}-\pi/4+\frac{1}{2}s'\left(\ln\left(\frac{\ell+d}{\ell-d}\right)\left(x'-1\right)d/\ell-\ln\left(\frac{1+x'}{1-x'}\right)+\ln 2-\ln\left(1-x\right)\right)\operatorname{sgn}\left(x'-1\right)\right\}dx$$

$$\sim\frac{1}{2^{1/4}\sqrt{\left|x'-1\right|}}\int_0^{\varepsilon}$$

$$\cos\left\{\lambda\left(x'-1\right)\frac{d}{4\ell}-\operatorname{sgn}\left(x'-1\right)\pi/4+\frac{1}{2}s'\left(\ln\left(\frac{\ell+d}{\ell-d}\right)\left(x'-1\right)d/\ell-\ln\left(\frac{1+x'}{1-x'}\right)+\ln 2-\ln v\right)\right\}v^{-1/4}dv$$

$$\sim\frac{1}{2^{5/4}\sqrt{\left|x'-1\right|}}$$

$$\exp\left\{i\left(\lambda\left(x'-1\right)\frac{d}{4\ell}-\operatorname{sgn}\left(x'-1\right)\pi/4+\frac{1}{2}s'\left(\ln\left(\frac{\ell+d}{\ell-d}\right)\left(x'-1\right)d/\ell-\ln\left(\frac{1+x'}{1-x'}\right)+\ln 2\right)\right)\right\}$$

$$\int_0^{\varepsilon}v^{-1/4-is'/2}dv$$

$$+\frac{1}{2^{5/4}\sqrt{\left|x'-1\right|}}$$

$$\exp\left\{-i\left(\lambda\left(x'-1\right)\frac{d}{4\ell}-\operatorname{sgn}\left(x'-1\right)\pi/4+\frac{1}{2}s'\left(\ln\left(\frac{\ell+d}{\ell-d}\right)\left(x'-1\right)d/\ell-\ln\left(\frac{1+x'}{1-x'}\right)+\ln 2\right)\right)\right\}$$

$$\int_0^{\varepsilon}v^{-1/4+is'/2}dv$$

$$\sim\frac{3\varepsilon^{3/4}}{2^{1/4}\left(9/4+s'^2\right)\sqrt{\left|x'-1\right|}}$$

$$\cos\left\{\lambda\left(x'-1\right)\frac{d}{4\ell}-\operatorname{sgn}\left(x'-1\right)\pi/4+\frac{1}{2}s'\left(\ln\left(\frac{\ell+d}{\ell-d}\right)\left(x'-1\right)d/\ell-\ln\left(\frac{1+x'}{1-x'}\right)+\ln\left(2/\varepsilon\right)\right)\right\}$$

$$-\frac{2s'\varepsilon^{3/4}}{2^{1/4}\left(9/4+s'^2\right)\sqrt{\left|x'-1\right|}}$$

$$\sin\left\{\lambda\left(x'-1\right)\frac{d}{4\ell}-\operatorname{sgn}\left(x'-1\right)\pi/4+\frac{1}{2}s'\left(\ln\left(\frac{\ell+d}{\ell-d}\right)\left(x'-1\right)d/\ell-\ln\left(\frac{1+x'}{1-x'}\right)+\ln\left(2/\varepsilon\right)\right)\right\}$$

Thus both are identical

$$\int_1^{1+\varepsilon}\left(x^2-1\right)^{-1/4}\frac{\cos\left\{\lambda\left|x'-x\right|\frac{d}{4\ell}-\pi/4-\left(p_2\left(x'd\right)-p_2\left(xd\right)\right)\operatorname{sgn}\left(x'-x\right)\right\}}{\sqrt{\left|x'-x\right|}}dx$$

$$\sim \frac{3\varepsilon^{3/4}}{2^{1/4}\left(9/4+s'^2\right)\sqrt{|x'-1|}}$$

$$\cos\left\{\lambda\left(x'-1\right)\frac{d}{4\ell}-\operatorname{sgn}\left(x'-1\right)\pi/4+\frac{1}{2}s'\left(\ln\left(\frac{\ell+d}{\ell-d}\right)\left(x'-1\right)d/\ell-\ln\left|\frac{1+x'}{1-x'}\right|+\ln\left(2/\varepsilon\right)\right)\right\}$$

$$-\frac{2s'\varepsilon^{3/4}}{2^{1/4}\left(9/4+s'^2\right)\sqrt{|x'-1|}}$$

$$\sin\left\{\lambda\left(x'-1\right)\frac{d}{4\ell}-\operatorname{sgn}\left(x'-1\right)\pi/4+\frac{1}{2}s'\left(\ln\left(\frac{\ell+d}{\ell-d}\right)\left(x'-1\right)d/\ell-\ln\left|\frac{1+x'}{1-x'}\right|+\ln\left(2/\varepsilon\right)\right)\right\}$$

$$\sim\int_{1-\varepsilon}^{1}\left(1-x^2\right)^{-1/4}\frac{\cos\left(\lambda\left|x'-x\right|\frac{d}{4\ell}-\pi/4-\left(p_1\left(x'd\right)-p_1\left(xd\right)\right)\operatorname{sgn}\left(x'-x\right)\right)}{\sqrt{|x'-x|}}dx$$

Next

$$\int_{1}^{1+\varepsilon}\left(x^2-1\right)^{-1/4}\frac{\sin\left(\lambda\left(x'+x\right)\frac{d}{4\ell}-\pi/4-p_2\left(x'd\right)-p_2\left(xd\right)\right)}{\sqrt{x'+x}}dx$$

$$=\int_{1}^{1+\varepsilon}\left(x^2-1\right)^{-1/4}\frac{\cos\left[\lambda\left(x'+x\right)\frac{d}{4\ell}-3\pi/4+\frac{1}{2}s'\left\{\ln\left(\frac{\ell+d}{\ell-d}\right)\left(x'+x\right)d/\ell-\ln\left(\frac{x'+1}{x'-1}\right)-\ln\left(\frac{x+1}{x-1}\right)\right\}\right]}{\sqrt{x'+x}}dx$$

$$\sim\frac{1}{2^{1/4}\sqrt{x'+1}}$$

$$\operatorname{Re}\exp\left[i\left(\lambda\left(x'+1\right)\frac{d}{4\ell}-3\pi/4+\frac{1}{2}s'\left\{\ln\left(\frac{\ell+d}{\ell-d}\right)\left(x'+1\right)d/\ell-\ln\left(\frac{x'+1}{x'-1}\right)-\ln 2\right\}\right)\right]\int_{0}^{\varepsilon}v^{-1/4+is'/2}dv$$

$$\sim\frac{4\varepsilon^{3/4}}{2^{1/4}\sqrt{x'+1}}$$

$$\operatorname{Re}\exp\left[i\left(\lambda\left(x'+1\right)\frac{d}{4\ell}-3\pi/4+\frac{1}{2}s'\left\{\ln\left(\frac{\ell+d}{\ell-d}\right)\left(x'+1\right)d/\ell-\ln\left(\frac{x'+1}{x'-1}\right)-\ln\left(2/\varepsilon\right)\right\}\right)\right]\frac{3/4-is'/2}{9/4+s'^2}$$

$$\sim\frac{3\varepsilon^{3/4}}{2^{1/4}\left(9/4+s'^2\right)\sqrt{x'+1}}\cos\left[\lambda\left(x'+1\right)\frac{d}{4\ell}-3\pi/4+\frac{1}{2}s'\left\{\ln\left(\frac{\ell+d}{\ell-d}\right)\left(x'+1\right)d/\ell-\ln\left(\frac{x'+1}{x'-1}\right)-\ln\left(2/\varepsilon\right)\right\}\right]$$

$$+\frac{2s'\varepsilon^{3/4}}{2^{1/4}\left(9/4+s'^2\right)\sqrt{x'+1}}\sin\left[\lambda\left(x'+1\right)\frac{d}{4\ell}-3\pi/4+\frac{1}{2}s'\left\{\ln\left(\frac{\ell+d}{\ell-d}\right)\left(x'+1\right)d/\ell-\ln\left(\frac{x'+1}{x'-1}\right)-\ln\left(2/\varepsilon\right)\right\}\right]$$

$$\sim \frac{3\varepsilon^{3/4}}{2^{1/4}\left(9/4+s'^2\right)\sqrt{x'+1}}\sin\left[\lambda\left(x'+1\right)\frac{d}{4\ell}-\pi/4+\frac{1}{2}s'\left\{\ln\left(\frac{\ell+d}{\ell-d}\right)\left(x'+1\right)d/\ell-\ln\left(\frac{x'+1}{x'-1}\right)-\ln\left(2/\varepsilon\right)\right\}\right]$$

$$-\frac{2s'\varepsilon^{3/4}}{2^{1/4}\left(9/4+s'^2\right)\sqrt{x'+1}}\cos\left[\lambda\left(x'+1\right)\frac{d}{4\ell}-\pi/4+\frac{1}{2}s'\left\{\ln\left(\frac{\ell+d}{\ell-d}\right)\left(x'+1\right)d/\ell-\ln\left(\frac{x'+1}{x'-1}\right)-\ln\left(2/\varepsilon\right)\right\}\right]$$

$$\int_{1-\varepsilon}^{1}\left(1-x^2\right)^{-1/4}\frac{\cos\left(\lambda\left(x'+x\right)\frac{d}{4\ell}-\pi/4-p_1\left(x'd\right)-p_1\left(xd\right)\right)}{\sqrt{x'+x}}dx$$

$$=\int_{1-\varepsilon}^{1}\left(1-x^2\right)^{-1/4}\frac{\cos\left(\lambda\left(x'+x\right)\frac{d}{4\ell}-\pi/4+\frac{1}{2}s'\left\{\ln\left(\frac{\ell+d}{\ell-d}\right)\left(x'+x\right)d/\ell-\ln\left(\frac{1+x'}{1-x'}\right)-\ln\left(\frac{1+x}{1-x}\right)\right\}\right)}{\sqrt{x'+x}}dx$$

$$\sim\frac{1}{2^{1/4}\sqrt{x'+1}}$$

$$\operatorname{Re}\exp\left[i\left(\lambda\left(x'+1\right)\frac{d}{4\ell}-\pi/4+\frac{1}{2}s'\left\{\ln\left(\frac{\ell+d}{\ell-d}\right)\left(x'+1\right)d/\ell-\ln\left(\frac{1+x'}{1-x'}\right)-\ln 2\right\}\right)\right]\int_0^{\varepsilon}v^{-1/4+is'/2}dv$$

$$\sim \frac{3\varepsilon^{3/4}}{2^{1/4}\left(9/4+s'^2\right)\sqrt{x'+1}}\cos\left[\lambda\left(x'+1\right)\frac{d}{4\ell}-\pi/4+\frac{1}{2}s'\left\{\ln\left(\frac{\ell+d}{\ell-d}\right)\left(x'+1\right)d/\ell-\ln\left(\frac{1+x'}{1-x'}\right)-\ln\left(2/\varepsilon\right)\right\}\right]$$

$$+\frac{2s'\varepsilon^{3/4}}{2^{1/4}\left(9/4+s'^2\right)\sqrt{x'+1}}\sin\left[\lambda\left(x'+1\right)\frac{d}{4\ell}-\pi/4+\frac{1}{2}s'\left\{\ln\left(\frac{\ell+d}{\ell-d}\right)\left(x'+1\right)d/\ell-\ln\left(\frac{1+x'}{1-x'}\right)-\ln\left(2/\varepsilon\right)\right\}\right]$$

Now the cross terms

$$\int_{1-\varepsilon}^{1}\left(1-x^2\right)^{-1/4}\frac{\cos\left(\lambda\left(x'-x\right)\frac{d}{4\ell}-\left(p_2\left(x'd\right)-p_1\left(xd\right)\right)\right)}{\sqrt{x'-x}}dx$$

$$=\int_{1-\varepsilon}^{1}\left(1-x^2\right)^{-1/4}\frac{\cos\left(\lambda\left(x'-x\right)\frac{d}{4\ell}+\frac{1}{2}s'\left\{\ln\left(\frac{\ell+d}{\ell-d}\right)\left(x'-x\right)d/\ell-\ln\left(\frac{x'+1}{x'-1}\right)+\ln\left(\frac{1+x}{1-x}\right)\right\}\right)}{\sqrt{x'-x}}dx$$

$$\sim\frac{1}{2^{1/4}\sqrt{x'-1}}\int_0^{\varepsilon}\cos\left(\lambda\left(x'-1\right)\frac{d}{4\ell}+\frac{1}{2}s'\left\{\ln\left(\frac{\ell+d}{\ell-d}\right)\left(x'-1\right)d/\ell-\ln\left(\frac{x'+1}{x'-1}\right)+\ln 2-\ln v\right\}\right)v^{-1/4}dv$$

$$\sim\frac{1}{2^{1/4}\sqrt{x'-1}}\operatorname{Re}\exp\left[i\left(\lambda\left(x'-1\right)\frac{d}{4\ell}+\frac{1}{2}s'\left\{\ln\left(\frac{\ell+d}{\ell-d}\right)\left(x'-1\right)d/\ell-\ln\left(\frac{x'+1}{x'-1}\right)+\ln 2\right\}\right)\right]$$

$$\int_0^{\varepsilon}v^{-1/4-is'/2}dv$$

$$\sim \frac{3\varepsilon^{3/4}}{2^{1/4}\left(9/4+s'^2\right)\sqrt{x'-1}}\cos\left[\lambda\left(x'-1\right)\frac{d}{4\ell}+\frac{1}{2}s'\left\{\ln\left(\frac{\ell+d}{\ell-d}\right)\left(x'-1\right)d/\ell-\ln\left(\frac{x'+1}{x'-1}\right)+\ln\left(2/\varepsilon\right)\right\}\right]$$

$$-\frac{2s'\varepsilon^{3/4}}{2^{1/4}\left(9/4+s'^2\right)\sqrt{x'-1}}\sin\left[\lambda\left(x'-1\right)\frac{d}{4\ell}+\frac{1}{2}s'\left\{\ln\left(\frac{\ell+d}{\ell-d}\right)\left(x'-1\right)d/\ell-\ln\left(\frac{x'+1}{x'-1}\right)+\ln\left(2/\varepsilon\right)\right\}\right]$$

$$\int_{1-\varepsilon}^{1}\left(1-x^2\right)^{-1/4}\frac{\cos\left(\lambda\left(x'+x\right)\frac{d}{4\ell}-p_2\left(x'd\right)-p_1\left(xd\right)\right)}{\sqrt{x'+x}}dx$$

$$=\int_{1-\varepsilon}^{1}\left(1-x^2\right)^{-1/4}\frac{\cos\left(\lambda\left(x'+x\right)\frac{d}{4\ell}+\frac{1}{2}s'\left\{\ln\left(\frac{\ell+d}{\ell-d}\right)\left(x'+x\right)d/\ell-\ln\left(\frac{x'+1}{x'-1}\right)-\ln\left(\frac{1+x}{1-x}\right)\right\}\right)}{\sqrt{x'+x}}dx$$

$$\sim \frac{1}{2^{1/4}\sqrt{x'+1}}\int_0^{\varepsilon}\cos\left(\lambda\left(x'+1\right)\frac{d}{4\ell}+\frac{1}{2}s'\left\{\ln\left(\frac{\ell+d}{\ell-d}\right)\left(x'+1\right)d/\ell-\ln\left(\frac{x'+1}{x'-1}\right)-\ln 2+\ln v\right\}\right)v^{-1/4}dv$$

$$\sim \frac{1}{2^{1/4}\sqrt{x'+1}}\operatorname{Re}\exp\left[i\left(\lambda\left(x'+1\right)\frac{d}{4\ell}+\frac{1}{2}s'\left\{\ln\left(\frac{\ell+d}{\ell-d}\right)\left(x'+1\right)d/\ell-\ln\left(\frac{x'+1}{x'-1}\right)-\ln 2\right\}\right)\right]$$

$$\int_0^{\varepsilon}v^{-1/4+is'/2}dv$$

$$\sim \frac{3\varepsilon^{3/4}}{2^{1/4}\left(9/4+s'^2\right)\sqrt{x'+1}}\cos\left[\lambda\left(x'+1\right)\frac{d}{4\ell}+\frac{1}{2}s'\left\{\ln\left(\frac{\ell+d}{\ell-d}\right)\left(x'+1\right)d/\ell-\ln\left(\frac{x'+1}{x'-1}\right)-\ln\left(2/\varepsilon\right)\right\}\right]$$

$$+\frac{2s'\varepsilon^{3/4}}{2^{1/4}\left(9/4+s'^2\right)\sqrt{x'+1}}\sin\left[\lambda\left(x'+1\right)\frac{d}{4\ell}+\frac{1}{2}s'\left\{\ln\left(\frac{\ell+d}{\ell-d}\right)\left(x'+1\right)d/\ell-\ln\left(\frac{x'+1}{x'-1}\right)-\ln\left(2/\varepsilon\right)\right\}\right]$$

Finally we need to treat the region about $x'$

$$\int_{x'-\varepsilon}^{x'+\varepsilon}\frac{\cos\left(\lambda\left|x'-x\right|\frac{d}{4\ell}-\pi/4-\left(p_2\left(x'd\right)-p_2\left(xd\right)\right)\operatorname{sgn}\left(x'-x\right)\right)}{\sqrt{\left|x'-x\right|}}dx$$

$$=\int_{x'-\varepsilon}^{x'+\varepsilon}\frac{\cos\left(\lambda\left|x'-x\right|\frac{d}{4\ell}-\pi/4+\frac{1}{2}s'\left\{\ln\left(\frac{\ell+d}{\ell-d}\right)\left(x'-x\right)d/\ell-\ln\left(\frac{x'+1}{x'-1}\right)+\ln\left(\frac{x+1}{x-1}\right)\right\}\operatorname{sgn}\left(x'-x\right)\right)}{\sqrt{\left|x'-x\right|}}dx$$

$$\sim \frac{1}{\sqrt{2}}\int_{x'-\varepsilon}^{x'+\varepsilon}\frac{dx}{\sqrt{\left|x'-x\right|}}=\sqrt{2}\int_0^{\varepsilon}\frac{du}{\sqrt{u}}=2\left(2\varepsilon\right)^{1/2}$$

$$\int_{x'-\varepsilon}^{x'+\varepsilon} \frac{\cos\left(\lambda\left|x'-x\right|\frac{d}{4\ell}-\pi/4-\left(p_1\left(x'd\right)-p_1\left(xd\right)\right)\operatorname{sgn}\left(x'-x\right)\right)}{\sqrt{\left|x'-x\right|}}dx$$

$$=\int_{x'-\varepsilon}^{x'+\varepsilon} \frac{\cos\left(\lambda\left|x'-x\right|\frac{d}{4\ell}-\pi/4+\frac{1}{2}s'\left\{\ln\left(\frac{\ell+d}{\ell-d}\right)\left(x'-x\right)d/\ell-\ln\left(\frac{1+x'}{1-x'}\right)+\ln\left(\frac{1+x}{1-x}\right)\right\}\operatorname{sgn}\left(x'-x\right)\right)}{\sqrt{\left|x'-x\right|}}dx$$

$$\sim \frac{1}{\sqrt{2}}\int_{x'-\varepsilon}^{x'+\varepsilon}\frac{dx}{\sqrt{\left|x'-x\right|}}=\sqrt{2}\int_0^{\varepsilon}\frac{du}{\sqrt{u}}=2\left(2\varepsilon\right)^{1/2}$$

# Distribution

1 Prof. Steven Anlage
University of Maryland
Office: 1367 Physics
College Park, MD 20742-4111

1 Dr. David A. Hill
Mailcode 818.02
325 Broadway
Boulder, CO 80305-3328

1 Dr. Kelvin S. H. Lee
ITT Industries/AES
1033 Gayley Avenue
Suite 215
Los Angeles, CA 90024

| | | |
|---|---|---|
| 1 | MS0188 | D. C. Chavez, LDRD Office, 01011 |
| 1 | MS0492 | K. C. Chen, 12332 |
| 1 | MS1152 | R. E. Jorgenson, 01652 |
| 1 | MS1152 | M. B. Higgins, 01653 |
| 1 | MS1152 | J. D. Kotulski, 01652 |
| 1 | MS1152 | M. E. Morris, 01652 |
| 5 | MS1152 | L. K. Warne, 01652 |
| 2 | MS9018 | Central Technical Files, 08944 |
| 2 | MS0899 | Technical Library, 04536 |